Targeting Mitochondrial ROS Production in Kidney Transplantation

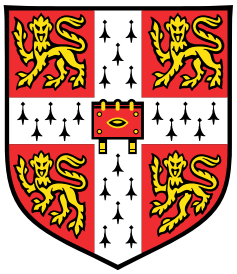

Timothy Elliott Beach

Supervisor: Mr Kourosh Saeb-Parsy, Prof. Michael P. Murphy

Department of Surgery
University of Cambridge

This dissertation is submitted for the degree of
Doctor of Philosophy

Peterhouse December 2019

Declaration

This dissertation was written in partial fulfilment of the requirements for the degree of Doctor of Philosophy. With the exception of any collaborations that are mentioned throughout the text, this dissertation describes my own work carried out under the supervision of Mr Kourosh Saeb-Parsy and Professor Michael P. Murphy from October 2016 until December 2019. Any information that is derived from other sources is referenced accordingly. It does not exceed the prescribed word limit for the Degree Committee.

Timothy Elliott Beach
December 2019

Abstract

Ischaemia reperfusion injury (IRI) is an inevitable consequence of transplant practices, but is associated with reduced levels of graft function and survival. In addition, concerns regarding the severity of IRI has restricted the greater use of organs from the available donor pool. Critically, no pharmacological therapies currently exist to ameliorate the effects of IRI in organ transplantation (or other IRI-related pathologies), partly due to an incomplete understanding of the underlying pathophysiology. Recently, a specific mechanism of mitochondrial reactive oxygen species (ROS) production, thought to initiate many of the downstream pathways resulting in IRI, has been described. This mechanism has identified a number of new therapeutic targets within mitochondria, including the respiratory complex succinate dehydrogenase (SDH). The aim of this thesis was to determine whether malonate ester prodrugs, which competitively inhibit SDH, may reduce mitochondrial ROS production and ameliorate IRI in models of kidney transplantation. Herein, I show that the metabolic changes required for mitochondrial ROS production on reperfusion, including succinate accumulation and the depletion of adenine nucleotides, occur in grafts retrieved from both DBD and DCD donors, despite differences in their exposure to warm ischaemia. This may partly relate to difficulties in efficiently cooling organs and suggests grafts from both donor types may benefit from therapies aimed at reducing mitochondrial ROS production. I describe a translational model of kidney transplantation in the pig and human as well as a model of renal IRI in the mouse. I show the mitochondrial ROS probe, MitoB, may be limited in its ability to accurately quantify the burst of mitochondrial ROS production that occurs during IRI in the kidney; however mitochondrial ROS production may instead be inferred indirectly in mouse, pig and human models by comparing the metabolic changes that occur on reperfusion to those previously described to drive mitochondrial ROS production *in vitro*. In addition, I identify key markers of oxidative damage, cell death and kidney function in the mouse, pig and human and subsequently show malonate ester prodrugs administered at reperfusion (but not prior to ischaemia) may reduce IRI in the mouse. Finally, I present pilot data in the pig providing important dosing and timing information for the use of malonate ester prodrugs in this model. Further work is needed to determine whether malonate ester prodrugs may inhibit mitochondrial ROS production in kidney transplantation; however, this thesis has

provided important inroads into the use of these compounds in a transplant setting as well as characterising a number of translational models that may pave the way to their use in future clinical trials.

Acknowledgements

I would first like to thank my two supervisors, Kourosh Saeb-Parsy and Mike Murphy. Kourosh, thank you for giving me the opportunity to undertake a PhD with you and for your endless support, time and optimism over the last three years. Thank you for sharing with me your positive mentality, for encouraging me to think outside the box and for giving me the experimental freedom to explore different ideas. You have been a huge inspiration as a clinician-scientist and I hope to continue to develop many of the traits you have instilled in me in future years to come. Mike, thank you for all your advice support and guidance over the last three years, for helping me to navigate the incredibly interesting but complex world of mitochondria, free radicals and redox biology, and for sharing in my enthusiasm for the kidney and heart! You have helped further develop my scientific mindset and I hope that from you I have learnt to become a better scientist.

Thank you also to everyone from the Department of Surgery and Mitochondrial Biology Unit who have been so welcoming over the last three years. In particular, thank you to Jack and Mazin for teaching me many of the surgical skills required to complete the experiments in this thesis. Thank you also to Anja and Hiran, for taking me under your wing and teaching me many of the biochemical techniques used in this project. I am also incredibly grateful to Krishnaa for all her help and insights with many aspects of this project. Thank you also to Andrew James for his insights and Sarah Hosgood and Prof. Nicholson for all their advice and support. I would also like to thank the CBS team and team at Huntingdon Life Sciences for their technical assistance over the last three years.

Thank you to everyone who has made the last three years so memorable. Kourosh, Nikola, Olivia, Nikitas, Anja, Krishnaa, Mazin, Jack, Maggie, Beth, Alba, Michelle, Abbie, John, Natasha, Alison G and Evans from the KSP group. Mike, Hiran, Filip, Nils, Fay, Amin, Jan, Nicole, Tracey, Angela, Georgina, Marie-Christine and AJ from the Murphy Lab. Ashley, Hannah, Jenna, Tom M, Tom A, Keziah, Patrick, Veena, Corina, Sylvia, Fay, Jackie, Alison W, Linda, Lila, Sarah, Mike and Vas from the Department. I hope that our friendships and good times together will continue for many years to come!

Last but not least thank you to Mum, Lily, Rowan and Ally for all your love and support. You have always encouraged me to be the best I can be and without you none of this would have been possible!

Table of contents

Abbreviations

ΔE_h	Redox driving force
Δp	Proton motive force
4-HNE	4-hydroxynonenal
AKI	Acute kidney injury
AMS	Diacteoxymethyl succinate
ATN	Acute tubular necrosis
AUC	Area under the curve
BTF	Back-table flush
BUN	Blood urea nitrogen
CDPA	Citrate-phosphate-dextrose-adenine
CIT	Cold ischaemia time
CKD	Chronic kidney disease
CoQ	Ubiquinone
$CoQH_2$	Ubiquinol
cyt C	Cytochrome C
DAMP	Damage associated molecular pattern
DBD	Donation after brainstem death
DCD	Donation after circulatory death

DGF	Delayed graft function
DIC	Dicarboxylate carrier
DMM	Dimethyl malonate
DMSO	Dimethyl sulfoxide
DNP	Dinitrophenylhydrazine
DSM	Disodium malonate
DTNB	5,5'-dithiobis-(2-nitrobenzoic acid)
ECD	Extended criteria donor
eGFR	Estimated glomerular filtration rate
EGL	Early graft loss
ER	Endoplasmic reticulum
ESR	Electron spin resonance
ETC	Electron transport chain
EVNP	*Ex vivo* normothermic perfusion
FAD	Oxidised flavin adenine dinucleotide
$FADH_2$	Reduced flavin adenine dinucleotide
FENa	Fractional excretion of sodium
FMN	Flavin mononuclear
GR	Glutathione reductase
GSH	Reduced glutathione
GSSG	Oxidised glutathione
HLA	Human leukocyte antigen
HMP	Hypothermic machine perfusion
IMM	Inner mitochondrial membrane

IMS	Intermembrane space
IRI	Ischamia reperfusion injury
IVC	Inferior vena cava
LAD	Left anterior descending
LD	Living donation
LN2	Liquid nitrogen
LPP	Lipid peroxidation product
MAM	Diacetoxymethyl malonate
MAS	Malate aspartate shuttle
MCU	Mitochondrial calcium uniporter
MDA	Malondialdehyde
MnSOD	Manganese superoxide dismutase
mPTP	Mitochondrial permeability transition pore
mtDNA	Mitochondrial DNA
NAD^+	Oxidised nicotinamide adenine dinucleotide
NADH	Reduced nicotinamide adenine dinucleotide
NADPH	Reduced nicotinamide adenine dinucleotide phosphate
NCX	Na^+/Ca^{2+} exchanger
NHE	Na^+/H^+ exchanger
NOX	NADPH oxidases
NRP	Normothermic regional perfusion
OMM	Outer mitochondrial membrane
$ONOO^-$	Peroxynitrite
OXPHOS	Oxidative phosphorylation

PLE	Pig liver esterase
PNC	Purine nucleotide cycle
PNF	Primary nonfunction
PVC	Polyvinyl chloride
RBF	Renal blood flow
RET	Reverse electron transport
ROS	Reactive oxygen species
SCr	Serum creatinine
SDH	Succinate dehydrogenase
SERCA	Sarcoplasmic reticulum Ca^{2+}-ATPase
TBARS	Thiobarbituric acid reactive species
TCA	Tricarboxylic acid
TIM	Translocase of the inner mitochondrial membrane
TLR	Toll-like receptor
TNB	2-nitro-5-thiobenzoate
TOM	Translocase of the outer mitochondrial membrane
TPP	Triphenylphosphonium
TUNEL	Terminal deoxynucleotidyl transferase dUTP nick end labelling
UW	University of Wisconsin
VDAC	Voltage dependent anion channels
XO	Xanthine oxidase

Chapter 1

Introduction

1.1 General Introduction

Kidney transplantation is the treatment of choice for end-stage renal failure offering a substantial improvement in quality of life and reduced risk of mortality compared to chronic dialysis [1]. As of 31st March 2019, 4,647 adult patients were registered on the kidney only transplant list with a median waiting time of 1.8 years [2]. However, due to an ongoing organ shortage, 23% of patients are still waiting for a transplant at three years post-registration and a further 11% are either no longer suitable for a transplant or have died. Whilst the number of active patients on the kidney only transplant list has significantly decreased over the last decade, the incidence of end-stage renal failure in the UK is increasing [3]. Meeting organ demand therefore remains a major challenge in kidney transplantation with total demand set to increase in coming years.

Between 1st April 2018 and 31st March 2019, 3,280 adult kidney only transplants were performed in the UK; however, changing donor demographics and growing pressure to meet organ demand has led to an increase in the use of more marginal organs including those with longer warm ischaemic times retrieved from donation after circulatory death (DCD) and so called extended criteria organs that historically would have been declined for transplantation [4] [5] [2]. Such organs are thought to endure increased levels of ischaemia reperfusion injury (IRI) upon transplantation and have been linked with poorer short- and long-term outcomes [6] [7] [8] [9]. Furthermore, a significant proportion of donated organs are declined for transplantation due to concerns IRI will lead to excessive damage in transplanted grafts on reperfusion [2] [10] [11]. Currently, no treatments exist to ameliorate the effects of IRI in kidney transplantation leading to an increase in recipient morbidity and mortality and barring the greater use of organs from the current donor pool [12] [13].

Over the last decade, our understanding of the pathological mechanisms underlying IRI has greatly improved [14]. Increasing evidence now points to a specific mechanism of mitochondrial reactive oxygen species (ROS) production that is thought to initiate many of the downstream pathways leading to organ damage and dysfunction [15] [16]. As a result, a number of novel therapeutic targets have been identified within mitochondria aimed at reducing mitochondrial ROS production and ameliorating IRI [17]. As IRI currently limits the availability donor organs in addition to causing a degree of injury in all transplanted grafts, inhibition of mitochondrial ROS production during kidney transplantation may help to increase organ supply as well as improving overall graft quality and survival.

In this thesis, I investigate whether malonate ester-prodrugs can ameliorate IRI in kidney transplantation by reducing mitochondrial ROS production upon reperfusion. In this chapter, I will first discuss IRI in the context of kidney transplantation, how it may vary under different conditions of organ donation and its effect on short and long term graft and patient survival. I will then discuss how mitochondria produce ROS during IRI and how this process may be targeted. Lastly, I will discuss how different malonate compounds may be targeted to mitochondria in order to inhibit mitochondrial ROS production during IRI and how clinical transplantation may be simulated in a variety of translational animal models.

1.2 Ischaemia Reperfusion Injury in Kidney Transplantation

1.2.1 Definition

Ischaemia reperfusion injury occurs upon the return of an oxygenated blood supply to an organ or tissue following a period of ischaemia or lack of oxygen [18] [16]. Paradoxically, the return of oxygenated blood leads to an increase in the level of injury over and above that which occurs during ischaemia alone [19] [18]. This is thought to be related to the production of ROS during reperfusion which go on to initiate much of the downstream damage leading to organ or tissue injury [20] [21]. Ischaemia reperfusion injury is inherent to current transplant practices but also underlies many other pathological conditions including myocardial infarction and ischaemic stroke [18] [22]. In this section I first discuss the pathophysiology underlying IRI in organ transplantation. I then discuss the clinical risk factors that influence the severity of IRI in kidney transplantation and their clinical consequences. Lastly, I discuss the therapeutic strategies currently used to ameliorate IRI in kidney transplantation.

1.2.2 Pathophysiology of IRI in Kidney Transplantation

Whilst much of our understanding surrounding the pathophysiology of IRI arises from studies in the heart, many of the underlying mechanisms of injury are thought to apply universally to all organs and tissues [14] [23]. A key difference between IRI in organ transplantation and myocardial infarction however, is that the injury following organ transplantation may be further complicated by the alloimmune response of the recipient's immune system to the donor allograft [24]. Whilst the details of the alloimmune response will not be discussed in detail here, the injury resulting from IRI may play an important role in initiating and modulating the severity of this response and may subsequently influence the rate of organ rejection [25] [26].

Pathophysiology of Ischaemia

During organ donation, the conditions and duration of ischaemia experienced by a graft vary depending on the donor type from which the organ is retrieved (discussed below); nonetheless, a number of key metabolic and biochemical changes are thought to occur in all donated organs regardless of the donor type [27]. During ischaemia, oxidative phosphorylation ceases and there is a metabolic switch to anaerobic glycolysis leading to the accumulation of lactate and reduction in intracellular pH [28]. ATP is hydrolysed to ADP by reversal of F_OF_1-ATP synthase within mitochondria and then further degraded to adenosine and inosine as high energy phosphate bonds are consumed by other enzymatic processes [29] [30]. ATP depletion and cellular acidosis subsequently lead to an increase in intracellular sodium due to decreased Na^+/K^+ ATPase activity and sodium entry via the Na^+/H^+ exchanger (NHE) [31]. Increased intracellular sodium leads to reversal of the Na^+/Ca^{2+} exchanger (NCX) and an increase in intracellular calcium which; alongside impaired sarcoplasmic reticulum Ca^{2+}-ATPase (SERCA) activity and endoplasmic calcium release; results in calcium overload [32] [33]. Lactate production, production of glycolytic intermediates and accumulation of sodium and calcium ions also leads to an increase in intracellular osmolarity resulting in water entry and cellular swelling [34] [35]. During donation, organs are rapidly cooled to less than 4 °C and placed in preservation solution in an attempt to minimise the metabolic and biochemical changes that occur during ischaemia [35]. Cooling organs reduces the metabolic rate in accordance with van't Hoff's equation, thereby slowing the rate of ATP depletion and accumulation of metabolic end-products. Meanwhile, a number of preservation solutions have been developed with a similar ionic composition to the intracellular space, thereby abolishing ionic and osmotic gradients across cell membranes, minimising intracellular Na^+ accumulation and cellular swelling [35] [36]. It is important to note however that depending

on the type of donation, organs may have experienced a prolonged period of warm ischaemia prior to cooling during which the processes described above occur at a much faster rate and significant biochemical and metabolic changes may have already occured [37].

Pathophysiology of Reperfusion

Following vessel anastomosis, the graft is reperfused resulting in the reactivation of the electron transport chain within cells and an increase in the mitochondrial membrane potential [23]. Re-establishment of the negative mitochondrial membrane potential drives calcium entry into mitochondria via the mitochondrial calcium uniporter (MCU) and calcium accumulation within the mitochondrial matrix [38]. There is also a burst of reactive oxygen species (ROS) from mitochondria on reperfusion that has historically been ascribed to the non-specific 'spill' of electrons from the electron transport chain [39]. Meanwhile, the NHE is reactivated and hydrogen is extruded from the cell resulting in an increase in intracellular pH. Restoration of intracellular pH alongside mitochondrial calcium entry and ROS production leads to opening of the mitochondrial permeability transition pore (mPTP) [40] [41]. The mPTP is a non-selective pore permeable to molecules up to 1.5 kDa. Cyclophilin D, a mitochondrial specific peptidyl-prolyl cis-trans isomerase, is thought to play an important role in pore formation with $CypD^{-/-}$ mice showing protection against IRI [42]. The other molecular components of the mPTP however are currently unclear and the exact nature of the pore is under much debate [43] [44]. Nonetheless, opening of the mPTP following IRI leads to dissipation of the mitochondrial membrane potential, uncoupling of oxidative phosphorylation, ATP depletion and necrotic cell death [45]. Swelling of the mitochondrial matrix following mPTP opening may also lead to outer mitochondrial membrane rupture and the release of pro-apoptotic factors including cytochrome C culminating in apoptosis [46]. In addition, ROS production on reperfusion can cause direct damage to lipids, proteins and DNA leading to further cellular dysfunction that may trigger numerous cell death pathways [47] [39]. Mitochondrial DNA (mtDNA) release into the cytoplasm via the mPTP may also activate a number of endogenous immune pathways through its action as an intracellular damage associated molecular pattern (DAMP) further contributing to cell death and inflammation [48] [49].

Cell death following IRI results in the release of a number of DAMPs including mtDNA into the extracellular space and activation of the innate immune response via toll-like receptors (TLRs) [50]. Activation of graft resident macrophages and dendritic cells through the release of DAMPs and other signalling molecules results in the release chemokines which enhance the recruitment of host immune cells to the graft [51]. Meanwhile, activated endothelial cells upregulate adhesion molecules including VCAM-1 and L-selectin promoting the entry of host immune cells into the transplanted graft [52]. Following the initial inflammatory

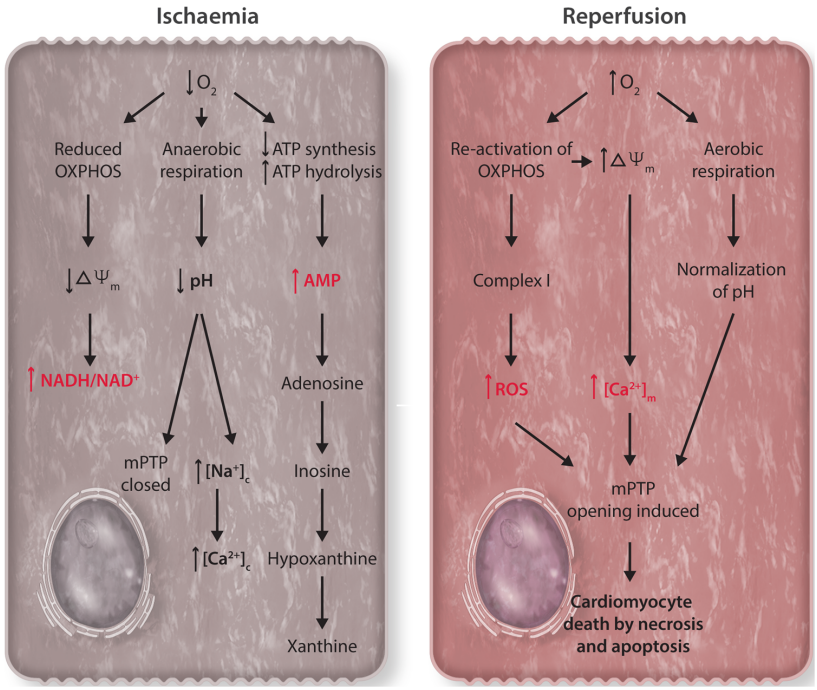

Figure 1.1 Pathophysiology of Ischaemia Reperfusion Injury. During ischaemia, oxidative phosphorylation ceases and a switch to anaerobic metabolism leads to lactate production and a decrease in intracellular pH. ATP is hydrolysed by reversal of mitochondrial F_OF_1-ATP synthase leading to inhibition of Na^+/K^+ ATPase and intracellular Ca^{2+} accumulation. On reperfusion, mitochondrial ROS production and calcium overload lead to opening of the mitochondrial permeability transition pore resulting in mitochondrial depolarisation and cellular necrosis. Figure adapted from Pell et al (2016).

response, host macrophages and dendritic cells migrate to draining lymph nodes where they may initiate an anti-donor adaptive immune response [53]. Ischaemia reperfusion injury and DAMP release may therefore influence the adaptive immune response to the graft in addition to their role in sterile inflammation [26].

1.2.3 Risk Factors Influencing IRI Severity in Kidney Transplantation

A number of factors are thought to influence the severity of IRI in kidney transplantation, including donor type, donor age, cold ischaemia and anastomosis time and these will be discussed in detail here.

Donor Type

Three types of kidney donation currently exist in the UK; living donation (LD) , donation after brainstem death (DBD) and donation after circulatory death (DCD).

In living donation, a relative, spouse, close friend or altruistic donor, may donate one of their kidneys to the recipient. This is possible due to the large reserve capacity of the kidney allowing a healthy donor to survive with a single organ. Usually the donor and recipient operation occur simultaneously in adjacent theatres, thus minimising the organ preservation period and cold ischaemia time (CIT) to which the graft is exposed. The donor operation is often performed laparoscopically and there is a very short period of warm ischaemia between ligation of the renal artery and vein and removal of the kidney from the abdominal cavity. Following retrieval from the donor, the kidney is flushed with ice-cold preservation solution (University of Wisconsin (UW) or Soltran) and submerged in slushed ice whilst the recipient is prepared for implantation [54]. Whilst most LD transplants occur in adjacent theatres with a short CIT, a number of donor-recipient pairs may be HLA or ABO incompatible and instead enter into a national organ sharing scheme. Here, donor-recipient pairs who are incompatible may exchange grafts in order to obtain the best match possible for each recipient. In these circumstances however, the CIT may be increased due to time taken to transport donated grafts between hospitals [55]. Between 1st April 2018 and 31st March 2019, 941 living donor transplants were performed in the UK [2].

Donation after brainstem death occurs in donors who meet brainstem death criteria but have not undergone circulatory arrest. The definition of brainstem death was introduced by Havard Medical School in 1968 to enable declaration of death in patients with catastrophic brain injury leading to irreversible coma; this was to help ease the burden of withdrawing life support in such patients but also overcome previous controversy with the use of organs from brain dead patients. In the UK, brainstem death may only be confirmed under the following conditions: (i) patients must be in a deep state of unconsciousness, apnoeic and mechanically ventilated and there should be no doubt the patient has suffered irreversible brain damage of known aetiology, (ii) potentially reversible contributions to a state of apnoeic coma such as sedative drugs, endocrine or metabolic abnormalities and hypothermia must be excluded, and (iii) formal testing of apnoea and brainstem reflexes must be performed to confirm brainstem death. Testing must be performed by two doctors together on two separate occasions before brainstem death can be confirmed [56]. Historically, DBD donors were typically young, healthy patients who had died from traumatic brain injury, however it is now more likely for a DBD donor to be over 50 years old and have died from intracerebral haemorrhage [57]. Following confirmation of death and consent for organ donation, DBD donors may be transferred to the surgical theatre where a laparotomy and dissection of organs for retrieval may be performed prior to withdrawal of life support and *in situ* cold flush thereby minimising the warm ischaemia time to which they are exposed. Slushed ice is usually placed intraperitoneally at the commencement of cold in situ flush to aid with topical

organ cooling. Following retrieval from the abdomen, kidneys undergo further cold flushing with preservation solution on the back table at the discretion of the retrieval team before being transferred to cold static storage. Between 1st April 2018 and 31st March 2019, 1,369 DBD transplants were performed in the UK [2].

A US study comparing transplant outcomes in LD compared to DBD reported that survival rates were significantly greater in kidneys retrieved from LD compared to DBD, even when there was a higher degree of human leukocyte antigen (HLA) mismatching between the donor and recipient in LD compared to DBD [58]. Furthermore, superior survival rates in kidneys from LD compared to DBD could not be attributed to shorter cold ischaemia times in LD and it is now thought that the injurious processes that occur during brainstem death may account for much of the disparity in graft survival between the two donor types [58] [59] [57]. During brainstem death a number of haemodynamic, hormonal and inflammatory changes occur in the body that may cause damage in the donor kidney and sensitise them to IRI injury, most notably of which are the catecholamine and cytokine storms [57] [60] [61] [62] [63]. The damaging effects of brainstem death on donor kidneys are thought to exacerbate the effects of IRI on transplantation resulting in poorer graft survival [64].

Donation after circulatory death describes organ donation following death from circulatory arrest in the donor. In the UK, death from circulatory arrest may only be confirmed following a five minute observational period during which time the organs of the body are exposed to warm ischaemia. There are 5 separate categories of DCD donation described by the Modified Maastricht Classification scheme as shown in Table 1.1. Uncontrolled donation rarely occurs in the UK and 90% of DCD donors fall under Maastricht category III. Such donors have often suffered irreversible brain injury but do not meet the brainstem death criteria. Instead, life support is withdrawn in a controlled environment and circulatory death is allowed to occur naturally. Organ retrieval teams are notified of potential DCD donors prior to withdrawal of life-support and if consent for donation is given, will prepare a surgical theatre so that organ retrieval may begin as close to the declaration of death as possible. On confirmation of circulatory death, a rapid laparotomy is performed and the aorta cannulated in order to flush organs with cold preservation solution *in situ* (converting warm ischaemia to cold ischaemia). Slushed ice is placed intraperitoneally to aid topical cooling of the organs and following retrieval from the abdomen, organs may undergo further cold perfusion on the back-table prior to cold storage at the discretion of the organ retrieval team. The median warm ischaemic time from circulatory arrest to *in situ* perfusion is currently 14 minutes with interquartile range of 11-17 minutes [9]. The number of DCD kidney transplants has

Modified Maastricht Category	Situation surrounding circulatory arrest	Conditions surrounding circulatory arrest
I	Dead on arrival at hospital	Uncontrolled
II	Unsuccessful resuscitation	Uncontrolled
III	Anticipated circulatory arrest	Controlled
IV	Circulatory arrest in a patient previously declared dead according to neurological criteria (brain death)	Controlled
V	Circulatory arrest in hospital	Controlled

Table 1.1 Donation after Circulatory Death Modified Maastricht Category from Longnus et al (2014).

increased over the last ten years from 527 in 2009 to 970 in 2018 to help meet organ demand [2].

A UK registry study of 9,134 deceased donor kidney transplants between 2000 and 2007 has found that whilst DCD kidneys had twice the risk of developing delayed graft function (DGF, see below) compared to DBD kidneys (50% of DCD grafts versus 25% DBD grafts) there was no significant difference in estimated glomerular filtration rate (eGFR) at 1-5 years post-transplant or 5-year graft survival between donor types [65]. Interestingly, whilst warm ischaemia time was thought to be largely responsible for the increased rate of DGF in DCD kidneys, warm ischaemia time was not associated with transplant outcome in this study. In a second UK registry study of 6,490 deceased kidney transplants from 2005 to 2010, which included a greater number of DCD kidney transplants and therefore more reflective of current donor demographics, authors reported higher rates of primary nonfunction (PNF) (4% vs 3%), DGF (49% vs 24%) and a marginally lower eGFR at 1-year post transplant in recipients of DCD kidneys compared to DBD kidneys however no significant difference in graft or patient survival (82.9% vs 85.0%) between recipients of DCD kidneys compared to DBD kidneys was reported at 3.6 years post-transplant [8]. A further follow-up paper subsequently reported graft and patient survival was not significantly different between DCD and DBD kidneys at 5 and 10 years post-transplant, reinforcing previous UK registry analysis [9]. These findings are in agreement with studies of larger US registries that have also reported no significant difference in mid- to long-term survival of DCD compared to DCD kidneys [66].

In addition to the warm ischaemia experienced during the observational period in DCD donation, some patients become haemodynamically unstable following the withdrawal of artificial life support in DCD donation, leading to organ hypoperfusion. A blood pressure of less than 50 mmHg is arbitrarily defined as the threshold for hypoperfusion below which organs may undergo a period of 'functional warm ischaemia' prior to circulatory arrest. This period is very difficult to predict and current UK guidelines state that organ retrieval teams may abandon a DCD retrieval if the period of functional warm ischaemia exceeds two hours [67]. However, a retrospective study of 117 DCD kidney transplants found the duration of functional warm ischaemia had no effect on transplant outcomes [68].

In summary, kidneys from living donors offer the best transplant outcomes. Kidneys from DBD donors have lower graft survival rates compared to kidneys from living donors which is thought to result from damage to DBD kidneys during brainstem death and possible increased sensitivity to IRI rather than from increased CITs alone. Kidneys from DCD kidneys have higher rates of DGF than DBD kidneys which is attributed to the exposure of DCD kidneys to warm ischaemia prior to organ retrieval however, at least in some studies, DCD and DBD show similar long term graft survival rates.

Donor Age and Extended Criteria Organs

Deceased donor grafts may be further categorised as meeting either standard or extended criteria. Extended criteria donor (ECD) grafts are defined as grafts retrieved from deceased donors over 60 years of age or aged over 50 years with at least two of the following risk factors: (i) a history of hypertension, (ii) a terminal serum creatinine >1.5 mg/dL or (iii) a cerebrovascular cause of death [69]. More recently, a separate measure of donor risk, the UK donor risk index, has been developed to encompass a wider spectrum of factors affecting transplant outcomes and is used in to improve allocation of 'higher risk' organs in the UK [70]. Under this classification the number of high risk DBD transplants has increased from 258 in 2009 to 536 in 2018 and is largely attributable to the use of older donors [2] [9]. Furthermore, the number of organ donors over 60 years of age has gradually been increasing in the last decade and constitutes roughly one third of the available donor pool [9].

In an initial UK registry study of 9,134 deceased donor kidney transplants between 2000 and 2007, kidneys from DCD donors aged 60 years or older was associated with poorer graft function as measured by eGFR at 3 months compared with DCD kidneys from donors aged less than 40 years [65]. The authors ascribed poorer function in older DCD kidneys to reduced functional reserve and increased vasculopathy, meaning older kidneys were less able to withstand transplant related injury. A second UK registry study of 6,490 deceased kidney transplants from 2005 to 2010, which included a greater number of DCD kidney

transplants and therefore more reflective of current donor demographics, showed that kidneys from donors aged more than 60 years had twice of the risk of graft failure within 3 years of transplantation than those from donors aged less than 40 years irrespective of whether kidneys were received from DCD or DBD donor, suggesting decisions regarding the use of older kidneys from DCD donors should be the same as for kidneys from DBD donors [8]. However, the authors warn that this analysis may have included an element of selection bias and only DCD kidneys of exceptional quality would have been transplanted [8].

Other factors such as history of hypertension and premortem serum creatinine concentration are more weakly associated with recipient outcome relative to donor age [8] [71]. UK registry analysis has shown kidneys from ECD donors have inferior survival compared to standard criteria organs however there was no significant difference in graft survival between ECD kidneys from DCD compared to DBD donors [9]. Again, this finding is further supported by analysis of larger US registries [72].

Cold Ischaemia Time

Following retrieval, organs from deceased and living donors are most commonly stored in preservation solution on ice in order to inhibit the pathological changes that occur during ischaemia. The metabolic rate of the tissue is slowed by a factor of 1.5-2 for every 10 °C reduction in temperature; therefore, the rate of metabolism is decreased approximately six-fold in donated organs cooled to 4 °C [73]. Whilst cooling an organ dramatically decreases enzymatic activity, pathological metabolic and biochemical changes still occur in the tissue and there is a limit to the duration of cold ischaemia a donated organ can tolerate. The major factors affecting CIT in clinical transplantation include transport time, time for taken for donor-recipient tissue cross matching, allocation and preparation of the recipient as well as access to surgical theatres. Nonetheless, CIT is more easily modified compared to other risk factors associated with IRI and a number of approaches have been adopted in order minimise CIT to which donated organs are exposed (see below). The median CIT for DBD donor kidney transplants has fallen from 16 hours in 2007 to 13 hours in 2018 and from 16 hours to 12.5 hours in DCD donor kidney transplants [2]. The median CIT in adult LD donor kidney transplants has marginally increased over the last 10 years, but is approximately 2-4 hours [2].

A number of conflicting studies have been published on the effect of CIT on graft and patient outcomes in recipients of grafts from different donor types. Much of this confusion may relate to whether CIT is analysed as a categorical (e.g. grafts are grouped together under fixed durations of CIT such 0-4 h, 5-8 h, 9-13 h etc) or continuous variable (where the actual CIT of each graft is considered individually e.g. 13.5 h, 9.2 h, 15.6 h etc). A US

study of 9,082 deceased donor kidney pairs from 2000 to 2009 showed that kidneys with longer CITs (analysed categorically) were at significantly higher risk of DGF but had limited bearing on long-term graft outcome [74]. Similarly, a Collaborative Transplant Study of 91,674 transplants from 1990 to 2005, reported that increasing CIT up to 18 h (analysed categorically) was not detrimental for graft outcome but the risk of graft failure did increase at longer increments of cold ischaemia [75]. Meanwhile a retrospective Dutch registry study of 6,322 deceased kidney transplants performed between 1990 and 2007, reported CIT was an independent risk factor for DGF and primary non-function (PNF, see below) in both DBD and DCD kidneys and shorter CITs (analysed categorically) were associated with better graft survival [76].

In contrast to the above studies, a UK registry study of 9,134 deceased donor kidney transplants between 2000 and 2007 showed that a CIT of greater than 24 h relative to a CIT of less than 12 h in DCD kidneys was associated with poorer graft function at measured by eGFR at 3 months post-transplantation [65]. In a second UK registry study of 6,490 deceased kidney transplants from 2005 to 2010, which included a greater number of DCD kidney transplants and therefore more reflective of current donor demographics, authors showed that the duration of cold ischaemia had no effect on the survival of DBD kidneys but was associated with an increased risk of graft failure in DCD kidneys, suggesting DCD kidneys are more susceptible to cold ischaemia. Meanwhile, in a US study of 14,230 kidney pairs, CIT was shown to a be a significant risk factor for the development of DGF in ECD kidneys but had no effect on graft or patient survival [77]. However, an analysis of French registry data of 6,891 kidney transplants from 2004 to 2011 showed that ECD allograft survival significantly improved with cold ischaemia times of 12 h or less [78].

In contrast to several US and UK registry studies, a French prospective cohort study of 3,839 DBD kidney transplants performed from 2000 to 2011 reported a significant proportional increase in the risk of both graft failure and patient death for each additional hour of cold ischaemia experienced by DBD kidneys when CIT was analysed as a continuous variable [79]. The authors argued that theirs was the first study to determine the proportional increase in the risk graft failure related to CIT in which CIT thresholds were not used. Debout et al [79] argue that use of CIT thresholds, such as those used by Kayler et al [77], Summers et al [65] and Opelz et al [75] may inadvertently reduce the power of their analysis and may explain their conflicting findings.

Lastly, a recent UK registry analysis of 9,156 LD kidney transplants from 2001 to 2014, reported that whilst a prolonged CIT of 4-8 h compared to 0-2 h led to a marginal but significant increase in DGF (8.6% vs 4.3%) and decrease in 1-year graft survival (96.2%

vs 97.1%), rates of DGF and graft failure were still much lower in LD than in cadaveric transplants [80]

In summary, there is evidence to suggest that cold ischaemia time is an independent risk factor for DGF and graft survival in all donor types as well as PNF in deceased donor kidneys. DCD and ECD kidneys may be more sensitive to cold ischaemia compared to DBD and standard criteria organs.

Anastomosis Time

During transplantation, the kidney is most commonly placed in the extraperitoneal space of the right iliac fossa. Here, the external iliac vessels are more superficial than on the left allowing easier (end-to-side) anastomsis. The temperature of the kidney increases exponentially during anastomosis and a second period of warm ischaemia is experienced by all grafts types whilst the graft is held within the abdominal cavity [81]. The graft is usually reperfused before the ureterneocystostomy is performed to keep the warm ischaemic time to a minimum. Some centres may wrap the kidney graft in ice gauze during anastomosis to slow the rise in graft temperature and minimise warm ischemia further, however this practice is often under the discretion of the surgeon.

A single centre study of 669 DBD kidney transplants from 2004 to 2012 in the Netherlands showed that anastomosis time independently increased the risk of DGF and impaired allograft function for up to three years post-transplant. In a sub-group of recipients, analysis of protocol biopsies showed prolonged anastomosis was also independently associated with an increased risk of interstitial fibrosis and tubular atrophy [82]. A similar association between anastomosis time and DGF was reported in a single centre retrospective study of 298 deceased kidney transplants performed between 2006 and 2012 in Canada [83]. A follow-up Eurotransplant study of 13,964 deceased donor transplants from 2004 to 2013 reported that the risk of graft failure at 5 years post-transplant increased more with every 10 minute increase in anastomosis time than with every 1 h increase in CIT in recipients of all deceased donor kidneys. However the effect of anastomosis time on graft loss was more pronounced in recipients of DCD kidneys than in recipients of DBD kidneys [84]. This was ascribed to the additive effect of anastomosis time to total donor warm ischaemia time which was greater in DCD than in DBD kidneys due to prolonged warm ischaemia experienced during organ retrieval. An increased risk of graft failure and death following prolonged anastomosis time has also been reported in other single centre studies and a large US registry analysis [85] [86].

A small number of studies on the effect of surface cooling during anastomosis have been published. A single centre randomised study of 46 consecutive kidney transplants in

which a specialised polyethylene bag containing slushed ice was used to maintain a low surface temperature during kidney anastomosis reported use of the bag led to an increase in graft function at 14 days post-transplant and a reduced cumulative incidence of DGF and acute rejection compared to grafts that were anastomosed following standard procedures [87]. Similar findings have also been reported in historic studies although larger randomised control trials are needed to validate these preliminary findings [88].

Recipient Factors

The main recipient risk factors influencing IRI severity in kidney transplantation include male gender, a body mass index greater than 30, African-American ethnicity, history of diabetes, anti-human leukocyte antigen (HLA) immunisation and requirement for dialysis before transplantation [89] [90]. These factors are often unmodifiable and further as part of this thesis.

1.2.4 Clinical Consequences of IRI in Kidney Transplantation

The clinical consequences of IRI on kidney transplant outcome include primary non-function, delayed graft function, acute and chronic rejection and graft dysfunction and will be discussed in detail here.

Primary Non-Function

Primary non-function (PNF) is rare and only occurred in 4% DCD and 3% DBD transplants in a UK registry analysis [8]. Primary non-function is a catastrophic outcome in transplantation resulting in significant medical and surgical complications, possible HLA sensitisation as well as the physical and emotional strain of returning to dialysis and/or retransplantation. However, a recent UK study of 801 deceased kidney transplants, reported that whilst early graft loss (EGL) including loss due to PNF, was associated with 12.28 times greater risk of death within the first year post-transplantation, long-term mortality was worse for patients remaining on the waiting list [91].

Delayed Graft Function

Delayed graft function (DGF) is commonly defined as the requirement of at least one session of dialysis in the first week following kidney transplantation. Alternative definitions of DGF including changes in serum creatinine have been previously trialled however the more easily calculated clinical definition is considered best based on its simplicity [92]. A French single

centre study of 263 deceased donor transplants performed between 1988 and 1997 reported the underlying cause of DGF to be acute tubular necrosis (ATN) in 92.1% of cases and acute rejection in 7.9% cases [93]. These findings have been corroborated by other single centre reports and ATN resulting from IRI is thought to be the main cause of DGF in kidney transplant recipients [94] [89]. A recent single centre retrospective UK study of 225 DCD kidney transplants performed between 2011 and 2016 reported the median duration of DGF was 6 days with an interquartile range of 2-11.75 days. Whilst patients with DGF may return to dialysis until ATN resolves, this is undesirable leading to increased patient morbidity, prolonged hospitalisation and increased healthcare costs [89].

Meanwhile, the exact relationship between DGF and long-term graft outcomes is still unclear. A meta-analysis performed in 2008 suggested DGF led to an increased risk of graft loss, increased serum creatinine and increased risk of acute rejection but did not affect patient survival [95]. A more recent retrospective single-centre study of 2,161 kidney transplants between 1999 and 2013 showed that patients with documented post-transplant DGF had between 3- and 5-year shorter graft half-lives when compared to recipients that did not experience DGF [96]. However, another retrospective study of 1,784 deceased donor transplants between 1983 and 2014 found that DGF only lead to a reduction in patient survival when it occurred alongside acute rejection [97]. UK registry analysis has suggested DGF was strongly predictive of inferior transplant outcomes in recipients of DBD kidneys but not DCD kidneys [65]. This may relate to problems surrounding the definition of DGF and lack of specificity with respect to the underlying injury. Meanwhile, other studies have reported a relationship between DGF duration, acute graft rejection and graft survival [98] [99] [100] [101].

Acute and Chronic Rejection

Ischaemia reperfusion injury has been shown to activate both the innate and adaptive immune system following kidney transplantation and is thought to contribute to acute and chronic graft rejection [6] [102] [103].

A number of recent experimental studies have re-emphasised the role of IRI in allograft rejection. In particular, IRI results in DAMP release promoting sterile inflammation but may also increase the activation of dendritic cells, the T-cell allograft response and production of graft specific antibodies [26] [104] [105] [106]. Ameliorating the effects of IRI during kidney transplantation may therefore dampen the immune response to the allograft and reduce rates of graft rejection.

Graft Dysfunction and Failure

Despite vast advances in immunosuppression over the last 50 years, mid- to long-term graft survival has changed little [107]. In a UK registry analysis, death-censored (i.e. controlling for patients with functioning graft who died from other causes) 10-year graft survival was 74.9% for DCD kidneys and 74.3% for DBD kidneys [9]. As previously stated there is no significant difference in long-term graft survival between DBD and DCD kidneys [8]. Living donor kidneys offer the best long-term outcomes with a 10-year graft survival of approximately 90% whilst ECD kidneys offer the poorest outcomes and are estimated to survive for only 5.1 years on average [108] [109].

Approximately 840 patients return to dialysis as a result of graft failure in the UK every year [110]. Return to dialysis is associated with increased morbidity and mortality, primarily due to cardiovascular complications and infection [111]. It is currently unclear whether dialysis should be given to transplant patients pre-emptively and the management of patients with failing grafts falls below the standards set for non-transplant chronic kidney disease (CKD) patients [112]. Furthermore, there are significant medical and surgical risks associated with the withdrawal of immunosuppression and removal of the failed graft [111]. Strategies to improve graft survival are therefore desirable in order to reduce patient morbidity and mortality and re-transplantation demand.

It is now thought that IRI during transplantation may be a major factor contributing to long-term graft function and survival [107]. This theory is supported by a greater understanding of the consequences of IRI in acute kidney injury (AKI) in which a single episode of AKI greatly increases the risk of developing CKD [113]. Recently, a number of experimental studies have greatly advanced our understanding of the mechanisms driving AKI to CKD transition. In particular, maladaptive repair and G2/M cell cycle arrest of proliferating tubule epithelial cells is thought to lead to the release of profibrotic mediators, pericyte to myofibroblast differentiation and tissue fibrosis [114]. The epigenetic changes that occur following ischaemia reperfusion are also of increasing interest in fibrosis development [115] [116]. The mechanisms contributing to kidney fibrosis following acute kidney injury are likely to also contribute to graft dysfunction in renal transplantation [6] [117]. Therefore therapeutic strategies aimed at ameliorating IRI in kidney transplantation may help reduce graft fibrosis and increase long-term graft function and survival.

1.2.5 Current Strategies to Reduce IRI in Kidney Transplantation

Strategies to reduce IRI during kidney transplantation have mainly focused on minimising CIT through improvements in organ allocation schemes as well as the use of novel technologies

such as machine perfusion [118] [119] [120]. Other approaches including pharmacological therapies aimed at reducing ROS production, immune activation and vascular dysfunction as well as the use of ischaemic pre and post-conditioning, cellular therapies, therapeutic gases and miRNAs to ameliorate the effects of IRI have been reviewed in detail elsewhere [121] [27]. Many of these therapeutic approaches are either in the early stages of development or have not shown significant benefit in human trials and as such are beyond the scope of this thesis. Meanwhile, other strategies are being developed to increase the use of otherwise discarded or declined kidneys including pre-implantation biopsies and quality assessment during normothermic machine perfusion [122] [123].

Virtual Cross Matching

During the organ allocation process, it is important to match an organ to a recipient that is not sensitised to the HLA of the donor graft [124]. The presence of alloantibodies directed against donor HLA in the recipient can lead to hyperacute rejection, resulting in increased morbidity and mortality. HLA-specific antibody screening is routinely performed on all patients on the kidney transplant waiting list and is used to identify unacceptable donor HLA mismatches [125]. To aid in efficient organ allocation, virtual crossmatching between the donor-recipient HLA and recipient antibody profile is performed in order to predict the most suitable recipient for a donated organ. However, a confirmatory crossmatch test is then performed in the recipient hospital prior to transplantation which may significantly increase the CIT to which an organ is exposed. A prospective study of 606 deceased donor kidney transplants from 1998 to 2008, showed that the pretransplant crossmatch test may be safely omitted in patients where it is predicted to be negative based on sensitisation history and HLA-specific antibody screening [119]. This led to a significant reduction in the CIT and rates of DGF in DBD kidney grafts in which cross matching was omitted whilst long-term graft survival and acute rejection rates were unaffected [119].

Organ Allocation Schemes

To promote equal access to transplantation and ensure organs are allocated to those most in need, a national allocation scheme was adopted in the UK in 2006 and further revised in 2015 and 2019 [126]. In this scheme, kidneys from deceased donors are allocated to recipients based on factors including recipient waiting time, sensitisation, human leukocyte antigen match and donor-recipient age difference [118]. Whilst this scheme promotes transplant equality, the additional transportation times between the donor and recipient hospitals can increase the CIT to which organs are exposed leading to an increase in IRI. Transport

distances in the UK are relatively small and do not usually affect transplant decisions, but become more significant in larger allocation schemes such as in the US and continental Europe.

Of note, transport distances and CITs become more significant in the UK where organs are declined by the initial recipient hospital and must be reallocated to a new recipient. Kidneys from DCD and ECD donors are at high risk of being discarded if declined by the initial recipient hospital due to concerns regarding their sensitivity to prolonged cold ischaemia times and the time taken to find a suitable recipient for so called 'hard to place' kidneys. In a bid to decrease the discard rate of otherwise transplantable DCD and ECD kidneys, a fast-track scheme has recently been implemented in the UK to allocate 'hard to place' kidneys more efficiently, thereby minimising CITs and maximising organ use [120].

Hypothermic Machine Perfusion

Hypothermic machine perfusion (HMP) describes the continuous or pulsatile recirculation of cold preservation solution through an organ at low pressure [127]. A European randomised controlled trial of 336 consecutive deceased donor transplants showed HMP significantly reduced the risk of delayed graft function and increased 1- and 3-year allograft survival [128] [129]. However, a UK multicentre randomised controlled trial of HMP in DCD kidneys showed no difference in the incidence of DGF between grafts assigned to HMP versus cold static storage and no significant difference in kidney function at 3- or 12-months post-transplantation was reported [130]. Meanwhile, a multivariate regression analysis of 90 randomised ECD kidney pairs in the initial European trial showed HMP significantly reduced the risk DGF and PNF as well as an increasing one year graft survival in ECD grafts [131].

In contrast to UK findings, a recent systematic review of sixteen studies comparing HMP to static cold storage in both Europe and the US has concluded HMP does significantly reduce the risk of delayed graft function in both DCD and DBD kidneys compared to cold static storage [132]. Nonetheless, the general consensus in the UK is that HMP offers little advantage in controlled DCD donation with mean CITs of around 14 h with cold static storage being cheaper and simpler, HMP may be used but at the discretion of the transplanting surgeon [130] [9]. Many questions remain to be answered in the use of HMP including whether perfusion should be continuous or applied for a short period prior to transplantation, whether HMP can prolong the CIT tolerated by deceased donor grafts in addition to further confirmation of the effect of HMP on long term graft outcome [133]. In addition, there is increasing interest in the use of hypothermic oxygenated machine perfusion (HOPE) in kidney preservation following a recent trial demonstrating the superiority of HOPE over HMP in the liver [134] [135].

Normothermic Machine Perfusion

Normothermic machine perfusion involves the perfusion of an organ ex situ with a warm, oxygenated red-cell based perfusate in order to restore metabolism and organ function. Not only does normothermic perfusion help to minimise cold ischaemia time but may also lead to reconditioning and repair of ischaemic injury [136]. A phase I study comparing the effect of normothermic machine perfusion on 18 ECD kidneys compared to 47 ECD kidneys that underwent cold static storage has shown normothermic perfusion led to a significant decrease in DGF on transplantation as well as demonstrating the safety and feasibility of the technique [137]. More recently, a multicentre randomised control trial of 220 liver transplants showed normothermic preservation led a significant reduction in graft injury as measured by hepatocellular enzyme release on transplantation compared to static cold storage and is one of the first randomised control trials to demonstrate the ability of normothermic perfusion to improve graft preservation [138]. Meanwhile, a multicentre randomised controlled trial to determine the effect of normothermic perfusion on DGF in DCD kidneys compared to conventional cold storage is currently underway with results expected in 2020 [139].

In addition to its effects on organ preservation, normothermic machine perfusion may also be used to assess the quality of an organ that would otherwise be declined for transplantation. A scoring system has been developed by Hosgood et al and has led to the successful transplantation of a number previously declined DCD kidneys; however greater use of declined DCD kidneys following assessment by normothermic machine perfusion is currently limited by their extended cold ischaemic time resulting from the organ offering process as discussed above [140] [122].

Normothermic Regional Perfusion

In addition to *ex situ* perfusion, organs from DCD donors may be reperfused with warmed oxygenated blood *in situ* following the confirmation of circulatory death using normothermic regional perfusion (NRP) [141]. This technique was first developed to facilitate the use of organs from uncontrolled DCD (Maastricht Category II) donors in Spain (see Table 1.1) [142]. The technique has subsequently been adapted to assess the viability of organs from controlled DCD (Maastricht Category III) donors in the UK to facilitate the greater use of organs from this donor type [143]. In addition, technique may have a conditioning effect leading to improved graft and recipient outcomes. Randomised control trials comparing NRP to other preservation methods are lacking in the UK where heparinisation prior to confirmation of death is prohibited (see Section 1.5.1) [144]. However, studies in other countries where pre-heparinisation or use of uncontrolled DCD (Maastricht Category II)

donors is more common have reported reduced rates of DGF and improved graft survival in kidneys exposed to NRP compared to conventional static cold storage [145].

1.2.6 Summary

Ischaemia reperfusion injury is inherent to current transplant practices leading to cellular injury, inflammation and reduced organ function in transplanted grafts. A number of risk factors may influence the severity of IRI on transplantation including donor type, donor age, warm and cold ischaemia times and recipient related factors. Both short and long-term graft outcomes may be affected by the severity of IRI on transplantation and a significant proportion of organs are currently declined for use due to concerns regarding IRI. Machine perfusion technologies and improvements to the organ allocation scheme have been used to reduce the cold ischaemic time experienced by donated organs in an attempt to minimise the severity of IRI on transplantation. Strikingly however, no pharmacological therapies currently exist to ameliorate the effects of IRI in organ transplantation or other IRI-related pathologies.

1.3 Mitochondrial ROS Production in Ischaemia Reperfusion Injury

1.3.1 Overview of Mitochondria

Mitochondria originated from an early endosymbiotic relationship between α-proteobacteria and primitive eukaryotic cells which subsequently resulted in the transfer of genetic material from mitochondria to the nucleus and loss of organelle autonomy [146]. The incorporation of mitochondria into eukaryotic cells is thought to have facilitated increased protein translation and greater genetic complexity without bioenergetic penalty [147]. Today, mitochondria are central to numerous cellular processes, most notably oxidative phosphorylation and ATP production, but also the synthesis of Fe-S clusters, nucleotides and amino acids, Fe^{2+}/Ca^{2+} handling, inflammation, apoptosis and numerous other cell death pathways [148]. In this section, I will first outline the structure and morphology of mitochondria before discussing oxidative phosphorylation and ATP production in detail. I will then briefly discuss the role of mitochondria within the cells of the kidney.

Mitochondrial Morphology and Dynamics

Mitochondria are composed of an outer and inner membrane, intermembrane space and matrix (see Figure 1.2) [149] [150]. The outer mitochondrial membrane (OMM) is similar in composition to the endoplasmic reticulum (ER) with an equal protein to phospholipid ratio [151]. Voltage dependent anion channels (VDAC) allow the passive movement of molecules of less than 6.8 kDa between the cytoplasm and intermembrane space (IMS) whilst larger molecules such as proteins are transported across the membrane by the translocase of the outer membrane (TOM) complex [152] [153]. Conversely, the inner mitochondrial membrane (IMM) is similar in composition to prokaryotic membranes with a greater protein to lipid ratio and presence of cardiolipin in place of cholesterol [151]. Movement across the IMM is more restricted than for the OMM with ions and small molecules requiring transport across the membrane via specific carriers whilst proteins are imported to the matrix by translocase of the inner mitochondrial membrane (TIM) complex [154] [155]. The IMS located between the outer and inner mitochondrial membranes contains the electron carrier cytochrome C (cyt C) as well as many other proteins involved in lipid synthesis, co-ordination of metal ions and protein transport [155] [156] [157]. The mitochondrial matrix enveloped by the IMM, forms a protein rich compartment and is the site of various anabolic and catabolic processes including the tricarboxylic acid (TCA) cycle, lipid and amino acid metabolism [149]. The mitochondrial matrix also contains hundreds of copies of mtDNA, a double-stranded circular DNA molecule encoding 22 tRNAs, 2 ribosomal RNAs and 13 polypeptide subunits belonging to various respiratory chain complexes [148]. The respiratory complexes I-IV are located on invaginations of the IMM that project into the mitochondrial matrix known as cristae, with dimers of F_OF_1-ATP synthase located at the cristae tips [158]. The increased surface area resulting from cristae formation, together with the proximity of the respiratory chain enzymes to F_OF_1-ATP synthase is thought to maximise the efficiency of ATP production.

Within the cell, mitochondria form highly dynamic reticular networks that continuously undergo fission and fusion enabling them to share proteins, DNA and other molecules [159]. Mitochondrial fission is mediated by the cytoplasmic protein Drp1, which oligomerises on the OMM to form a ring-like structure resulting in mitochondrial siscision whilst mitochondrial fusion is a two-part process mediated by the proteins Mfn1 and Mfn2 on the OMM and OPA1 on the IMM [160]. In addition, damaged mitochondria may be targeted for degradation via mitophagy through PINK1-PARKIN mediated ubquitination [161]. Mitochondrial biogenesis may replace degraded mitochondria and is tightly controlled by numerous nutrient sensing pathways to ensure the mitochondrial population can continue to meet the energy demands of the cell [162].

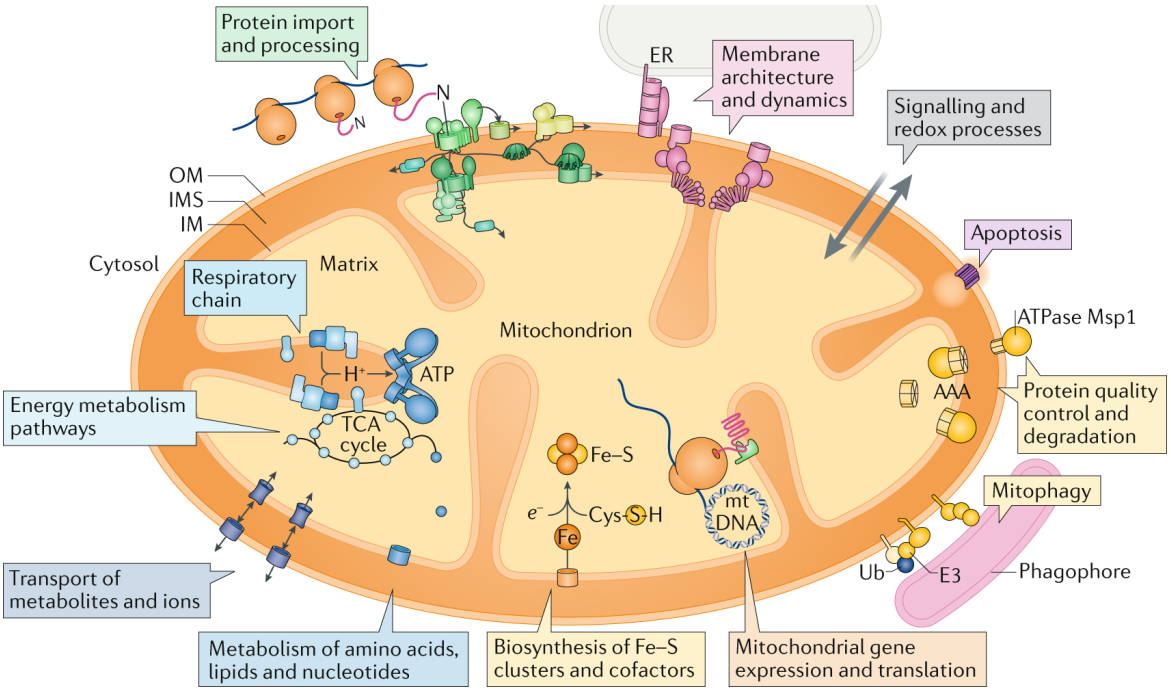

Figure 1.2 Mitochondrial Morphology and Function. Mitochondria consist of four compartments, the outer membrane (OM), intermembrane space (IMS), inner membrane (IM) and matrix. The various functions of mitochondria are depicted in the figure including energy metabolism, mitochondrial gene expression, Fe-S cluster synthesis, transport of metabolites and ions and control of apoptosis. Figure adapted from Pfanner et al (2019).

Oxidative Phosphorylation

Oxidative phosphorylation (OXPHOS) refers to the phosphorylation of ADP to ATP using the energy derived from the oxidation of different foodstuffs by the electron transport chain (ETC) [163]. Within mitochondria, the TCA cycle acts as the primary oxidative pathway for the generation of reducing equivalents nicotinamide adenine dinucleotide (NADH) and flavin adenine dinucleotide ($FADH_2$) from carbohydrates, lipids and amino acids. The pathway consists of eight enzymes as shown in Figure 1.3 [164]. Succinate dehydrogenase (SDH) forms Complex II of the ETC and contains oxidised flavin adenine dinucleotide (FAD) [165]. Oxidation of succinate to fumarate reduces FAD to $FADH_2$ within SDH which then reduces the electron carrier ubiquinone (CoQ) to ubiquinol ($CoQH_2$) . As the rate of succinate to fumarate conversion is controlled by the ubiquinol/ubiquinone ratio within the IMM, SDH activity may form part of a feedback mechanism between the TCA cycle and OXPHOS [163]. Meanwhile, NADH is oxidised to NAD^+ by the flavin mononuclear (FMN) site of Complex I which subsequently reduces CoQ to $CoQH_2$ at its quinone binding site (see Figure 1.4). Ubiquinol is then oxidised by Complex III which transfers electrons to the electron carrier cyt C which in turn is oxidised by Complex IV which transfers electrons to the terminal electron acceptor oxygen, forming water [166]. As electrons pass along the ETC, their reduction potential increases resulting in the release of free energy. This energy is utilised by complexes I, III and IV to pump protons across the IMM generating a proton motive force (Δp) comprising of the membrane potential and pH gradient [167] [163]. The Δp is then utilised by F_0F_1-ATP synthase to drive phorphorylation of ADP to ATP by allowing the protons to re-enter the mitochondrial matrix down the proton electrochemical potential gradient [163] [168].

Role of Mitochondria in the Kidney

The kidney has the second highest mitochondrial content of any organ after the heart [169]. The energy produced by mitochondria is mostly used by Na^+/K^+ ATPases to produce ionic gradients for the reabsorption of nutrients and ions from the glomerular filtrate [170]. Approximately 80% of the filtrate is reabsorbed by the epithelial cells of the proximal tubule which contain the most mitochondria and rely on β-oxidation of fatty acids as a fuel source for OXPHOS with little glycolytic capacity [169]. Conversely, glomerular cells including podocytes, endothelial and mesangial cells play a more passive role in kidney function and contain fewer mitochondria relying mainly on glycolysis [171]. As a result, the different cell types of the kidney may show different sensitivities to IRI and mitchondrial dysfunction depending on their reliance on OXPHOS [170].

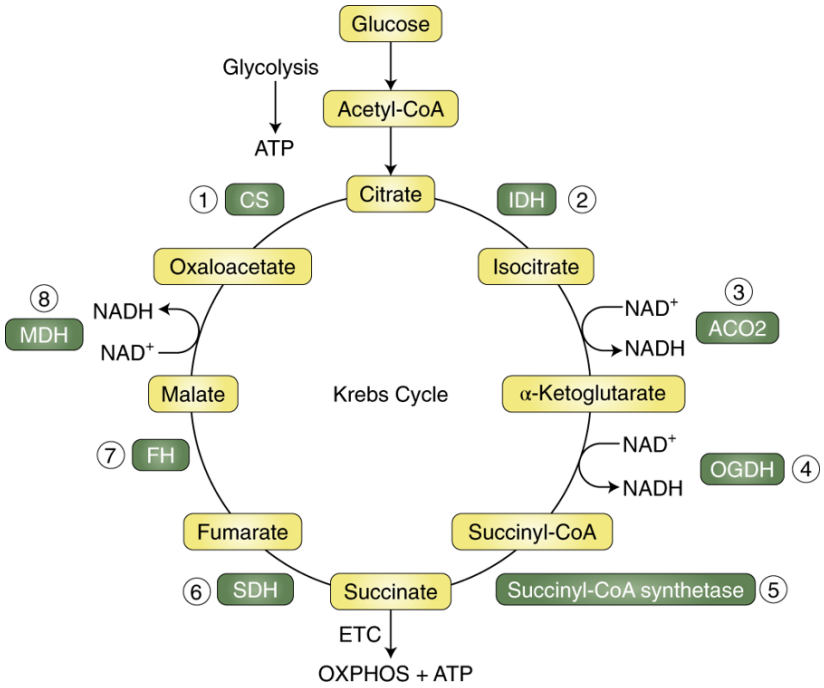

Figure 1.3 The Tricarboxylic Acid Cycle. The tricarboxylic acid cycle (TCA) is the primary oxidative pathway for the generation of reducing equivalents NADH and $FADH_2$ in aerobic organisms. The pathway is situated within the mitochondrial matrix and consists of eight enzymes; citrate synthase (1), isocitrate dehydrogenase (2), aconitase (3), α-ketoglutarate dehydrogenase (4), succinyl-CoA synthetase (5), succinate dehydrogenase (6), fumarate hydratase (7) and malate dehydrogenase (8). Succinate dehydrogenase (SDH) contains FAD and forms Complex II of the ETC. Figure adapted from Ryan et al (2019).

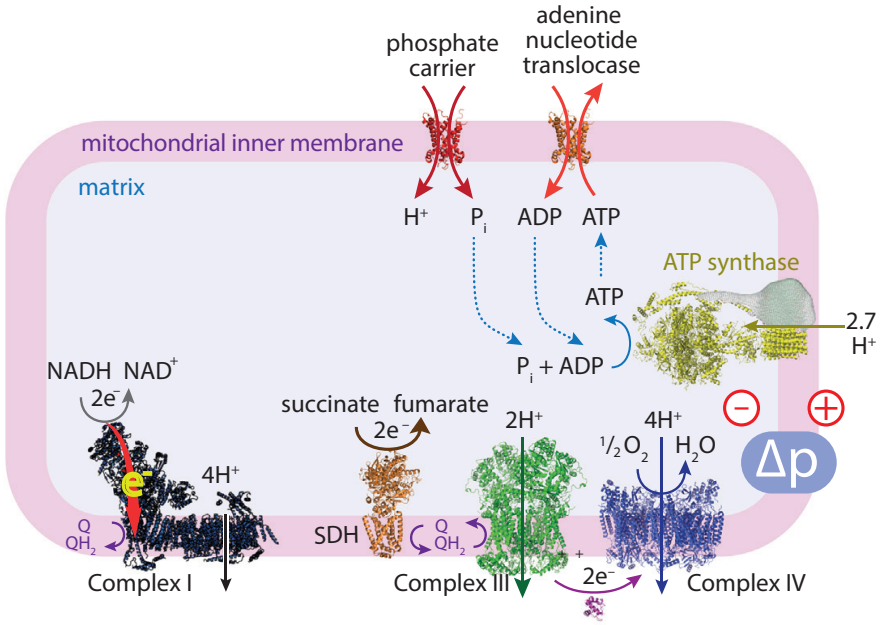

Figure 1.4 The Electron Transport Chain and F_0F_1-ATP Synthase. Electrons enter the electron transport chain (ETC) at the FMN site of Complex I and via reduction of FAD at Complex II (which also forms SDH within the TCA cycle and oxidises succinate to fumarate, see Figure 1.3). The electron carrier ubiquinone (CoQ) transfers electrons from Complex I and II to Complex III. The electron carrier cytochrome C (cyt C) transfers electrons from Complex III to IV. Oxygen acts as the terminal electron acceptor in the ETC combining with hydrogen to form water. As electrons pass down the ETC their reduction potential increases resulting in the release of free energy. This energy is used to pump protons across the inner mitochondrial membrane generating a proton motive force (Δp). The Δ is then utilised by F_OF_1-ATP synthase for the phosphorylation of ADP to ATP. Figure adapted from Chouchani et al (2016).

Despite receiving approximately 20% of cardiac output at rest, the oxygenation of renal cortex and medulla is relatively low. The renal cortical P_{O2} is approximately 4-9.5 kPa and the renal medulla P_{O2} is approximately 2 kPa despite an arterial P_{O2} of 12.5 kPa at the renal hila [172]. The low cortical P_{O2} is thought to result from an arteriovenous shunt between the interlobar artery and vein prior to reaching the cortex. The reason for this anatomical shunt may be to protect the kidney from over-oxygenation and oxidative stress whilst maintaining a sufficient rate of ultafiltration [173]. The P_{O2} decreases further in the renal medulla as it receives only 1% of the blood supply to the kidney via the vasa recta [170]; this is to allow a high solute concentration to build up within the medulla and facilitate the production of concentrated urine. As a result of low tissue oxygenation however, the mitochondria within the kidney operate close to conditions of hypoxia.

1.3.2 A Unifying Mechanism of Mitochondrial ROS Production

Reactive oxygen species production was previously thought to occur as a result of damage to mitochondrial components during IRI and the spill of electrons onto oxygen in a non-specific manner. However, an increasing body of evidence now points towards a specific mechanism of mitochondrial ROS production [14] [15]. In this section, I will first discuss the metabolic changes during ischaemia which prime mitochondria for superoxide production. I will then discuss the mechanisms leading to reverse electron transport (RET) and superoxide production at the FMN site of Complex I. Lastly, I will discuss other sources of ROS production following IRI and how these likely contribute to secondary tissue damage following the initial ROS burst from mitochondria [174].

Succinate Accumulation During Ischaemia

Comparative metabolomic analysis has shown that only three metabolites - succinate, xanthine and hypoxanthine - are universally increased across tissues during ischaemia [14]. Hypoxanthine and xanthine are known breakdown products of ATP whilst succinate is a key intermediate in the TCA cycle (see Figure 1.3). Succinate accumulation during ischaemia is thought to act as a store of electrons and source of reactive oxygen species on reperfusion. However, ATP degradation is also required before mitochondrial ROS production can occur (see below). Succinate accumulation alongside ATP degradation during ischaemia thus primes mitochondria for superoxide production on reperfusion [15].

Succinate accumulation is thought to occur due to reverse action of SDH with a contribution from glutaminolysis and canonical TCA cycle action [14] [175]. Development of a highly reduced CoQ pool within mitochondria during ischaemia is thought to drive SDH

reversal and reduction of fumarate to succinate. The fumarate required for reverse action of SDH is supplied by two pathways in ischaemic tissue; the purine nucleotide cycle (PNC) and malate aspartate shuttle (MAS) (see Figure 1.5). The PNC is activated by the accumulation of AMP during ischaemia which is metabolised to adenylosuccinate and then fumarate by adenylosuccinate lyase. To enter mitochondria, fumarate must be converted to malate and exchanged for mitochondrial succinate by the dicarboxylate carrier (DIC) . Meanwhile, the MAS is stimulated by a high NADH/NAD^+ ratio leading to the transamination of aspartate and production of malate which is also exchanged for mitochondrial succinate by the DIC. Within mitochondria, malate is then converted to fumarate by fumarate hydratase for subsequent reduction by SDH [14] [15].

Succinate cannot be further metabolised during ischaemia due to depletion of GTP and CoA required for conversion to succinyl-CoA. and therefore accumulates within the cytosol of the cell. Accumulated succinate acts as a large store of electrons, which if rapidly oxidised on reperfusion may drive RET and superoxide production from the FMN site Complex I [15]. However, RET will only occur on reperfusion where ATP has also been largely degraded. The period of ischaemia required for mitochondria to become primed for ROS production may vary amongst different tissue types depending on their rate of ATP degradation and succinate accumulation. In addition, succinate may also act as a signalling molecule during ishaemia and reperfusion stimulating various inflammatory and hypoxia signalling pathways [164].

Mitochondrial ROS Production on Reperfusion

Upon reperfusion, mitochondria are thought to produce a burst of reactive oxygen species that drive much of the subsequent damage resulting from IRI [18] [176]. Increasing evidence points to RET and superoxide production from the FMN site of Complex I as the major site of ROS production on reperfusion and will be discussed in detail here [15].

In vitro, complex I is known to produce superoxide under two conditions; either during forward electron transport at the FMN site following damage or inhibition to the mitochondrial respiratory chain (Mode 1) or at the FMN as a result of RET in the presence of a highly reduced CoQ pool and near maximal proton motive force (Δp) (Mode 2) [177]. Reverse electron transport is possible as Complex I operates close to thermodynamic equilibrium. During forward electron transport, the redox driving force (ΔE_h) that pushes two electrons from NADH to CoQ is greater than the energy required to pump four electrons across the inner mitochondrial membrane against the Δp. However, as the overall reaction is not displaced far from thermodynamic equilibrium, electrons may flow backward through Complex

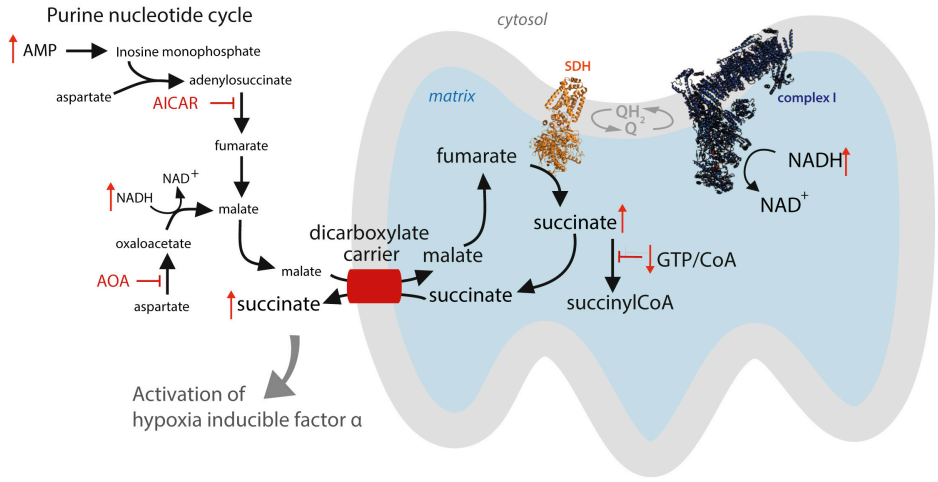

Figure 1.5 Succinate Accumulation During Ischaemia. During ischaemia, succinate is thought to accumulate due to the reverse action of succinate dehydrogenase. Fumarate required for reversal of SDH is thought to be supplied by the purine nucleotide cycle, stimulated by the accumulation of AMP during ischaemia, and the malate aspartate shuttle, stimulated by a high NADH/NAD^+ ratio. Succinate cannot be further metabolised under conditions of ischaemia and is exported from mitochondrial matrix via the dicarboxylate carrier (DIC). Figure adapted from Chouchani et al (2016).

I onto the FMN site and then oxygen if the Δp exceeds the ΔE_h resulting in mitochondrial superoxide production [15].

A near maximal Δp is required for RET *in vitro* and is achieved by limiting the supply of ADP to mitochondria and consumption of the Δp by ATP synthase. *In vivo*, the breakdown of adenine during ischaemia results in lack of substrate for ATP synthase on reperfusion, allowing a large Δp to develop. Meanwhile, succinate accumulation during ischaemia acts as a store of reducing equivalents capable of maintaining a highly reduced CoQ pool on reperfusion. The highly reduced CoQ pool is able to drive both proton pumping by complexes III and IV in order to establish a high Δp as well as RET through Complex I resulting in superoxide production [15]. Mitochondrial superoxide production from the FMN site complex I is therefore likely to be responsible for the initial burst of mitochondrial reactive oxygen species during IRI as the store of succinate is rapidly oxidised. Meanwhile, other sites of ROS production within the mitochondria, such as Complex III, are thought to only make a minor contribution to superoxide production on reperfusion.

Other Sources of Reactive Oxygen Species

Other sites outside mitochondria may also contribute to superoxide production following IRI including cytoplasmic xanthine oxidase (XO) and NADPH oxidases (NOX) [178] [179]. Importantly however, superoxide production from these sources is thought to occur after the

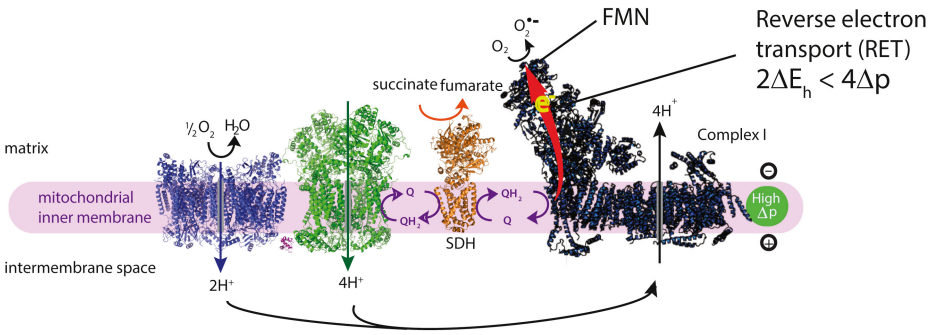

Figure 1.6 Mitochondrial ROS Production on Reperfusion. During reperfusion, return of the terminal electron acceptor oxygen leads to the reactivation of Complex III and IV, proton pumping and regeneration of the proton motive force (Δp). However, as ADP is mostly degraded during prolonged ischaemia, there is a lack of substrate for F_OF_1-ATP synthase allowing Δp to reach near maximal levels. Coupled with a highly reduced CoQ pool resulting from rapid succinate oxidation, a near maximal Δp enables electrons to pass backwards through Complex I via reverse electron transport and combine with oxygen at the flavin mononuclear (FMN) site of the complex forming a superoxide radical. Figure adapted from Chouchani et al (2016).

initial burst of superoxide from mitochondria and as a result contributes to secondary tissue damage [174].

1.3.3 Consequences of Mitochondrial ROS Production

Reactive oxygen species are radical and non-radical molecules formed from the partial reduction of oxygen, such as superoxide, hydrogen peroxide and the hydroxyl radical [180]. They are primarily produced by mitochondria but also originate from other sites within the cell as described above. Under physiological conditions, ROS are thought to play important signalling roles within the cell through the post-translational modification of cysteine residues [181]. Through this mechanism the mitochondria communicate their metabolic status to the remaining cell and nucleus. In addition, ROS production is central to the antimicrobial defence mechanism of neutrophils [182]. During IRI however, ROS production is over and above that which occurs under physiological conditions and overwhelms the antioxidant defences which prevent ROS from damaging cellular components [39]. In this section, I will discuss the fate of superoxide produced by mitochondria during early reperfusion, the antioxidant defences within mitochondria and how ROS cause oxidative damage leading to tissue injury.

Fate of Superoxide

Superoxide produced at Complex I during the initial reperfusion is very rapidly dismutated to hydrogen peroxide by manganese superoxide dismutase (MnSOD) , present at high concentrations within mitochondria [177]. Hydrogen peroxide is a two electron oxidant but reacts poorly with most biological molecules due to a high activation energy [183]. However, it may also undergo one electron oxidations in the presence of transition metals to form a hydroxyl radical or activated metal complexes, a process referred to as Fenton(-like) chemistry [184]. Hydroxyl radicals are extremely reactive with a low activation energy barrier and react non-specifically with most biological molecules at diffusional controlled rates [184].

Some superoxide may also escape dismutation by MnSOD and react with NO to produce peroxynitrite ($ONOO^-$) . Peroxynitrite is a strong oxidant and may react with thiols, iron-sulfur centres and zinc fingers. Alternatively, $ONOO^-$ may react with carbon dioxide to produce a highly reactive carbonate radical with a similar reactivity to the hydroxyl radical [185].

Antioxidant Defences

Cells have a number of defences to remove hydrogen peroxide and prevent the formation of hydroxyl radicals including both enzymatic and non-enzymatic antioxidants. Within mitochondria, the major enzymatic antioxidants include the thiol peroxidases, peroxiredoxin and glutathione peroxidase (see Figure 5.2) [184] [186]. Hydrogen peroxide typically reacts slowly with thiols to produce sulfenic acid followed by reaction with another thiol to produce a disulphide bond. This reaction is greatly accelerated by peroxiredoxin and glutathione peroxidase which polarise the -O-O bond of hydrogen peroxide facilitating electrophilic attack of the thiolate anion. Glutathione peroxidase contains a selenocyteine active site and catalyses the reaction of hydrogen peroxide with reduced glutathione (GSH) to produce oxidised glutathione (GSSG) , water and oxygen. GSSG may then be converted back to GSH by glutathione reductase (GR) which uses nicotinamide adenine dinucleotide phosphate (NADPH) as an electron donor. Similarly, peroxiredoxins react with hydrogen peroxide and form interchain disulphide bonds. Oxidised peroxiredoxins may then be converted back to their reduced form by reaction with NADPH catalysed by thioredoxin reductases [186]. In addition to their roles in antioxidant defence, redox modifications of thiol proteins by hydrogen peroxide and other reactive species are thought to act as an important means of communication between mitochondria and the rest of the cell under normoxic conditions [183] [187].

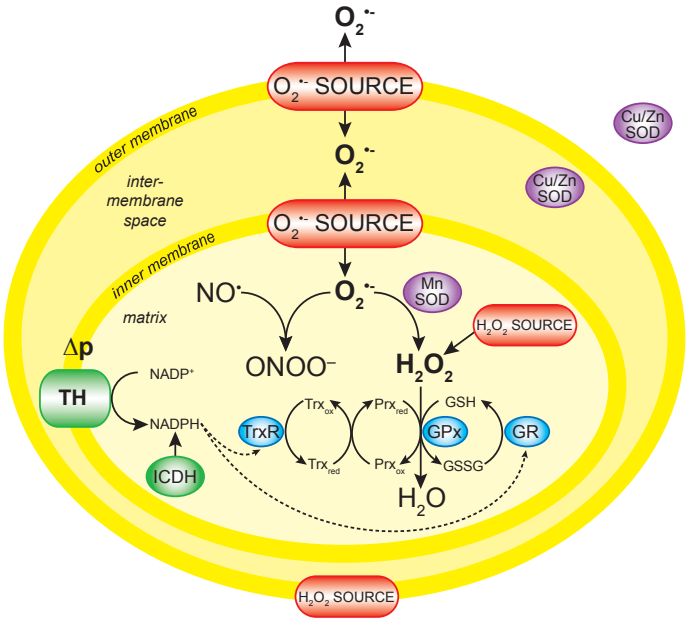

Figure 1.7 Antioxidant Defences within Mitochondria. Mitochondria possess a number of antioxidant defences including peroxiredoxin (Prx) and glutathione peroxidase (GPx) which catalyse the conversion of hydrogen peroxide to water in order to prevent the formation of hydroxyl radicals. Following reaction with hydrogen peroxide, oxidised thiol peroxidases are converted back to their reduced form by reaction with NADPH. Figure adapted from Murphy et al (2009).

Oxidative Stress and Damage following IRI

During IRI, the antioxidant defences within the mitochondria may become overwhelmed leading to oxidative stress and damage [186] [185]. Mitochondrial DNA is particularly susceptible to oxidative stress due to a lack protective histones and poor DNA repair mechanisms [188]. Meanwhile, the inner mitochondria membrane contains a relatively large number of polyunsaturated fatty acids and is thus prone to lipid peroxidation [189]. Not only does lipid peroxidation lead to changes in membrane permeability but may also release lipid peroxidation products (LPPs) such as 4-hydroxynonenal (4-HNE) and malondialdehyde (MDA) . LPPs are highly reactive and go on to cause further damage to proteins and DNA via covalent modification [190] [185]. Proteins, including components of the mitochondrial respiratory chain, may also react with ROS produced during IRI and indirectly with oxidation products leading to protein carbonyl formation, protein-protein cross linkages and protein fragmentation [191] [192]. As mitochondria are the major source of superoxide following IRI, these organelles often bear the brunt of oxidative damage leading to mitochondrial dysfunction, further ROS production, mitochondrial permeability transition, cell death and inflammation.

1.3.4 Strategies to Target Mitochondrial ROS Production

Elucidation of the mechanism underlying mitochondrial ROS production during early reperfusion has led to identification of a number of novel therapeutic targets within mitochondria. These may be targeted at different stages during IRI to inhibit either succinate accumulation or ROS production (see Figure 1.8). As mitochondrial ROS production is thought to initiate much of the downstream damage arising from IRI, targeting mitochondrial ROS production poses as an attractive therapeutic nexus. In this section, I will discuss how mitochondrial ROS production may be targeted at different stages during IRI drawing on examples from early *in vivo* experimental studies.

Targeting Succinate Accumulation

Succinate accumulation during ischaemia acts as a large store of electrons capable of driving mitochondria ROS production on reperfusion. Inhibition of succinate accumulation during ischaemia may therefore prevent mitochondrial ROS production by abolishing the store of electrons required to drive RET. During ischaemia, succinate accumulation is thought to primarily occur through the reverse action of succinate dehydrogenase. Inhibition of succinate dehydrogenase during ischaemia may therefore reduce succinate accumulation. Administration of the competitive inhibitor of SDH, malonate, as the membrane-permeable

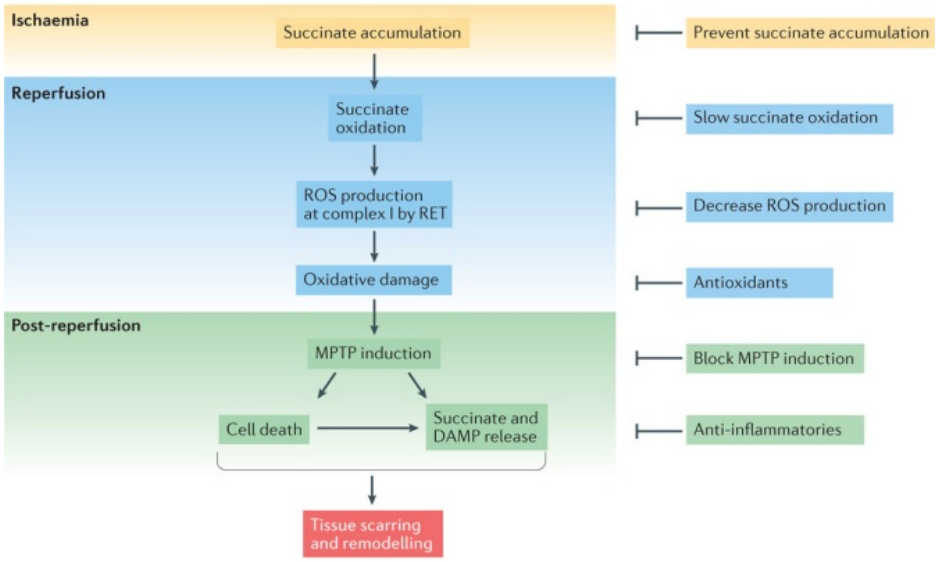

Figure 1.8 Therapeutic Targets within Mitochondria during IRI. Mitochondria may be targeted at various stages during IRI. Therapeutic strategies include inhibition of succinate accumulation during ischaemia, prevention of succinate oxidation on reperfusion, inhibition ROS production by Complex I, scavenging of ROS with antioxidants as well as inhibition of the downstream effects of ROS production including mPTP induction and inflammation. Figure adapted from Murphy et al (2018).

precursor, dimethyl malonate (DMM) , significantly reduced the level of succinate accumulation in the ischaemic mouse heart and led to a reduction in mitochondrial superoxide production and infarct size on reperfusion [14]. Similar findings were also demonstrated a mouse model of heart transplantation [193].

Targeting Succinate Oxidation

Rapid oxidation of succinate by SDH on reperfusion of ischaemic tissue is to thought result in a highly reduced CoQ pool required for RET and superoxide production at Complex I [15] [177]. Inhibition of succinate oxidation by SDH on reperfusion may therefore inhibit ROS production by preventing RET. Disodium malonate (DSM) has also been shown to inhibit succinate oxidation and reduce infarct size when given at the onset of reperfusion following a period of global ischaemia in the isolated mouse heart, most likely through inhibition of ROS production [194]. Similarly, DSM administered at the onset of reperfusion reduced infarct size in a translational model of myocardial infarction in the pig [195].

Targeting RET at Complex I

Reverse electron transport and superoxide production at the FMN site of Complex I is thought to be the major source of reactive oxygen species during the initial reperfusion. Many inhibitors of Complex I have been shown to protect against IRI by inhibiting RET including rotenone [196] and amobarbitol [176]. Complex I is also known to undergo a conformational change known as the active/deactive transition during ischaemia with a half life of 10-12 minutes [197] [15]. Transition to the deactive state prevents RET through Complex I and reveals a critical cysteine residue, Cys39, on the ND3 subunit. Reversible modification of the exposed Cys39 residue by thiol-reactive agents, such as MitoSNO, may temporarily lock Complex I in the deactive state and thereby prevent RET and ROS production [15]. MitoSNO has been shown to inhibit ROS production and reduce infarct size following left anterior descending (LAD) coronary artery occlusion in the mouse [198].

Mitochondria-Targeted Antioxidants

As the initial burst of reactive oxygen species are thought to originate from mitochondria following ischaemia-reperfusion, mitochondria-targeted antioxidants, such as MitoQ, may aid in reducing oxidative damage and subsequent injury by scavenging reactive species before they damage mitochondrial and cellular components. MitoQ consists of a ubiquinone moiety linked to a triphenylphosphonium (TPP) cation by a 10-carbon alkyl chain. The positive charge of the TPP cation is distributed over a large surface area allowing the molecule to pass easily through membranes and accumulate several hundred fold in the negatively charged matrix of mitochondria [199]. Within mitochondria, the ubiquinone moiety of MitoQ is reduced to ubiquinol and may subsequently act as an effective antioxidant against lipid peroxidation becoming oxidised to ubiquinone and preventing propagation of lipid radicals. Oxidised ubiquinone may be reduced back to ubiquinol by Complex II restoring its antioxidant activity [200]. MitoQ has been shown to be protective in a mouse model of cardiac and renal IRI as well as a mouse model of cardiac transplantation [201] [202] [203].

1.3.5 Summary

Mitochondria are highly dynamic organelles central to oxidative phosphorylation and many other cellular processes. During IRI, mitochondrial ROS production is thought to initiate many of the downstream processes leading to cellular damage and injury. Whilst mitochondrial ROS production was previously thought to occur via a relatively non-specific mechanism, increasing evidence points towards reverse electron transport and superoxide

production from the FMN site of Complex I as a major source of ROS production. Reverse electron transport is thought to be driven by the rapid oxidation of succinate which accumulates across tissues during ischaemia. A number of novel therapeutic targets have subsequently been identified within mitochondria with early experimental studies targeting this mechanism showing promising results.

1.4 Development of Malonate Compounds for Use in Ischaemia Reperfusion Injury

In this thesis, I primarily focus on whether malonate compounds may be used to reduce mitochondrial ROS production and IRI in kidney transplantation. Malonate may be used to inhibit succinate accumulation during ischaemia or succinate oxidation on reperfusion by competitive inhibition of SDH as discussed above. In this section, I discuss the rationale behind the use of malonate over other SDH inhibitors during IRI and different mechanisms used to target malonate to mitochondria *in vivo*.

1.4.1 Choice of Malonate as an SDH Inhibitor

Succinate dehydrogenase may be inhibited at either the succinate or CoQ binding site [165]. Succinate binding site inhibitors competitively inhibit SDH activity and include the dicarboxylates malonate and oxaloacetate [204] [205] [206]. Ubiquinone site inhibitors are similar in structure to ubiquinone however are not readily reversible and have been reported to induce apoptosis [207]. Competitive succinate binding site inhibitors are therefore better suited to the transient inhibition of SDH during ischaemia reperfusion avoiding toxic long term effects.

Whilst oxaloacetate is a more potent inhibitor of SDH than malonate, it is unstable in aqueous environments, undergoing spontaneous decarboxylation to pyruvate and carbon dioxide with a half-life of 10 min; this has precluded the use of oxaloacetate with most efforts in our lab focusing development of novel malonate compounds. Malonate has an IC_{50} of a few μM and is metabolised relatively quickly following its administration, making it ideally suited to transient inhibition of SDH during IRI [208] [209] [210]. However, malonate is posses a double negative charge at physiological pH ($pK_a \sim 2.85$) preventing it from passing directly through lipid membranes. Assuming malonate does not have a carrier, in order to cross cell membranes and inhibit SDH within mitochondria *in vivo*, malonate must be chemically modified to increase its membrane permeability either by the synthesis

of malonate ester pro-drugs or conjugation of malonate to mitochondrial targeting molecules such as TPP.

1.4.2 Development of Malonate Ester Pro-Drugs

Pro-drugs are molecules with little or no pharmacologial activity that are converted to the active parent drug *in vivo* by enzymatic or chemical reactions or by a combination of the two [211]. Short-chain hydrocarbon pro-moieties are commonly used to mask charged groups such as the carboxylic acids on malonate forming a lipophilic alkyl ester with increased membrane permeability [211]. Alkyl ester pro-drugs can then be converted to their active parent compound by ubiquitously expressed carboxylesterases within their target tissue. Up to five potential carboxylesterase genes have been identified in humans however, only two isoforms, CES1 and CES1 have been extensively studied [212]. CES1 favours the hydrolysis of small alcohol or large acyl groups whilst CES2 favours the opposite.

Caboxylesterases are differentially expressed in the body with particularly high concentrations reported in the liver, kidney and intestine (likely related to their role in xenobiotic detoxification) [213]. The differential expression and substrate specificity of carboxylesterase isoforms may have numerous consequences for pro-drug delivery, requiring malonate ester pro-drugs to be 'tuned' for delivery to a particular tissue type [214] [211]. Furthermore, carboxylesterases are not specific to mitochondria and are located within numerous other subcellular compartments [215]. Malonate ester pro-drugs may therefore undergo hydrolysis at numerous intracellular locations but to inhibit SDH must be subsequently transported into mitochondria.

Two of the most promising malonate ester pro-drugs currently under investigation are DMM and diacetoxymethyl malonate (MAM) . DMM is hydrolysed at a much slower rate than MAM by non-specific esterase, such as pig liver esterase (PLE) , when assessed *in vitro* (personal communication, Hiran A Prag). The rate of hydrolysis of malonate ester pro-drugs may have important consequences for the stage of ischaemia reperfusion the different compounds should be given. Furthermore, an increased tissue malonate concentration was achieved in liver, kidney, heart and brain following intravenous administration of MAM compared to DMM via tail vein injection in mice (personal communication, Hiran A Prag). As such, it may be that a lower concentration of MAM compared to DMM is required to achieve the same therapeutic concentration of malonate in a tissue during IRI. Again, this may have important consequences for the use of malonate ester pro-drugs *in vivo*, as lower concentrations of the pro-drug will likely lead to fewer off-target and adverse effects.

1.4.3 Development of Mitochondria Targeted Malonate Compounds

An alternative to malonate ester prodrugs is the conjugation of malonate to mitochondria targeting moieties such as the lipophilic cation, TPP. Lipophilic cations such as TPP exploit the large charge difference across the inner mitochondrial membrane to drive several hundred fold accumulation within mitochondria whilst distribution of the positive charge across the molecule and large hydrophobic surface area provided by the three lipophilic phenyl groups, greatly reduces the activation energy required for the molecule to pass through plasma and mitochondrial membranes [216].

Charged molecules such as malonate may be conjugated to TPP via an ester linkage and released within the matrix by carboxylesterases in a similar manner to malonate ester prodrugs [217]. Directly targeting malonate to mitochondria may help to reduce ester hydrolysis occurring at other cellular locations and increase the malonate concentration achieved within the mitochondrial matrix. This may permit the use of lower doses of malonate whilst achieving the same therapeutic effect as in non-targeted methods. TPP molecules are also rapidly taken up by cells and mitochondria on administration which may be of particular benefit in targeting succinate oxidation during early reperfusion. However, the uptake of TPP-linked molecules has been shown to vary in different organs depending on the bioactive cargo and mitochondrial membrane potential within the tissue [218]. The properties of TPP-linked malonate compounds may therefore need to be 'tuned' for therapeutic use in different organs. Nonetheless, TPP molecules have shown a good safety profile in Phase II trials with excretion of the TPP moiety occuring via redistribution into the extracellular fluid, extracellular metabolism and biliary excretion [219] [220].

TPP-linked malonate esters are currently being developed by the Hartley Lab (WestChem, University of Glasgow, UW) and Murphy Lab (MRC Mitochondrial Biology Unit, University of Cambridge, UK). One promising compound under development is TPP_{11}-malonate which has shown rapid uptake and hydrolysis in tissues when administered to mice *in vivo* (personal communication, Hiran A Prag). Furthermore, TPP_{11}-malonate led to a reduction in infarct size when administered at reperfusion in a mouse model of myocardial infarction (unpublished data, Mr Hiran A Prag).

1.4.4 Use of Disodium Malonate

Disodium malonate is the sodium salt of malonate. It has previously been shown to reduce IRI when administered on reperfusion in the mouse and pig [194] [195]. However, it is currently unclear how DSM efficiently crosses cell membranes under conditions of normoxia in order to reach mitochondria (personal communication, Mr Hiran A Prag). It may be that

IRI leads to changes in membrane permeability, facilitating cell entry of DSM on reperfusion; however, this hypothesis requires further investigation.

1.4.5 Summary

Malonate is ideally suited to the transient inhibition of SDH during IRI. However, it is a charged molecule and must be administered in a chemically-altered form in order to pass through cellular membranes and enter mitochondria *in vivo*. Two strategies currently used to increase the membrane permeability of malonate include the synthesis of malonate ester pro-drugs or conjugation of malonate to lipophilic cations. However, these modifications may affect the rate of accumulation and activation of malonate within cells and mitochondria and the optimal time during IRI when each compound should be given is currently under investigation.

1.5 Use of Novel Therapeutics in Kidney Transplantation

In the translation of mitochondrial therapies from experimental studies to clinical practice, it is important to consider at what stages during the transplant process novel therapies might be given. Legal, technical and logistical barriers may restrict the number of opportunities to administer different compounds with significant consequences for their ability to inhibit mitochondrial ROS production and ameliorate IRI. Early consideration of the current (and possibly future) opportunities to administer mitochondrial therapies during organ transplantation, as well as an in depth understanding of the pathological mechanisms occurring during ischaemia and reperfusion may therefore help to select the most promising targets, compounds and treatment strategies, leading to quicker, more efficient translation of novel therapies to clinical practice.

1.5.1 Use in Organ Donors

Administration of mitochondrial therapies such as malonate compounds prior to the onset of ischaemia may help to prevent the pathological changes that occur within cells during warm and cold ischaemia and reduce the severity of IRI on subsequent organ transplantation. Administration of DMM prior to onset of warm ischaemia in the mouse model of cardiac transplantation has shown to reduce succinate accumulation and protect against IRI on reperfusion [193]. Mitochondrial therapies may theoretically be administered to organ donors prior to the onset of ischaemia, although a number of technical and legal barriers first must be overcome (see below). Translational models will be important in demonstrating

the protective effect of mitochondrial compounds administered prior to ischaemia in organ transplantation whilst a continuing organ deficit may prompt legal barriers preventing the treatment of potential organ donors prior to declaration of death to be revisited in order to increase organ supply and quality.

Administration to DBD Donors

Therapeutic interventions aimed at optimising organ quality for donation are currently administered to DBD donors following the confirmation of brainstem death. These include the correction of hypovolaemia with fluids and vasopressors, correction of diabetes insipidus with antidiuretic hormone, inhibition of inflammatory responses with methylprednisolone and hormone replacement therapy to counteract endocrine and metabolic changes following brainstem death [221]. It is therefore foreseeable that if mitochondrial compounds were fully approved for clinical use, they could be administered to DBD donors prior to organ retrieval in order to prevent succinate accumulation and reduce IRI during transplantation as has been demonstrated in a mouse model of heart transplantation [193].

Administration to DCD Donors

In the UK, it is currently illegal to administer a therapy to a patient that is not for the primary benefit of that patient, including during organ donation. Therefore, therapies aimed at improving the quality of organs for subsequent transplantation can only be given after the death of an organ donor has been confirmed. As previously discussed, organs retrieved following donation after circulatory death are exposed to a significant period of warm ischaemia prior to *in situ* flush and organ cooling. Mitochondrial therapies aimed at reducing the pathological changes that occur during warm ischaemia, such as the accumulation of succinate, could therefore not be administered at the optimal time during DCD donation under current UK law [222].

However, in the US, pre-mortem heparin is commonly given prior to the withdrawal of life support in DCD donation to reduce clot formation in the organs subsequently retrieved for transplantation. Whilst pre-mortem heparin is not given for the primary benefit of the patient, it is not thought to accelerate patient death or cause harm to a potential organ donor but may help to facilitate the patient's wishes to donate their organs where consent has been obtained; these arguments have been used to justify the use of pre-mortem heparin during DCD donation [223]. Mitochondrial therapies would need to meet similar criteria if their use is to be permitted in potential organ donors prior to declaration of patient death in the US and other countries. In addition, substantial evidence would be needed to demonstrate treatment

of organs prior to patient death in DCD donors would lead to a significant improvement in organ quality and function [222] [224]. This is where translational models such as the pig and ex vivo normothermic perfusion of declined human kidneys may be extremely important in providing preliminary data to inform ethics committees. Whilst treatment of DCD donors prior to patient death remains illegal in the UK, the ageing population and increasing demand-supply mismatch in organ donation may lead to changes in the law in future years.

Administration to Living Donors

In living organ donation, a similar dilemma exists in whether therapies aimed at improving organ quality should be administered to the donor as such therapies are not of direct benefit to them. However, the altruistic nature of living donation and the fact the donor has already consented to a considerable level of harm may mean what is in their best interest is to provide the highest quality organ possible. A clear ethical and legal framework for the administration of novel mitochondrial therapies to living donors is currently lacking. Whilst kidneys from living donors experience short ischaemic times and typically show very low rates of delayed graft function they still experience a degree of IRI and mitochondrial therapies may be of benefit in increasing the long term function and survival. Again, translational studies will be extremely important in determining the effect of mitochondrial therapies on grafts from living donors and will be important in shaping future attitudes to the treatment of potential grafts within living patients.

1.5.2 Use in Organ Preservation

As a number of legal and technical barriers must be overcome in order to administer mitochondrial therapies to organ donors an alternative approach may be to administer mitochondrial therapies immediately following organ retrieval during either back-table flush and cold static storage or ex vivo normothermic perfusion.

Administration during Back-Table Flush and Cold-Static Storage

Administration of mitochondrial therapies to grafts during back table flush would occur after warm ischaemia in DCD donors but close to the onset of ischaemia in DBD and living donation. Metabolic processes are greatly inhibited during cold ischaemia but continue to occur at a slow rate. Malonate compounds may therefore inhibit succinate accumulation that occurs during cold ischaemia as well as rapid succinate oxidation on subsequent reperfusion. Already a number of compounds such as the xanthine oxidase inhibitor allopurinol are added

to University of Wisconsin solution to inhibit oxidative damage and improve organ quality on reperfusion meaning there are no legal hurdles to overcome in the administration of mitochondrial therapies to organs during cold preservation [35]. Furthermore, if primarily aimed at reducing mitochondrial ROS production at reperfusion, mitochondrial therapies may be administered to organs at the point of organ flush regardless of donor type and pre-exposure to warm ischaemia. Lastly, current organ donation practices would not need to change if mitochondrial targeted therapies could be given during in situ or back-table flush and would greatly ease the introduction of their use. Development of mitochondrial therapies that could be given during cold preservation and reduce IRI on subsequent transplantation are therefore highly attractive.

Administration during Normothermic Perfusion

In addition to the assessment and reconditioning of marginal organs, the use of *ex vivo* normothermic perfusion as a drug delivery platform during organ preservation is increasingly being explored [225] [136] [226]. Ex vivo normothermic perfusion allows direct delivery of compounds to the metabolically active organ and may help to overcome difficulties in systemic drug delivery and adverse, off-target effects. Furthermore, ex vivo normothermic perfusion may permit the use of lower drug concentrations and otherwise toxic compounds. Different malonate compounds could be added to the perfusate before, during or at the end of ex vivo normothermic perfusion depending on the desired effect. Translational models such as ex vivo normothermic perfusion of pig and declined human kidneys could be easily used to simulate human kidney perfusion and determine the appropriate doses and administration times of malonate compounds to inform future clinical trials.

1.5.3 Use in Organ Recipients

Organ transplant recipients already receive a number of therapeutic compounds before and after organ transplantation in order to improve transplant outcomes, most notably immunosuppressives such as the IL-2 receptor antagonist basiliximab, calcineurin inhibitors, steroids and antiproliferatives [227]. No legal barriers therefore need to be overcome in the administration of mitochondrial compounds to transplant recipients to reduce IRI and improve organ quality *per se* however ethical approval would still be required for trials of new therapies in transplant recipients. Mitochondrial therapies would need to be administered at reperfusion and accumulate rapidly within the mitochondria of the transplanted graft in order to effectively reduce ROS production. However, targeting of mitochondrial compounds to the graft may be difficult and high concentrations of the compound may be required, increasing the risk

of off-target or toxic effects. Again translational models will be important in exploring the administration of mitochondrial therapies to the recipient during organ transplantation.

1.5.4 Summary

There are multiple opportunities to administer mitochondrial therapies to donor grafts during the transplant process however, depending on the donor type and stage of IRI targeted, a number of logistical and legal barriers may need to be overcome. Translational models of kidney transplantation will play an important role in informing ethical committees and early clinical trials as the optimal mitochondrial therapy and stage of administration in different donor types. Ideally, mitochondrial therapies could be administered at the same stage in all donor types and incorporation into current retrieval and transplant protocols would greatly ease their clinical implementation.

1.6 Translational Models of Kidney Transplantation

In order to investigate the contribution of mitochondrial ROS production to IRI in human kidney transplantation and the potential for novel mitochondrial therapies to improve transplant outcomes, translational models of kidney transplantation are needed to bridge the gap between basic experimental models of IRI and clinical transplant practices. Use of translational models of kidney transplantation are can help identify the most promising therapeutic compounds for use in clinical practice as well as informing early clinical trials as to the likely route, dose and timing of their administration. In this section, I discuss how translational models in the mouse, pig and human may be used to investigate the effect of novel mitochondrial therapies during IRI in kidney transplantation.

1.6.1 Mouse Models

A model of kidney transplantation has previously been developed for the study of allograft rejection in the mouse [228] [229] [230]. Whilst this model is ideally suited to the investigation of the alloimmune responses in kidney transplantation, it is less well suited to the investigation of transplant IRI. The procedure itself is technically demanding requiring a high level of training whilst any variations in the time taken to retrieve the donor kidney and perform the recipient anastomosis make the severity and reproducibility of IRI difficult to control [231]. In addition, the length of the procedure results in a high level of injury and it is usually necessary for one native kidney to be retained in the recipient mouse in order to avoid death related to delayed graft function [232] [233]. However, the presence

of the native kidney may fully compensate for reduced function in the transplanted kidney preventing measures such as serum creatinine from being used to assess graft function [234]. This model is therefore not well suited to investigate the effect of mitochondrial therapies on IRI experienced during kidney transplantation.

An alternative to the kidney transplant model is a model of renal IRI in which the blood supply to one or both kidneys is occluded by a micro-serrefine clamp placed over the renal hila and then removed at the time of reperfusion [235] [236]. This model has the advantage of being less technically challenging than the kidney transplant model and the duration of ischaemia is more easily controlled. This results in a more reproducible level of injury between experiments as long as other factors such as core temperature, hydration status and anaesthesia time are also tightly controlled [236] [237]. The level of injury experienced by the kidneys on reperfusion may also be adjusted by altering the warm ischaemia time to which they are exposed and fatal renal insufficiency as experienced in the kidney transplant model can be avoided [238]. Furthermore, a recent comparison of the transcriptional changes that occur during early reperfusion in human kidney transplants to the changes that occur in mouse kidneys following ischaemia reperfusion, showed a highly significant degree of concordance between the two, suggesting similar injury processes occur in mouse IRI to human kidney transplantation [239] [240]. The mouse model of kidney IRI is therefore ideally suited to investigate the effects of mitochondrial therapies on the kidney injury and function in the mouse and may be used to inform subsequent studies that more closely resemble transplant practices.

1.6.2 Large Animal Models

Whilst mouse models of disease offer cost effective and relatively easy opportunities for the investigation of novel drug compounds, many of the therapies trialled in rodents do not show the same efficacy in humans [241]. This is often related to differences in rodent anatomy, physiology and metabolism in comparison to humans as well as a disparity between experimental models of disease and clinical practices [241]. Larger animal models may resemble human anatomy, physiology and metabolism more closely and therefore aid in more efficient translation of novel therapies to clinical trials [242]. Furthermore, ineffective compounds may be identified at an earlier stage of drug development with the use of larger animal models enabling resources to be focused on the most promising therapies.

Pig, dog and non-human primates have all been used in translational models of kidney transplantation, the most popular of which being the pig [243]. The multilobular, multipapillary architecture of the pig kidney has a high degree of similarity to the human compared to the unilobular, unipapillary kidney in rodents and dogs [244] [245]. The body size and

vasculature of the mini-pig (60-70 kg) also closely resembles the human allowing surgical procedures to be more accurately simulated [246]. Similarities in body size and metabolism also allow for easier estimation of therapeutic doses in humans from pig studies whilst pigs have the added advantages of being easily bred and harbouring little public resentment for use in scientific research [245] [243]. However, larger animal models can be expensive and consequent studies often consist of low animal numbers. Furthermore, pigs rapidly exceed the size and weight of humans, making handling more difficult and most experiments are done on very young, healthy adults [245] [243].

To partly overcome the high costs involved in large animal studies, *ex vivo* normothermic perfusion (EVNP) may be used as an experimental model of kidney transplantation to investigate IRI during early reperfusion [247]. In such studies, organ retrieval from the animal and preservation of the organ during transportation closely resemble the clinical scenario; however instead of transplanting the organ into a living recipient, organs are reperfused *ex vivo* on a modified cardiopulmonary bypass machine using a warm, oxygenated, whole blood perfusate [248]. Not only does this model dramatically reduce the cost of large animal studies but also allows close monitoring of numerous functional parameters during early reperfusion including renal blood flow, urine output, creatinine secretion and fractional excretion of sodium that would not be possible following transplantation in living recipient. Furthermore, multiple blood, urine and tissue samples may be taken at different stages during reperfusion which would also not be possible in a full transplant model, maximising the amount of information gained from each experiment. Currently however, organs may only be reperfused for several hours using EVNP due to gradual haemolysis of the whole blood perfusate within the reperfusion circuit and the technique is not suitable for the long term study of organ function [136]. Other limitations include the possible recirculation effects of the perfusate and the reperfusion of the organs in isolation [249]. Nonetheless, EVNP is ideally suited to investigate the translation of mitochondrial therapies to kidney transplantation and their effect on early IRI, the results from which could later be used to inform full transplant experiments in larger animals as well as early human trials.

1.6.3 Use of Declined Human Kidneys

In addition to its use in large animal models, EVNP has also been used to assess the function of declined human kidneys following organ retrieval and cold static storage [250] [122]. Favourable assessment of kidney function during EVNP has led to the successful transplantation of previously declined human kidneys in a number of cases [251] [140] [137]. In other instances, EVNP of declined human kidneys may be used as an experimental model of kidney transplantation in order to investigate kidney pathology or the safety and efficacy of

novel therapies in human tissue [252] [253]. Again, multiple tissue, blood and urine samples can be taken from the kidney during EVNP which would not be possible as part of a human trial. *Ex vivo* normothermic perfusion of declined human kidneys could therefore be used to investigate the use of novel mitochondrial compounds in kidney transplantation and help inform Phase II clinical trials

1.6.4 Summary

Translational models of kidney transplantation may be used to investigate the safety and efficacy of novel mitochondrial therapies under conditions that more closely resemble clinical practice. *Ex vivo* normothermic perfusion of pig and human kidneys may be used as a cheaper alternative to full transplant studies with the added benefit of allowing close monitoring of kidney function and increased sampling of tissues across a range of time points. Ultimately, it is hoped that experiments in translational models of kidney transplantation will inform early clinical trials of mitochondrial therapies in kidney transplant patients.

1.7 Thesis Hypotheses

My overall hypothesis for this thesis is that malonate ester pro-drugs may be used to reduce IRI in kidney transplantation.

1.8 Thesis Aims

In this thesis, I aim to investigate whether malonate ester pro-drugs can be used to ameliorate IRI in kidney transplantation using the experimental approach shown in Figure 1.9. In particular, I plan to address four main aims;

1. To determine how succinate accumulation and mitochondrial ROS production are determined by conditions under which kidneys are retrieved during organ donation
2. To determine whether malonate ester pro-drugs can be used to inhibit mitochondrial ROS production during IRI in kidney transplantation
3. To determine at what stage in the transplant process different malonate ester pro-drugs may be effectively given
4. To determine whether inhibition of mitochondrial ROS production leads to improved initial graft function in kidney transplantation

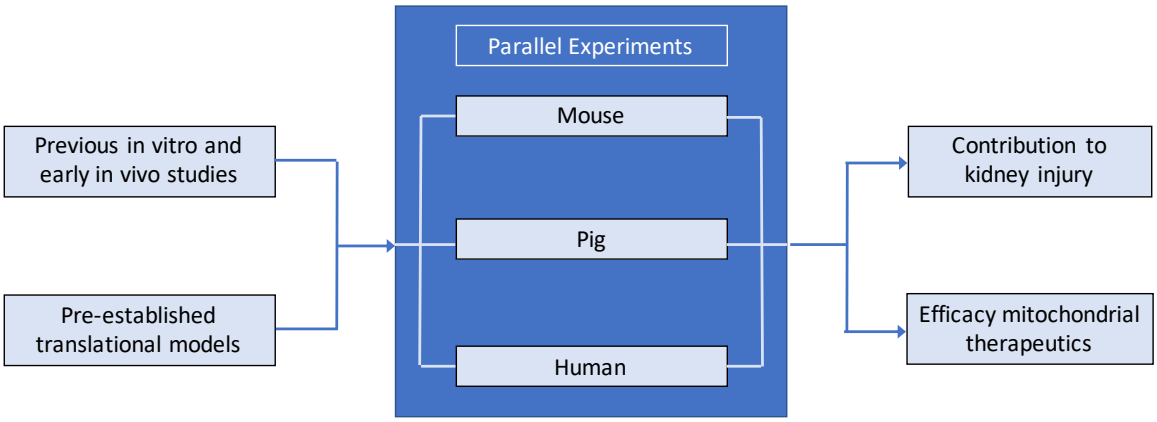

Figure 1.9 Experimental Approach to Investigate the Effect of Malonate Ester Pro-Drugs on IRI in Kidney Transplantation. Previous *in vitro* ad early *in vivo* studies alongside pre-established translational models of kidney transplantation were used to inform experiments in the mouse, pig and human. A mouse model of bilateral renal IRI, pig model of kidney transplantation using EVNP and EVNP of declined human kidneys were used. Experiments in the mouse, pig and human were conducted in parallel to aid in the rapid translation of malonate ester-prodrugs from early *in vitro* studies to Phase I clinical trials.

In the following chapters, I first investigate the metabolic changes that occur in the kidney under the different conditions of organ donation and whether malonate ester pro-drugs may be used to inhibit succinate accumulation. I then go on to the characterise the level of mitochondrial ROS production in the different models of kidney transplantation and investigate whether malonate ester pro-drugs given at various stages in the transplant process may be used to inhibit ROS production on reperfusion. Lastly, I investigate the effect of malonate ester pro-drugs on kidney function during early reperfusion in each of the different models of kidney transplantation. So each Chapter may be read in isolation, I have intentionally re-introduced some aspects of this introduction at the beginning of Chapter's 3, 4 and 5.

Chapter 2

Materials and Methods

2.1 Chemicals Reagents and Stocks

All reagents were obtained from Merch (formerly Sigma-Aldrich), UK unless otherwise stated. Diacetoxymethyl malonate was synthesised by Ms Laura Pala in the lab of Professor Richard C. Harley (WestCHEM School of Chemistry, University of Glasgow, UK).

2.2 Surgical Procedures

All procedures were approved by the UK Home Office under the Animals (Scientific Procedures) Act 1986.

2.2.1 Murine Model of Renal Ischaemia Reperfusion Injury

Animal Husbandary

Female C57BL/6 mice (Charles River Laboratories, UK) were maintained in specific pathogen free facilities with ad libitum food and water. All procedures were conducted under Project Licence number P7720A3D6.

Anaesthesia and Pre-Operative Care

Pre-operative care was performed by a surgical technician in an adjacent room to the surgical theatre. Mice were placed in an induction chamber and anaesthesia was induced using 3-5 % isoflurane (Abbott Laboratories, USA) and 2.0 L/min oxygen. Following induction, anaesthesia was maintained with 1.5-2 % isoflurane and 2.0 L/min oxygen delivered via a nose cone. The abdomen of the mouse shaved using electrical clippers and wiped clean with

chlorhexidine (Molnlycke, Sweden). For non-terminal procedures, a subcutaneous injection buprenorphine (0.1 mg/kg) was given for pain relief following surgery.

Surgical Procedure

Anaesthetised mice were placed on a heat mat attached to a homeothermic monitoring system (Havard Apparatus, UK). The core temperature of the animal was measured with a rectal temperature probe and maintained at 36.0 $\pm$ 0.5 °C throughout the procedure. A midline laparotomy was performed and the renal hila were dissected. To induce ischaemia, a micro-serrofine clamp (15 mm, Fine Science Tools, Germany) was placed over the renal hilum of each kindey to occlude the renal artery and vein. During ischaemia, the midline laparotomy was closed using 5-0 absorbable suture (Safil®, Braun, Germany) to maintain core body temperature and minimise evaporational losses. Successful occlusion of the renal vessels could be confirmed by development of a purplish colour to each kidney. For reperfusion experiments, micro-serrefine clamps were removed from the renal hila following ischaemia and return to normal colour was noted.

Infusions

In all experiments, compounds were administered as an infusion in a total volume of 160 µL saline. A syringe driver was used to deliver compounds at a rate of 16 µL/min through an infusion line (Portex Polyethylene Tubing, Smiths Medical International, UK) inserted directly into the inferior vena cava (IVC) with a 30 G needle. In experiments aimed at inhibiting succinate accumulation, saline or DMM (0.8, 1.6, 3.2, 6.4 and 12.8 mg) were administered as an infusion beginning 10 mins prior to the onset of ischaemia. In experiments aimed at inhibiting succinate oxidation on reperfusion, saline, DMM (3.2 mg), 1 % dimethyl sulfoxide (DMSO) or MAM (0.32 mg) in 1 % DMSO were administered as a 10 minute infusion beginning 5 mins prior to the onset of reperfusion.

Administration of MitoB

MitoB (20 nmol) in 50 µL saline (5 % DMSO) was given as an intravenous injection directly into the IVC 30 mins prior to the onset of ischaemia where stated.

Animal Recovery

In non-terminal procedures, the abdominal wall was closed in two layers with 5-0 absorbable suture (Safil, Braun, Germany) and mice were re-hydrated with 500 µL saline injected

subcutaneously. Mice were then recovered in an incubator set at 28 °C on soft, dry bedding with access to food and water.

Sample Collection & Storage

Tissue, whole blood and urine were collected from mice under terminal anaesthesia. Approximately 500 µL whole blood was collected directly from the IVC using a 1 mL syrine and 27 G needle. Whole blood was transferred to 250 µL capillary action collection tubes and allowed to clot. Tubes were then cetrifuged at 3000 g for 10 mins to separate the clot from the serum. The serum was then collected and stored at -70 °C until further processing and analysis. Kidneys for biochemical analysis were rapidly excised from the mouse and frozen in liquid nitrogen (LN2) using Wollenburg clamps. Frozen tissue was then stored at -70 °C until further processing. Kidneys for histological analysis were excised from the mouse and divided along the renal hilum using a scapel. One half was placed in 10 % neutral buffered formalin and the other in optimal cutting temperature compound which was then cooled on dry ice and stored -70°C until further processing. Urine was collected directly from the urethra of the mouse in a 250 µL capillary action collection tube by compressing the bladder with a cotton bud. Urine was then centrifuged at 3000 g for 10 mins and the supernatent was stored at -70 °C until further processing.

2.2.2 Retrieval of Pig Kidneys

Animal Husbandary

Large male and female Landrace pigs weighing 40-70 kg were supplied by Envigo, Huntington, UK. All procedures were conducted under Envigo Protocol Number WRS0001.

Anaesthesia and Pre-Operative Care

Pigs were medicated with intramuscular ketamine (10 mg/kg), medetomidine (0.02 mg/kg) and midazolam (0.1 mg/kg). A peripheral intravenous catheter was placed in the marginal ear vein and anaesthesia was induced with propofol to effect. Pigs were intubated and 100 % oxygen supplied with intermittent positive pressure ventilation was used to maintain normocapnia. Anaesthesia was maintained with continuous infusions of propofol (starting at 10 mg/kg/hr and titrating down to effect) and either remifentanil (starting at 2.4 µg/kg/h and titrating up to effect) or alfentanil (starting at 30 µg/kg/h and titrating up to effect). If required, isoflurane was provided at approximately 2 % to maintain anaesthesia. Saline was administered intravenously at approximately 10 mL/kg/hr. During anaesthesia a Datex

Ohmeda Cardiocap patient monitoring system was used to monitor ECG waveform, pulse oximetry, temperature and capnography parameters.

Surgical Procedure

A midline laparotomy was performed and the bowel mobilised to expose the renal hila. The hila were dissected and the renal arteries and veins slung using a 3-0 vicryl tie (Ethicon, Johnson & Johnson, UK) on both sides. The ureters were identified and each kidney was freed from the underlying connective tissue. Heparin (500 IU/kg, CP Pharmaceuticals, UK) was then given via the marginal ear vein and allowed to circulate for approximately 5 mins.

Immediately before the retrieval of each kidney a wedge tissue biopsy was taken and clamp frozen in LN2 using Wollenburg clamps. Each renal artery and vein was then tied and the renal vessels and ureter were divided. Kidneys undergoing warm ischaemia were left in the abdomen at 38 °C for 30 mins before being removed and flushed with cold preservation solution. Kidneys undergoing cold ischaemia only were immediately removed from the abdomen of the pig to be flushed with cold preservation solution on the back-table.

Following retrieval of both kidneys, approximately 1 L of blood was collected from the distal aorta in two 500 mL citrate-phosphate-dextrose-adenine (CDPA) blood bags (Fresenius Kabi, Germany). The pig was then euthanised by an overdose of pentobarbitone at approximately 200 mg/kg.

Back-Table Flush and Cold Preservation

On removal from the abdomen, the renal artery was cannulated with a 10 F catheter and kidneys were immediately flushed with approximately 500 mL ice-cold Soltran preservation solution (0.86% (w/v) potassium citrate, 0.82 % (w/v) sodium citrate, 3.38 % (w/v) mannitol and 1.0 % (w/v) magnesium sulphate; Baxter Healthcare, US) whilst submerged in slushed ice. Following back-table flush, kidneys were sealed in bags containing ice-cold Soltran solution and packed in organ storage boxes on ice for 6 h to mimic the conditions of static cold storage.

Measurement of Tissue Temperature

Where indicated, the surface and core temperature of the kidney was measured during back-table flush using a K type thermocouple (Hanna Instruments, UK) and data logger (EasyLog EL-USB-TC-LCD, Lascar Electronics, UK). Thermocouples were inserted into the kidney prior to the commencement of back-table flush and the temperature recorded to the nearest 0.5 °C every second.

2.2.3 Acceptance of Declined Human Kidneys for Research

Human kidneys declined for organ transplantation were accepted for research as per NHS Blood and Transplant and Addenbrooke's Hospital guidelines. Full ethical approval for the use of human kidneys for the investigation of ischaemia reperfusion injury had been awarded in advance (NREC 15/NE/0408).

2.3 *Ex Vivo* Normothemic Perfusion of Pig and Human Kidneys

2.3.1 Circuit Preparation

Circuit Components

The EVNP circuit consists of several disposable and non-disposable components. Non-disposable components include a Bioconsole including centrifugal pump & pressure transducer (Bio-console 560, Medtronic, Watford, UK), flow probe (BioProbe TX 50P, Medtronic, Watford, UK), heated circulating bath (Grants Instruments, Cambridge, UK), temperature probe (Oakton Instruments, Vernon Hills, IL, USA), glass kidney chamber, two Gemini PC-2 infusion pumps (Imed, San Diego, CA, USA) and a catheter bag. Disposable perfusion sets (Medtronic, Watford, UK) include a biohead pump, venous reservoir, polyvinyl chloride (PVC) tubing and a membrane oxygenator/heat exchanger.

The perfusion circuit is assembled such that perfusate flows from the venous reservoir to the centrifugal paediatric pump and then onto the membrane oxygenator and heat exchanger, as shown in Figure 2.1. The perfusate then passes through the flow probe before entering the glass kidney chamber. The venous outflow of the kidney is collected by the glass chamber and then returned to the venous reservoir to circulate again.

Circuit Perfusate

The circuit perfusate consisted of 300 mL whole blood, 300 mL Ringer's solution (Baxter Healthcare, US), 2.5 g mannitol, 0.06 g creatinine, 10 mL 8.4 % sodium bicarbonate and 500 IU heparin (CP Pharmaceuticals, UK). The perfusate was added to the reperfusion circuit 30 mins prior to the start of reperfusion. Once at a temperature of 37.0 ± 1.0 °C, the pH of the perfusate was tested using a blood gas analyser. If the pH of the perfusate was too low, additional sodium bicarbonate (8.4 %) could be added to adjust the pH prior to reperfusion of the kidney.

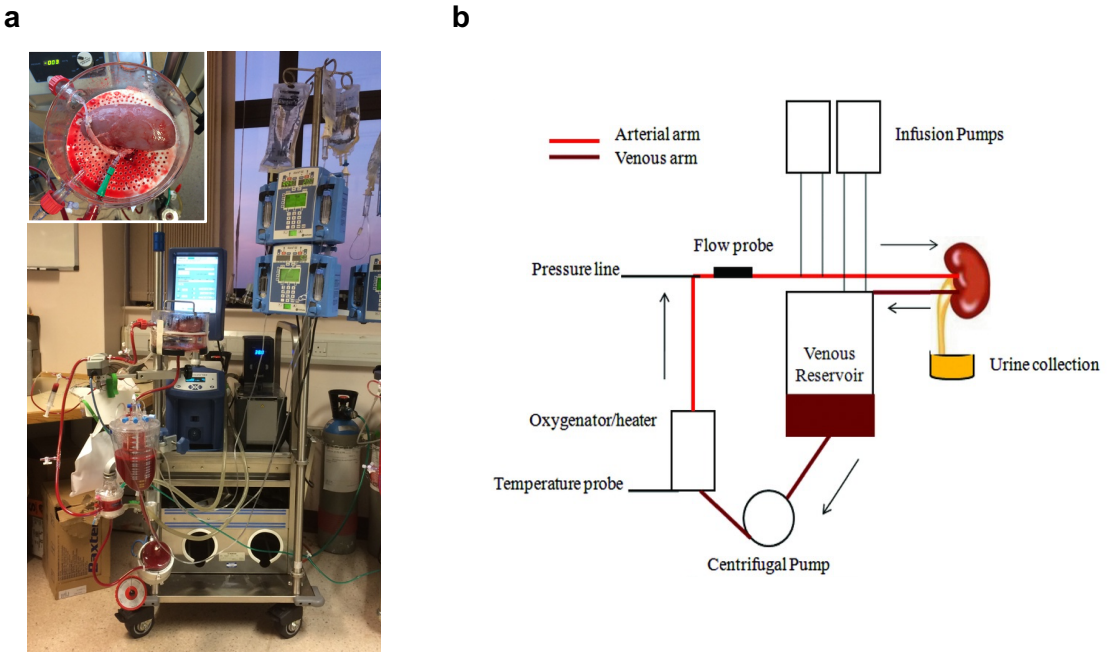

Figure 2.1 ***Ex Vivo*** **Normothermic Perfusion Circuit**. **(a)** Photograph of the EVNP circuit and a kidney undergoing perfusion in the glass chamber. **(b)** Schematic diagram of the EVNP circuit showing the individual circuit components. During EVNP, the whole blood based perfusate passes from the venous reservoir to the centrifugal pump and then onto the membrane oxygenator and heat exchanger before entering the perfusion chamber where the kidney is reperfused via cannulation of the renal artery. The venous outflow from the kidney is collected by the perfusion chamber and returned to the venous reservoir where it may circulate again. The temperature of the perfusate is measured using a temperature probe at the heat exchanger and the flow rate of the perfusate measured using a flow probe proximal to the perfusion chamber. Urine produced by the kidney during EVNP was collected via cannulation of the ureter and catheter bag. A number of infusions were given to the kidney during EVNP including Ringer's solution to replace the volume of perfusate lost in urine, a glucose solution (5 %) and an amino acid solution (Synthamin 17 10.0 %) supplemented with sodium bicarbonate (15 mL, 8.4 %) and insulin (500 IU). These were delivered to the venous reservoir via a set of infusion pumps. Figure adapted from Nicholson et al (2013).

Circuit Infusions

A number of infusions were added to the venous reservoir of the circuit during perfusion in order to maintain the physiological conditions of the perfusate. Ringer's solution (Baxter Healthcare, US) was given to replace the fluid lost in the urine produced by each kidney during reperfusion with the rate of infusion adjusted to match the rate of urine production. In addition, a 5 % glucose (Baxter Healthcare, US) solution was given at a rate of 5 mL/h and an amino acid solution (Synthamin 17 10.0 %, Baxter Healthcare, UK) with added insulin (100 IU per 500 mL Synthamin) and sodium bicarbonate 8.4 % (15 mL per 500 mL Synthamin) was given a rate of 20 mL/h.

Reperfusion Conditions

Each kidney was reperfused at a centrifugal pump speed of 1500 rpm, at a temperature of 37.0 $\pm$ 1.0 °C and the perfusate was oxygenated with a 95 % oxygen: 5 % carbon dioxide gas mixture.

2.3.2 Preparation of Pig and Human Kidneys for Perfusion

Kidneys were removed from cold storage approximately 30 mins prior to reperfusion and submerged in a bowl containing slushed ice and ice cold Soltran solution (Baxter Healthcare, US). The renal vessels and ureter were identified and any residual fat or connective tissue was removed from the kidney. The renal artery was then cannulated using a size 12 F soft silastic catheter (Pennine, UK) and held in place with a 3-0 Vicryl tie (Ethicon, Johnson & Johnson, UK). The ureter was also cannulated using a size 10 F soft silastic catheter again held in place with a 3-0 Vicryl tie (Ethicon, Johnson & Johnson, UK). A 20 mL syringe was used to flush each kidney with 100 mL Ringer's solution at the end of cold storage prior to connection to the reperfusion circuit.

2.3.3 Kidney Monitoring and Sampling during Perfusion

Renal Blood Flow

Renal blood flow (RBF) could be measured directly by the flow probe during reperfusion and recorded every 5 mins for the first 15 mins of reperfusion, then half-hourly from 30 mins after the start of reperfusion.

Urine Output

The urine produced by each kidney was collected in a catheter bag and the total amount recorded hourly. The total hourly urine output was used to adjust the rate of Ringer's infusion to maintain the circulating volume of the perfusate.

Fall in Serum Creatinine

Fall in serum creatinine (SCr) was used as a measure of kidney function on reperfusion. This was chosen instead of creatinine clearance as a bolus dose of creatinine was added to the perfusate at the start of reperfusion rather than a continuous infusion of creatinine being given throughout. As a result creatinine concentration within the perfusate decreased over time making creatinine clearance difficult to calculate accurately at low serum creatinine concentrations. Serum creatinine was measured by obtaining an arterial perfusate sample prior to addition of the kidney to the circuit and at 1 h, 3 h and 6 h of reperfusion. Samples were stored at 4 °C and sent to Core Biochemical Assay Laboratory, Addenbrooke's Hospital, Cambridge, UK for analysis.

Fractional Excretion of Sodium

Fractional excretion of sodium (FENa) at 1 h reperfusion was used as measure of damage to the proximal tubules of the kidney following ischaemia reperfusion. Sodium excretion by a healthy kidney is usually less than 1 % however following ischaemia, dysregulation of proximal tubule polarity and ATN leads to disrupted sodium reabsorption and loss of sodium in the urine [254]. An arterial perfusate sample and urine sample were taken at 1 h reperfusion sent to the Core Biomedical Assay Laboratory, Addenbrooke's Hospital, UK for analysis of serum and urine sodium and creatinine concentration. Fractional excretion of sodium was subsequently calculated as follows;

$$FENa = ([Na]_{\text{urine}}[Cr]_{\text{plasma}})/([Na]_{\text{plasma}}[Cr]_{\text{urine}})$$

Tissue Wedge Biopsies

Wedge tissue biopsies were taken from the kidney cortex and rapidly clamp frozen in LN2 using Wollenburg clamps where indicated. Frozen tissue samples were then stored at -70 °C until further processing and analysis.

2.4 Liquid-Chromatography Tandem Mass Spectrometry (LC-MS/MS)

2.4.1 Extraction of Polar Metabolites

Polar metabolites were extracted from clamp frozen tissue samples using a protocol developed by the Frezza Lab (MRC Cancer Unit, University of Cambridge, UK). For each each sample, approximately 20 mg of clamp frozen tissue was weighed out on dry ice into a pre-cooled Precellys tube (Hard tissue homogenising CK28-R - 2 mL; Bertin Instruments, France). After weighing, 25 µl/mg of pre-cooled extraction buffer (50 % (v/v) MS-grade methanol (Thermo Fisher Scientific, UK), 30 % (v/v) MS-grade acetonitrile (Romil, UK), 20 % MS grade-water (Thermo Fisher Scientific, UK) and 100 ng/mL HEPES free acid) was added to each sample along with 20 µl internal standard containing 100 pmol ^{13}C-succinate and 100 pmol ^{13}C-malonate. Samples were homogensied using a Precellys 24 tissue homogeniser (6500 rpm, 2 x 15 s, Bertin Instruments, France) and transferred back onto dry ice. Following homgenisation samples were centrifuged (17,000 g, 10 min, 4 °C) and the supernatent transferred to a pre-cooled microcentrifuge tube on wet ice. Samples were centrifuged again (17,000 g, 10 min, 4 °C) and the supernatent transferred to a pre-cooled MS vials. Vials were stored at -70 °C until analysis.

2.4.2 Extraction of MitoP & MitoB

MitoP and MitoB were extracted from clamp frozen tissue samples using a protocol developed by the Murphy Lab (Mitochondrial Biology Unit, University of Cambridge, UK). For each sample, approximately 50 mg of clamp frozen tissue was weighed out on dry ice into a 2 mL microcentrifuge tube. One spatula of zirconium oxide beads (Next Advance, USA), approximately the size of the tissue, was added to each sample along with 200 µl MitoP/B extraction buffer A (60 % (v/v) MS-grade acetonitrile (Romil, UK), 0.1 % MS-grade formic acid (Merck, UK), 39.9 % MS-grade water (Thermo Fisher Scientific, UK)) and 10 µl internal standard containing 100 pmol d_{15}-MitoB and 50 pmol d_{15}-MitoP. Samples were then homogenised using a Bullet Blender (speed 8, 4 min, Next Advance, USA) and left for 30 minutes at 4 °C. Samples were then centrifuged (17,000 g, 10 min) and the supernatent transferred to a 96 well filter plate. The sample pellet was then resuspended in 200 µl MitoP/B extraction buffer A, vortexed for approximately 30 seconds and centrifuged again (17,000 g, 10 min). The second supernatent was then added to first supernatent in the corresponding well of the filter plate and samples were vacuum filtered into the collection plate. The filtered supernatent of each sample was then transferred to a fresh 2 mL microcentrifuge tubes

and dried in a speed vac overnight (40 °C). Dried samples were then resuspended in 250 µl MitoP/B extraction buffer B 20 % (v/v) MS-grade acetonitrile (Romil, UK), 0.1% MS-grade formic acid (Merck, UK), 79.9 % MS-grade water (Thermo Fisher Scientific, UK)), vortexed for 5 minutes and centrifuged (17,000 g, 10 min). The supernatent was then transferred to MS vials and stored at -70 °C until analysis.

2.4.3 Sample Analysis

LC-MS/MS analysis of malonate and succinate were performed by Mr Hiran A. Prag (MRC Mitochondrial Biology Unit, University of Cambridge, UK). LC-MS/MS analysis of MitoP/MitoB ratio were performed by Ms Angela Logan (MRC Mitochondrial Biology Unit, University of Cambridge, UK) and Mr Hiran A. Prag (MRC Mitochondrial Biology Unit, University of Cambridge, UK). Samples were analysed using an LCMS-8060 mass spectrometer (Shimadzu, UK) with a Nexera X2 UHPLC system (Shimadzu, UK). Sample separation was achieved using a SeQuant®ZIC®-HILIC column (3.5 µg,100 Å, 150 x 2.1 mm, 30 °C column temperature;MerckMillipore, UK) with a ZIC®-HILIC guard column (200Å, 1 x 5 mm). The mass spectrometer was operated in negative ion mode with multiple reaction monitoring (MRM). Sample spectra were acquired using Labsolutions software (Shimadzu, UK) and the peak area for each compound of interest measured relative to the internal standard. Sample concentrations were then calculated from a standard curve of known compound concentrations produced by LC-MS/MS in a similar manner.

2.5 Laboratory Assays

2.5.1 ATP/ADP Luciferase Assay

ATP and ADP concentrations were measured using a Luciferase based assay as described by Strehler et al. [255]. Frozen tissue samples were homogenised in ice-cold perchloric acid extractant (3 % (v/v) $HClO_4$, 2 mM Na_2-EDTA, 0.5 % Triton X-100). The supernatant was diluted to a concentration of 1 mg frozen tissue per mL. Samples, ATP and ADP standards were pH neutralized using a potassium hydroxide solution (2 M KOH, 2 mM Na_2-EDTA, 50 mM MOPS), vortexed until formation of a white precipitate ($KClO_4$), then centrifuged (17, 000 X g for 1 min at 4°C). For ADP measurements, 250 µl neutralised sample supernatant was mixed with 250 µl ATP sulfurylase assay buffer (20 mM $Na2MoO_4$, 5 mM GMP, 0.2 U ATP sulfurylase (New England Biolabs, USA), in Tris-HCl buffer (100 mM Tris-HCl, 10 mM $MgCl_2$ (pH 8.0)), incubated for 30 min at 30 °C with shaking (500 rpm), heated at 100 °C for 5 min and then cooled on ice. Standards (100 µl), samples for ATP measurement (100 µl)

or samples for ADP measurement (200 µl) (in duplicate) were added to 400 µl Tris-acetate (TA) buffer (100 mM Tris, 2 mM Na_2-EDTA, 50 mM $MgCl_2$, pH 7.75 with glacial acetic acid) in luminometer tubes. 10 µl pyruvate kinase solution (100 mM PEP, 6 U pyruvate kinase suspension (Sigma #P1506)) were added to one set of samples for ADP measurement and incubated for 30 min at 25°C in the dark to convert ADP to ATP. The other duplicate tube (without addition of pyruvate kinase solution) served as an ADP 'blank' value. The samples were then all assayed for ATP content in a Berthold AutoLumat Plus luminometer by addition of (100 µl) Luciferase/Luciferin Solution (7.5 mM DTT, 0.4 mg/ml BSA, (1.92 µg) luciferase/ml (SIGMA #L9506), 120 μM D-luciferin (SIGMA #L9504), made in TA buffer (25% (v/v) glycerol)), delivered via auto injection, protected from light. Bioluminescence of the ATP- dependent luciferase activity was measured for 45 s post injection and the data quantified against standard curves [193].

2.5.2 Glycogen Assay

Tissue glycogen concentration was measured using an assay adapted from Passonneau et al whereby the production of NA(D)PH was measured during the oxidation of glycogen-derived glucose to 6-phosphogluconate [256]. Frozen tissue (5-10 mg) was minced finely before being treated with 250 µl hot acid (2 M HCl; 100 °C) or alkali (2 M NaOH; 100 °C) to hydrolyse glycogen or as an unhydrolysed control respectively (100 °C, 1 h, vigorous shaking every 10 min). Samples were subsequently cooled to RT and neutralised to pH 7 with either 2 M NaOH or HCl and the addition of (500 µl) 400 mM Tris (pH 7.4). Neutralised samples were vortexed before centrifuging (17,000 x g, 10 min, RT). 60 µl of sample supernatant was plated in duplicate in a 96-well plate together with a glucose standard curve (0,10, 20, 40, 80, 160 µg glucose/ml). 200 µl glucose assay reagent (Sigma, #G3293) was added to each well and the plate incubated (5 min, RT) prior to measuring absorbance at 340 nm in a Spectramax Plus 384 plate reader (Molecular Devices, UK). The average absorbance of each sample was interpolated using the standard curve and multiplied by the final volume after pH adjustment to give μg of glycogen (or glucose for NaOH control) in original sample. This was divided by the weight of tissue added and the NaOH control was subtracted from the HCl sample to give μg glycogen per mg frozen tissue. Measurement of of tissue glycogen concentration was performed by Ms Fay M Allen (MRC Mitochondrial Biology Unit, University of Cambridge, UK).

2.5.3 Measurement Oxidative Damage to Mitochondrial DNA

Use of quantitative PCR to detect mitochondrial DNA lesions was based on the method described by Santos et al. [257] and performed using the following primers at 10 μM in the mouse: forward primer FWD: 5'-GCC AGC CTG ACC CAT AGC CAT AAT-3'. Reverse primer for the long 10090 bp PCR product: REV: 5'-GAG AGA TTT TAT GGG TGT AAT GCG G-3'. Reverse primer for the short 127 bp PCR product: REV: 5'- GCC GGC TGC GTA TTC TAC GTT A -3'. Sample DNA was extracted using the Qiagen DNeasy Tissue Kit (Qiagen, UK) following the provided instructions and quantified using the PicoGreen dsDNA Assay Kit (Invitrogen, US). QPCR was performed on 15 ng DNA in 35 µl reactions on a PCR thermocycler (Biometra, analytikjena, Germany). 1 U TaKaRa LA Taq was used per reaction (TakaRa Bio Inc, Japan). PCR master mix was prepared following the TaKaRa LA Taq instructions. Linearity of the PCR reaction was confirmed for each sample by running a 1:2 diluted sample simultaneously. Cycling parameters for the short reaction were 94ºC for 5 mins followed by 18 cycles of 94 °C for 30 s, 64 °C for 45 s, 72 °C for 45 s, followed by 72 °C for 10 mins. Conditions for the long amplification were 94 °C for 5 mins followed by 18 cycles of 94 °C for 15s and 64 °C for 12 minutes, followed by 72 °C for 10 mins. The PCR reaction was confirmed on 1% agarose gels and concentrations of the PCR product were determined by PicoGreen dsDNA Assay Kit. Amplification of the long PCR target was then normalised to that of the short target.

2.5.4 Measurement of Protein Carbonyls

Total protein carbonyl concentration in tissue was determined by ELISA using the Bio-Cell PC test kit (Biocell Corp, New Zealand) according to the manufacturer's instructions. Approximately 40 mg clamp frozen tissue was weighed out on dry ice into a pre-cooled Precellys tube (Hard tissue homogenising CK28-R - 2 mL; Bertin Instruments, France). After weighing, 150 µl pre-cooled RIPA buffer (Thermo Fisher Scientific, UK) supplemented with a protease inhibitor cocktail (cOmplete, mini, EDTA-free tabs, Roche) was added to each sample and homogenised using a Precellys 24 tissue homogeniser (6500 rpm, 2 x 15 s, Bertin Instruments, France). Samples were then centrifuged (17,000 g, 10 min, 4 °C) and the supernatant was transferred to 2 mL microcentrifuge tubes on wet ice. The protein concentration of the supernatant was determined relative to bovine serum albumin using a BCA assay kit (Thermo Fisher Scientific, UK) and adjusted to a protein concentration 10 mg/mL.

Protein samples were then reacted with dintirophenylhydrazine (DNP) to derivatise protein carbonyls and non-specifically adsorbed onto an ELISA plate. Excess protein and

non-protein constituents were washed away whilst the adsorbed protein was probed with biotinylated anti-DNP antibody followed by horseradish peroxidase. A chromatin reagent containing H_2O_2 was then added which catalysed the oxidation of 3,3',5,5'-tetramethylbenzidine (TMB). The reaction was followed at 650 nm until the highest standard reached the value 0.3 OD. The reaction was then stopped by the addition of a proprietary acid reagent and the absorbance was measured for each well at 450 nm. The protein carbonyl concentration of each sample was then related to a standard curve prepared for serum albumin containing increasing proportions of hpochlorous acid-oxidised protein.

2.5.5 Thiobarbituric Acid Reactive Species Assay

The thiobarbituric acid reactive species (TBARS) assay was used to measure tissue malondialdehyde (MDA) concentration, a product of lipid peroxidation, and was adapted from the method described by Kelso et al. [258]. Thiobarbituric acid reacts with MDA to form a fluorescent product which excites at 515 nm and emits at 532 nm. Approximately 20 mg of clamp frozen tissue was weighed out on dry ice into a pre-cooled Precellys tube (Hard tissue homogenising CK28-R - 2 mL; Bertin Instruments, France). After weighing, 60 µl butylated hydroxytoluene (DMSO), 200 µl 35 % (w/v) perchloric acid and 200 µl 1 % (w/v) thiobarbituric acid was added to each sample and homogenised using Precellys 24 tissue homogeniser (6500 rpm, 4 x 15 s, Bertin Instruments, France). Samples were then incubated at 100 °C for 15 min, cooled to room temperature and transferred to a 15 mL falcon centrifuge tube containing 2 mL MillQ and 2 mL Butan-1-ol. Samples were vortexed for approximately 10 s and then left until the MilliQ and Butan-1-ol had re-separated. 250 µl of the butan-1-ol (top) layer was then be transferred to a 96-well plate and read using a Spectramax Plus 384 plate reader (Molecular Devices, UK). Positive control samples were homogenised in 200 µl 35% perchloric acid and 200 µl 1% thiobarbituric acid only. A final concentration of 50 μmol $FeCl_2$ and 50 μmol t-butylated hydroxytoluene added to the homogenate and positive control samples were vortexed and incubated for 1 hour at 37 °C. Samples were then incubated at 100 °C for 15 min and added to MilliQ Butan-1-ol solution as described above. The relative emission values for control, treatment and positive control samples were subsequently compared to determine the relative MDA concentration in the tissue. Measurement of tissue MDA concentration using the TBARs assay was performed by Ms Margaret Huang (Department of Surgery, University of Cambridge, UK).

2.5.6 Glutathione Recycling Assay

The glutathione recycling assay was adapted from the protocol described by Griffith et al. [259]. In the assay, the rate of 2-nitro-5-thiobenzoate (TNB) production is followed at 412 nm from the reaction of reduced glutathione (GSH) with 5,5'-dithiobis-(2-nitrobenzoic acid) (DTNB) . Reaction of GSH with DTNB forms TNB and a mixed GS-TNB disulphide which may be reduced by another GSH molecule to give oxidised glutathione (GSSG) and further TNB. GSSG may then be recycled back to 2 molecules of GSH by glutathione reductase in an NAD(P)H dependent manner. The rate of TNB production is therefore proportional to the GSH concentration within the sample and may be compared to a set of GSH standards. Approximately 10 mg of clamp frozen tissue was weighed out on dry ice into a pre-cooled Precellys tube for each sample (Hard tissue homogenising CK28-R – 2 mL; Bertin Instruments, France). After weighing, 20 µl/mg of 5% (w/v) sulfosalicylic acid, pre-cooled on wet ice, was added to each sample and homogenised using a Precellys 24 tissue homogeniser (6500 rpm, 4 x 15 s, Bertin Instruments, France). Homogenised tissue samples were then rapidly transferred back onto wet ice. Subsequently, 10 µl of homogenised sample and glutathione standards (0, 0, 20 30, 40, 50, 60 and 70 nmoles made in 5% (w/v) sulfosalicyclic acid) were analysed for total glutathione concentration on a 96-well plate. Samples and standards were incubated with NAD(P)H (0.5 mM), 5,5'-dithiobis-(2-nitrobenzoic) (DTNB; 0.5 mM) and glutathione reductase from baker's yeast (4 U/ml). Reduction of DTNM to 2-nitro-5-thiobenzoate (TNB) was then followed at 412 nm using a spectrophotometer (SpectraMax Plus 384; Molecular Devices, UK) over 20 min, with sample kinetic rates compared to GSH standards.

2.5.7 Measurement of Serum Creatinine

Serum creatinine was measured on an automated biochemical analyser (Siemens Dimension RxL analyser, Siemens AG, Healthcare Division, Germany) by the Jaffe reaction. In this reaction pictrate reacts with creatinine in the presence of NaOH to form a red chromophore. The rate of increasing absorbance at 510 nm due to chromophore formation is directly proportional to the creatinine concentration in the plasma sample and may be quantified using a standard curve. This assay was performed by by Cambridge Biochemical Analysis Laboratory, Addenbrooke's Hospital, Cambridge, UK.

Step	Reagent	Incubation Time (h)
1	50% EtOH	1
2	70% EtOH	1
3	80% EtOH	1
4	95% EtOH	1
5	100% EtOH	1
6	100% EtOH	1
7	100% EtOH	1
8	Xylene	1.5
9	Xylene	1.5
10	Paraffin	2
11	Paraffin	2
12	Paraffin	2

Table 2.1 Automated Embedding Programme

2.5.8 Measurement of Blood Urea Nitrogen

Blood urea nitrogen (BUN) was measured on an automated biochemical analyser (Siemens Dimension RxL analyser, Siemens AG, Healthcare Division, Germany) using urease. In this reaction, urease hydrolyses urea to form ammonia which is then converted to L-glutamate by glutamate dehydrogenase in the presence of α-ketoglutarate and NADH. The change in absorbance at 340 nm due to the oxidation of NADH to NAD^+ is directly proportional to the BUN concentration and may be quantified using a standard curve. This assay was performed by by Cambridge Biochemical Analysis Laboratory, Addenbrooke's Hospital, Cambridge, UK.

2.6 Histology

2.6.1 Tissue Fixation and Embedding

Following retrieval, kidney tissue was placed in 10% neutral buffered formalin for 24 hours at room temperature. Samples were then transferred to 70 % ethanol and stored at 4 °C for a minimum of 48 hours prior to embedding. Samples were processed by an automated benchtop tissue processor (Leica TP1020, Leica Biosystems Inc, US) as shown in Table 2.1 and embedded in paraffin blocks using a paraffin embedding station (HistoCoreAradia II, Leica Biosystems Inc, US).

Deparaffinization and Rehydration	
2 x 3 min	Xylene
2 x 3 min	100% EtOH
1 x 3 min	95% EtOH
1 x 3 min	80% EtOH
1 x 5 min	ddH_2O
Haematoxylin Staining	
1 x 1 min	Haematoxylin
Rinse	ddH_2O
1 x 5 min	Tap water
Dip 8-12x	Acid Ethanol
2 x 1 min	Tap water
1 x 2 min	ddH_2O
Eosin Staining and Dehydration	
1 x 30s	Eosin
3 x 5 min	95% EtOH
3 x 5 min	100% EtOH
3 x 15 min	Xylene

Table 2.2 Haemotoxylin & Eosin Staining Protocol

2.6.2 Sectioning and Staining

Paraffin embedded tissue was sectioned using a microtome (Leica Biosystems Inc, US). Serial sections of 3.5 µm thickness were cut and mounted on polysine glass slides (VWR International, UK). Sections were then stained with eosin and haemotoxylin as shown in Table 2.2. Following staining, a coverslip was placed over each section using histomount (National Diagnostics, UK) and left to dry overnight.

2.6.3 Imaging and Analysis

Kidney tissue sections were imaged at 20 x magnification using an Olympus IX81 microscope (Olympus, Japan). Ten separate images of equal spacing were taken of cortical tissue in each tissue section. One tissue section was imaged for each kidney sample. Images were then analysed using ilastik software [260]. As necrotic tissue is less eosinophilic than viable tissue, image thresholds could be adjusted to separate viable, necrotic and background areas of an image. A training library, containing one image from each kidney sample was used to determine thresholds for background necrotic and viable tissue. Thresholds were then

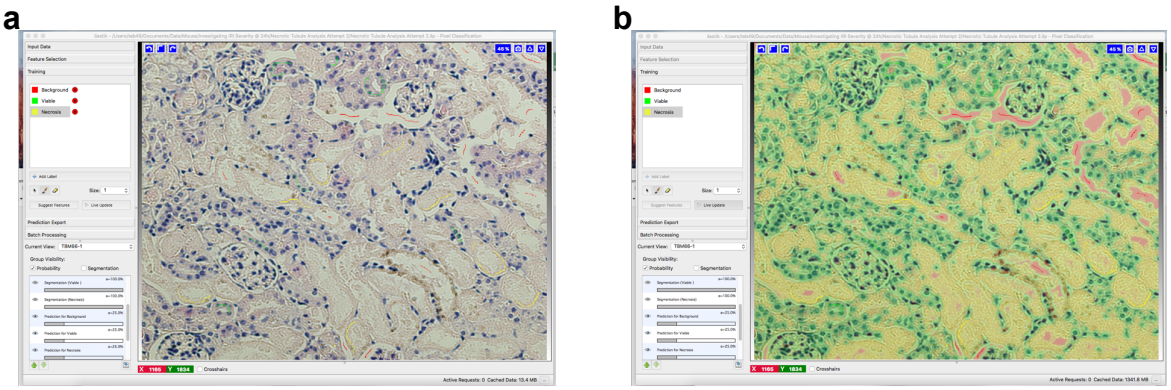

Figure 2.2 Generation of Image Masks Using ilastik Software. **(a)** Background, necrotic and viable areas marked on image within ilastik software. **(b)** Probability map calculated by random forest classifier and used to generate image masks for background (red), necrotic (yellow) and viable (green) areas for analysis in ImageJ.

used to create image 'masks' of background, necrotic and viable tissue for the remaining 9 images of each kidney sample as shown in Figure 2.2. The area of each mask could then be calculated using ImageJ software [261] and the total necrotic area calculated as a percentage of the total tissue area. Note that ilastik software does not perform any analysis or alter the image properties in any way; instead a random forest classifier is used to generate a probability map of each annotated area which can be confirmed visually. The probability map can then be transformed into individual objects or 'masks' using image thresholding. A separate threshold for background, necrotic and viable tissue can be set using a different threshold for each colour channel of the RGB image.

2.7 Statistical Analysis

Data are presented as mean ± SEM unless otherwise stated. Statistical analysis was performed using Prism 7.0 (Graphpad, USA). Comparisons between two datasets were assessed using a two-tailed unpaired t-test assuming equal variance. Comparisons between multiple datasets were assessed using one or two-way analysis of variance (ANOVA) followed by Dunnett's or Sidak's multiple comparisons test. P values <0.05 were considered to be statistically significant.

2.8 Collaborative Experiments

Where experiments were conducted by or with collaborators, these are explicitly stated in the figure legend. Mr Kourosh Saeb-Parsy (University of Cambridge Department of Surgery,

UK), Mr Jack L Martin (University of Cambridge Department of Surgery, UK), Mr Mazin O Hamid (University of Cambridge Department of Surgery, UK) and Ms Kirshnaa Mahbubani (University of Cambridge Department of Surgery, UK) assisted with the surgical retrieval of kidneys in the pig. Mr Hiran A Prag (MRC Mitochondrial Biology Unit, University of Cambridge, UK), Ms Angela Logan (MRC Mitochondrial Biology Unit, University of Cambridge, UK) and Ms Ana S H Costa (MRC Cancer Unit, University of Cambridge, UK) ran extracted samples on the mass spectrometer and analysed peak traces. Mr Jack L Martin (University of Cambridge Department of Surgery, UK) and Ms Anja Gruszczyk (MRC Mitochondrial Biology Unit, University of Cambridge, UK) provided heart data for comparison with the kidney in Chapter 3. Measurement of tissue glycogen concentration in Chapter 3 was performed by Ms Fay M Allen (Mitochondrial Biology Unit, University of Cambridge, UK). Measurement of tissue malondialdehyde concentration in Chapter 5 was performed by Ms Margaret M Huang (University of Cambridge Department of Surgery, UK).

Chapter 3

Metabolic Changes in the Kidney During Organ Retrieval and Preservation

3.1 Introduction

Ischaemia reperfusion injury is a two-stage process involving an ischaemic phase where an organ or tissue is deprived of an oxygenated blood supply and a reperfusion phase where the oxygenated blood supply to that organ or tissue is returned. The metabolic changes that occur during the ischaemic phase, namely succinate accumulation and adenine nucleotide depletion, play an important role in mitochondrial ROS production during the reperfusion phase. This is thought to initiate much of the downstream damage resulting from IRI [16]. A recent comparative metabolomic analysis reported that succinate, xanthine and hypoxanthine accumulate universally across multiple tissues during ischaemia [14]. Accumulation of succinate is thought to act as a large store of electrons capable of driving RET and superoxide production from Complex I when rapidly oxidised on reperfusion. Xanthine and hypoxanthine are derived from the depletion of adenine nucleotides and facilitate mitochondrial ROS production on reperfusion by restricting the substrate available for F_OF_1-ATPase allowing a near maximal Δp required for RET to develop [15]. Therefore, this model suggests that mitochondrial ROS production will only occur following both succinate accumulation and adenine nucleotide depletion during ischaemia.

Succinate accumulates during ischaemia due to reverse action of SDH driven by a highly reduced CoQ pool as well as glutaminolysis and canonical CAC action [14] [175]. Fumarate required for reversal of SDH is supplied by the PNC stimulated by an increase in AMP concentration during ischaemia and the MAS stimulated by a high $NADH/NAD^+$ ratio in the cytosol, as shown in Figure 3.1 [14]. Succinate dehydrogenase may therefore act as a thera-

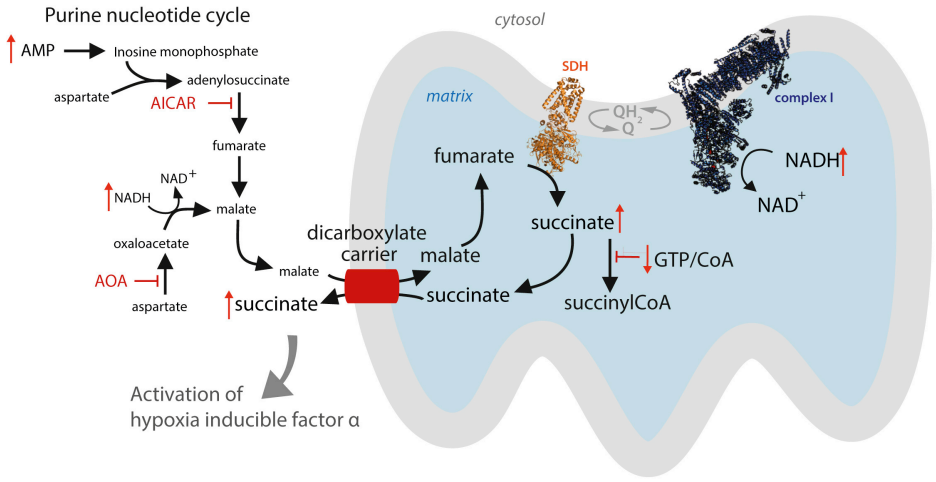

Figure 3.1 Succinate Accumulation During Ischaemia. During ischaemia, succinate is thought to primarily accumulate due to the reverse action of SDH. Fumarate required for reversal of SDH is thought to be supplied by the purine nucleotide cycle, stimulated by the accumulation of AMP during ischaemia, and the malate aspartate shuttle, stimulated by a high NADH/NAD$^+$ ratio. Succinate cannot be further metabolised under conditions of ischaemia and is exported from mitochondrial matrix via the DIC. Figure adapted from Chouchani et al (2016).

peutic target in IRI, the inhibition of which may reduce ischaemic succinate accumulation and thus the 'store' of electrons available for mitochondrial ROS production on reperfusion [23] [17]. Inhibition of SDH with the competitive inhibitor malonate, administered as the membrane permeable precursor DMM, has previously been shown to significantly reduce ischaemic succinate accumulation in a mouse model of myocardial infarction leading to a reduction in mitochondrial ROS production and infarct size on reperfusion [14].

Malonate is a charged molecule and must be given as a cell permeable precursor in order to enter cells and inhibit SDH *in vivo*. Malonate ester prodrugs, such as DMM, increase the membrane permeability of malonate by 'masking' the negatively charged carboxyl groups with a short-chain hydrocarbon pro-moiety to form an alkyl ester. However, the ester bond formed between the carboxyl group and alcohol must subsequently be hydrolysed by intracellular carboxylesterases in order to release malonate and enable SDH inhibition to occur [211]. Carboxylesterases are located in multiple subcellular compartments and DMM may either be hydrolysed within the mitochondrial matrix or transported into mitochondria via the DIC following hydrolysis in the cytoplasm. The rate of hydrolysis of malonate ester pro-drugs varies depending on the alkyl ester side groups used, which may determine how close to the onset of ischaemia different compounds should be given. Succinate accumulation occurs over a number of minutes during ischaemia and a sufficient malonate concentration must be present within mitochondria prior to the onset of ischaemia for effective inhibition of SDH reversal to occur. Therefore, the targeting of succinate accumulation via inhibition of

SDH during ischaemia may only be feasible in controlled situations of IRI where the onset of ischaemia is anticipated, for example in organ DBD, LD or other surgical procedures such as partial resection of renal tumours and abdominal aortic aneurysm repair. Dimethyl malonate is hydrolysed relatively slowly by PLE *in vitro* (personal communication, Hiran A Prag) and was given as an infusion beginning 10 mins prior to the onset of ischaemia in the mouse model of myocardial infarction [14]. Other malonate ester pro-drugs, such as MAM, are hydrolysed more rapidly by PLE (personal communication, Hiran A Prag) and may be administered closer to ischaemia onset. However, much of our understanding of when different malonate ester pro-drugs should be given during IRI is under active investigation; this Chapter specifically focuses on the administration of malonate ester pro-drugs prior to ischaemia in order to inhibit succinate accumulation. In Chapter 4, the administration of malonate ester compounds at other stages of ischaemia-reperfusion is investigated and discussed in more detail.

Most previous work on IRI has focused on the role of succinate accumulation and adenosine nucleotide depletion in the context of myocardial infarction; IRI is also central to organ transplantation but the role of succinate accumulation in this context has not been previously investigated [14] [194] [175]. In contrast to myocardial infarction, organ transplantation involves periods of both warm and cold ischaemia. Cold ischaemia reduces the metabolic activity within ischaemic tissue and may inhibit the rate of succinate accumulation and adenosine nucleotide depletion during cold preservation of donated organs. However, grafts retrieved from different donor types experience varying periods of warm ischaemia prior to organ cooling during which succinate accumulation and adenine nucleotide depletion may occur more rapidly. Kidneys retrieved following DCD experience on average 14 minutes of warm ischaemia prior to organ cooling as a result of the stand-off period required to confirm circulatory arrest [9]. In contrast, kidneys retrieved following DBD remain perfused with oxygenated blood up until the point of *in situ* flush with cold preservation solution and experience minimal warm ischaemia [57]. It may therefore be postulated, that succinate accumulation would be significantly greater in organs retrieved from DCD compared to DBD donors, leading to increased mitochondrial ROS production and injury on transplantation. Consistent with this hypothesis, it is known that grafts from DCD donors experience increased rates of DGF compared to DBD grafts on transplantation which is thought to be related to their increased exposure to warm ischaemia [8]. A recent time-resolved metabolomic analysis of heart tissue exposed to warm and cold ischaemia showed succinate accumulation was significantly reduced in cold ischaemic tissue compared to warm ischaemic tissue [193]. Importantly, the onset of ischaemia is often anticipated in organ donation with both DCD and DBD donation occurring under controlled conditions in the UK. Succinate accumulation

may therefore be amenable to inhibition with malonate ester prodrugs administered prior to the onset of ischaemia in organ donation. However, depending on the donor type from which organs are retrieved there may be a number of legal and logistical barriers to overcome before the use of malonate ester prodrugs in organ transplantation can progress to human trials as discussed previously.

In this chapter, I first compared the metabolic changes that occur during warm and cold ischaemia in the kidney to those in the heart, in which most previous work has been conducted. The aim was to determine whether the key metabolic changes that occur during ischaemia in the heart are conserved in the kidney and whether similar therapeutic targets may be used in both organs. Heart tissue for comparison with the kidney was collected in collaboration with by Mr Jack L Martin (University of Cambridge Department of Surgery, UK), Ms Anja V Gruszczyk (MRC Mitochondrial Biology Unit, University of Cambridge, UK) and Ms Fay M Allen (MRC Mitochondrial Biology Unit, University of Cambridge, UK). I then investigated the rate of organ cooling during back-table flush in the pig kidney and heart to determine how quickly metabolic activity may be inhibited during organ donation. I next investigated whether there was a difference in succinate accumulation and adenosine nucleotide depletion between declined human kidneys retrieved from different donor types. The aim was to determine whether there was a difference in succinate accumulation between organs retrieved from DCD compared to DBD donors which may explain increased rates of DGF in DCD organs on transplantation. Lastly, I investigated whether DMM can inhibit succinate accumulation when administered prior to warm ischaemia in a mouse and pig model of kidney donation.

3.1.1 Aims

1. To compare the metabolic changes that occur during warm and cold ischaemia in the kidney relative to the heart in the mouse, pig and human

2. To investigate the metabolic profile of human kidneys retrieved under the different conditions of organ donation

3. To determine whether DMM can be used inhibit succinate accumulation during warm ischaemia in model of kidney donation in the mouse and pig

3.1.2 Hypotheses

1. Increased succinate accumulation occurs in kidney and heart grafts retrieved following donation after circulatory death compared to donation after brainstem death

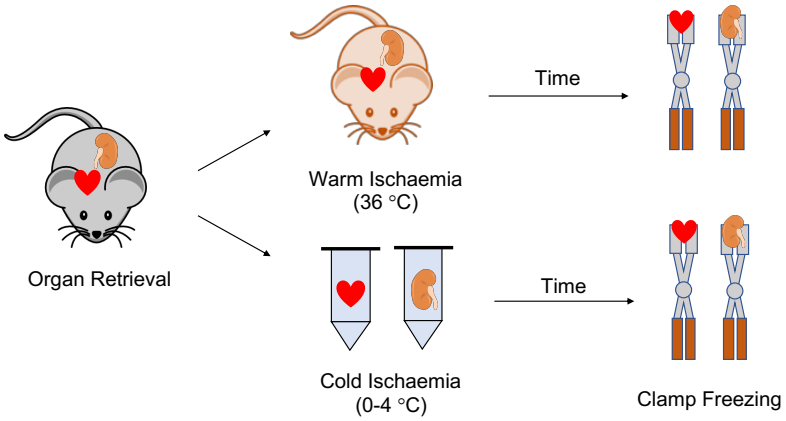

Figure 3.2 Modelling Warm and Cold Ischaemia in the Mouse. Organs were rapidly retrieved from mice following exsanguination under terminal anaesthesia and placed in either ice cold UW solution at 0-4 °C or left in the carcass of the animal maintained at 36 °C. Following 6, 12 or 30 mins of ischaemia, organs were clamp frozen in LN2 using Wollenburg clamps and stored at -70 °C until further processing and analysis. Control organs were rapidly retrieved from normoxic mice and immediately clamp frozen in LN2. The retrieval of kidneys and hearts from mice was conducted by Mr Jack L Martin (University of Cambridge Department of Surgery, UK).

2. Accumulation of succinate during warm ischaemia in the kidney can be inhibited by prior addition of malonate ester prodrugs

3.2 Metabolic Changes during Warm and Cold Ischaemia in the Mouse

The metabolic changes that occur during warm and cold ischaemia in the mouse kidney compared to the mouse heart were investigated as shown in Figure 3.2.

3.2.1 Succinate Accumulation

Succinate reached a near maximal tissue concentration of approximately 1200 pmol/mg (Figure 3.3a) after 6 mins of warm ischaemia in the mouse kidney and was approximately 15-fold (Figure 3.3b) greater than normoxic levels. In contrast, succinate accumulated to a much greater level (3000 pmol/mg) (Figure 3.3b & 3.3e) in the mouse heart reaching a maximum concentration at approximately 30 mins warm ischaemia. In comparison to normoxic values however, the relative increase in succinate concentration in the mouse heart was similar to in the mouse kidney (Figure 3.3d).

During cold ischaemia, succinate increased at a much slower rate, reaching a concentration of approximately 500 pmol/mg (Figure 3.3a) or 7-fold (Figure 3.3c) normoxic levels following 480 mins cold ischaemia in the mouse kidney and 2000 pmol/mg (Figure 3.3b) or 10-fold normoxic levels (Figure 3.3d) in the mouse heart. In contrast to changes during warm ischaemia, succinate increased by a greater amount in both absolute (Figure 3.3f) and relative terms (Figure 3.3c & 3.3d) during cold ischaemia in the mouse heart compared to the kidney.

3.2.2 Changes in ATP and ADP Concentrations and Ratio

Under conditions of normoxia, the ATP/ADP ratio was approximately 3 in the mouse kidney (Figure3.4a) and 6 in the mouse heart (Figure 3.4b). During warm ischaemia, the ATP/ADP ratio decreased rapidly in the mouse kidney and reached a minimum value of 0.4 (Figure3.4a) after 10 mins warm ischaemia, roughly 20% (Figure 3.4c) of the normoxic ratio. In the mouse heart, the ATP/ADP ratio decreased more gradually during warm ischaemia reaching a minimum value of 0.5 (Figure 3.4b) at 30 mins, roughly 10% (Figure 3.4d) of the normoxic ratio. Despite decreasing more gradually, there was no significant difference in the ATP/ADP ratio between the mouse heart and kidney after 12 mins warm ischaemia (Figure 3.4e). Under conditions of cold ischaemia, the ATP/ADP ratio decreased at a much slower rate in the mouse kidney and heart. At 480 mins cold ischaemia, the ATP/ADP ratio was approximately 1.2 (Figure 3.4a) or 40% (3.4c) the normoxic ratio in the mouse kidney and 0.8 (Figure 3.4b) or 15% (Figure 3.4d) the normoxic ratio in the mouse heart. However, despite these differences there was no significant difference in the ATP/ADP ratio between the mouse kidney and heart at 30 or 480 mins cold ischaemia (Figure 3.4f).

Similar to the ATP/ADP ratio, the sum of the ATP and ADP concentration was greater in the mouse heart (approximately 6 nmol/mg) (Figure 3.5b) than in the mouse kidney (approximately 3 nmol/mg) (Figure 3.5a). During warm ischaemia, the sum of the ATP and ADP concentration decreased rapidly in the mouse kidney and reached a minimal level of approximately 0.2 nmol/mg (Figure 3.5a), about 7% the normoxic value (Figure 3.5c) at 30 mins. In contrast the sum of the ATP and ADP concentration decreased more gradually in the mouse heart and reached a minimum value of 0.25 nmol/mg (Figure 3.5b) at 30 mins warm ischaemia, approximately 5% the normoxic value (Figure 3.5d). Despite decreasing more gradually however, there was no significant difference in the sum of the ATP and ADP concentrations in the mouse kidney and heart at 12 or 30 mins warm ischaemia (Figure 3.5e). Under conditions of cold ischaemia, the sum of the ATP and ADP concentration decreased at a much slower rate in the mouse kidney and heart. As a result, the sum of the ATP and ADP concentration in the mouse heart was significantly greater than in the kidney at 6, 12 and 30 minutes cold ischeamia (Figure 3.5f). At 480 mins however, the sum of the ATP and

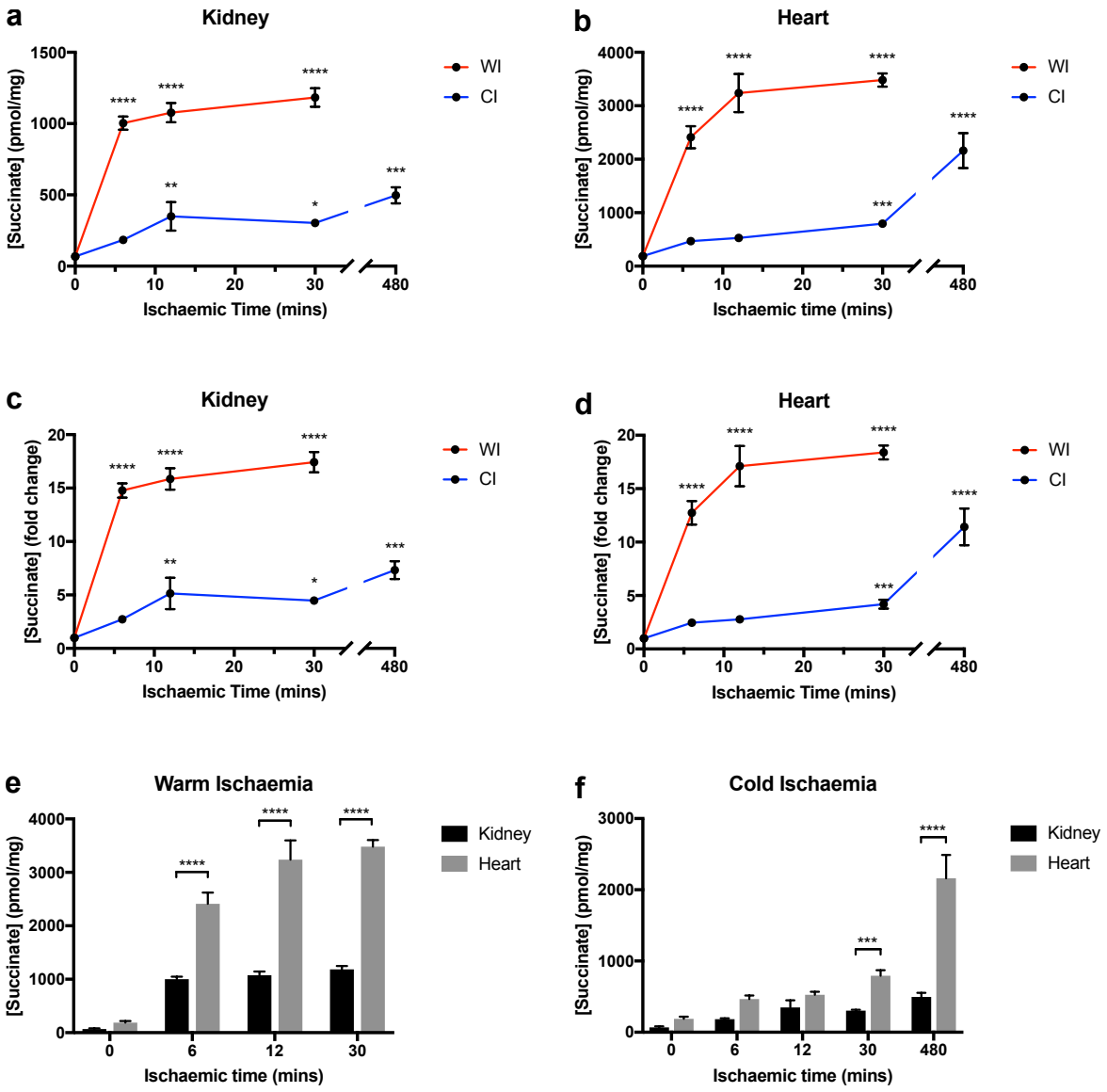

Figure 3.3 Succinate Accumulation during Warm and Cold Ischaemia in the Mouse Kidney and Heart. Tissue succinate concentration during warm ischaemia (WI) at 36 °C and cold ischaemia (CI) at 0-4 °C in the kidney (**a**) (n=4) and heart (**b**) (n=5-6). Relative change in succinate concentration compared to normoxia during WI and CI in the kidney (**c**) and heart (**d**). Comparison of tissue succinate concentration in the kidney and heart during WI (**e**) and CI (**f**). *P < 0.05, **P < 0.01, ***P < 0.001, ****P < 0.0001. P values were calculated by one-way analysis of variance (ANOVA) with Dunnett's multiple comparison test (**a**-**d**) and two-way ANOVA with Sidak's multiple comparisons test (**e**-**f**). Data are mean ± SEM.

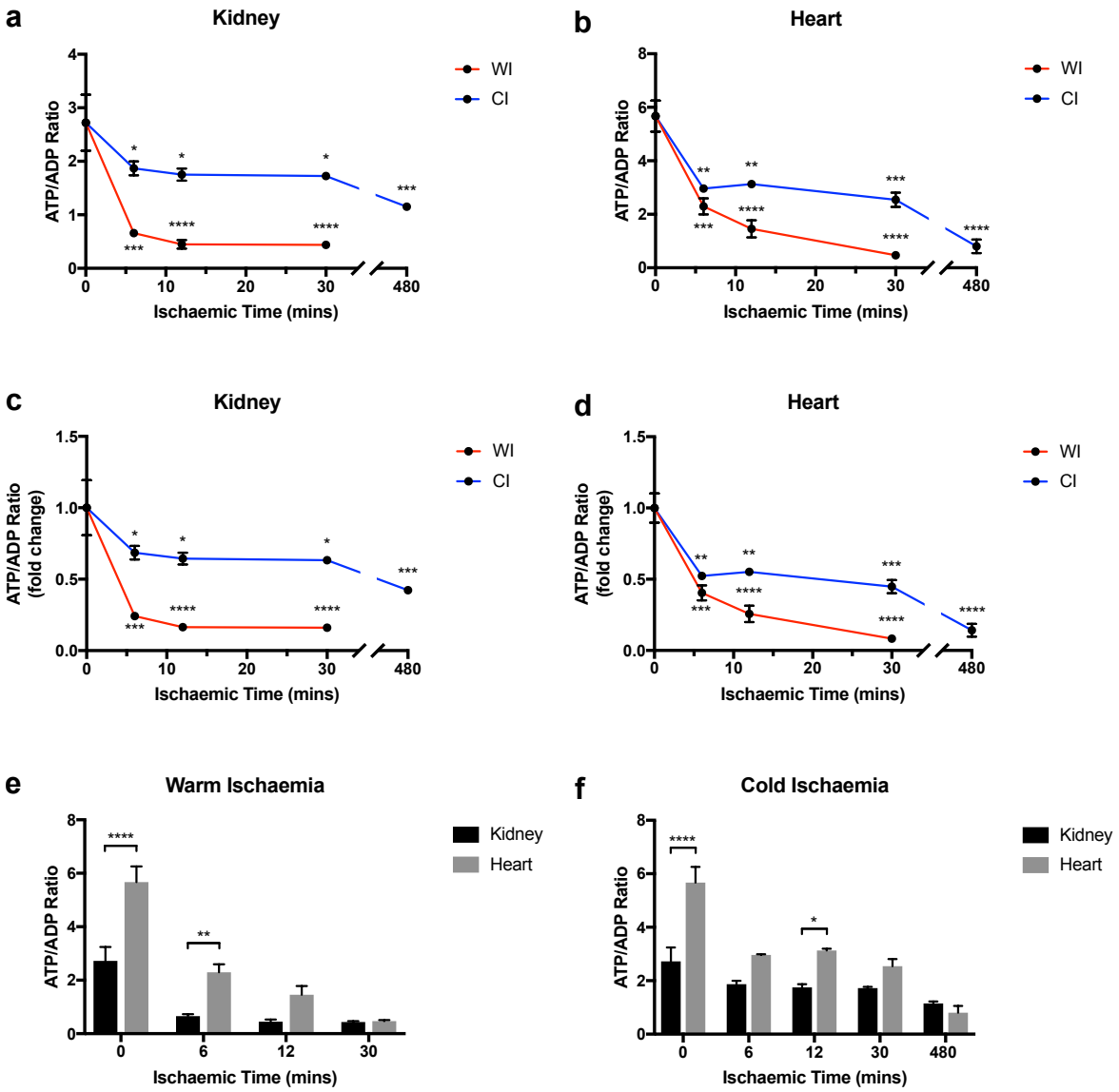

Figure 3.4 Changes in the ATP/ADP Ratio during Warm and Cold Ischaemia in the Mouse Kidney and Heart. Tissue ATP/ADP ratio during warm ischaemia (WI) at 36 °C and cold ischaemia (CI) 0-4 °C in the kidney (**a**) (n=3-4) and heart (**b**) (n=3-4, except 6 & 12 mins CI where n=2). Relative change in tissue ATP/ADP ratio compared to normoxia during WI and CI in the kidney (**c**) and heart (**d**). Comparison of tissue succinate concentration in the kidney and heart during WI (**e**) and CI (**f**). *P < 0.05, **P < 0.01, ***P < 0.001, ****P < 0.0001. P values were calculated by one-way analysis of variance (ANOVA) with Dunnett's multiple comparison test (**a**-**d**) and two-way ANOVA with Sidak's multiple comparisons test (**e**-**f**). Data are mean ± SEM except 6 & 12 mins CI in the heart where data are mean ± range. Measurement of heart ATP and ADP concentration was performed by Ms Anja V Gruszczyk (MRC Mitochondrial Biology Unit, University of Cambridge, UK).

ADP concentration was 0.4 nmol/mg (Figure 3.5a) or approximately 14% (Figure 3.5c) the normoxic value in the mouse kidney and 0.5 nmol/mg (Figure 3.5b) or approximately 9% (Figure 3.5d) the normoxic value in the mouse heart and there was no significant difference between the two organs (Figure 3.5f).

3.2.3 Glycogen Consumption

Under conditions of normoxia, tissue glycogen concentration (Figure 3.6a) was approximately 2 μg/mg in the mouse kidney and 4 μg/mg in the mouse heart. During warm ischaemia, glycogen decreased in both organs however it plateaued at a higher concentration of 1 μg/mg in the mouse heart and at a lower concentration of 0.5 μg/mg in the mouse kidney (Figure 3.6a). However, in relative terms, tissue glycogen concentration decreased to approximately 30% normoxic levels in both organs (Figure 3.6b). It was not possible to measure tissue glycogen concentration under conditions cold ischaemia in this experiment as organs were placed in UW preservation solution containing hydroxyethyl starch that we found artifactually raised glycogen values measured via the assay.

3.3 Metabolic Changes during Warm and Cold Ischaemia in the Pig

The metabolic changes that occur during warm and cold ischaemia in the pig kidney and heart were investigated as shown in Figure 3.7. It is important to note that the whole kidney was exposed to conditions of warm and cold ischaemia compared to wedge biopsies taken from the heart. This was primarily due to restrictions on when different organs could be retrieved under the Home Office Licence. The heart could only be retrieved from the pig following confirmation of circulatory arrest. To obtain a baseline measurement of tissue succinate, ATP and ADP values as close to normoxia in the pig heart as possible, a wedge biopsy was rapidly retrieved from the apex of the heart through an incision in the diaphragm, immediately following confirmation of circulatory arrest by the attending vet. Circulatory arrest occurred within seconds of administering a lethal dose of intravenous pentobarbitol to the pig and retrieval of a wedge biopsy from the apex of the heart took a further 10-20 s. A section of the wedge biopsy was then immediately clamp frozen using Wollenburg clamps to act as a baseline control and the remaining tissue exposed to either warm and cold ischaemia as described in Figure 3.7. Whilst the baseline tissue sample from the heart was exposed to approximately 30 s warm ischaemia in total, it was still possible to investigate further metabolic changes in the tissue during subsequent warm and cold ischaemia. Furthermore,

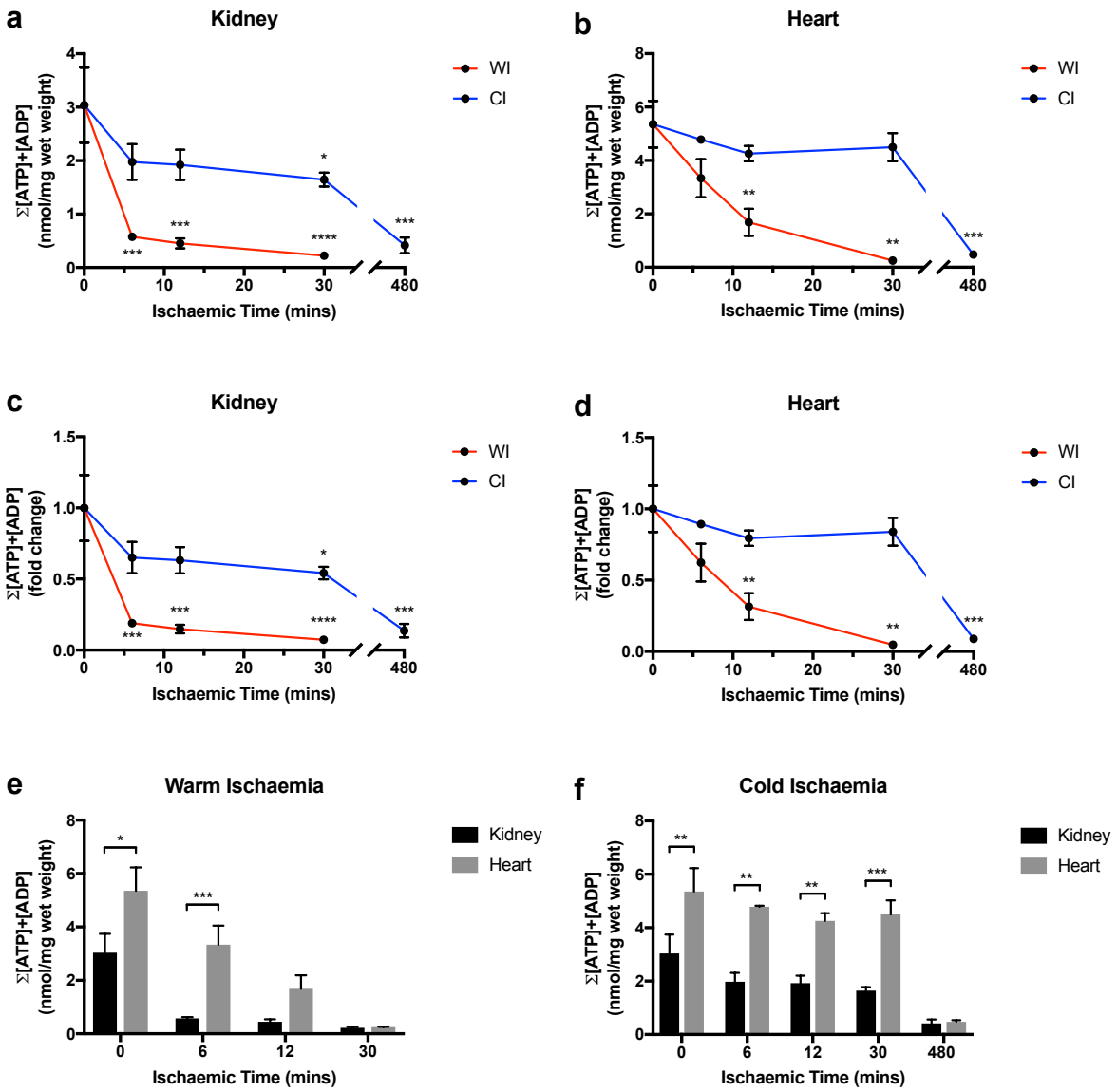

Figure 3.5 Total ATP and ADP Concentration during Warm and Cold Ischaemia in the Mouse Kidney and Heart. Total ATP and ADP concentration during warm ischaemia (WI) at 36.0 °C and cold ischaemia (CI) at 0-4 °C in the kidney (**a**) (n=3-4) and heart (**b**) (n=3-4, except 6 & 12 mins CI where n=2). Relative change in total ATP and ADP concentration compared to normoxia during WI and CI in the kidney (**c**) and heart (**d**). Comparison of tissue succinate concentration in the kidney and heart during WI (**e**) and CI (**f**). *P < 0.05, **P < 0.01, ***P < 0.001, ****P < 0.0001. P values were calculated by one-way analysis of variance (ANOVA) with Dunnett's multiple comparison test (**a**-**d**) and two-way ANOVA with Sidak's multiple comparisons test (**e**-**f**). Data are mean ± SEM except 6 & 12 minutes CI in the heart where data are mean ± range. Measurement of heart ATP and ADP concentration was performed by Ms Anja V Gruszczyk (MRC Mitochondrial Biology Unit, University of Cambridge, UK).

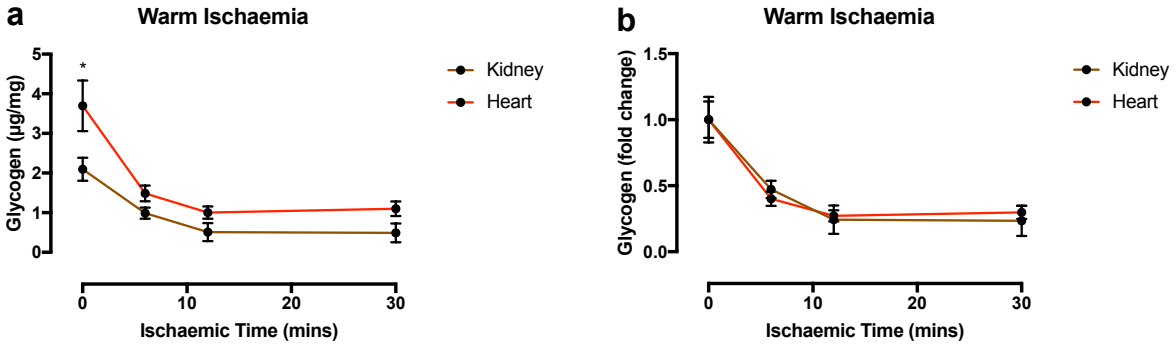

Figure 3.6 Glycogen Consumption during Warm Ischaemia in the Mouse Kidney and Heart. (**a**) Tissue glycogen concentration during warm ischaemia (WI) at 36 °C in the kidney (n=3-5 except 0 & 30 mins where n=2) and heart (n=5). (**b**) Relative change in tissue glycogen concentration compared to normoxia during WI in the kidney and heart. *P < 0.05. P values were calculated by two-way analysis of variance (ANOVA) with Sidak's multiple comparison test. Data are mean ± SEM except 0 & 30 minutes WI in the kidney where data are mean ± range. Measurement of tissue glycogen concentration was performed by Ms Fay M Allen (MRC Mitochondrial Biology Unit, University of Cambridge, UK).

the use of multiple organs from each pig experiment in this way enabled a greater amount of information to be gained from each pig experiment, reducing the total number of animals required in accordance with the principle of the 3Rs (refine, reduce, replace) as set out by the National Centre for the Replacement, Refinement & Reduction of Animals in Research.

3.3.1 Succinate Accumulation

Similar to the situation in the mouse, the tissue succinate concentration increased rapidly in the pig kidney and reached a maximum concentration of 1200 pmol/mg (Figure 3.8a), approximately 5-fold the normoxic value (Figure 3.8b) at 30 mins warm ischaemia. The relative increase in succinate concentration during warm ischaemia in the pig was much lower than in the mouse. However, this difference may partly relate to a longer delay (10-20 s vs <5 s in the mouse) in clamp freezing the normoxic sample from the pig as a result of the greater complexity of the procedure. During this delay, succinate may have increased in the tissue as it became ischaemic, artificially raising the normoxic level. Comparison of the fold changes between species and models should therefore be interpreted carefully with differences in the surgical procedure, complexity and method of tissue sampling taken into consideration. The tissue succinate concentration increased to a greater level in the pig heart than in the pig kidney (Figure 3.8e), again similar to the mouse. The tissue succinate concentration reached a maximum concentration of 4500 pmol/mg (Figure 3.8b) at 30 mins warm ischaemia, approximately 12-fold (Figure 3.8d) the normoxic value. Again, the difference in the relative

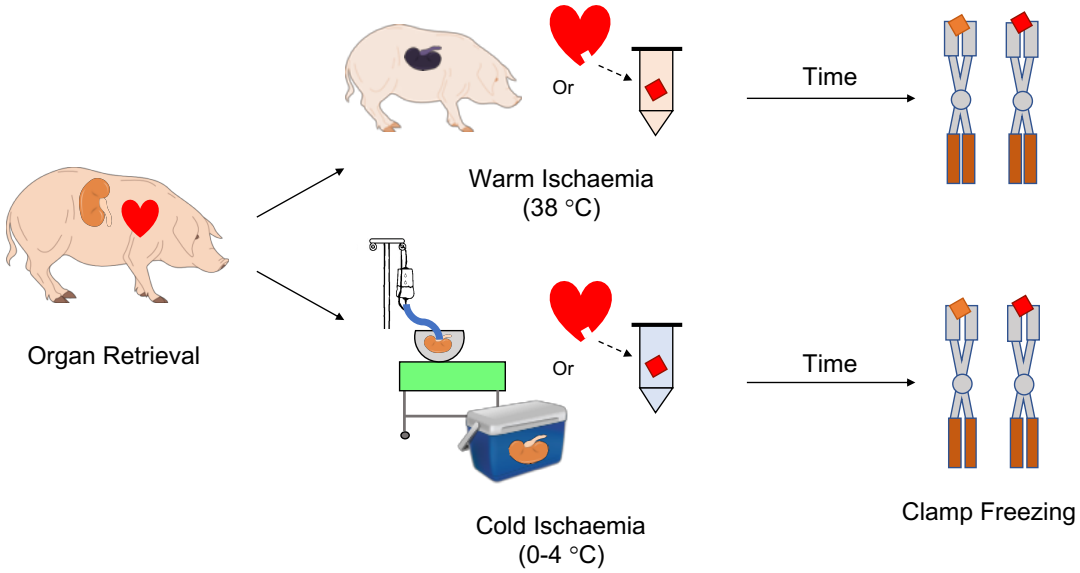

Figure 3.7 Modelling Warm and Cold Ischaemia in the Pig. Kidneys were retrieved from the pig under general anaesthesia. Hearts were retrieved from the pig immediately following euthanasia. A 0 mins wedge biopsy was taken prior to retrieval in the kidney but following retrieval from the thorax in the heart. All wedge biopsies were rapidly clamp frozen in LN2 using Wollenburg clamps. During warm ischaemia, the kidney was maintained at 38 °C in the abdomen of the pig whilst wedge biopsies from the heart were placed in humidified eppendorf tubes maintained at 38 °C in a heat block. During cold ischaemia, the kidney was rapidly submerged in slushed ice and flushed with 500 mL ice cold Soltran solution before being packed on ice and stored in an organ preservation box whilst wedge biopsies from the heart were placed in eppendorf tubes containing cold UW solution stored on ice. Heart and kidney wedge biopsies were then clamp frozen at 6, 12 and 30 mins warm ischaemia and 6, 12, 30 and 360 mins cold ischaemia. Frozen tissue samples were stored at -70 °C until further processing and analysis. Mr Kourosh Saeb-Parsy (University of Cambridge Department of Surgery, UK), Mr Jack L Martin (University of Cambridge Department of Surgery, UK), Mr Mazin O Hamed (University of Cambridge Department of Surgery, UK) and Ms Krishnaa T Mahbubani (University of Cambridge Department of Surgery, UK) assisted with the surgical retrieval of kidneys and hearts.

increase in succinate concentration between the mouse and pig may relate to differences in the experiment design.

During cold ischaemia, succinate increased at a much slower rate. At 360 mins, the tissue succinate concentration was approximately 500 pmol/mg (Figure 3.8a) or 4 fold (Figure 3.8c) the normoxic value in the pig kidney and 500 pmol/mg (Figure 3.8b) or 1.3 (Figure 3.8d) fold the normoxic value in the pig heart. The absolute succinate concentration was significantly greater in the pig heart at 30 mins cold ischaemia but there was no significant difference in the succinate concentration between the pig heart and kidney at 360 mins cold ischaemia (Figure 3.8e).

3.3.2 Changes in ATP and ADP Concentrations and Ratio

Under conditions of normoxia, the ATP/ADP ratio in the pig kidney was approximately 1.5 (Figure 3.9a) and significantly lower (Figure 3.9e) than the ratio in the pig heart, measuring approximately 12 (Figure 3.9b). During 30 mins warm ischaemia, the ATP/ADP ratio rapidly declined to 0.5 (Figure 3.9a) or 50% the normoxic ratio in the pig kidney and approximately 2.5 (Figure 3.9b) or 20% the normoxic ratio in the pig heart. However, there was no significant difference in the ATP/ADP ratio between the pig kidney and heart at 5, 12 or 30 mins warm ischaemia (Figure 3.9e). Under conditions of cold ischaemia, the ATP/ADP ratio decreased more gradually, reaching a value of 0.6 (Figure 3.9a) or 40% (Figure 3.9c) the normoxic ratio at 360 mins in the pig kidney and 3.7 (Figure 3.9b) or 30% (Figure 3.9d) the normoxic ratio in the pig heart. The ATP/ADP ratio was significantly greater in the pig heart at 6 minutes cold ischaemia but not at 30 or 360 mins (Figure 3.9f).

The sum of the ATP and ADP concentration under conditions of normoxia was also significantly lower in the pig kidney than in the pig heart (Figure 3.10e), measuring approximately 0.9 nmol/mg (Figure 3.10a) in pig kidney and 7.9 nmol/mg Figure 3.10b) in the pig heart. During warm ischaemia the sum of the ATP and ADP concentration decreased rapidly, reaching a value of 0.2 nmol/mg (Figure 3.10a) or 20% (Figure 3.10c) the normoxic value at 30 mins in the pig kidney and 2.3 nmol/mg (Figure 3.10b) or 30% (Figure 3.10d) the normoxic value in the pig heart. At 12 and 30 mins warm ischaemia however, there was no significant difference in the sum of the ATP and ADP concentration between the two organs (Figure 3.10e). Under conditions of cold ischaemia, the sum of the ATP and ADP concentration decreased more gradually, reaching a value of 0.3 nmol/mg (Figure 3.10a) or 24% (Figure 3.10c) the normoxic value at 360 mins in the pig kidney and 2.6 nmol/mg (Figure 3.10b) or 30% (Figure 3.10d) the normoxic value in the pig heart. The sum of the ATP and ADP concentration was significantly greater in the pig heart than in the pig kidney at 6, 12 and 30 mins cold ischaemia but not at 360 mins cold ischaemia (Figure 3.10f).

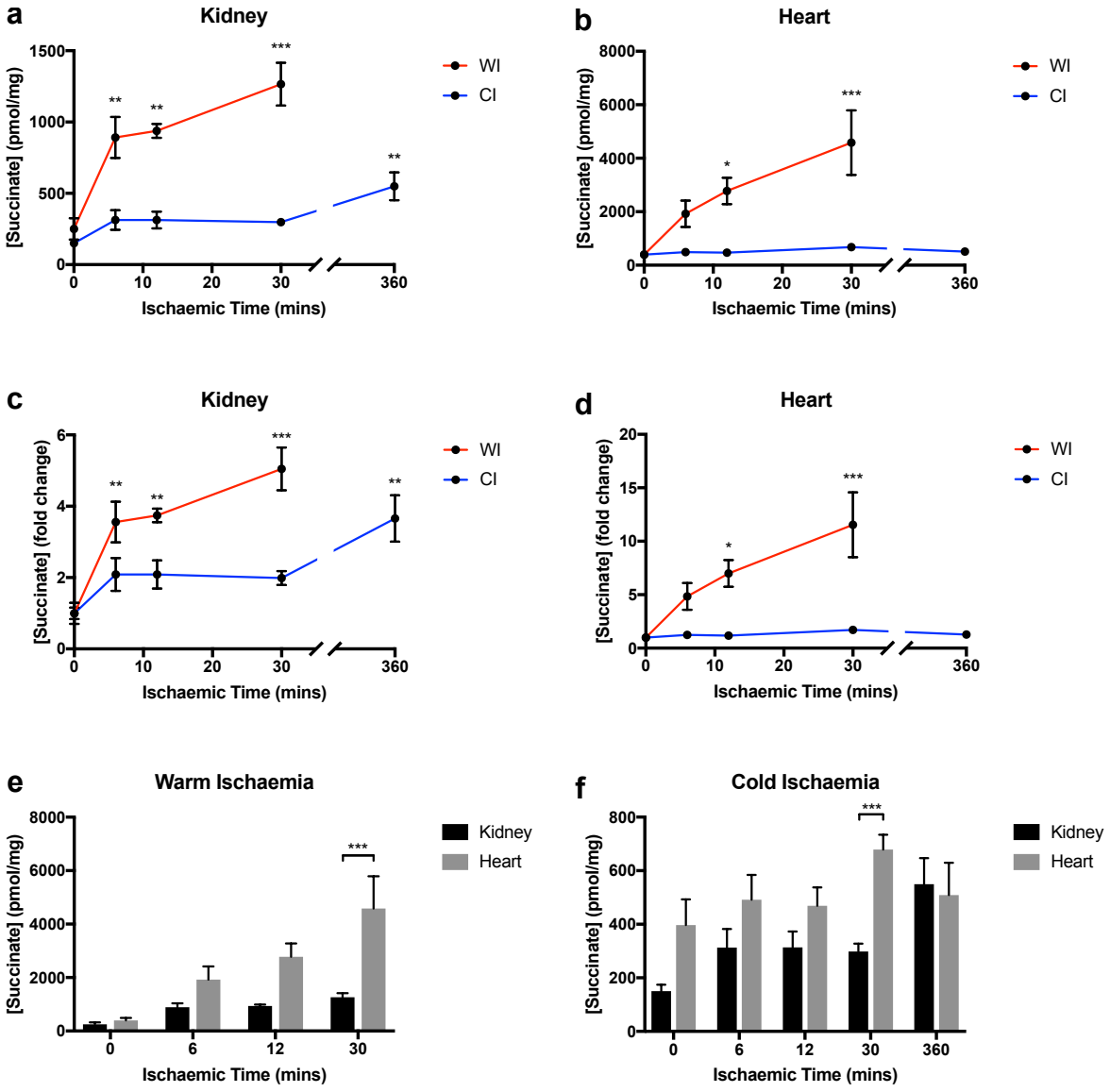

Figure 3.8 Succinate Accumulation during Warm and Cold Ischaemia in the Pig Kidney and Heart. Tissue succinate concentration during warm ischaemia (WI) at 38 °C and cold ischaemia (CI) at 0-4 °C in the kidney (**a**) (n=4) and heart (**b**) (n=5-6). Relative change in tissue succinate concentration compared to normoxia during WI and CI in the kidney (**c**) and heart (**d**). Comparison of tissue succinate concentration in the kidney and heart during WI (**e**) and CI (**f**). *P < 0.05, **P < 0.01, ***P < 0.001, ****P < 0.0001. P values were calculated by one-way analysis of variance (ANOVA) with Dunnett's multiple comparison test (**a**-**d**) and two-way ANOVA with Sidak's multiple comparisons test (**e**-**f**). Data are mean ± SEM.

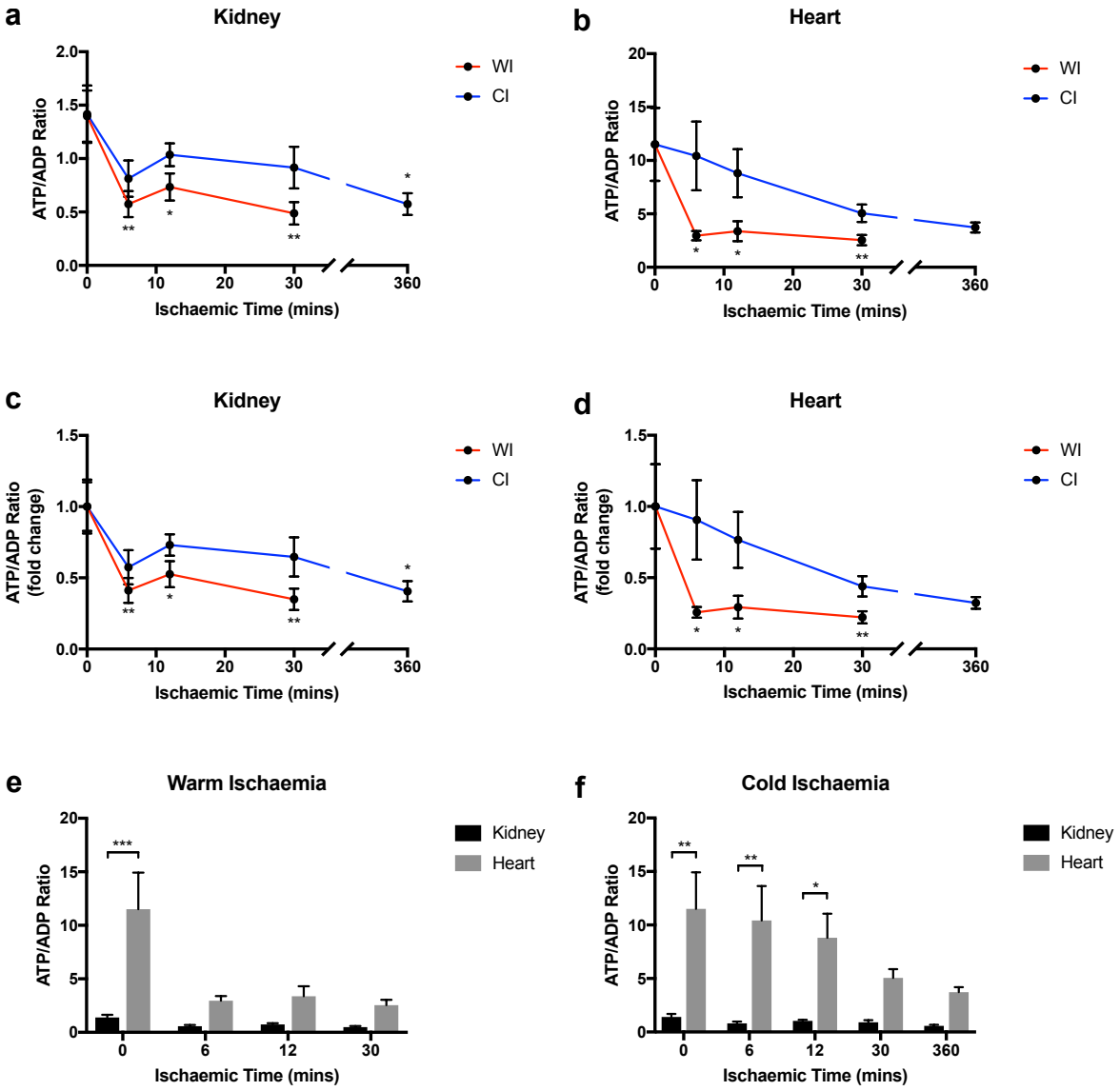

Figure 3.9 Changes in the ATP/ADP Ratio during Warm and Cold Ischaemia in the Pig Kidney and Heart. Tissue ATP/ADP ratio during warm ischaemia (WI) at 38 °C and cold ischaemia (CI) at 0-4 °C in the kidney (**a**) (n=4) and heart (**b**) (n=5). Relative change in tissue ATP/ADP ratio compared to normoxia during WI and CI in the kidney (**c**) and heart (**d**). Comparison of tissue succinate concentration in the kidney and heart during WI (**e**) and CI (**f**). *P < 0.05, **P < 0.01, ***P < 0.001, ****P < 0.0001. P values were calculated by one-way analysis of variance (ANOVA) with Dunnett's multiple comparison test (**a**-**d**) and two-way ANOVA with Sidak's multiple comparisons test (**e**-**f**). Data are mean ± SEM. Measurement of heart ATP and ADP concentration was performed by Ms Anja V Gruszczyk (MRC Mitochondrial Biology Unit, University of Cambridge, UK).

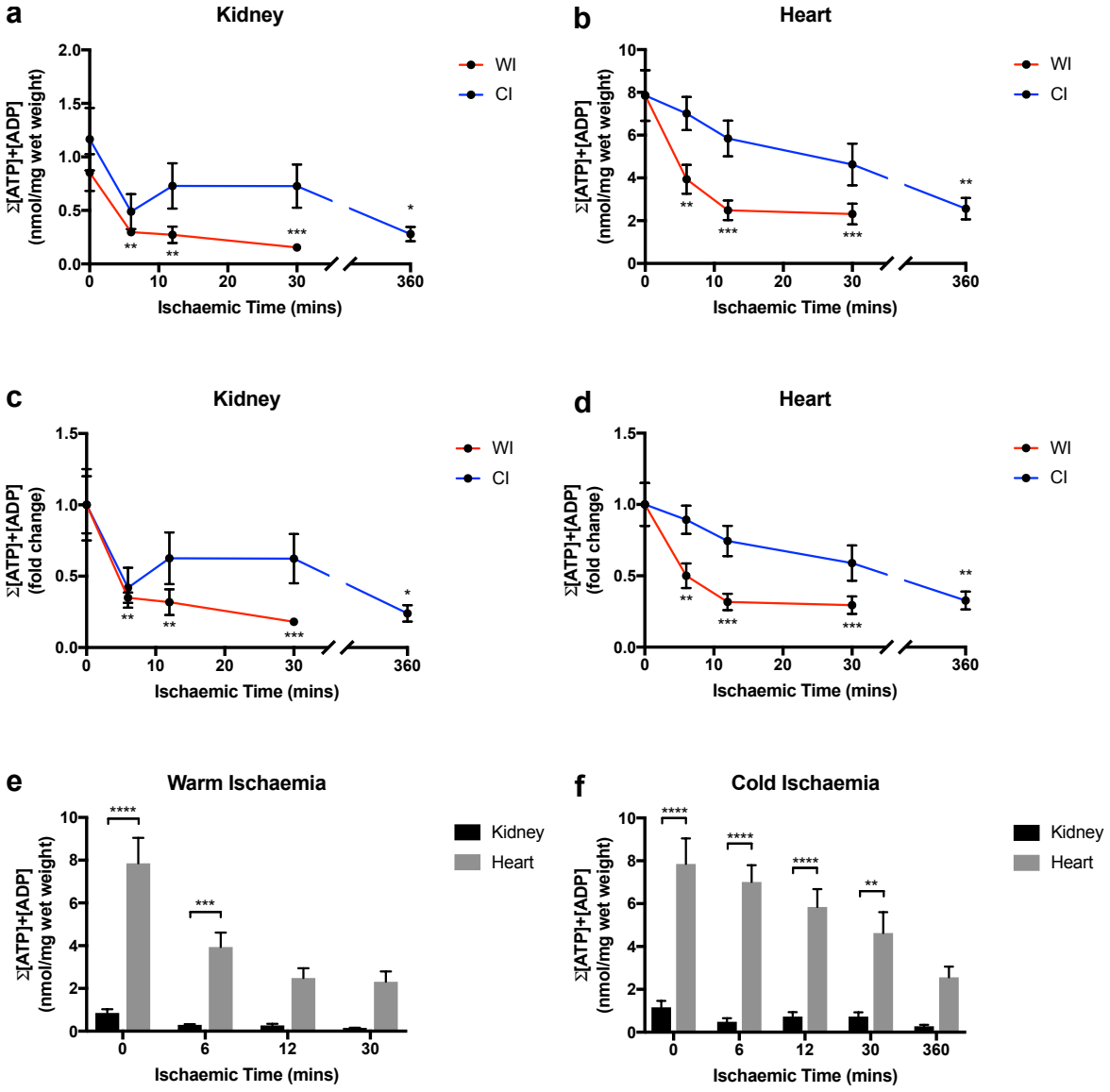

Figure 3.10 Total ATP and ADP Concentration during Warm and Cold Ischaemia in the Pig Kidney and Heart. Total ATP and ADP concentration during warm ischaemia (WI) at 38 °C and cold ischaemia (CI) at 0-4 °C in the kidney (**a**) (n=4) and heart (**b**) (n=5). Relative change in total ATP and ADP concentration compared to normoxia during WI and CI in the kidney (**c**) and heart (**d**). Comparison of tissue succinate concentration in the kidney and heart during WI (**c**) and CI (**d**). *P < 0.05, **P < 0.01, ***P < 0.001, ****P < 0.0001. P values were calculated by one-way analysis of variance (ANOVA) with Dunnett's multiple comparison test (**a**-**d**) and two-way ANOVA with Sidak's multiple comparisons test (**e**-**f**). Data are mean ± SEM. Measurement of heart ATP and ADP concentration was performed by Ms Anja V Gruszczyk (MRC Mitochondrial Biology Unit, University of Cambridge, UK).

3.4 Interim Summary I

The overall metabolic changes that occur during warm and cold ischaemia are conserved between the kidney and heart in mice and pigs. The absolute increase in succinate is greater in the heart than in the kidney during ischaemia which may be related to differences in underlying organ function and physiology. Fold changes relative to normoxia between species should be interpreted carefully in the above experiments as normoxic values may be affected by a delay (of even 10-20 s) in clamp freezing tissue in more complex animal models or due to legal restrictions on when tissue samples may be taken. Importantly however, succinate accumulation in the kidney acts as a potential therapeutic target during IRI in a similar manner to the heart.

3.5 Efficiency of Organ Cooling during Back-Table Flush

As shown above, succinate accumulates to near maximal levels within a few minutes of warm ischaemia and it has previously been shown that the rate of succinate accumulation within the ischaemic mouse heart is directly proportional to the temperature of the tissue (Figure 3.11a) [193]. A difference in succinate accumulation between DCD and DBD grafts, which may potentially explain the difference in rates of DGF between graft types as discussed above, is therefore likely to only exist if kidneys from DBD donors are cooled rapidly and to a sufficiently low temperature during the initial stages of organ retrieval. Organs from DBD donors are often flushed with ice-cold preservation solution *in situ* at the start of organ retrieval and topically cooled with slushed ice placed in the abdominal cavity. Following *in situ* flush, organs are dissected and retrieved from the donor before being packed on ice or undergo further flushing on the back-table. However, it is currently unclear as to the temperature the intra-abdominal organs reach during this process. If DBD kidneys are not cooled effectively during retrieval, increased succinate accumulation may occur leading to increased mitochondrial ROS production on transplantation. As mitochondrial ROS production is thought to initiate much of the downstream damage leading to IRI, minimising mitochondrial ROS production in kidney transplantation may be of benefit to both short and long-term graft function as previously discussed.

It has been shown that the mouse heart may be cooled to 4 °C in under 60 s of retrieval when submerged in ice cold preservation solution resulting in very limited succinate accumulation (Figure 3.11b) [193]. However, the mouse heart is small with a large surface area to volume ratio enabling rapid heat exchange to occur between the organ and preservation solution. In contrast, pig and human organs are much larger than in the mouse with a smaller

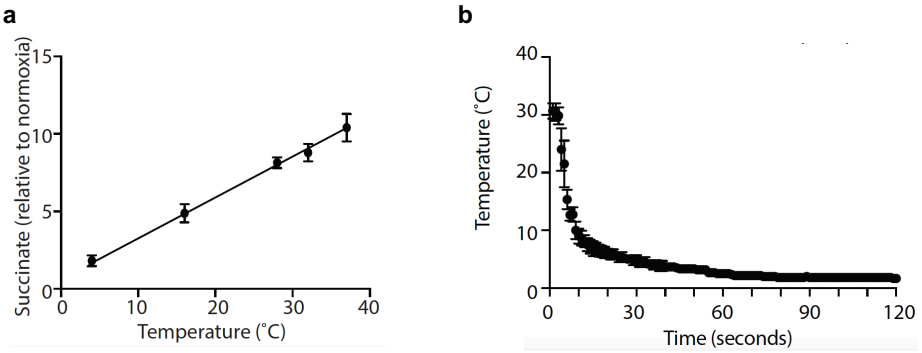

Figure 3.11 Succinate Accumulation During Organ Cooling in the Mouse Heart. (**a**) Succinate concentration relative to normoxia in the mouse heart following 12 mins ischaemia at various temperature (n=4-5). (**b**) Mouse heart temperature following rapid retrieval and submersion in ice cold preservation solution (n=3). Data are mean ± SEM. Figure adapted from Martin et al (2019).

surface area to volume ratio. Heat exchange between these larger organs and the preservation solution is therefore less efficient, likely taking much longer to reach a target temperature of 4 °C. Increased succinate accumulation may therefore occur in the larger organs in comparison to the mouse depending on the rate of cooling and final temperature reached. To investigate further, the temperature and succinate concentration of the pig kidney and heart was measured during organ cooling as shown in Figure 3.12. Again, due to restrictions under the Home Office Licence it was not possible to simulate the clinical protocol for the retrieval of organs from a DBD donor in the pig. Instead, the rate of organ cooling was investigated following rapid retrieval of the organ from the pig followed by ice-cold flush and submersion in slushed ice on the back-table, similar to the protocol used to cool kidney grafts from living donors. However, important information relating to the accumulation of succinate during the cooling of larger organs could still be gained and used to inform future experiments and aid in further hypothesis generation.

3.5.1 Surface and Core Temperature

During back-table flush, the core and surface temperature of the pig kidney (Figure 3.13a) and heart (Figure 3.13b) cooled to 10 °C in less than 10 mins; however, it took up to 30 mins for the core and surface tissue to reach a target temperature of 4 °C suggesting organ cooling became less efficient at lower temperatures. Pig kidneys weighed approximately 150 g and pig hearts approximately 300 g however there was no significant difference in time taken for the surface ((Figure 3.13c) or core ((Figure 3.13d) temperature of the two organs to reach 20, 10 or 4 °C.

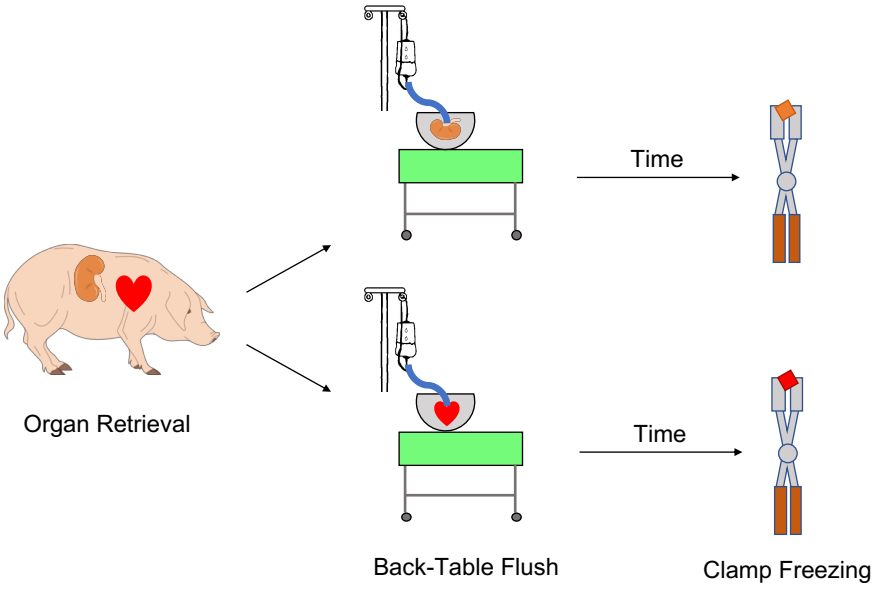

Figure 3.12 Modelling Organ Back-Table Flush in the Pig. Kidneys were retrieved from the pig under general anaesthesia. Hearts were retrieved from the pig immediately following euthanasia. A 0 mins surface wedge and core needle biopsy was taken from the kidney under conditions of normoxia prior to retrieval and from the heart on removal from the thorax. Organs were rapidly transferred to the back-table where the renal artery or coronary vessels were cannulated and temperature probes placed in the core and surface tissue of the organ. Organs were then submerged in slushed ice and flushed with either 500 mL ice cold Soltran (kidney) or UW (heart) solution. Wedge surface and core needle biopsies were taken at 6, 12 and 30 mins and rapidly clamp frozen in LN2. Tissue samples were then stored at -70 °C until further processing and analysis. Mr Kourosh Saeb-Parsy (University of Cambridge Department of Surgery, UK) and Ms Krishnaa T Mahbubani (University of Cambridge Department of Surgery, UK) assisted with the surgical procedure.

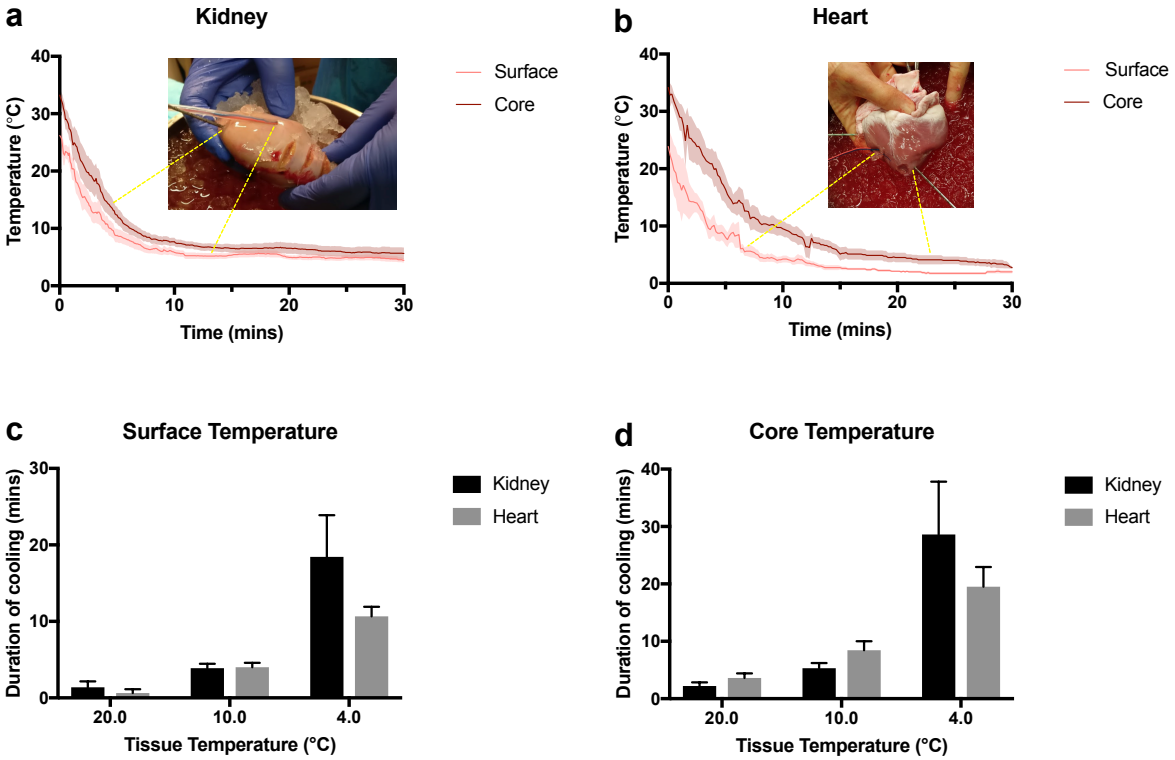

Figure 3.13 Temperature Changes during Back-Table Flush in the Pig Kidney and Heart. Surface and core temperature measured during back-table flush in the kidney (**a**) (n=4) and heart (**b**) (n=4). Comparison of the duration of organ cooling in the heart and kidney at the organ surface (**c**) and core (**d**). Data are mean ± SEM.

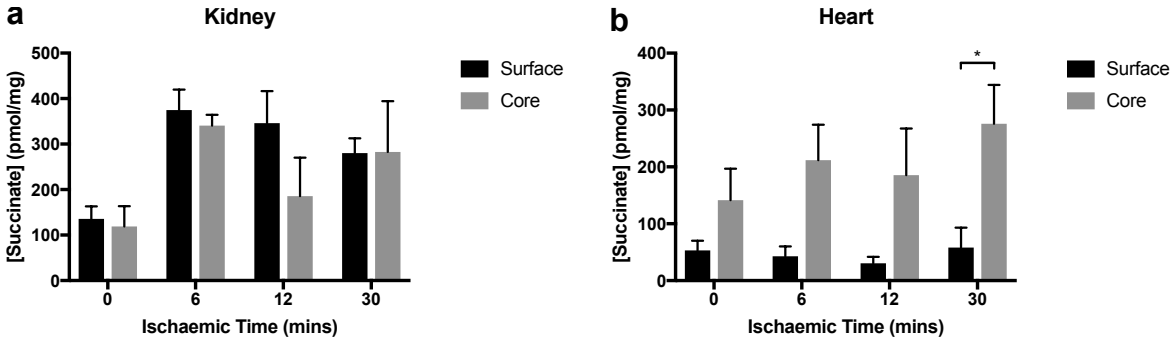

Figure 3.14 Tissue Succinate Concentration during Back-Table Flush in the Pig Kidney and Heart. Surface and core succinate concentration measured during back-table flush in the kidney (**a**) (n=3) and heart (**b**) (n=3). *P < 0.05. P values were calculated by two-way analysis of variance (ANOVA) with Sidak's multiple comparisons test. Data are mean ± SEM.

3.5.2 Succinate Accumulation

The surface succinate concentration increased in the kidney (Figure 3.14a) but not in the heart (Figure 3.14b) during back-table flush. This may partly relate to differences in the duration and complexity of organ retrieval or a delay in placing the organ in slushed ice during the insertion of the temperature probes. The core succinate concentration increased in both the kidney and heart during back-table flush and may relate to a slower rate of cooling of the core tissue compared to the surface tissue. As discussed above, this may relate to a smaller surface area to volume ratio in the pig kidney and heart compared to the mouse resulting in a slower rate of heat exchange between the organ and preservation solution. Whilst organs were actively flushed with cold preservation solution, the flow rate was relatively slow taking approximately 12.8 ± 4.2 mins to flush 500 mL preservation solution whilst the average temperature of the preservation solution entering the pig kidney was 8.5 ± 1.3 °C. Comparing the surface and core succinate concentration in the kidney and heart with the temperature values in Figure 3.13 suggests that whilst the surface may cool very rapidly to inhibit succinate concentration, the slower rate of cooling in the core of the tissue may enable greater succinate to occur due to the linear relationship between tissue temperature and succinate accumulation as shown in Figure 3.11a.

3.6 Metabolic Profile of Declined Human Kidneys

To determine whether a difference in succinate accumulation and adenine nucleotide levels existed between kidneys retrieved from DCD compared to DBD donors, declined human kidneys retrieved from deceased donors following standard procedures but subsequently deemed unsuitable for organ transplantation were accepted for research under full ethical approval

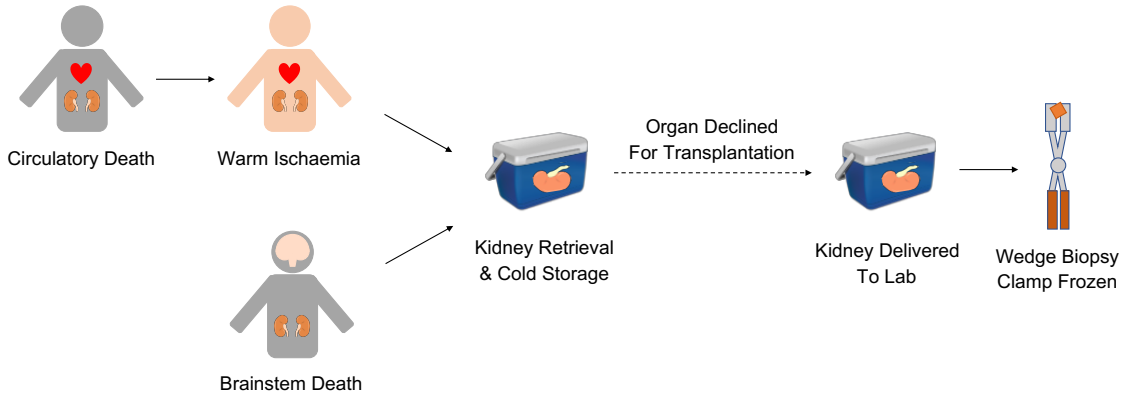

Figure 3.15 Acceptance of Declined Human Kidneys for Scientific Research. Human kidneys accepted for scientific research were retrieved from DBD and DCD donors following standard procedures. Organs from donation after cardiac death were exposed to a period of warm ischaemia prior to organ retrieval and cold storage whilst organs from donation after brainstem death were not. This is due to a mandatory 5 minute stand off period following cardiac arrest in order to confirm circulatory death. Following confirmation, organs experience an additional period of warm ischaemia whilst the aorta is accessed in order to begin *in situ* flush and organ cooling. This is in contrast to retrieval from DBD donors, in which organs remained perfused under conditions of normoxia until *in situ* flush begins. The average warm ischaemia time experienced by kidneys retrieved from DCD donors is currently 12 minutes in the UK. In the above diagram, grey figures represent normoxic organs *in situ* and pink figures represent organs undergoing warm ischaemia *in situ*.

and informed consent from donor families. Tissue succinate, ATP and ADP concentration were measured at the time of arrival of declined human kidneys to the laboratory under conditions of static cold storage as shown in Figure 3.15. Donor and organ characteristics for DCD and DBD kidneys accepted for research are detailed in Table 3.1

There was no significant difference in tissue succinate concentration between DCD and DBD kidneys, despite DCD kidneys undergoing 11 $\pm$ 4 mins of warm ischaemia prior to organ cooling (Figure 3.16a). Kidneys accepted from DBD donors underwent 9.5 $\pm$ 2.6 h of cold ischaemia whilst kidneys from DCD donors underwent 15.9 $\pm$ 2.3 h cold ischaemia (Table 3.1). The ATP/ADP ratio was lower in DCD kidneys however was not significantly different from the ratio in DBD kidneys (Figure 3.16b). The sum of the ATP and ADP concentration was similar in kidneys from both donor types (Figure 3.16c).

Donor Type	**DBD**	**DCD**
Age	68y 7m (±10y 7m)	55y 11m (±11y 7m)
Gender		
Male	4 (57%)	5 (83%)
Female	3 (43%)	1 (17%)
BMI	33.6 (±6.7)	27.6 (±4.5)
Cause of Death		
Intracranial Haemorrhage	3 (43%)	2 (33%)
Intracranial Thrombosis	2 (29%)	1 (17%)
Hypoxic Brain Damage	2 (29%)	3 (50%)
Kidney		
L	3 (43%)	2 (33%)
R	4 (57%)	4 (67%)
Type of Perfusate		
Soltran	2 (29%)	5 (83%)
UW	5 (71%)	1 (17%)
Quality of Perfusion		
Good	5 (71%)	5 (83%)
Fair	2 (29%)	1 (17%)
WIT	-	00:11 (±00:04)
CIT	09:32 (±02:37)	15:56 (±03:20)
Reason For Decline		
Donor history	1 (14%)	1 (17%)
Organ pathology	3 (43%)	3 (50%)
Atherosclerotic vessels	2 (29%)	-
Anatomy	1 (14%)	-
Poor perfusion	-	1 (17%)
Suspected malignancy	-	1 (17%)

Table 3.1 Donor & Organ Characteristics of Declined Human Kidneys. Kidneys were retrieved from either donation after brainstem death (DBD, *n*=7) or donation after circulatory death (DCD, *n*=6) donors under standard surgical procedures but subsequently deemed unsuitable for transplantation. Data are mean ± SD or absolute number. Organ pathology includes presence of multiple cysts, diabetic changes, parenchymal damage and unidentified masses.

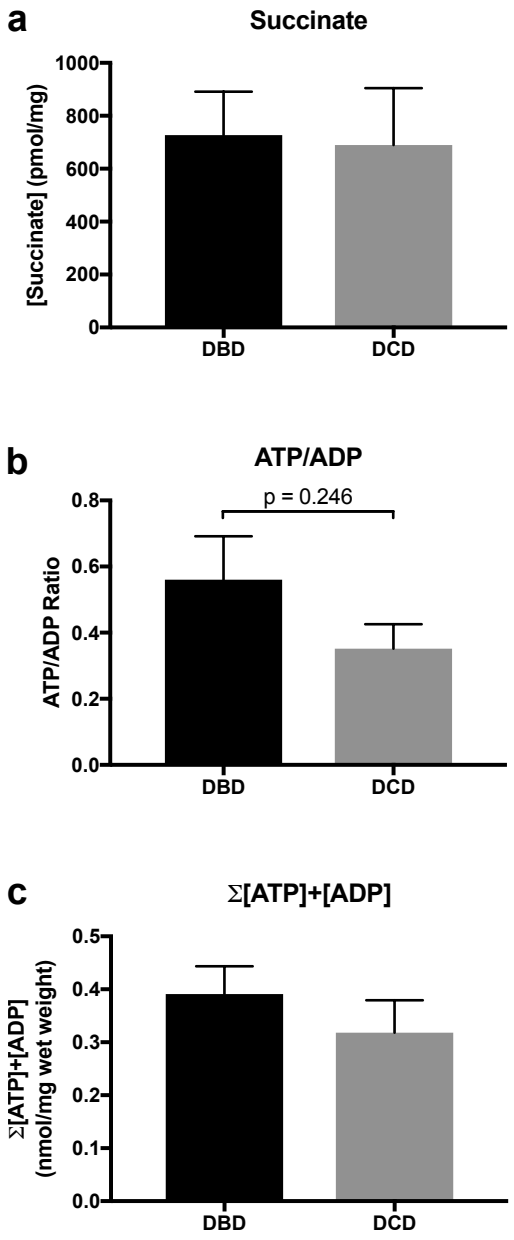

Figure 3.16 Metabolic Profile of Declined Human Kidneys Tissue succinate concentration (**a**), ATP/ADP ratio (**b**) and total ATP and ADP nucleotide concentration (**c**) ratio in human kidneys retrieved from DBD (n=7) and DCD (n=6) donation but subsequently declined for transplantation. P values were calculated using a two-tailed unpaired t test. Data are mean ± SEM.

3.7 Metabolic Changes during Warm Ischaemia in the Human Kidney

In order to quantify succinate accumulation in human kidneys during organ retrieval and cold storage, it was important to determine the baseline succinate concentration in the human kidney under conditions of normoxia. However, it was not possible to obtain a normoxic tissue sample from a living human for obvious ethical reasons. It was also not possible to biopsy a kidney from a DBD donor prior to *in situ* flush, again due to lack of ethical approval and as most kidneys are not declined for human transplantation until after retrieval and examination on the back-table. However, as succinate is known to rapidly return to normoxic levels on reperfusion, EVNP was used to determine the concentration of succinate in the human kidney under conditions of normoxia and confirm succinate accumulation had occurred during organ retrieval and preservation of human kidneys from DBD and DCD donors. *Ex vivo* normothermic perfusion refers to the reperfusion of an organ outside the body with an oxygenated whole blood perfusate at 36 °C. This is achieved using an adapted cardio-pulmonary bypass circuit as discussed in Chapter 2 (see Figure 2.1). In addition to investigation of the metabolic changes that occur during organ retrieval and cold storage in human kidneys, ethical approval was obtained for a wedge biopsy to be taken from the heart of DBD donors that were not suitable for cardiac transplantation. Part of the biopsy could be rapidly clamp frozen in liquid nitrogen as soon as it was taken from the donor to determine the normoxic succinate concentration in the heart and the remaining tissue exposed to either warm or cold ischaemia as shown Figure 3.17. Similarly, following EVNP, human kidneys could be re-exposed to warm or cold ischaemia to investigate succinate accumulation and changes in ATP and ADP concentration under more controlled conditions. The differences between the human kidney and heart could then be compared in a similar manner to the mouse and pig, to determine whether the metabolic changes measured in these models reflect those in the human and whether succinate accumulation may be targeted in similar manner in the human kidney and heart to that in the mouse and pig.

Succinate levels were similar in the kidney and heart under conditions of normoxia and succinate accumulation had occurred in declined human kidney during organ retrieval and cold preservation. In contrast to the pig, the succinate concentration was similar in the kidney and heart at 30 mins warm ischaemia, reaching a concentration of 890 pmol/mg (Figure 3.18a) or 5-fold (Figure 3.18b) the normoxic value in kidney and 1370 pmol/mg (Figure 3.18a) or 9-fold (Figure 3.18b) the normoxic value in the heart. However, values in the heart were variable and may have resulted from difficulties in maintaining the temperature of heart tissue at 36 °C. Interestingly, the succinate concentration in the kidney at 30 mins warm

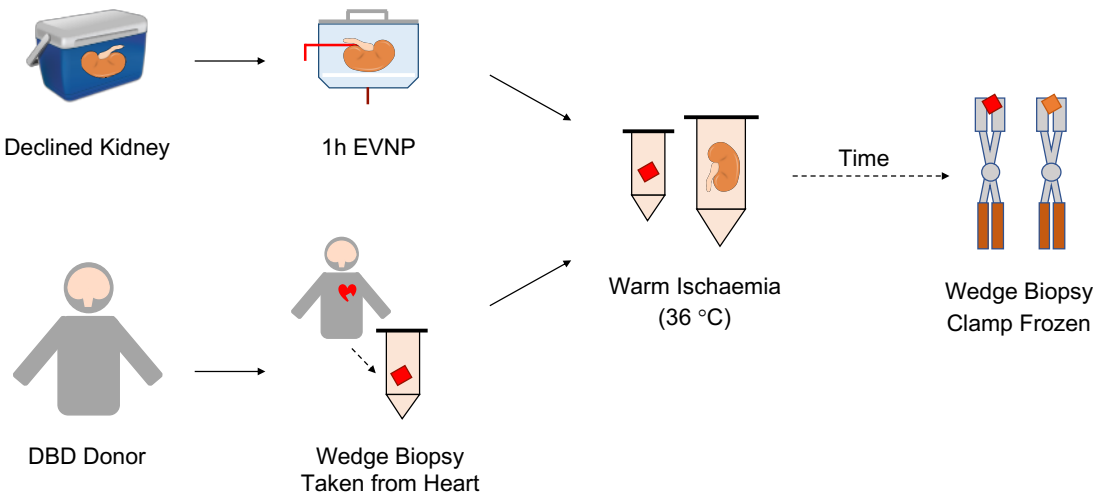

Figure 3.17 Investigating the Metabolic Changes That Occur During Warm Ischaemia in the Human Heart and Kidney. Declined human kidneys were accepted for research as previously described and reperfused for 1 h using EVNP (see Figure 2.1) to 'reset' their metabolic profile. After one hour EVNP, a tissue wedge biopsy was then taken from the kidney under conditions of normoxia and rapidly clamp frozen in LN2 using Wollenburg clamps to act as a baseline control. Kidneys were then placed in a bag and submerged in a water bath set to 36 °C to simulate conditions of warm ischaemia. Meanwhile, ethical approval was obtained for a wedge biopsy to be taken from the heart of a DBD donor under conditions of a normoxia. A section of the wedge biopsy was immediately clamp frozen in LN2 to act as a baseline control. The remaining tissue was placed in a humidified eppendorf tube maintained at 36 °C in a heat block to simulate conditions of warm ischaemia. Wedge tissue biopsies from kidney and heart were rapidly clamp frozen in LN2 using Wollenburg clamps immediately after 30 mins warm ischaemia. Tissue samples were then stored at -70 °C until further processing and analysis. Mr Kourosh Saeb-Parsy (University of Cambridge Department of Surgery, UK), Mr Jack L Martin (University of Cambridge Department of Surgery, UK), Ms Anja V Gruszczyk (MRC Mitochondrial Biology Unit, University of Cambridge, UK) and Ms Krishnaa Mahbubani (University of Cambridge Department of Surgery, UK) assisted with the collection of heart tissue from human DBD donors.

ischaemia was similar to levels measured in declined human kidneys from DBD and DCD donors and may represent a maximum succinate concentration.

Similar to in the pig, the ATP/ADP ratio was significantly greater in the human heart than in the human kidney under conditions of normoxia, although the human kidney had only undergone 1 h EVNP following a period of cold static storage and the ATP/ADP levels may have not fully recovered due to nucleotide depletion and cellular necrosis. The ATP/ADP ratio was 1.4 (Figure 3.18c) in the human kidney following 1 h EVNP and 6.7 (Figure 3.18c) in the human heart. Following subsequent exposure to 30 mins warm ischaemia, the ATP/ADP ratio decreased to 0.4 (Figure 3.18c) or 30% (Figure 3.18d) the normoxic value in the human kidney and 1.6 (Figure 3.18c) or 24% (Figure 3.18d) the normoxic value in the human heart. However there was no significant difference in the ATP/ADP ratio between the two organs. The sum of the ATP and ADP concentration was also significantly greater in the human heart than in the human kidney under conditions of normoxia but again may partly relate to the previous exposure of the human kidney to ischaemia and short duration of EVNP. The sum of the ATP and ADP concentration under conditions of normoxia was 1.0 pmol/mg (Figure 3.18e) in the human kidney and 7.4 pmol/mg (Figure 3.18e) in human heart. Following 30 mins subsequent warm ischaemia, the sum of the ATP and ADP concentration decreased to 0.26 pmol/mg (Figure 3.18e) or 25% (Figure 3.18f) the normoxic value in the human kidney and 1.6 pmol/mg (Figure 3.18e) or 22% (Figure 3.18f) the normoxic value in the human heart; however there was again no significant difference in the sum of the ATP and ADP concentrations between the organs at this time point. Overall, the changes measured in the ATP/ADP ratio and sum of the ATP and ADP concentration closely reflected those measured in the pig, further supporting the use of the pig as a translational model in organ transplant studies.

3.8 Interim Summary II

There was no significant difference in succinate concentration in kidneys retrieved from DCD donors compared to DBD donors and succinate accumulation had occurred during organ retrieval and cold storage in both donor types. The tissue succinate concentration measured in declined human kidneys was similar to that measured following exposure of human kidneys to 30 mins warm ischaemia and may reflect a maximal succinate concentration, measuring approximately 800 pmol/mg or 5-fold normoxic levels. As succinate accumulation appeared to be near maximal in kidneys retrieved from both DCD and DBD donors, grafts from both donor types may benefit from interventions aimed at reducing succinate accumulation that occurs during organ retrieval and cold static storage. This may subsequently lead to a

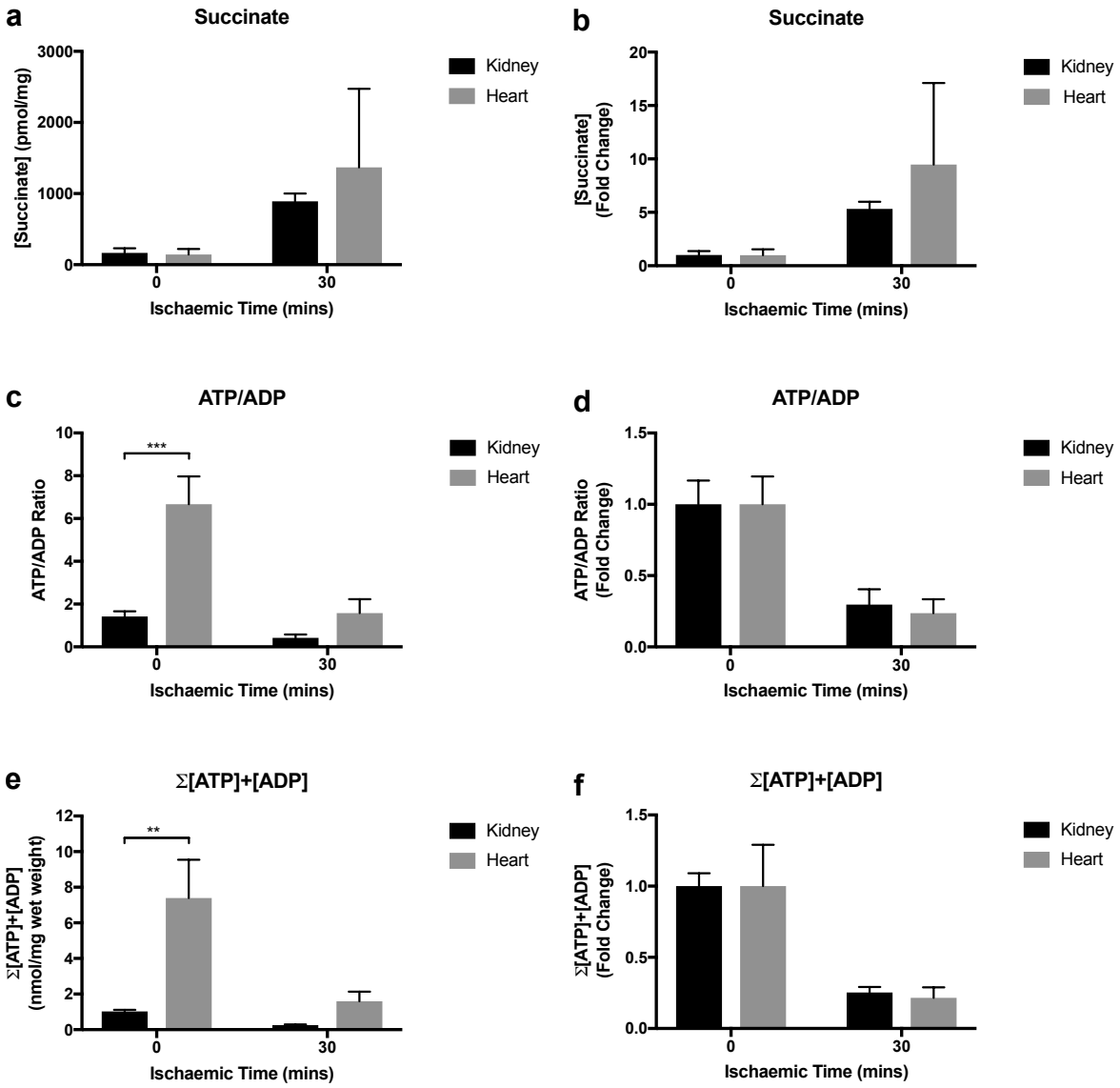

Figure 3.18 Metabolic Changes During Warm Ischaemia in the Human Kidney and Heart. Tissue succinate concentration (**a**), ATP/ADP ratio (**c**) and total ATP and ADP nucleotide concentration (**f**) in human kidneys (n=4) and heart (n=3) immediately before and after 30 mins warm ischaemia. The fold change in succinate (**b**), ATP/ADP ratio (**d**) and total ATP and ADP nucleotide concentration (**f**) in kidney and heart is also shown relative to normoxic values. **P < 0.01, ***P < 0.001. P values were calculated using two-way analysis of variance (ANOVA) with Sidak's multiple comparison test. Data are mean ± SEM. Measurement of heart ATP and ADP concentration was performed by Ms Anja V Gruszczyk (MRC Mitochondrial Biology Unit, University of Cambridge, UK).

reduction in mitochondrial ROS production on transplantation (via the mechanisms discussed above), ultimately reducing the level of IRI and improving both short and long-term graft outcomes.

3.9 Effect of Malonate Ester Pro-Drugs on Succinate Accumulation during Warm Ischaemia

Inhibition of succinate accumulation during organ retrieval and preservation may reduce mitochondrial ROS production and organ injury on transplantation, thereby resulting in improved graft and patient outcomes. To investigate whether succinate accumulation may be inhibited with malonate ester pro-drugs during organ retrieval and preservation, DMM was administered prior to warm ischaemia in mouse and pig models of kidney donation.

3.9.1 Effect of DMM on Succinate Accumulation in the Mouse Kidney During Warm Ischaemia

To determine whether succinate accumulation could be inhibited during warm ischaemia in a mouse model of kidney donation, DMM was administered to mice prior to onset of warm ischaemia as shown in Figure 3.19. Tissue malonate, succinate, ATP/ADP ratio and total ATP and ADP nucleotide concentration following administration of DMM and at the end of 20 mins warm ischaemia is shown in Figure 3.20.

Tissue malonate concentration significantly increased with increasing doses of DMM and a high tissue malonate concentration was present in kidneys immediately following administration of DMM (Figure 3.20a, Pre-Isc, black bars) and at the end of warm ischaemia (Figure 3.20a, End Isc, grey bars). However, administration of DMM did not appear to inhibit the accumulation of succinate during 20 mins warm ischaemia and succinate levels were even significantly increased at the end of warm ischaemia following administration of 3.2 and 6.4 mg DMM (Figure 3.20b, End-Isc, grey bars). Succinate concentration was also significantly increased following administration of 6.4 and 12.8 mg DMM prior to the onset of warm ischaemia (Figure 3.20b, Pre-Isc, black bars) and was possibly due to forward inhibition of SDH by malonate under conditions of normoxia. Meanwhile, tissue ATP/ADP ratio (Figure 3.20c) and the sum of the ATP and ADP concentration (Figure 3.20d) were unaffected by administration of DMM.

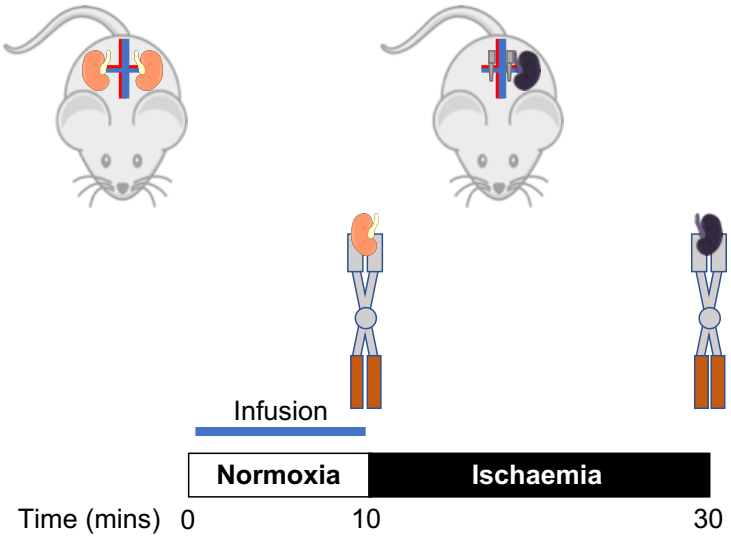

Figure 3.19 Targeting Succinate Accumulation During Warm Ischaemia in the Mouse. Mice were anaesthetised and the renal hila dissected. An infusion of DMM (0.8, 1.6, 3.2, 6.4 or 12.8 mg) or saline control was given over a period of 10 mins immediately prior to the onset of ischaemia. One kidney was rapidly retrieved and clamp frozen in liquid nitrogen using Wollenburg clamps at the end of the infusion immediately prior to the onset of ischaemia. The second kidney was then rapidly retrieved and clamp frozen following 20 mins warm ischaemia induced by placing a micro-serrefine clamp over the renal hila. Successful occlusion of the renal hila resulted in a change colour of each kidney from orange to dark purple. The core temperature of the mouse was maintained at 36 °C at all times by a closed loop temperature control system. Tissue samples were stored at -70 °C until further processing and analysis.

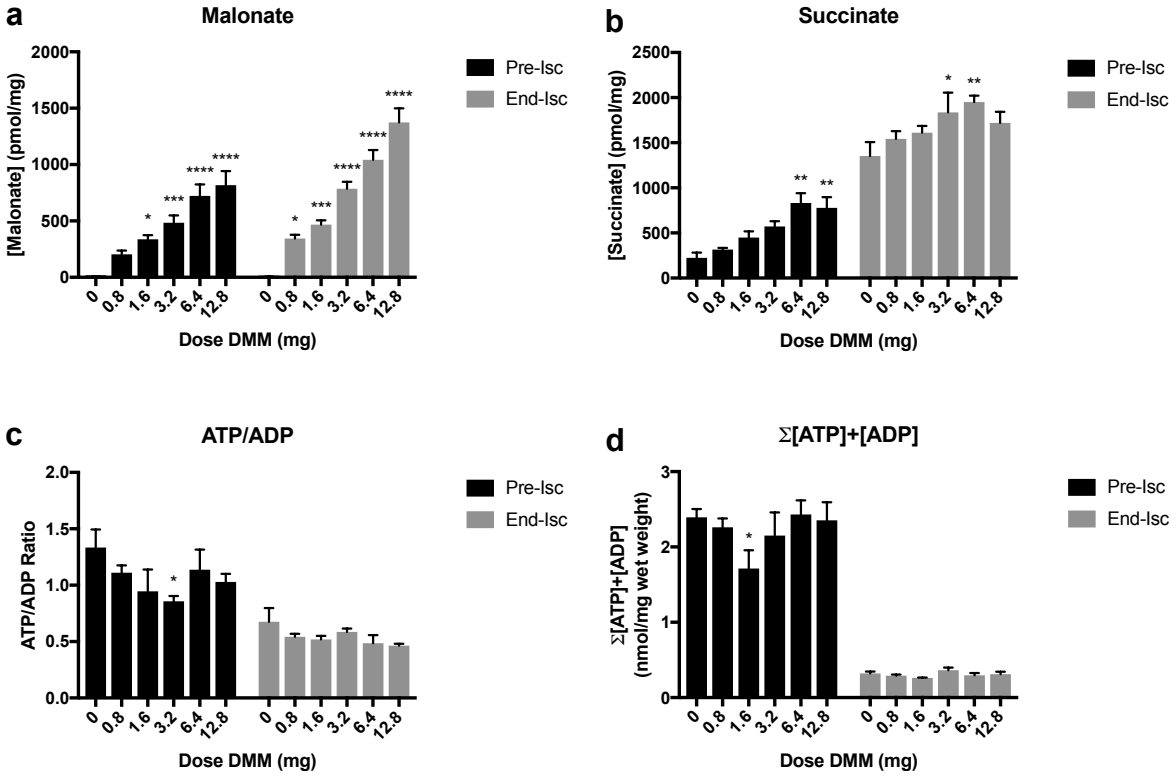

Figure 3.20 Metabolic Changes during Warm Ischaemia in the Mouse Kidney following Administration of DMM. Tissue malonate (**a**) (n=4), succinate (**b**) (n=4), ATP/ADP ratio (**c**) (n=4) and total ATP and ADP concentration (**d**) (n=4) immediately following infusion of DMM (0.8, 1.6, 3.2, 6.4 or 12.8 mg) or saline control (0) prior to the onset of ischaemia (black bars) and after 20 mins warm ischaemia (grey bars) in the mouse kidney. *P < 0.05, **P < 0.01, ***P < 0.001, ****P < 0.0001. P values were calculated by two-way analysis of variance with Sidak's multiple comparisons test. Data are mean ± SEM.

3.9.2 Effect of DMM on Succinate Accumulation in the Pig Kidney during Warm Ischaemia

To determine whether succinate accumulation could be inhibited during warm ischaemia in a more clinically relevant model of kidney donation, a preliminary set of experiments were performed in the pig. This was to determine the feasibility of administering DMM to larger animals (to better inform human studies) prior to warm ischaemia and to investigate the dose of DMM required. Dimethyl malonate was administered as an intravenous bolus dose to the pig via the ear vein prior to onset of warm ischaemia as shown in Figure 3.21. Following administration, DMM was allowed to circulate in the pig for either 5, 10 or 30 mins prior to the kidney retrieval and onset and warm ischaemia. Tissue malonate and succinate concentrations were measured immediately before and at the end of 30 mins warm ischaemia. Doses of DMM were chosen based on allometric scaling of effective doses previously reported in the mouse [262] [14]. Allometric scaling was conducted on the basis of differences in body surface area between species using a conversion table produced by the Food and Drug Administration of the United States (FDA). The underlying principle of scaling of drug doses based on body surface area is that larger animals are thought to have a reduced ability to gather and dissipate energy and so have adapted to this limitation by reducing their underlying rate of metabolism. As a result a smaller dose of a drug is required to achieve the same therapeutic effect per unit weight in larger animals owing to their decreased rates of drug metabolism [262]. In addition, as it was not possible to give DMM as an infusion to the pig due to restrictions under the Home Office Licence, DMM was given as an intravenous bolus dose. This meant that a steady state level of malonate could not be established in the kidney prior to retrieval as in the mouse and instead a number of different time points (5, 10 and 30 mins) following the administration of the DMM bolus were investigated in order to determine the point at which the malonate concentration within the kidney was greatest (as DMM must first distribute to the kidney following injection and subsequently undergo hydrolysis to release active malonate) [263].

Figure 3.22 shows the tissue malonate and succinate concentration immediately before and after 30 mins warm ischaemia in the pig kidney following systemic administration of 840 mg DMM. This dose was based on allometric scaling of the reported effective dose of 160 mg/kg in the mouse for a 60 kg pig. DMM was given as a bolus injection into the ear vein and was allowed to circulate systemically in the pig for either 5, 10 or 30 mins prior to warm ischaemia. Administration of DMM led to an increase in malonate concentration in the kidney prior to warm ischaemia and was highest after 5 mins systemic circulation (Figure 3.22a, Pre-Isc, black bars). During warm ischaemia, tissue malonate concentration increased further in the kidney suggesting hydrolysis of DMM continued to occur in ischaemic tissue

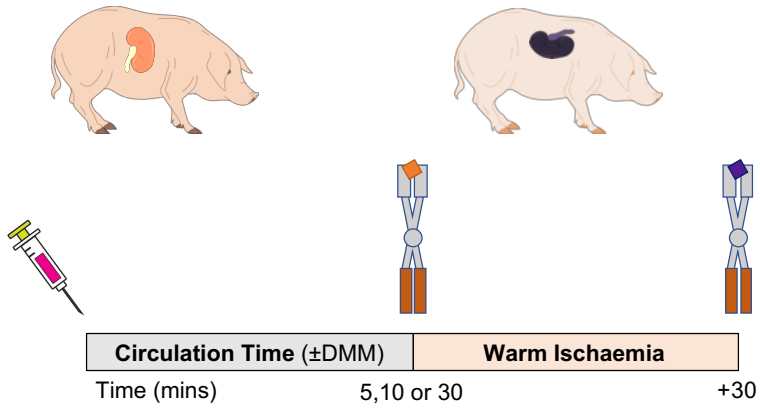

Figure 3.21 Targeting Succinate Accumulation During Warm Ischaemia in the Pig. One kidney was retrieved from the pig prior to administration DMM and exposed to 30 mins warm ischaemia in order to act as a control (not shown). A wedge biopsy was taken *in situ* and following 30 mins warm ischaemia from the control kidney and rapidly clamp frozen in LN2 using Wollenburg clamps (not shown). Dimethyl malonate was then administered as a bolus injection into the ear vein of the pig and allowed to circulate systemically for 5, 10 or 30 mins. Following 5, 10 or 30 mins circulation, an *in situ* wedge biopsy was taken from the second kidney and rapidly clamp frozen. The renal vessels were then tied and divided and the kidney was exposed to 30 mins warm ischaemia in abdomen of the pig maintained at 38 °C. During warm ischaemia pig kidneys became purple in colour due to the presence of deoxygenated blood within the microvasculature. Following 30 mins warm ischaemia, a second wedge biopsy was taken and rapidly clamp frozen. Tissue samples were stored at -70 °C until further processing and analysis. Mr Kourosh Saeb-Parsy (University of Cambridge Department of Surgery, UK) and Miss Krishnaa T Mahbubani (University of Cambridge Department of Surgery, UK) assisted with the surgical retrieval of kidneys from the pig.

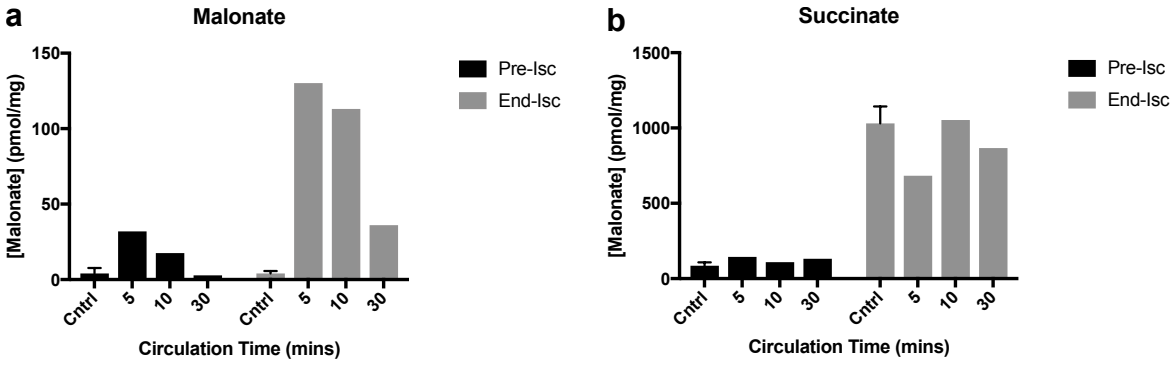

Figure 3.22 Metabolic Changes during Warm Ischaemia in the Pig Kidney following Administration of DMM. 840 mg DMM in 20 mL saline was administered as a bolus injection into the ear vein and allowed to circulate systemically within the pig for either 5, 10 or 30 mins (n=1 per time point). Tissue malonate (**a**) and succinate (**b**) concentration were then measured immediately before (black bars) and after (grey bars) 30 mins warm ischaemia. DMM treated kidneys were compared to control kidneys (Cntrl) retrieved from the pig and exposed to 30 mins warm ischaemia prior to the administration of DMM (n=3). Data are mean of technical replicates measured from DMM treated kidneys and mean $\pm$ SEM of control kidneys.

and was greatest in kidneys that had been retrieved following 5 mins DMM circulation time (Figure 3.22a, End-Isc, grey bars). In addition, administration of DMM did not appear to affect tissue succinate concentration prior to warm ischaemia in contrast to the mouse (Figure 3.22b, Pre-Isc, black bars). At the end of 30 mins warm ischaemia, succinate concentration appeared to be decreased in the kidney treated with 840 mg DMM and retrieved after 5 mins systemic circulation (Figure 3.22b, End-Isc, grey bars) however repeat experiments and statistical testing would be needed to validate this finding in order to show a true reduction in succinate occurred and this preliminary result was not due to chance.

Administration of a ten times higher dose of DMM was also investigated in the pig as shown in Figure 3.23 as malonate concentrations achieved with 840 mg were roughly ten times lower than those achieved in the mouse. This led to a much higher malonate concentration in the pig kidney following 5 mins systemic circulation and at the end of 30 mins warm ischaemia. However, tissue succinate concentration was also increased following 5 mins systemic circulation, possibly due to forward inhibition of SDH activity and was greater than control values at the end of 30 mins warm ischaemia. Tissue malonate concentration following 10 mins systemic circulation of 8400 mg DMM was similar to doses achieved following 5 mins systemic circulation of 840 mg DMM. Tissue succinate concentration was not increased in kidneys following 10 mins systemic circulation of 8400 mg DMM and succinate concentration at 30 mins warm ischaemia was decreased compared to control values. It is also important to note that administration of 8400 mg DMM led to significant bradycardia and near cardiac arrest over the administration period and disodium

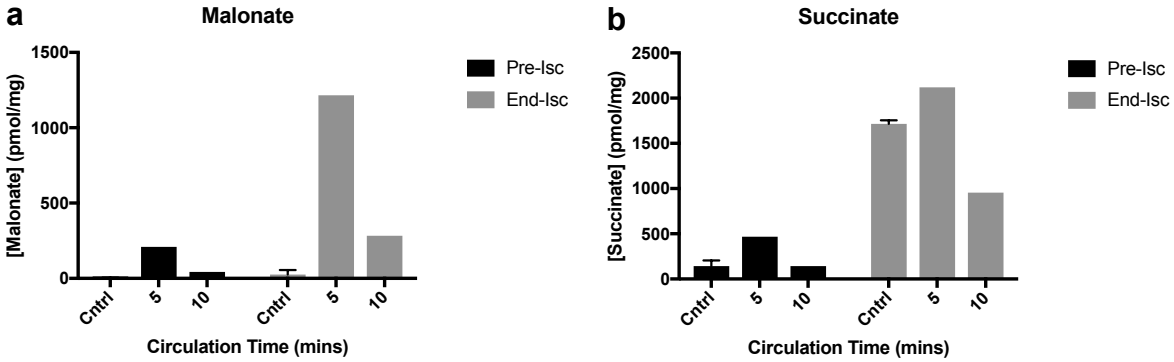

Figure 3.23 Metabolic Changes during Warm Ischaemia in the Pig Kidney following Administration of DMM. 8400 mg DMM in 100 mL saline was administered as a bolus injection into the ear vein and allowed to circulate systemically within the pig for either 5 or 10 mins (n=1 per time point). Tissue malonate (**a**) and succinate (**b**) concentration were then measured in DMM-treated kidneys immediately before (black bars) and after (grey bars) 30 mins warm ischaemia. DMM treated kidneys were compared to control kidneys (Cntrl) retrieved from the pig and exposed to 30 mins warm ischaemia prior to the administration DMM (n=3). Data are mean of technical replicates measured from DMM treated kidneys and mean ± SEM of control kidneys.

malonate has previously been reported to inhibit cardiac function at high doses in the mouse heart [194].

3.10 Discussion

3.10.1 Metabolic Changes During Warm and Cold Ischaemia in the Mouse and Pig Kidney

Overall, the metabolic changes that occur during warm and cold ischaemia in the kidney were similar to those in the heart in which most previous work had been conducted. Note that a maximal warm ischaemia time of 30 mins was chosen based on previous experiments demonstrating further changes in tissue succinate, ATP and ADP concentration do not occur beyond this time [193]. Succinate accumulated rapidly during warm ischaemia in both organs, increasing to 5-10 fold normoxic levels within a few minutes of ischaemia. In contrast, the rate of succinate accumulation was greatly reduced under conditions of cold ischaemia in the kidney and heart (provided the tissue could be cooled rapidly), with a 5-10 fold increase in succinate concentration occurring after 6-8 h cold ischaemia. Similar responses in the ATP/ADP ratio and sum of the ATP and ADP concentration in the kidney and heart were also measured during warm and cold ischaemia. The ATP/ADP ratio and the sum of the ATP and ADP nucleotides decreased rapidly during warm ischaemia reaching a minimal value

within 30 mins. In comparison the ATP/ADP ratio and sum of the ATP and ADP nucleotides decreased more gradually during cold ischaemia and had not reached the minimum value measured during warm ischaemia at 6-8 h cold storage. The similarities in the metabolic changes in the mouse and pig, kidney and heart strongly suggests a conserved mechanism of succinate accumulation occurs across the two organs as well as between species. However, succinate accumulated to a much higher concentration in the heart than in the kidney during warm ischaemia and took longer to reach its maximal tissue concentration. This may partly relate to the greater ATP and ADP concentration in the heart compared to the kidney under conditions of normoxia which may subsequently provide a greater supply of fumarate via the PNC for SDH reversal and succinate accumulation during ischaemia. Interestingly the rate of succinate accumulation appears to mirror the rate of ATP and ADP degradation in both the heart and the kidney but requires further investigation. Increased levels of succinate accumulation during ischaemia have been shown to lead to increased ROS production upon reperfusion suggesting a larger burst of mitochondrial ROS may occur in the heart than in the kidney on reperfusion but again this hypothesis requires further investigation within an *in vivo* system [14]. Nevertheless, the metabolic conditions required for mitochondrial ROS production on reperfusion are established during ischaemia in the kidney and inhibition of succinate accumulation may reduce mitochondrial ROS production and severity of ischaemia reperfusion injury in the kidney as in the heart [14].

3.10.2 Metabolic Changes During Organ Retrieval and Preservation of Declined Human Kidneys

Succinate concentration was not significantly greater in declined human kidneys retrieved from DCD compared to DBD donors and was greater than the succinate concentration measured in the human kidney under conditions of normoxia, suggesting succinate accumulation occurred during retrieval and cold preservation of grafts from both donor types. Investigation of organ cooling showed that core and surface tissue was rapidly reduced to 10 °C during back-table flush but took up to 30 mins to reach a target temperature of 4 °C. The rate of succinate accumulation varies linearly with temperature and increased succinate accumulation will occur where organs are not cooled efficiently [193]. During human organ donation, organs are first flushed with cold preservation solution *in situ* via cannulation of the aorta and slushed ice is applied topically to the organs in the abdominal cavity. However, organs must then be dissected and retrieved from the abdominal cavity before they are transferred to the back-table for further flushing and cold storage on ice. Given the difficulty and duration required to cool organs to 4 °C under the experimental conditions described in Section 3.5,

it is unlikely that large human organs are efficiently cooled to 4 °C during clinical organ donation. Inefficient organ cooling during back-table flush has also been reported by Kuiper et al [264]. Together, these findings suggest inefficient cooling may result in the accumulation of succinate during the retrieval of grafts from both DBD and LD despite rapid *in situ* and back-table flush.

Furthermore, succinate accumulation is not completely inhibited during cold ischaemia at 4 °C and continues to occur at a slow rate as shown in the mouse and pig. Given the relatively long duration of cold ischaemia experienced by DCD and DBD grafts prior to transplantation, a significant degree of succinate accumulation during cold preservation is also likely to occur. Succinate reached a maximum concentration after 12 h cold ischaemia in the mouse heart (Martin et al, 2019) and the succinate concentration measured in declined human kidneys following either 9.5 $\pm$ 2.6 h (DBD) or 15.9 $\pm$ 2.3 h (DCD) cold preservation was similar to the maximum succinate concentration measured in human kidneys following exposure to 30 mins warm ischaemia. Nevertheless, this finding suggests that both DCD and DBD kidneys may benefit from therapeutic interventions aimed at reducing succinate accumulation during organ retrieval and cold storage.

3.10.3 Effect of DMM on Succinate Accumulation in the Mouse and Pig Kidney during Warm Ischaemia

Whilst DMM has previously been shown to inhibit succinate accumulation during warm ischaemia in the mouse heart [14], administration of DMM prior to ischaemia in a mouse model of kidney donation did not lead to a reduction in tissue succinate concentration following 20 mins warm ischaemia. The metabolic conditions required for succinate accumulation via SDH reversal during ischaemia are thought to include a highly reduced NAD^+/NADH pool, inactivation of complexes III and IV and upregulation of the PNC. It is unlikely that these conditions occur instantaneously on the onset of ischaemia but probably develop over seconds to minutes, after which SDH reversal may begin. In the intervening period other pathways, such as glutaminolysis and canonical CAC action, may contribute to succinate accumulation [175]. Interestingly, approximately 15% of whole-body glutamine flux is taken up by the kidney and is primarily used in the process of ammoniagenesis with the resulting α-ketoglutarate entering the CAC cycle [265]. Whilst the mechanisms of succinate accumulation during ischaemia have been investigated in the mouse heart, the same is not true for the kidney. This is partly due to lack of a suitable model in the kidney equivalent to the Langendorff system in the heart and the difficulty in performing metabolic tracing experiments *in vivo* [266]. However, a better understanding of the underlying mechanisms of

succinate accumulation in different tissues and organs may be crucial in effectively targeting this process in organ transplantation and other ischaemia reperfusion related pathologies.

Meanwhile, preliminary experiments in the pig model of kidney donation mirrored findings in the mouse at high concentrations of DMM, however inhibition of succinate accumulation may have occurred at certain lower concentrations of DMM. Again, these findings re-emphasise that the correct timing and dose of malonate ester pro-drugs is crucially important in achieving therapeutic effects and that these important issues are not yet fully understood requiring further investigation.

3.11 Summary

In summary, increased succinate accumulation dose not occur following donation after cardiac death compared to donation after brainstem death and near maximal succinate accumulation occurs in grafts from both human DCD and DBD donors. This is likely due to inefficiencies in organ cooling during retrieval and continued succinate accumulation during cold preservation. Grafts from both donor types may benefit from inhibition of succinate accumulation however further work is needed to determine whether malonate ester pro-drugs may be used to inhibit succinate accumulation when administered prior to organ ischaemia. Alternatively, rapid oxidation of succinate may be targeted in grafts from both donor types on reperfusion, restricting the re-entry of electrons into the electron transport chain and driving force for mitochondrial ROS production and will be discussed in the next Chapter.

Chapter 4

Mitochondrial ROS Production in Kidney Transplantation

4.1 Introduction

As previously discussed, IRI is a two-stage process involving an ischaemic phase where an organ or tissue is deprived of oxygenated blood and a reperfusion phase where the supply of oxygenated blood to the organ or tissue is returned. Paradoxically, the injury that occurs during the reperfusion phase is over and above that which occurs during the ischaemia phase alone and is thought to result from a burst of ROS from mitochondria [16]. Whilst this process was previously attributed to the general 'spill' of electrons from damaged mitochondrial components upon reperfusion, increasing evidence now points to a more specific mechanism of mitochondrial ROS production [15]. In brief, the accumulation of succinate during ischaemia acts as a store of electrons capable of driving RET and ROS production from the FMN site of Complex I on reperfusion [14]. As Complex I operates close to thermodynamic equilibrium, it can reverse its action when the Δp across the inner mitochondrial membrane is greater than the ΔE_h required to push two electrons from NADH to CoQ. On reperfusion, a near maximal Δp develops across the inner mitochondrial membrane due to the depletion of adenine nucleotides and lack of substrate for $F_O F_1$-ATPase. Meanwhile, the rapid oxidation of accumulated succinate by SDH results in a highly reduced CoQ pool which drives RET through Complex I, culminating in superoxide production (Figure 4.1) [15]. Inhibition of SDH on reperfusion may therefore reduce ROS production by restricting the re-entry of electrons into the electron transport chain and hence the driving force required for RET to occur [17].

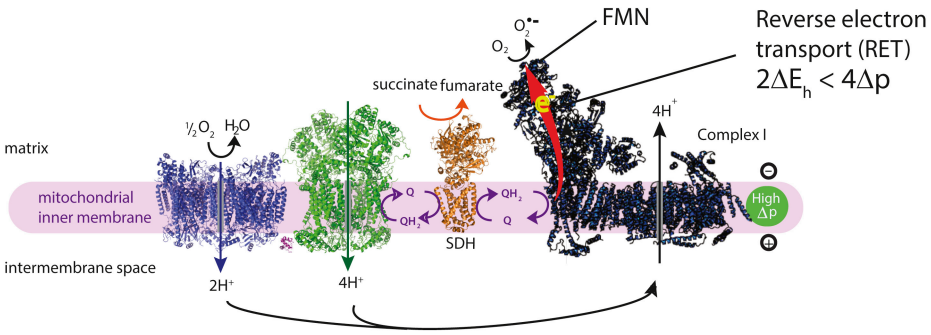

Figure 4.1 Mitochondrial ROS Production on Reperfusion. During reperfusion, return of the terminal electron acceptor oxygen leads to the reactivation of Complex III and IV, proton pumping and regeneration of the proton motive force (Δp). However, as ADP is mostly degraded during prolonged ischaemia, there is a lack of substrate for F_OF_1-ATP synthase allowing Δp to reach near maximal levels. Coupled with a highly reduced CoQ pool resulting from rapid succinate oxidation, a near maximal Δp enables electrons to pass backwards through Complex I via reverse electron transport and combine with oxygen at the flavin mononuclear (FMN) site of the complex forming a superoxide radical. Figure adapted from Chouchani et al (2016).

Malonate is a competitive inhibitor of SDH but as a charged molecule, must be given in a cell permeable form in order to pass through lipid membranes and enter mitochondria *in vivo* [211]. Succinate oxidation and ROS production occur within minutes of reperfusion and malonate must be present within mitochondria or accumulate rapidly within these organelles on reperfusion in order to effectively inhibit ROS production [267] [17]. Disodium malonate has been shown to reduce infarct size in an isolated model of myocardial infarction in the mouse and translational model of myocardial infarction in the pig when administered at the onset of reperfusion [195] [194]. However, it is currently unclear how this charged molecule enters mitochondria and whether its therapeutic effect is due to SDH inhibition, necessitating further investigation. Malonate ester pro-drugs, including DMM and MAM are designed to increase the lipophilicity of malonate so that they can pass through lipid membranes more easily. However, before they can inhibit SDH, their side groups must be hydrolysed by cellular carboxylesterases [211]. As previously discussed, hydrolysis of DMM by PLE *in vitro* is relatively slow and DMM may not be hydrolysed rapidly enough to inhibit succinate oxidation within mitochondria when administered at reperfusion (personal communication, Hiran Prag). To date, no studies have investigated the effect of DMM administered at reperfusion in an *in vivo* model of IRI. However, administration of DMM prior to ischaemia may result in an increased malonate concentration within mitochondria at reperfusion due to the hydrolysis DMM during the preceding ischaemic period. Administration of DMM prior to ischaemia may therefore not only inhibit succinate accumulation as previously shown in a mouse model of myocardial infarction but also inhibit

succinate oxidation on reperfusion, further contributing to its protective effect [17] [14]. In contrast to DMM, MAM is hydrolysed more rapidly by PLE *in vitro* and may be capable of inhibiting rapid oxidation of succinate by SDH when administered at reperfusion *in vivo* (personal communication, Hiran Prag). In preliminary experiments, MAM has been shown to reduce infarct size when administered at reperfusion in a mouse model of myocardial infarction suggesting hydrolysis and mitochondrial malonate accumulation is rapid enough to inhibit ROS production when administered at this time point (personal communication, Hiran Prag). Other strategies to inhibit ROS production at reperfusion include use of mitochondria-targeted malonate compounds, reversible S-nitrosation of Complex I in the inactive state and use of mitochondria-targeted antioxidants as discussed in Chapter 1 [198] [199] [202].

As shown in the previous chapter, succinate accumulates to a near maximal level in kidneys retrieved from both DBD and DCD donors and may subsequently drive mitochondrial ROS production on transplantation. Inhibition of succinate oxidation on transplantation may therefore help ameliorate IRI in grafts from both donor types, leading to improved short and long-term graft outcomes. During organ transplantation, mitochondrial therapies may be administered at multiple stages throughout the transplant process. Although a number of legal and logistical barriers must be addressed, it is feasible for malonate ester pro-drugs to be administered to a donor prior to organ retrieval, to an organ during preservation or to the recipient during transplantation. The optimal time to administer malonate ester pro-drugs to an organ will likely depend on the stage of mitochondrial ROS production being targeted (e.g. succinate accumulation during ischaemia or rapid oxidation on reperfusion), the rate of hydrolysis of the malonate ester prodrug and rate of accumulation within mitochondria. For example when attempting to inhibit rapid succinate oxidation on reperfusion, malonate ester pro-drugs that are hydrolysed relatively slowly by tissue carboxylesterases, such as DMM, may need to be administered to an organ donor prior to organ retrieval or during organ preservation to allow sufficient time for hydrolysis to occur and malonate to accumulate to a sufficient concentration within mitochondria to inhibit SDH on reperfusion, as discussed above. Alternatively, malonate ester pro-drugs that are hydrolysed relatively rapidly by tissue carboxylesterases, such as MAM, may be administered to the organ recipient at the time of reperfusion. In this scenario, malonate is able to reach a sufficient effective concentration within the mitochondria of the donor graft to inhibit succinate oxidation by SDH, and thus prevent ROS production.

The use of malonate ester pro-drugs to inhibit succinate oxidation on reperfusion in organ transplantation has not been previously investigated. In this Chapter, I investigate the use of malonate ester pro-drugs to inhibit mitochondrial ROS production on reperfusion when administered at various stages throughout the transplant process. I used the mitochondrial

ROS probe MitoB, a ratiometric mass spectrometry probe comprising an arylboronic acid conjugated to a TPP cation to measure mitochondrial ROS production on reperfusion *in vivo* [268]. The arylboronic acid of MitoB reacts selectively with hydrogen peroxide and peroxynitrite to form a stable phenol (see Figure 4.2a). As superoxide produced by mitochondria on reperfusion is rapidly converted to hydrogen peroxide by mitochondrial MnSOD, MitoB may be used to measure mitochondrial ROS production during IRI [177] [269]. Meanwhile, the positive TPP cation targets MitoB to the mitochondria several 100-fold as shown in Figure 4.2b [269]. In this Chapter, MitoB was first used to investigate the relationship between warm ischaemia and mitochondrial ROS production in the mouse kidney and whether mitochondrial ROS production was increased following administration of DMS. I then investigated whether the metabolic changes leading to mitochondrial ROS production in the mouse kidney also occur on reperfusion of pig and human kidneys using EVNP. Lastly, I investigated whether mitochondrial ROS production could be reduced by the administration of malonate ester pro-drugs to the mouse kidney prior to the onset of ischaemia (to simulate administration to an organ donor) or at the point of reperfusion (to simulate administration to an organ recipient) and to the pig kidney during back-table flush (to simulate administration during organ storage).

4.1.1 Aims

1. To investigate the effect of warm ischaemia time and succinate concentration on mitochondrial superoxide production during early reperfusion in the mouse kidney

2. To investigate the metabolic changes that occur in the pig and human kidney on reperfusion

3. To determine whether mitochondrial superoxide production during early reperfusion may be inhibited by administration of malonate ester pro-drugs prior to ischaemia (to simulate administration to an organ donor) or at reperfusion (to simulate administration to an organ recipient) in the mouse kidney

4. To determine whether malonate ester pro-drugs may be given during back-table flush in a pig model of kidney transplantation

4.1.2 Hypothesis

Mitochondrial superoxide production upon reperfusion is dependent on succinate accumulation during ischaemia and may be inhibited with malonate ester pro-drugs.

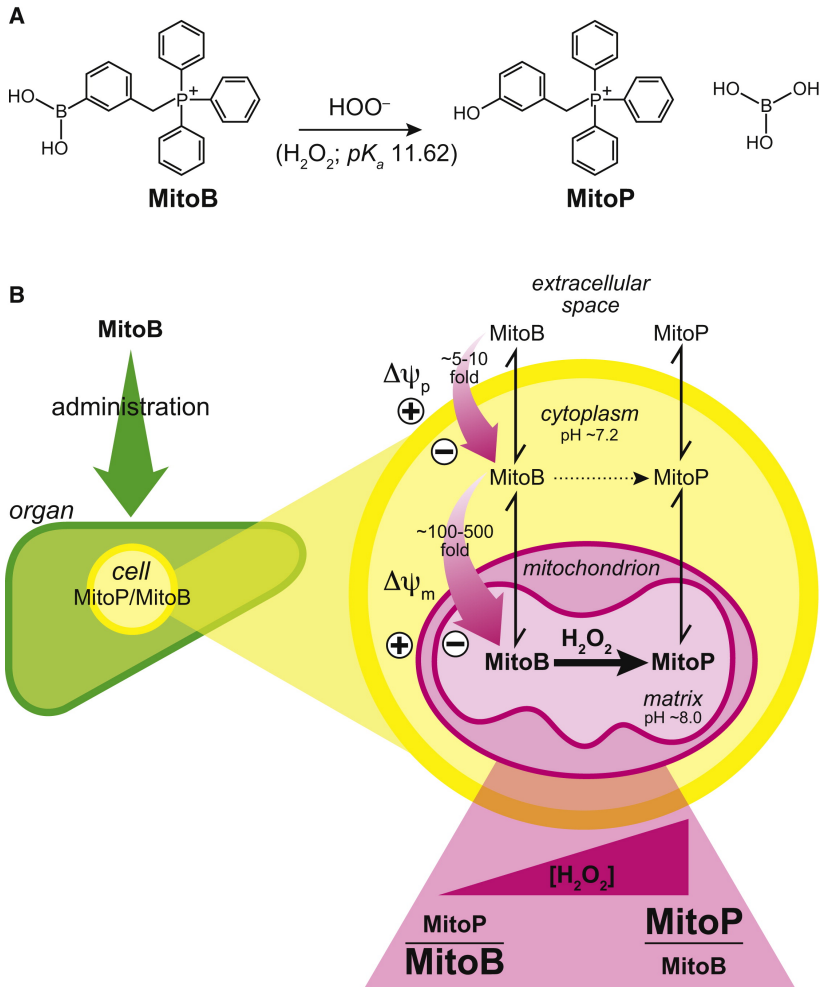

Figure 4.2 The Ratiometric Mass Spectrometry Probe, MitoB. MitoB is a ratiometric mass spectrometry probe that may be used to measure mitochondrial hydrogen peroxide production *in vivo*. (**a**) MitoB is comprised of a arylboronic acid conjugated to a triphenylphosphonium (TPP) cation and reacts selectively with hydrogen peroxide to form a stable phenol (MitoP). The MitoP/MitoB ratio may subsequently be used to determine the degree of mitochondrial ROS production in a tissue with an increase in hydrogen peroxide production leading to an increase in the MitoP/MitoB ratio. (**b**) MitoB accumulates several hundred fold within mitochondria due to the electrochemical driving force experienced by the positively charged TPP molecule across the cellular and mitochondrial membranes. Furthermore, as the positive charge of the TPP cation is distributed over the entire moiety, the activation energy required for MitoP to pass through a lipid membrane is greatly reduced, facilitating its passage through the cellular and mitochondrial membranes and enabling accumulation within mitochondria to occur. Figure adapted from Cocheme et al (2011).

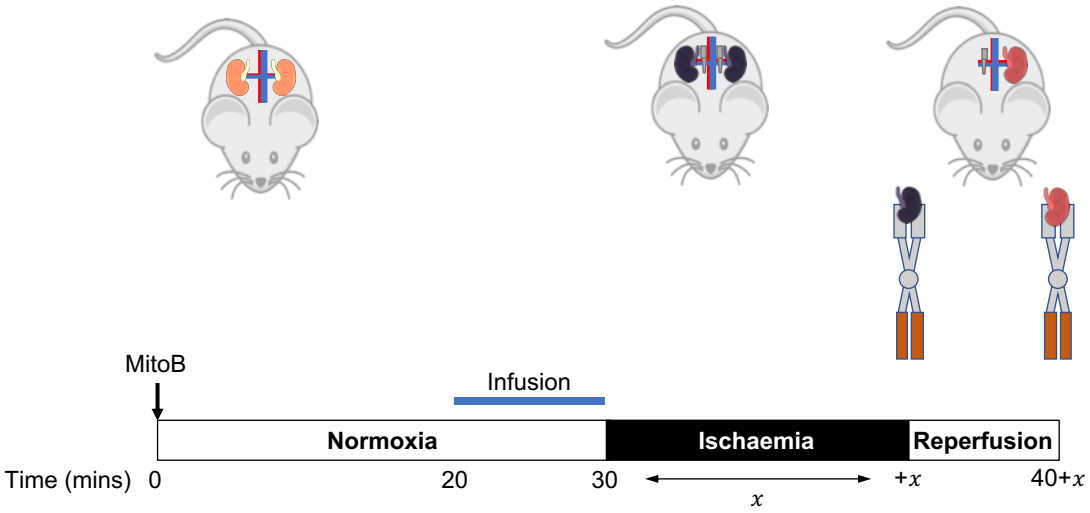

Figure 4.3 Investigating Mitochondrial Superoxide Production during Ischaemia-Reperfusion in the Mouse Kidney. MitoB was given as an intravenous injection into the IVC 30 mins prior to the onset of ischaemia. 10 mins prior to the onset of ischaemia an intravenous infusion of saline was given into the IVC. Following infusion, both kidneys were exposed to x (5, 10, 15, 20, 25, 30 or 45) minutes warm ischaemia by occluding the renal hila with a micro-serrefine clamp. Successful occlusion of the renal hila resulted in a change colour of each kidney from orange to dark purple. Following x (5, 10, 15, 20, 25, 30 or 45) minutes warm ischaemia, one kidney was rapidly retrieved and clamp frozen using Wollenburg clamps in LN2. The micro-serrefine clamp was removed from the hila of the second kidney which underwent 10 mins reperfusion. Successful reperfusion could be confirmed by a change in colour of the kidney from dark purple to orangey-pink. At 10 mins reperfusion the second kidney was also rapidly retrieved and clamp frozen in LN2. In DMS experiments, 6.4 mg DMS was given as an infusion 10 minutes prior to the onset of ischaemia as described above. Both kidneys were then exposed to 20 mins warm ischaemia. One kidney was clamp frozen at the end of ischaemia and the second following 10 mins reperfusion. All frozen tissue samples were stored at -70 °C until further processing and analysis

4.2 Mitochondrial ROS Production in the Mouse Kidney

4.2.1 Effect of the Duration of Warm Ischaemia on Mitochondrial ROS Production

To investigate the effect of warm ischaemia on mitochondrial ROS production at reperfusion, mouse kidneys were exposed to varying periods of warm ischaemia and reperfused for 10 mins as shown in Figure 4.3. For each experiment, one kidney was clamp frozen at the end of ischaemia to act as an internal control and was then compared with the second kidney which was clamp frozen after 10 mins reperfusion in order to determine the metabolic changes that occur in the tissue during reperfusion. Tissue MitoP/MitoB ratio, succinate concentration, ATP/ADP ratio and total ATP and ADP nucleotide concentration at the end

of warm ischaemia and after 10 mins of reperfusion are shown in Figure 4.4. There was a significant increase in the MitoP/MitoB ratio on reperfusion following 10 and 20 mins warm ischaemia (Figure 4.4a). The MitoP/MitoB ratio also showed an increasing trend following 15, 25, and 30 mins warm ischaemia but was not significant.

Tissue succinate concentration was significantly increased at the end of warm ischaemia across ischaemic times (Figure 4.4b). At 10 mins reperfusion, tissue succinate concentration decreased across ischaemic times and was not significantly different to control levels except following 45 mins ischaemia where succinate was still significantly increased at 10 mins reperfusion and may have been due to impaired reperfusion.

The ATP/ADP ratio was significantly decreased at 10 mins reperfusion following 10, 30 and 45 mins warm ischaemia (Figure 4.4c). Meanwhile the sum of the ATP and ADP concentration was significantly decreased at the end of warm ischaemia and at 10 mins reperfusion across ischaemic times except following 5 mins warm ischaemia where the sum ATP and ADP concentration returned to control values on reperfusion Figure 4.4d).

4.2.2 Effect of Succinate Accumulation During Ischaemia on Mitochondrial ROS Production

To determine the effect of succinate concentration on mitochondrial ROS production at reperfusion, 6.4 mg dimethyl succinate (DMS) was administered to mice as an infusion prior to the onset of 20 mins of warm ischaemia as shown Figure 4.3. Tissue succinate concentration and MitoP/MitoB ratio at the end of ischaemia and at 10 mins reperfusion is shown in Figure 4.5. Administration of DMS led to a significant increase in succinate concentration at the end of 20 mins warm ischaemia (Figure 4.5a). At 10 mins reperfusion, the succinate concentration in DMS treated kidneys had decreased and was not significantly different from control kidneys suggesting succinate was rapidly oxidised within the tissue. However, there was no significant difference in the MitoP/MitoB ratio between DMS treated and control kidneys at the end of ischaemia or at 10 mins reperfusion (Figure 4.5b) suggesting the increased ischaemic succinate concentration in DMS treated kidneys did not lead to an increase in mitochondrial ROS production as measured by the ratiometric probe MitoB.

4.3 Interim Summary I

A burst of mitochondrial ROS production was measured upon reperfusion of the mouse kidney following 10, 15, 20, 25 and 30 mins warm ischaemia but not 5 mins warm ischaemia. This may be explained by the rapid recovery of tissue ATP and ADP levels on reperfusion

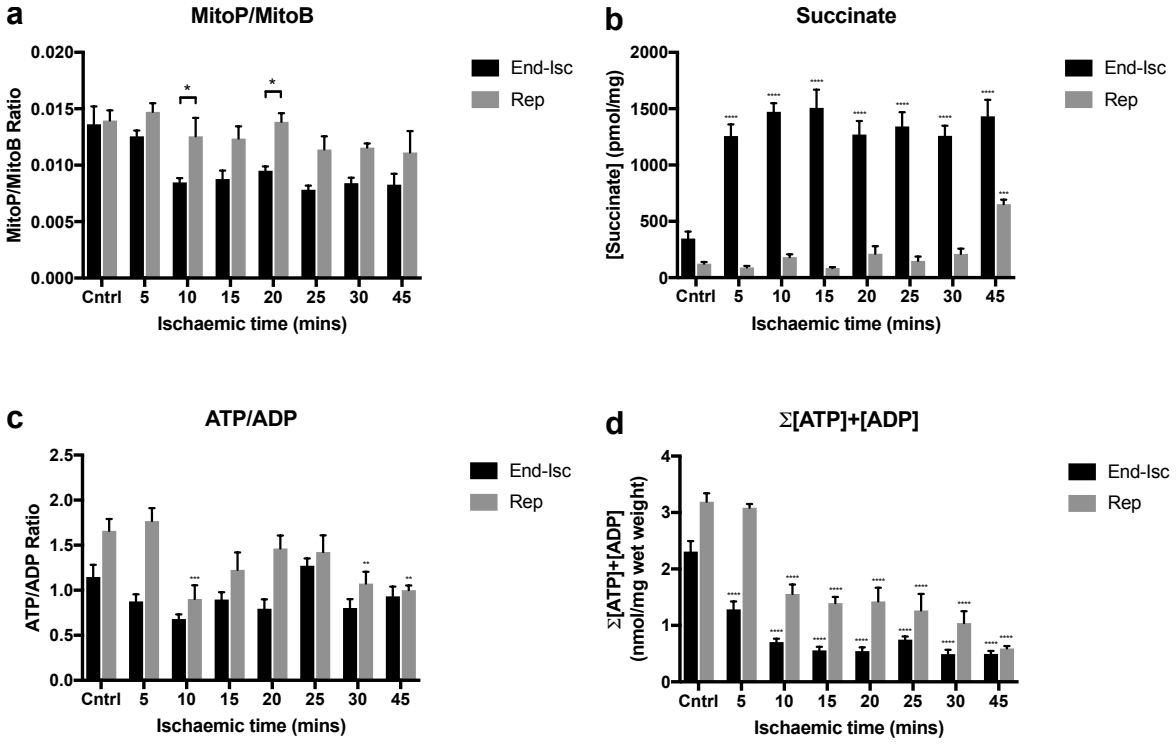

Figure 4.4 Effect of Warm Ischaemic Time on Mitochondrial ROS Production during Ischaemia-Reperfusion in the Mouse Kidney. MitoP/MitoB ratio **(a)** (n=3-4), succinate concentration **(b)** (n=4), ATP/ADP ratio **(c)** (n=3-4) and total ATP and ADP nucleotide levels **(d)** (n=3-4) at the end of ischaemia (black bars) and at 10 mins reperfusion (grey bars) following various periods of warm ischaemia. *P < 0.05, **P < 0.01, ***P < 0.001, ****P < 0.0001. P values were calculated by two-way analysis of variance (ANOVA) with Sidak's multiple comparisons test. Data are mean ± SEM.

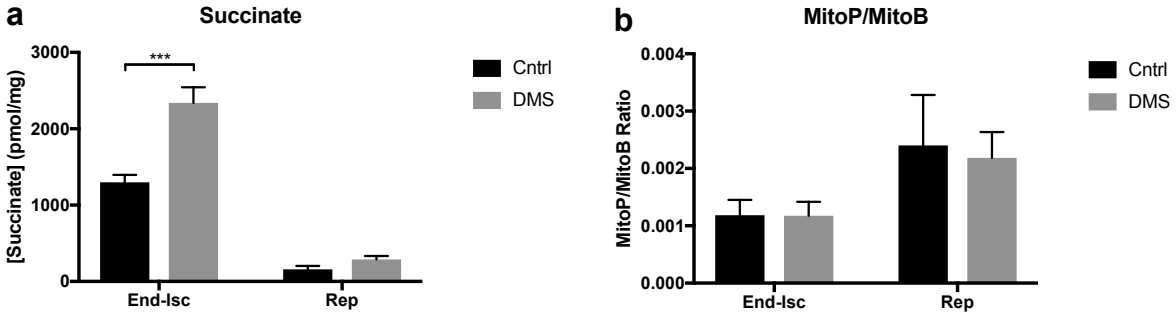

Figure 4.5 Effect of Succinate Concentration on Mitochondrial ROS Production during Ischaemia-Reperfusion in the Mouse Kidney. Succinate concentration **(a)** (n=3-4) and MitoP/MitoB ratio **(b)** (n=3-4) at the end of 20 mins warm ischaemia and 10 mins reperfusion following administration of saline (black bars) or 6.4 mg dimethyl succinate (DMS) (grey bars) as an infusion prior to the onset of ischaemia as shown in Figure 4.3. ***P < 0.001. P values were calculated by two-way analysis of variance (ANOVA) with Sidak's multiple comparisons test. Data are mean ± SEM.

following 5 mins warm ischaemia but not after longer warm ischaemia times. Rapid recovery of ATP and ADP levels on reperfusion suggests depletion of the adenosine nucleotide pool had not fully occurred and substrate was still available for F_OF_1-ATPase on reperfusion. F_OF_1-ATPase activity will have prevented a near maximal Δp required for reversal of Complex I from being reached and therefore RET and ROS production from occurring [15]. Administration of DMS prior to the onset of 20 mins warm ischaemia led to an increase in tissue succinate concentration at the end of ischaemia immediately prior to reperfusion. However, an increase in tissue succinate concentration at the end of 20 mins ischaemia did not lead to an increase in mitochondrial ROS production as measured by the MitoP/MitoB ratio at 10 mins reperfusion.

4.4 Metabolic Changes on Reperfusion in the Pig Kidney

As kidneys from the mice in the above experiments experienced only warm ischaemia prior to reperfusion and did not undergo cold ischaemia, mitochondrial ROS production was also investigated in a more clinically relevant translational model of kidney transplantation in the pig. However, it was not possible to administer MitoB to the pig in order to directly measure the degree of mitochondrial ROS production on reperfusion. This was due to the greater complexity of the retrieval procedure and uncertainty as to the dose, toxicity and optimal administration time of MitoB in this model. Preliminary experiments performed in our laboratory showed 250 nmol MitoB administered at 3 minutes EVNP in the pig kidney resulted in significantly worse renal function as measured by the FENa and clearance of creatinine compared to untreated control kidneys (personal communication, Anna Dare). This suggested MitoB administered at this dose may be toxic to pig kidney and as pig experiments were far more costly than in the mouse, it was not economical (or ethical) to further optimise the use of MitoB in this model at this stage. Nevertheless, a burst of mitochondrial superoxide production upon reperfusion may be inferred in pig kidneys on reperfusion by assessing whether the same metabolic changes occur in the pig as in the mouse during the initial reperfusion period. To simulate conditions of DBD and DCD donation, pig kidneys were exposed to either 0 or 30 mins warm ischaemia respectively, as shown in Figure 4.6. Kidneys then underwent 6 h cold static storage on ice followed by 6 h EVNP. *Ex vivo* normothermic perfusion refers to the reperfusion of an organ outside the body with an oxygenated whole blood perfusate at 36 °C [247] [137]. This is achieved using an adapted cardio-pulmonary bypass circuit as discussed in Chapter 2 (see Figure 2.1). The tissue succinate, ATP and ADP concentrations were measured in the pig kidney under conditions of normoxia (*In situ*), at the end of cold static storage (End-Isc) and following

10 mins EVNP (Rep) as shown in Figure 4.7 and compared to the metabolic changes in the mouse to determine whether mitochondrial ROS production is likely to have occured under these conditions. Note that whilst 30 mins represents a more extreme warm ischaemia time, rarely experienced by kidneys retrieved from DCD donors in the UK, this time was chosen to represent the maximum tissue injury that may be experienced by a kidney graft due to warm ischaemia during transplantation. The more severe warm ischaemia time adopted also enabled the range of injury that may be experienced by pig kidneys undergoing EVNP to be determined and thus the scope for improvement with a therapeutic intervention using the EVNP model (see Chapter 5). If this scope was too narrow (as may have occurred with shorter warm ischaemic times) then detecting an improvement in kidney injury with a therapeutic intervention during EVNP would become more difficult. Lastly, whilst the average warm ischaemia time from circulatory death to *in situ* flush is approximately 14 minutes (IQR 11-17 minutes) in the UK, grafts from DCD donors may also experience a period 'functional' warm ischaemia (defined as a systemic BP < 50 mmHg) ranging from minutes to hours following the withdrawal of life support during which time kidneys may become hypoperfused and undergo a prolonged period of hypoxia [9] [68]. Grafts from all donor types also experience a further period of ischaemia at a temperature between 0-4 °C and 36°C during graft anastomosis which was not simulated as part of the pig model [84]. When considering these factors, the choice of 30 mins of warm ischaemia to represent clinical DCD donation in an experimental model of kidney transplantation using kidneys from young, healthy pigs may be deemed more reasonable. Human kidneys are also known to withstand 30 mins warm ischaemia or longer periods in other clinical scenarios such as partial nephrectomy of renal tumours and abdominal aortic aneurysm repair. As such, the experimental data gained from this model may also help to inform the future use of malonate ester pro-drugs in surgical procedures such as these [270] [271].

In the translational model of kidney transplantation described in Figure 4.6, succinate concentration was significantly increased in kidneys exposed to 30 mins warm ischaemia and 6 h cold static storage at the end of ischaemia (Figure 4.7a). Following 10 mins reperfusion, tissue succinate concentration had decreased and was not significantly different from normoxic controls suggesting rapid succinate oxidation had occurred. In kidneys exposed to 6 h cold static storage only, succinate did not significantly increase from normoxic levels during ischaemia. There was a decrease in succinate concentration upon reperfusion, suggesting that if there was a small (but non-significant) increase in during ischaemia, it was oxidised upon reperfusion. The ATP/ADP ratio (Figure 4.7b) and the sum of the ATP and ADP concentrations (Figure 4.7c) significantly decreased in kidneys exposed to both 30 mins warm ischaemia and 6 h cold storage and 6 h cold storage only. Following 10 mins reperfusion

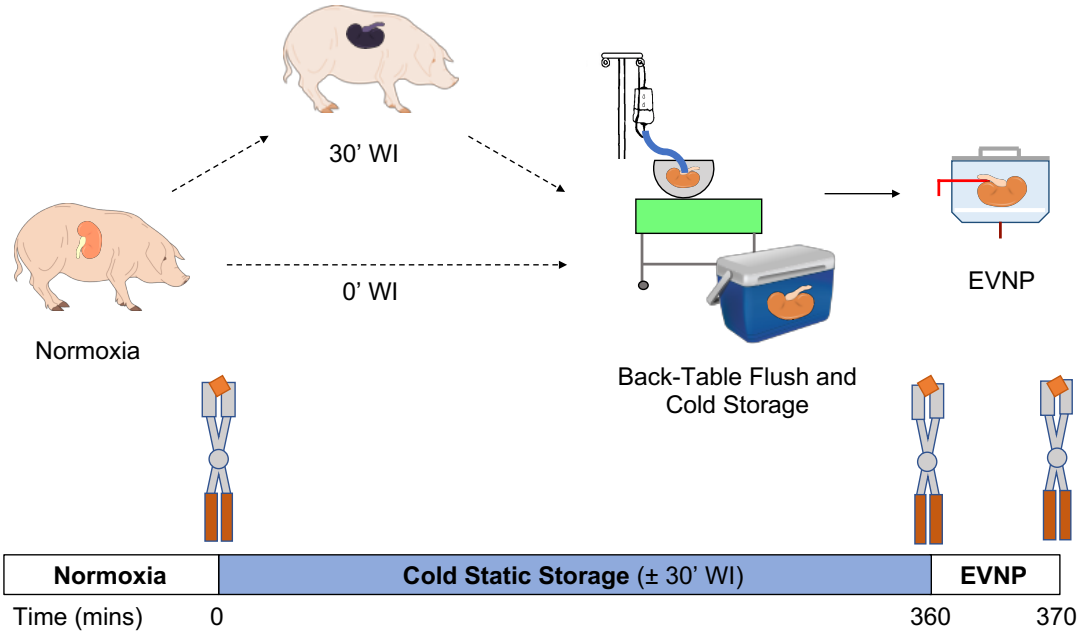

Figure 4.6 Investigating the Metabolic Changes on Reperfusion in the Pig Kidney. Pig kidneys were retrieved under general anaesthesia and exposed to either 30 mins warm ischaemia (30' WI) and 6 h cold static storage or 0 mins warm ischaemia (0' WI) and 6 h cold static storage. Prior to back-table flush, kidneys exposed to 30 mins warm ischaemia became darker and more purple in colour. Kidneys were then reperfused using EVNP for 6 h. Tissue wedge biopsies were taken from kidneys *in situ* under conditions of normoxia, at the end of cold static storage and following 10 mins EVNP to investigate the metabolic changes that occured in tissue upon repefusion. Tissue wedge biopsies were rapidly clamp frozen in liquid nitrogen using Wollenburg clamps and stored at -70°C until further processing and analysis.

however, the ATP/ADP ratio and total ATP and ADP concentrations returned to normoxic levels in kidneys exposed to 6 h cold storage only but remained significantly decreased in kidneys exposed to 30 mins warm ischaemia and 6 h cold static storage. This may suggest that the adenosine nucleotide pool was more depleted in kidneys exposed to 30 mins warm ischaemia and 6 h cold static storage. This has implications on the substrate availability for the ATP synthase and magnitude of the Δp upon reperfusion. In the absence of substrate for ATP synthase, a near maximal Δp may develop facilitating reverse electron transport and mitochondrial ROS production at FMN site Complex I. Succinate accumulation during ischaemia, rapid succinate oxidation on reperfusion and depletion of adenosine nucleotides during ischaemia and on reperfusion in kidneys exposed to 30 mins warm ischaemia and 6 h cold static storage supports our model of the production of mitochondrial ROS upon reperfusion as previously described by Chouchani et al [15]. In addition, these results concur with MitoB experiments demonstrating mitochondrial ROS production under similar conditions in the mouse kidney (Figure 4.4).

4.5 Metabolic Changes on Reperfusion in the Human Kidney

Similar to the pig, it was not possible to measure mitochondrial ROS production on reperfusion directly in human kidneys using ratiometric probe MitoB due to uncertainties regarding the dose and toxicity of MitoB in this model. As mentioned above, a set of preliminary experiments performed in our laboratory has shown that MitoB may be toxic to the pig kidney resulting in poor function during EVNP (personal communication, Anna Dare). Furthermore, human kidneys were only received in the laboratory following retrieval and cold storage and it was unknown whether MitoB administered to the declined human kidneys at reperfusion would distribute rapidly enough within the graft to accurately reflect early mitochondria ROS production. As declined human kidneys were precious and infrequent, I decided that MitoB should not be used. Instead, EVNP of declined human kidneys was used to determine whether the same metabolic changes that lead to mitochondrial ROS production on reperfusion in the mouse also occur in the human.

In addition, after measuring the metabolic changes that occur during initial reperfusion, declined human kidneys were subsequently re-exposed to 30 mins warm ischaemia and 6 h cold storage to investigate the metabolic changes in the tissue and mitochondrial ROS production under more controlled conditions, as shown in Figure 4.8. Re-exposure of declined human kidneys followed by a second period of EVNP has not previously been

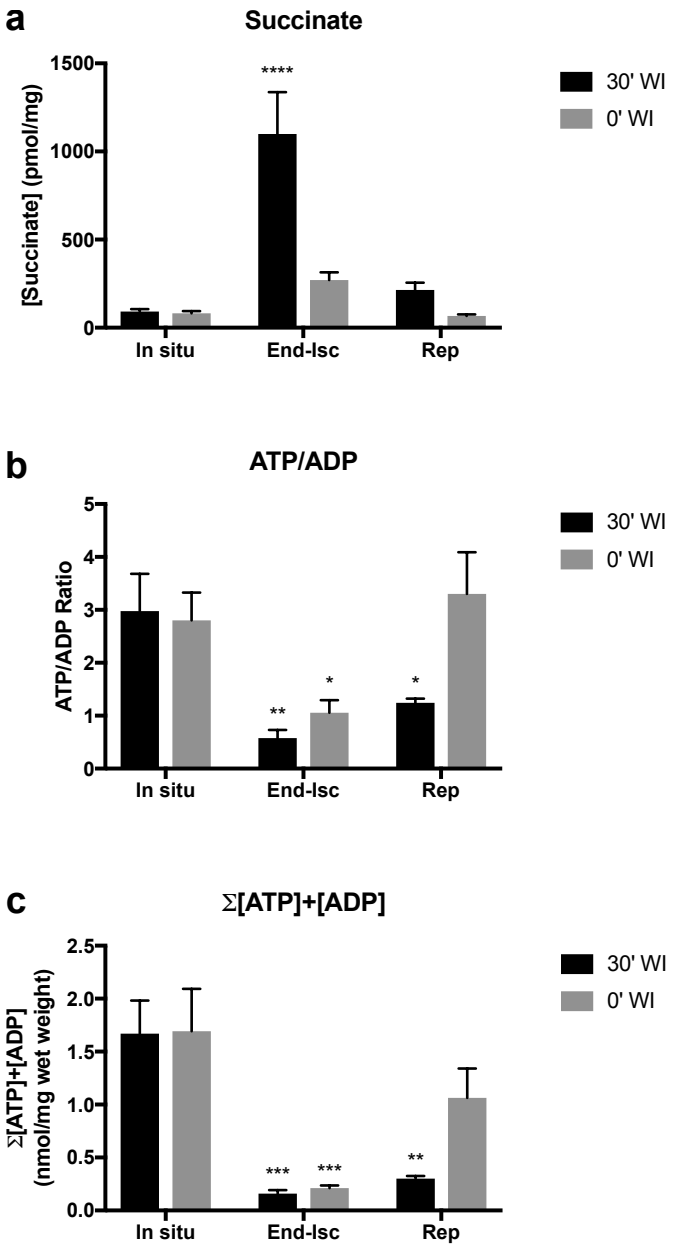

Figure 4.7 Metabolic Changes on Reperfusion in the Pig Kidney. Tissue succinate concentration **(a)** (n=4), ATP/ADP ratio **(b)** (n=4) and total ATP and ADP nucleotide concentration **(c)** (n=4) in pig kidneys under conditions of normoxia (In situ), at the end of cold static storage (End-Isc) and following 10 mins *ex vivo* normothermic perfusion (Rep). Pig kidneys were exposed to either 30 mins warm ischaemia and 6 h cold static storage (30' WI) or 0 mins warm ischaemia and 6 h cold static storage (0' WI) as shown in Figure 4.6. *P < 0.05, **P < 0.01, ***P < 0.001, ****P < 0.0001. P values were calculated by two-way analysis of variance (ANOVA) with Sidak's multiple comparisons test. Data are mean ± SEM.

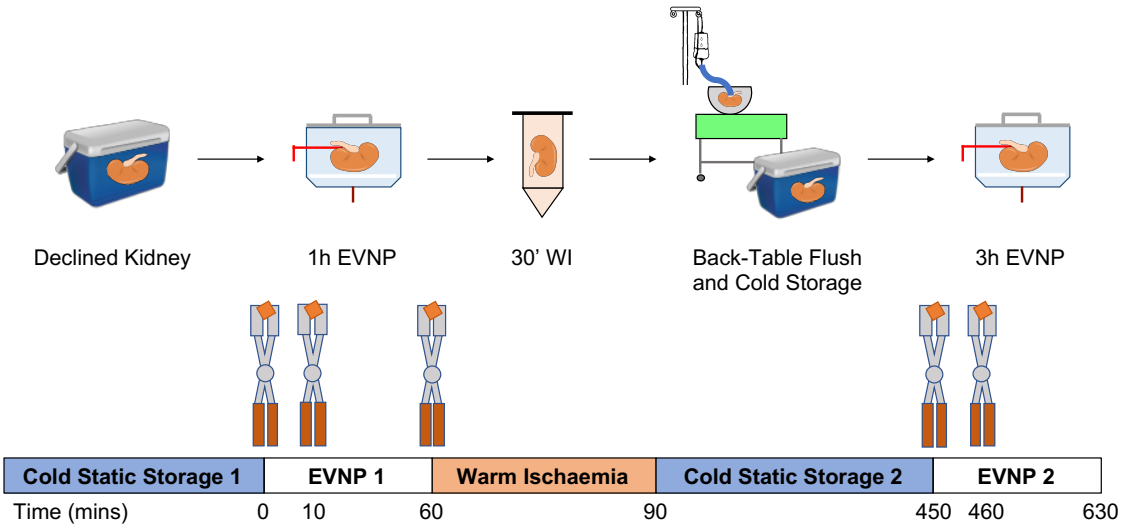

Figure 4.8 Investigating the Metabolic Changes on Reperfusion in the Human Kidney. Declined human kidneys were accepted for research and underwent 1 h EVNP on arrival to the laboratory. Kidneys were then exposed to 30 mins warm ischaemia at 36.0 °C followed by back-table flush and 6 h cold static storage. Kidneys were then reperfused for a second time 3 h period of EVNP.

conducted, however it was hoped that if successful, this model (which is similar to the model in the pig) could be used for the future investigation of malonate ester prodrugs in human kidneys and inform early clinical trials. Furthermore, as discussed in Chapter 3, it was not possible to obtain a normoxic tissue sample from human kidneys prior to organ retrieval and so the metabolic changes that occurred on initial reperfusion could not be compared to baseline levels. However, as succinate rapidly returns to normoxic levels upon reperfusion, EVNP of human kidneys followed by re-exposure to warm and cold ischaemia enabled the changes in tissue succinate, ATP and ADP during ischaemia and reperfusion to be compared to a baseline value and could subsequently be interpreted more accurately [267].

4.5.1 Metabolic Changes on Reperfusion of Declined Human Kidneys

The metabolic changes on initial reperfusion of declined human kidneys were investigated as shown in Figure 4.8. A tissue wedge biopsy was taken and rapidly clamp frozen using Wollenburg clamps at the end of cold static storage 1 (End-Isc 1) and after 10 mins reperfusion (Rep 1). Tissue succinate concentration decreased on reperfusion but was not significant (Figure 4.9a, $p = 0.11$). The ATP/ADP ratio significantly increased on reperfusion (Figure 4.9b). The sum of the ATP and ADP concentration increased but was not significant (Figure 4.9c). The trends in succinate and in ATP and ADP, generally reflect those measured in the mouse and support mitochondrial ROS production on reperfusion. While the changes in

tissue succinate concentration on reperfusion showed a lack of signifcance, this may partly reflect the low sample number.

4.5.2 Metabolic Changes on Reperfusion of Declined Human Kidneys Re-Exposed to Warm and Cold Ischaemia

To determine a baseline level of tissue succinate, and of ATP and ADP concentrations, declined human kidneys were reperfused for 1 h using EVNP and then re-exposed to warm and cold ischaemia before undergoing a second period of EVNP to further investigate the metabolic changes that occur during initial reperfusion as shown in Figure 4.8. Wedge biopsies were taken at the end of 1 h EVNP (End-EVNP 1), at the end of 30 mins warm ischaemia and 6 h cold static storage (End-Isc 2) and following 10 mins reperfusion (Rep 2). Tissue succinate concentration, ATP/ADP ratio and total ATP and ADP nucleotide concentration are shown in Figure 4.10.

There was a significant increase in tissue succinate concentration in human kidneys exposed of 30 mins warm ischaemia and 6 h cold static storage (End-Isc 2) compared to baseline levels measured at the end of 1 h EVNP (End-EVNP 1) (Figure 4.10a). The tissue succinate concentration in declined human kidneys measured at 10 mins reperfusion in the second period of EVNP (Rep 2) was not significantly different from baseline values measured at the end of the initial 1 h period of EVNP (End-EVNP-1) suggesting rapid oxidation had occurred. The ATP/ADP ratio was significantly decreased at the end of 30 mins warm ischaemia and 6 h cold static storage (End-Isc 2) compared to the baseline level measured after 1 h EVNP (End-EVNP 1), but not at 10 mins reperfusion in the subsequent second period of EVNP (Rep 2) (Figure 4.10b). However, the total ATP and ADP nucleotide concentration was significantly decreased at the end of 30 mins warm ischaemia and 6 h cold static storage (End-Isc 2) and 10 mins reperfusion (Rep 2) compared to baseline levels measured at the end of 1 h EVNP (End-EVNP 1). This suggests that there was a limited supply of ADP upon reperfusion and that significant depletion of the adenosine nucleotide pool had occurred (Figure 4.10c). Again, these findings support the production of mitochondrial superoxide from the FMN site of complex I via reverse electron transport and suggest inhibition of succinate oxidation by succinate dehydrogenase during initial reperfusion may help to ameliorate IRI during organ transplantation.

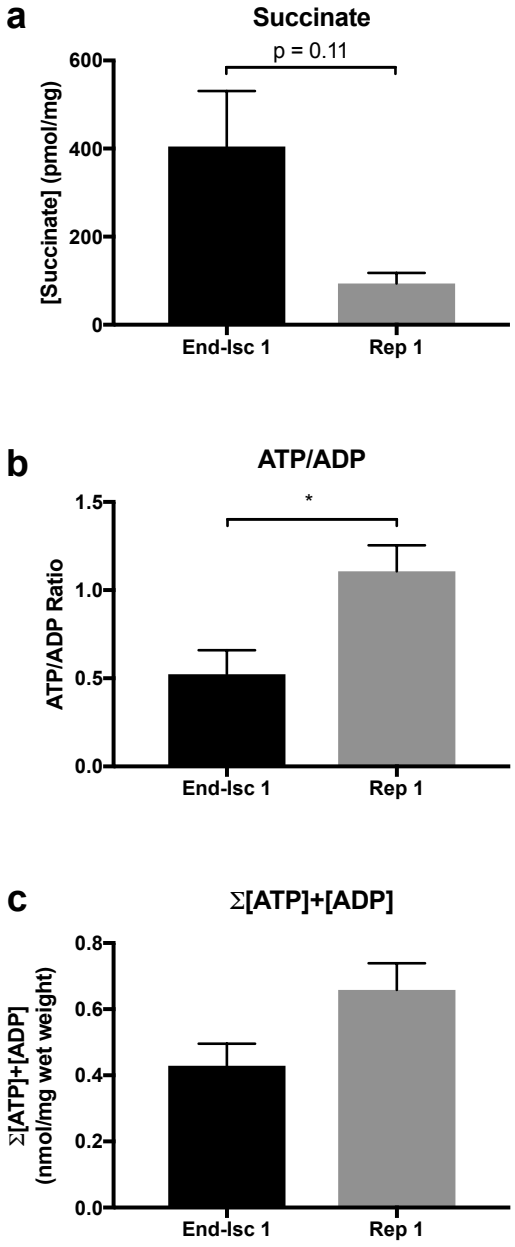

Figure 4.9 Metabolic Changes on Reperfusion of Declined Human Kidneys. Tissue succinate concentration **(a)** (n=4), ATP/ADP ratio **(b)** (n=4) and total ATP and ADP nucleotide concentration **(c)** (n=4) in declined human kidneys at the end of cold static storage (End-Isc 1) and following 10 mins *ex vivo* normothermic perfusion (Rep 1). *P < 0.05. P values were calculated by two-tailed paired t-test. Data are mean ± SEM.

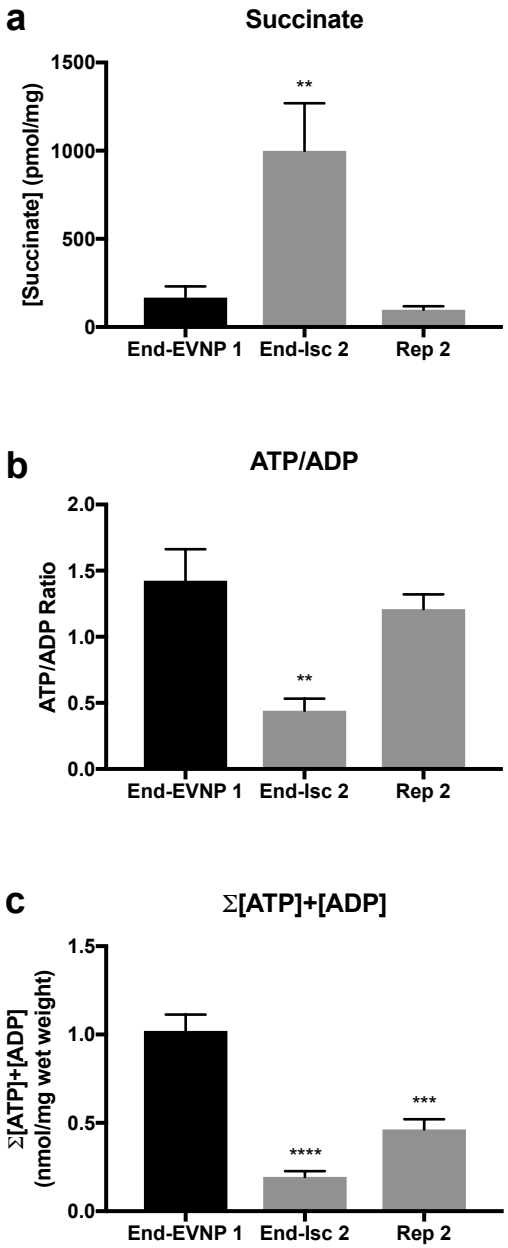

Figure 4.10 Metabolic Changes on Reperfusion of the Human Kidney following Re-Exposure to Warm and Cold Ischaemia. Tissue succinate concentration **(a)** (n=4), ATP/ADP ratio **(b)** (n=4) and total ATP and ADP nucleotide concentration **(c)** (n=4) in declined human kidneys following one hour ex vivo normothermic perfusion (End-EVNP 1), thirty minutes warm ischaemia and six hours cold static storage (End-Isc 2) and at ten minutes reperfusion (Rep 2) as shown in Figure 4.8. **P < 0.01, ***P < 0.001 ****P < 0.0001. P values were calculated by one-way analysis of variance (ANOVA) with Dunnett's multiple comparisons test. Data are mean ± SEM.

4.6 Interim Summary II

The metabolic changes in the pig kidney following 30 mins warm ischaemia and 6 h cold static storage closely mimicked those leading to ROS production in the mouse. This suggests that ROS production may have also occurred in the pig kidney under these conditions. In contrast, the ATP/ADP ratio and total ATP and ADP concentration recovered rapidly in pig kidneys exposed to 6 h cold static storage only, suggesting substrate availability for F_OF_1-ATPase on reperfusion, which as is the case in the mouse, may have prevented a maximal Δp required for RET and ROS from being established. The metabolic changes in declined human kidneys reperfused via EVNP also mimicked those leading to ROS production in the mouse kidney. Again this suggests that ROS production occurred under these conditions. Furthermore, human kidneys re-exposed to 30 mins warm ischaemia and 6 h cold static storage following 1 h EVNP enabled the changes in succinate and ATP and ADP concentrations to be compared to baseline levels. This provided further evidence that the metabolic changes required for ROS production occur in the human kidney under these conditions. Both pig and human translational models of kidney transplantation in which kidneys were exposed to 30 mins warm ischaemia and 6 h cold static storage may therefore be used to investigate the use of malonate ester pro-drugs to reduce mitochondrial ROS production in organ transplantation.

4.7 Effect of Malonate Ester Pro-Drugs on Mitochondrial ROS Production in the Mouse Kidney

4.7.1 Administration of DMM Prior to Ischaemia

As previously discussed, DMM is hydrolysed relatively slowly by pig liver esterase (PLE) *in vitro* suggesting malonate may not be released rapidly enough to inhibit succinate oxidation and mitochondrial ROS production if administered to an ischaemic tissue at the point of reperfusion, e.g. to the organ recipient at the point of reperfusion of the transplanted graft. However, as shown in the previous chapter, administration of DMM prior to ischaemia resulted in an increased tissue malonate concentration at reperfusion due to the ongoing hydrolysis of DMM within the tissue during ischaemia. Whilst administration of DMM prior to ischaemia was not able to inhibit succinate accumulation in the mouse kidney during warm ischaemia (see Figure 3.20), the increased malonate concentration within the tissue at the point of reperfusion may instead inhibit the rapid oxidation of succinate by SDH upon reperfusion, thereby reducing the supply of electrons to the electron transport chain and

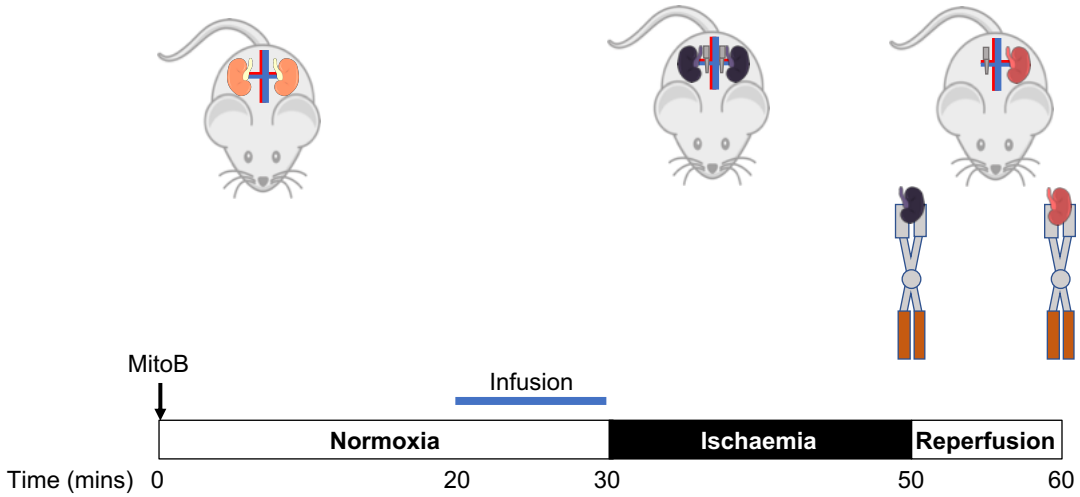

Figure 4.11 Targeting Mitochondrial ROS Production Prior to Ischaemia. MitoB was given as an intravenous injection into the IVC 30 mins prior to the onset of ischaemia. 10 mins prior to the onset of ischaemia an intravenous infusion of DMM (3.2) or saline was given into the IVC. Following infusion, both kidneys were exposed to 20 mins warm ischaemia by occluding the renal hila with a micro-serrefine clamp. Successful occlusion of the renal hila resulted in a change colour of each kidney from orange to dark purple. Following 20 mins of warm ischaemia, one kidney was rapidly retrieved and clamp frozen in LN2 using Wollenburg clamps. The micro-serrefine clamp was removed from the hila of the second kidney which underwent 10 mins reperfusion. Successful reperfusion could be confirmed by a change in colour of the kidney from dark purple to orangey-pink. At 10 mins reperfusion the second kidney was also rapidly retrieved and clamp frozen in LN2. Frozen tissue samples were stored at -70 °C until further processing and analysis.

driving force required for mitochondrial ROS production to occur. Administration of DMM to an organ donor prior to organ retrieval may therefore result in an increased malonate concentration within the donated graft at the point of reperfusion in the organ recipient, leading to a reduction in mitochondrial ROS production and IRI. To investigate further, DMM was administered to mice as infusion prior to the onset of 20 mins warm ischaemia as shown in Figure 4.3. The MitoP/MitoB ratio within kidneys treated with and without DMM was measured at the end of 20 mins warm ischaemia and at 10 mins reperfusion to determine whether an increased tissue malonate concentration at the onset of reperfusion led to a reduction in mitochondrial ROS production. Tissue MitoP/MitoB ratio, succinate concentration and malonate concentration at the end of 20 mins of warm ischaemia and at 10 mins of reperfusion are shown in Figure 4.12.

Effect of Dimethyl Malonate

Administration of 3.2 mg DMM prior to the onset of ischaemia led to a significant increase in tissue malonate concentration at the end of 20 mins of warm ischaemia and at 10 mins of

reperfusion in treatment versus control kidneys, as shown in Figure 4.12a. However, there was no significant difference in the MitoP/MitoB ratio between control and treatment kidneys at the end of 20 mins of warm ischaemia or at 10 mins reperfusion as shown in Figure 4.12b, suggesting mitochondrial ROS production was not inhibited. There was no significant difference in tissue succinate concentration at the end of 20 mins warm ischaemia between control and treatment kidneys. However, tissue succinate concentration was significantly greater in treatment kidneys than control values at 10 mins reperfusion, as shown in Figure 4.12c. This may be due to either reduced oxidation of ischaemic succinate at 10 mins reperfusion in treatment kidneys or inhibition of the forward action SDH as previously shown in Figure 3.20.

4.7.2 Administration of DMM and MAM on Reperfusion

As previously discussed, malonate ester pro-drugs administered upon reperfusion must be rapidly hydrolysed within (or subsequently transported into) mitochondria in order to effectively inhibit succinate oxidation and ROS production. Dimethyl malonate is hydrolysed relatively slowly by PLE *in vitro* and may be less well suited to inhibition of mitochondrial ROS production when administered at the point of reperfusion as discussed above. Diacetoxymethyl malonate on the other hand is hydrolysed more rapidly by PLE *in vitro* and preliminary experiments in a mouse model of myocardial infarction showed administration of MAM at reperfusion led to a reduction in infarct size (personal communication, Hiran Prag). Diacetoxymethyl malonate may therefore be capable of inhibiting mitochondrial ROS production in a donor graft when administered to an organ recipient at the point of reperfusion. To investigate further, DMM and MAM were given as an infusion to mice five minutes prior to the onset of kidney reperfusion as shown in Figure 4.13. The MitoP/MitoB ratio at the end of ischaemia in control versus malonate ester pro-drug treated kidneys was compared to that following ten minutes reperfusion to determine whether a reduction in mitochondrial ROS production had occurred.

Of note, DSM has previously been shown to a reduce infarct size when administered at reperfusion in an isolated mouse model of myocardial infarction and translational model of myocardial infarction in the pig [195] [194]. However, as DSM is a charged molecule it is currently unclear how this molecule enters mitochondria *in vivo* and whether its therapeutic effect occurs as result of SDH inhibition, requiring further investigation. As such, the effect of DSM administered at reperfusion on mitochondrial ROS production in the mouse kidney was not investigated as part of this thesis.

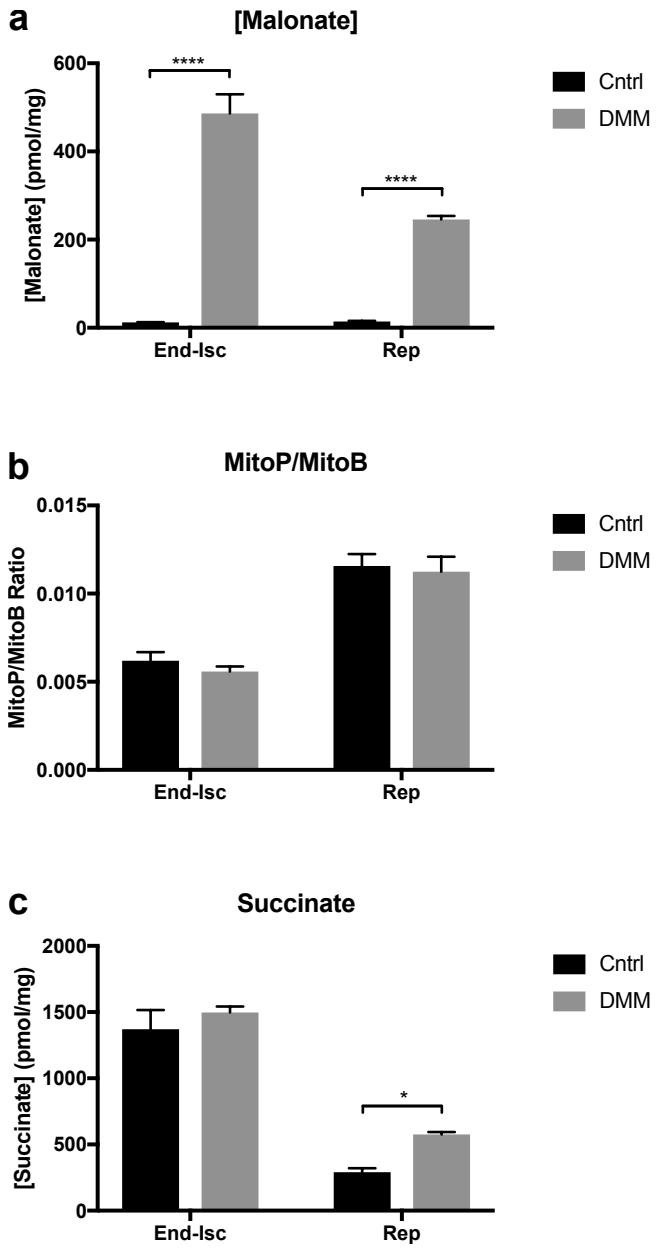

Figure 4.12 Targeting Mitochondrial ROS Production with Administration of DMM Prior to Ischaemia in the Mouse Kidney. MitoP/MitoB ratio **(a)** (n=8), succinate **(b)** (n=8) and malonate **(c)** (n=8) concentration at the end of 20 mins warm ischaemia and at 10 mins reperfusion following administration of saline (black bars) or 3.2 mg dimethyl malonate (DMM) (grey bars) as an infusion prior to the onset of ischaemia as shown in Fig 4.3. *P < 0.05, ****P < 0.0001. P values were calculated by two-way analysis of variance (ANOVA) with Sidak's multiple comparisons test. Data are mean ± SEM.

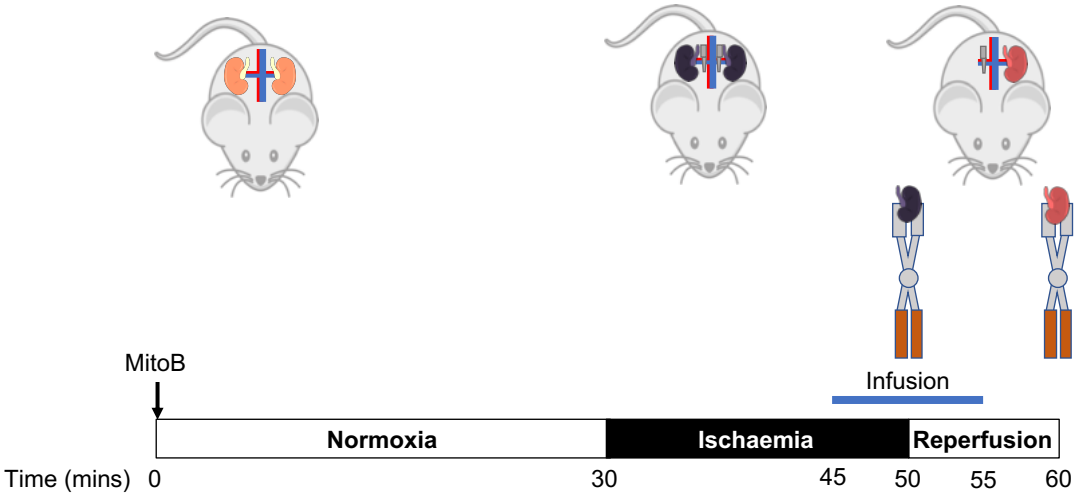

Figure 4.13 Targeting Mitochondrial ROS Production at Reperfusion in the Mouse Kidney. MitoB was given as an injection into the inferior vena cava 30 mins prior to the onset of ischaemia. Both kidneys then were exposed to 20 mins warm ischaemia by occluding the renal hila with a micro-serrefine clamp. Successful occlusion of the renal hila resulted in a change colour of each kidney from orange to dark purple. A 10 min infusion of a malonate (DMM or MAM) or control (saline or 1% DMSO) compound was started 5 mins prior to the onset of reperfusion as shown. At the end of 20 mins warm ischaemia, one kidney was rapidly retrieved and clamp frozen in LN2 using Wollenburg clamps. The micro-serrefine clamp was removed from the hila of the second kidney which underwent 10 mins reperfusion. Successful reperfusion could be confirmed by a change in colour of the kidney from dark purple to orangey-pink. At 10 mins reperfusion the second kidney was also rapidly retrieved and clamp frozen in LN2. Frozen tissue samples were stored at -70 °C until further processing and analysis.

Effect of Dimethyl Malonate

Dimethyl malonate was administered 5 minutes prior to the reperfusion of ischaemic mouse kidneys as shown in Figure 4.13. This was done to determine whether mitochondrial ROS production could be inhibited by an increase in tissue malonate concentration during early reperfusion. Tissue MitoP/MitoB ratio, succinate and malonate concentrations at the end of 20 mins of warm ischaemia and at 10 mins of reperfusion are shown in Figure 4.14. There was no significant difference in MitoP/MitoB ratio at the end of warm ischaemia or at 10 mins of reperfusion in treatment or control kidneys (Figure 4.14a), suggesting mitochondrial ROS production was not inhibited by administration of DMM on reperfusion. There was no significant difference in tissue succinate concentration at the end of warm ischaemia between control and treated kidneys however tissue succinate concentration was significantly greater in treated kidneys at 10 mins of reperfusion (Figure 4.14b). Similarly, there was no significant difference in tissue malonate concentration between control and treated kidneys at the end of warm ischaemia however tissue malonate concentration was significantly greater in treated versus control kidneys at 10 mins of reperfusion (Figure 4.14c). The increased succinate concentration at 10 mins of reperfusion in treatment kidneys may be due to reduced oxidation of the ischaemic succinate at 10 mins of reperfusion in treated kidneys or due to inhibition of forward action of SDH, as previously shown in Figure 3.20.

Effect of Diacetoxymethyl Malonate

Diacetoxymethyl malonate was administered 5 mins prior to the onset of reperfusion as shown in Figure 4.13 to determine whether mitochondrial ROS production could be inhibited by an increase in tissue malonate concentration during early reperfusion. Tissue MitoP/MitoB ratio, succinate concentration and malonate concentration at the end of 20 mins of warm ischaemia and at 10 mins of reperfusion are shown in Figure 4.15. There was no significant difference in the MitoP/MitoB ratio at the end of warm ischaemia or at 10 mins of reperfusion in treated or control kidneys, (Figure 4.15a), suggesting mitochondrial ROS production was not inhibited by administration of 0.32 mg MAM prior to reperfusion. Similarly, there was no significant difference in tissue succinate concentration at the end of warm ischaemia, or at 10 mins of reperfusion between control and treated kidneys (Figure 4.15b). There was no significant difference in tissue malonate concentration between control and treated kidneys at the end of warm ischaemia however tissue malonate concentration was significantly greater in treated versus control kidneys at 10 mins reperfusion (Figure 4.15c).

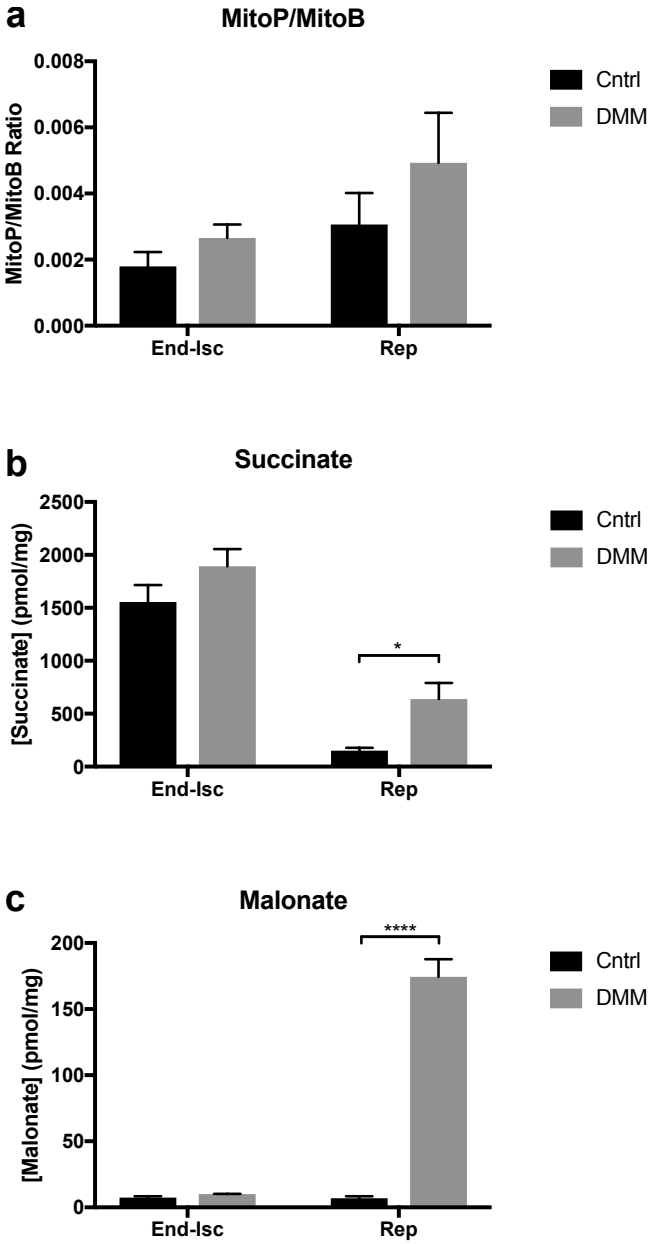

Figure 4.14 Targeting Mitochondrial ROS Production with Administration of DMM at Reperfusion in the Mouse Kidney. MitoP/MitoB ratio **(a)** (n=4), succinate **(b)** (n=4) and malonate **(c)** (n=4) concentration at the end of 20 mins warm ischaemia and at 10 mins reperfusion following administration of saline (black bars) or 3.2 mg dimethyl malonate (DMM) (grey bars) as an infusion prior to the onset of reperfusion as shown in Figure 4.13. *P < 0.05, ****P < 0.0001. P values were calculated by two-way analysis of variance (ANOVA) with Sidak's multiple comparisons test. Data are mean ± SEM.

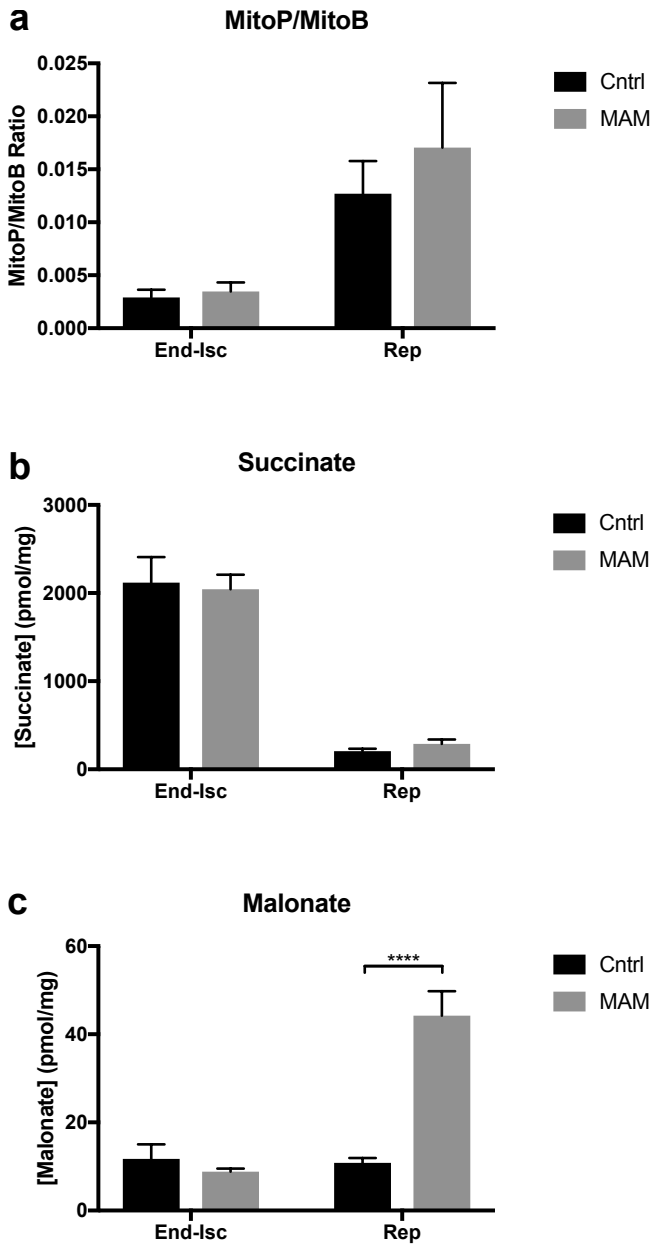

Figure 4.15 Targeting Mitochondrial ROS Production with Administration of MAM at Reperfusion in the Mouse Kidney. MitoP/MitoB ratio **(a)** (n=3-4), succinate **(b)** (n=3-4) and malonate **(c)** (n=3-4) concentration at the end of 20 mins warm ischaemia and at 10 mins reperfusion following administration of 1% DMSO (black bars) or 0.32 mg diacetoxymethyl malonate in 1% DMSO (MAM) (grey bars) as an infusion prior to the onset of reperfusion as shown in Figure 4.13. ****P < 0.0001. P values were calculated by two-way analysis of variance (ANOVA) with Sidak's multiple comparisons test. Data are mean ± SEM.

4.8 Effect of Malonate Ester Pro-Drugs on the Metabolic Changes in the Pig Kidney on Reperfusion

4.8.1 Administration of DMM during Back-Table Flush

Whilst the model of kidney IRI in the mouse may be used to investigate certain aspects of kidney transplantation, it is limited in its ability to replicate the clinical conditions under which donated organs are retrieved and preserved. In addition to the administration of malonate ester prodrugs to an organ donor or recipient, compounds may also be administered to a donated graft during back-table flush (BTF) and organ preservation in clinical transplantation. Importantly, this method of administration is currently associated with the fewest legal and logistical barriers to the use of malonate ester prodrugs in humans as discussed in Chapter 1. Whilst the conditions of BTF and organ preservation are not easily simulated in the mouse, they may be closely replicated in a translational model of kidney transplantation in the pig. In a similar manner to administration to an organ donor, administration of malonate ester prodrugs to a graft during BTF may lead to the accumulation of the prodrug within the tissue and subsequent hydrolysis during cold static storage, resulting in an increased malonate concentration within mitochondria at the point of reperfusion. The increased malonate concentration may subsequently inhibit rapid succinate oxidation by SDH on reperfusion of the graft in the recipient, leading to a reduction in mitochondrial ROS production and IRI. To investigate further, DMM was administered to the pig kidney during back-table flush as described in Figure 4.16. Pig kidneys were exposed to 30 mins warm ischaemia prior to back-table flush in order to simulate the conditions of DCD donation as previously described in Section 4.4. A dose of 80 mg DMM was administered to the pig kidney during BTF based on the weight of a pig kidney ($\sim$100 g) and the previously reported therapeutic dose in the mouse (160 mg/kg). Kidneys were flushed with a total volume of 500 mL ice cold Soltran solution containing 16 mg/100 mL DMM. Allometric scaling was not used in this experiment as DMM was not administered systemically to the pig. Earlier pilot data had indicated 50-100 mg DMM to be an appropriate dose to administer during BTF leading to a similar increase in tissue malonate as measured in the mouse. In addition to investigating the effect of DMM on mitochondrial ROS during reperfusion, it was hoped that the tissue concentration of malonate achieved in this experiment could also inform future pig and human experiments as to the optimal malonate concentration required to inhibit SDH in the kidney.

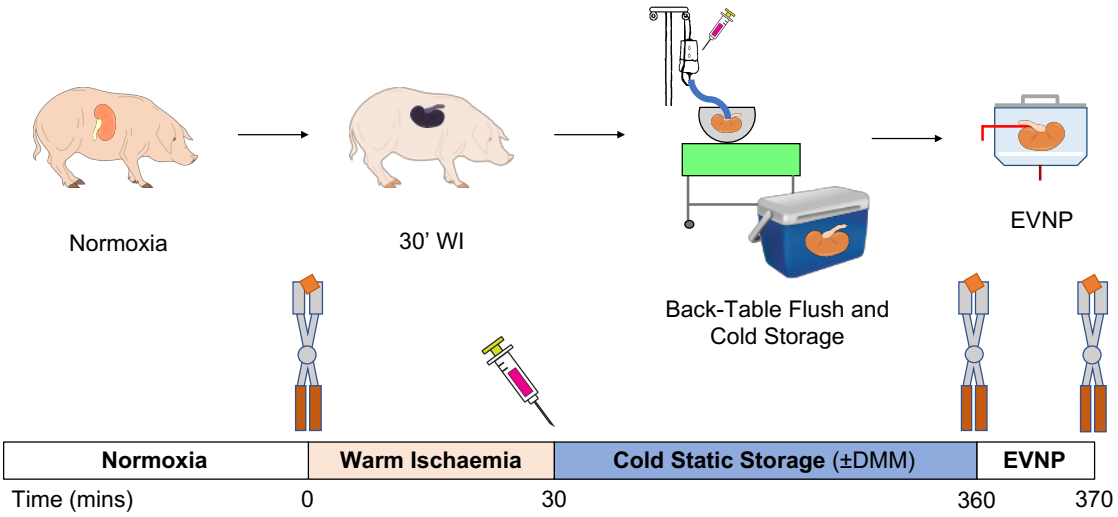

Figure 4.16 Investigating the Effect of DMM Administered During Back-Table Flush on the Metabolic Changes in the Pig Kidney on Reperfusion. Kidneys were retrieved from pigs under general anaesthesia and exposed to 30 mins warm ischaemia (30' WI). During warm ischaemia pig kidneys became purple in colour due to the presence of deoxygenated blood within the microvasculature. Kidneys were then flushed with ice cold Soltran (Cntrl) or ice cold Soltran containing 80 mg DMM and underwent 6 h cold static storage. Following cold static storage, kidneys were reperfused for 6 h using EVNP. Tissue wedge biopsies were taken from kidneys *in situ* under conditions of normoxia, at the end of cold static storage and following 10 mins EVNP to investigate the metabolic changes occurring in tissue with and without DMM during initial reperfusion. Tissue wedge biopsies were rapidly clamp frozen in LN2 using Wollenburg clamps and stored at -70 °C until further processing and analysis.

Effect of Dimethyl Malonate

As previously discussed, it was not possible to administer MitoB to the pig kidney prior to warm ischaemia due to the greater complexity of the surgery and uncertainty regarding the optimal dose. As a result mitochondrial ROS production could not be measured directly in the pig kidney on reperfusion via EVNP. However, measurement of tissue succinate and malonate concentration at the end of ischaemia and at 10 mins reperfusion could still be informative as to whether rapid succinate oxidation occurred on repefusion and whether sufficient levels of malonate within the tissue were achieved. Figure 4.17 shows the tissue malonate and succinate concentrations in pig kidneys treated with DMM during back-table flush under conditions of normoxia (In situ), at the end of cold static storage (End-Isc) and at 10 mins reperfusion (Rep). Tissue malonate concentration was significantly greater in DMM treated kidneys compared to controls at the end of cold static storage and at 10 mins reperfusion (Figure 4.17a), suggesting hydrolysis of DMM occurred during cold static storage in pig kidneys and remained elevated during the initial reperfusion period. Interestingly tissue succinate concentration was significantly lower at the end of cold static storage in kidneys that had been treated with DMM (Figure 4.17b) suggesting that further accumulation of succinate during cold static storage may have been inhibited by malonate in DMM treated kidneys compared to controls. Lastly, there was no significant difference in tissue succinate concentration between DMM treated and control kidneys at 10 mins reperfusion. It is unclear whether the malonate concentration in the tissue was able to inhibit succinate oxidation and mitochondrial ROS production from this data alone however further assays, such as that of aconitase, could be used to investigate whether increased tissue malonate concentration in DMM treated kidneys led to a reduction in mitochondrial ROS production as discussed below.

4.9 Discussion

4.9.1 Mitochondrial ROS Production in the Mouse Kidney

Effect of the Duration of Warm Ischaemia

The effect of the duration of warm ischaemia on mitochondrial ROS production on reperfusion in the mouse kidney was investigated using the ratiometric mass spectrometry probe MitoB, comprising an arylboronic acid conjugated to a TPP cation. The arylboronic acid reacts selectively with hydrogen peroxide and also with peroxynitrite, to form a stable phenol whilst the positive TPP cation targets MitoB to the mitochondria [269]. As mitochondrial

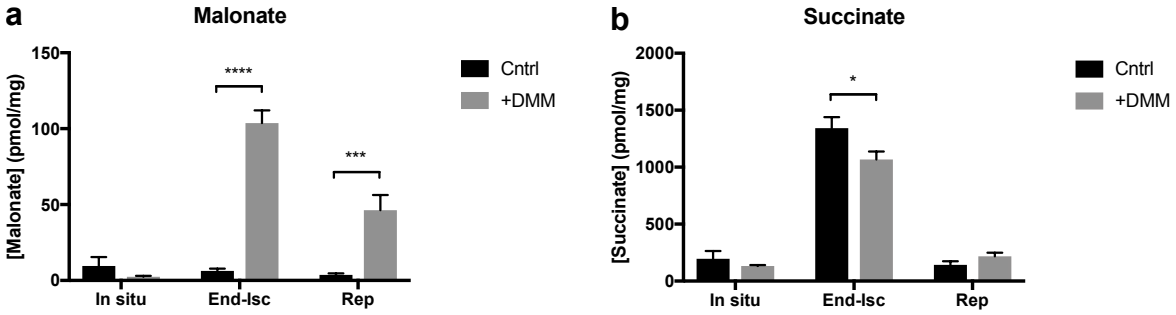

Figure 4.17 Effect of DMM Administered During Back-Table Flush on the Metabolic Changes in the Pig Kidney on Reperfusion. Tissue malonate **(a)** (n=3) and succinate **(b)** (n=3) concentration under conditions of normoxia (In situ), at the end of cold static storage (End-Isc) and following 10 mins ex vivo normothermic perfusion (Rep). Pig kidneys were exposed to 30 mins warm ischaemia and 6 h cold static storage as shown in Figure 4.16. During back-table flush kidneys were flushed with (+DMM) or without (Cntrl) 80 mg dimethyl malonate (DMM). *P < 0.05, ***P < 0.01, ****P < 0.0001. P values were calculated by two-way analysis of variance (ANOVA) with Sidak's multiple comparisons test. Data are mean ± SEM.

superoxide is very rapidly converted to hydrogen peroxide on reperfusion by mitochondrial superoxide MnSOD, MitoB may be used to measure mitochondrial ROS production on reperfusion *in vivo* [177] [269].

Increasing warm ischaemic time did not lead to increased mitochondrial superoxide production on reperfusion as measured by MitoP/MitoB ratio at 10 mins reperfusion. Instead, a similar increase in the MitoP/MitoB ratio was measured across the warm ischaemic times investigated, suggesting a similar quantity of mitochondrial ROS was produced at 10 mins reperfusion in each condition. This largely supports our working hypothesis of succinate being the key driver of mitochondrial superoxide production upon reperfusion as the succinate concentration had reached a maximum value after 5 mins warm ischaemia. Similarly, the ATP/ADP ratio and the sum of the ATP and ADP concentration appeared to be maximally depleted by 10 mins warm ischaemia and showed only partial recovery upon reperfusion. Adenosine nucelotide breakdown and lack of substrate for ATP synthase on reperfusion enables the large Δp required for RET and superoxide production at Complex I to develop. Interestingly, the ATP/ADP ratio and total ATP and ADP nucleotide levels fully recovered following 5 mins warm ischaemia and a smaller increase in MitoP/MitoB ratio was measured, further supporting the need for a near maximal Δp in order for mitochondrial superoxide production to occur. This hypothesis could be further tested by administering oligomycin, an inhibitor of ATP synthase, on reperfusion in future experiments. Of further note, kidneys exposed to 45 mins warm ischaemia showed poor initial reperfusion. This led to a reduced MitoP/MitoB ratio, increased succinate concentration, reduced ATP/ADP ratio and reduced

ATP and ADP nucleotide concentration at 10 mins reperfusion likely due to continued tissue ischaemia.

Effect of Succinate Concentration

Dimethyl succinate, a cell permeable derivative of succinate, has previously been shown to increase succinate concentration and mitochondrial ROS production on reperfusion in primary cardiomyocytes [14]. Here, 3.2 mg DMS was given as an infusion prior to 20 mins warm ischaemia in the mouse kidney as shown in Figure 4.3. Tissue succinate concentration was significantly increased compared to control kidneys at the end of 20 mins of warm ischaemia immediately prior to reperfusion however there was no significant difference in MitoP/MitoB ratio at 10 mins reperfusion in DMS versus control kidneys suggesting greater mitochondrial ROS production did not occur.

There are a number of possible explanations for this result. Firstly, the experiment may have been under powered given the variability in the MitoP/MitoB ratio measured in control kidneys at 10 mins reperfusion. Secondly, the experiment re-emphases the difficulty in accurately measuring ROS *in vivo* [272]. MitoB is not specific for mitochondrial superoxide production at Complex I and may also react with hydrogen peroxide and peroxynitrite produced at other sites within mitochondria on reperfusion. Furthermore, the reactivity of MitoB is pH-dependent and occurs slowly with hydrogen peroxide at a rate of $\sim$9 M^{-1} s^{-1}. Whilst this may be ideal for measuring steady-state levels of hydrogen peroxide, MitoB may be outcompeted by faster endogenous degradation pathways such as the peroxidases during the initial reperfusion period, which typically react with hydrogen peroxide at a rate of $\sim$2 x 10^7 M^{-1} s^{-1} [268]. Conversely, the measurement of the MitoP/MitoB ratio at 10 mins reperfusion may have been too long after the initial burst of ROS from mitochondria occurs on reperfusion, after the which the MitoP/MitoB signal may have become saturated by reaction with hydrogen peroxide from other sources. Lastly, it is currently unclear what proportion of accumulated succinate is oxidised by mitochondria on reperfusion. Up to two-thirds of ischaemic succinate may be exported from cells and washed out of ischaemic tissue on reperfusion [175]. The increased succinate concentration measured in Figure 4.5 may have been largely extracellular and therefore unable to increase mitochondrial superoxide production. Alternative succinate derivatives, such as diacteoxymethyl succinate (AMS) are hydrolysed more rapidly within mitochondria and may be better suited to increase mitochondrial succinate concentration and subsequent oxidation by SDH under the conditions required for RET and ROS production to occur [273]. Recently, AMS has been shown to increase the level of injury heart transplantation model in the mouse, supporting the role of succinate in mitochondrial ROS production and IRI [193].

4.9.2 Metabolic Changes on Reperfusion in the Pig and Human Kidney

Metabolic Changes on Reperfusion in the Pig Kidney

Although it was not possible to administer MitoB to the pig kidney due to the greater complexity of the procedure and uncertainty regarding the dose and side effects, mitochondrial ROS production on reperfusion could be implied by comparing the metabolic changes that occur in the pig to those in the mouse. The metabolic changes that occurred in pig kidneys exposed to 30 mins warm ischaemia and 6 h cold static storage followed by 10 mins EVNP strongly resembled the metabolic changes that lead on to mitochondrial ROS production in the mouse. Conversely, succinate did not significantly increase above baseline levels in pig kidneys exposed to 6 h cold static storage only. In addition, ATP and ADP levels recovered after 10 mins reperfusion in pig kidneys exposed to 6 h cold static storage, suggesting that the conditions required for mitochondrial ROS production did not occur. This could be further validated in future experiments by measuring alternative markers of mitochondrial ROS production such as the aconitase assay (see below). If only minimal mitochondrial ROS production occurred in kidneys exposed to 6 h cold storage, then they may act as an ideal negative control in future experiments in which mitochondrial ROS production in pig kidneys exposed to warm ischaemia is targeted.

Metabolic Changes on Reperfusion in the Human Kidney

Similar to the situation in the pig, MitoB could not be administered to human kidneys due to uncertainties regarding the compounds efficacy in the EVNP system. Instead, the metabolic changes on reperfusion of declined human kidneys were compared to those leading to mitochondrial ROS production in the mouse, to determine whether mitochondrial ROS production was likely to have occurred in the human kidney upon reperfusion. Succinate concentration decreased rapidly upon the reperfusion of declined human kidneys whilst ATP and ADP levels recovered more gradually, consistent with mitochondrial ROS production. It was not possible to gain a normoxic tissue sample from human kidneys. However, as succinate levels are known to return to normoxic values on reperfusion, human kidneys were re-exposed to warm and cold ischaemia to further investigate the metabolic changes thought to lead to mitochondrial ROS production compared to a normoxic baseline value. Re-exposure of human kidneys to ischaemia and a second period of EVNP has not previously been conducted. However, it has recently been shown that succinate accumulation during ischaemia is not affected by ischaemic pre-conditioning in the mouse heart [267]. As such, use of EVNP to 'reset' the metabolic profile of human kidneys followed by re-exposure to

ischaemia and second period of reperfusion, is an attractive model to investigate the use and efficacy of novel compounds under controlled conditions of ischaemia reperfusion in the human kidney.

4.9.3 Effect of Malonate Ester Pro-Drugs on ROS Production in the Mouse Kidney

Administration of Malonate Ester Pro-Drugs Prior to Ischaemia

Administration of dimethyl malonate (DMM) prior to warm ischaemia in the mouse kidney led to an increase in tissue malonate concentration at the end of ischaemia and at 10 mins reperfusion. However, this did not inhibit mitochondrial superoxide production on reperfusion as measured by the MitoP/MitoB ratio. The increased succinate concentration in DMM treated kidneys at 10 mins reperfusion suggests tissue malonate concentration is sufficient to inhibit succinate dehydrogenase however whether this is sufficient to inhibit the oxidation of high concentrations of succinate present at the end of ischaemia is unclear. Furthermore, DMM is not targeted to mitochondria in the same way as MitoB and it is unclear what proportion of the malonate concentration measured in the tissue is located within the mitochondria matrix and what proportion is located elsewhere in the cell or extracellular space. Lastly, as the use of MitoB to measure mitochondrial superoxide production on reperfusion is relatively insensitive, an alternative method to asses mitochondrial superoxide production on reperfusion, such as via aconitase activity may be informative. Aconitase catalyses the conversion of citrate to *cis*-aconitate and contains an iron-sulfur centre that is inactivated by superoxide. Aconitase activity may be assessed in frozen tissue extracts by monitoring the rate of NADPH production at 340 nm, with differences in aconitase activity used to determine the degree of mitochondrial ROS production that occurred on reperfusion [274].

Administration of Pro-Drugs upon Reperfusion

Administration of dimethyl malonate (DMM) and diacetoxymethyl malonate (MAM) 5 mins prior to reperfusion in the mouse kidney led to an increase in tissue malonate concentration at 10 mins reperfusion but did not inhibit mitochondrial superoxide production as measured by the MitoP/MitoB ratio. In order to inhibit mitochondrial superoxide production on reperfusion, DMM and MAM must be rapidly hydrolysed within (or subsequently transported into) mitochondria in order to inhibit succinate oxidation. The acetoxymethyl groups of MAM are favoured by carboxylesterases within cells and hydrolysed far more rapidly than the

methyl groups of DMM. However, neither molecule is specifically targeted to mitochondria and may be hydrolysed at numerous other subcellular locations requiring subsequent transport into mitochondria [275]. More specific mitochondria-targeting mechanisms, such as TPP linkage, may therefore be needed to deliver malonate compounds to mitochondria at a rate and concentration large enough inhibit succinate oxidation when administered on reperfusion [199].

4.9.4 Effect of Malonate Ester Pro-Drugs on the Metabolic Changes in the Pig Kidney on Reperfusion

Administration of DMM to the pig kidney during back-table flush inhibited further succinate accumulation during cold static storage. Furthermore, there was an increase in the tissue malonate concentration at the end of ischaemia and at ten minutes *ex vivo* reperfusion during which time succinate returned to normoxic levels. It was not possible to measure mitochondrial ROS production using MitoB in the pig due to the greater complexity of the surgery and concerns regarding its toxicity however, it may be possible to measure a difference in mitochondrial ROS production between control and treatment groups using the aconitase assay in future experiments as described above. Nonetheless, the presence of an increased tissue malonate concentration over the initial reperfusion period within the range shown to inhibit SDH in the previous Chapter (see Figures 3.22 & 3.23) is encouraging and suggests that by following up this approach it may be possible to inhibit the rapid oxidation of succinate upon reperfusion.

4.10 Summary

Our working hypothesis is that mitochondrial ROS production upon reperfusion appears to depend on the depletion of adenosine nucleotides and the accumulation of succinate during ischaemia. Inhibition of succinate oxidation upon reperfusion may therefore reduce mitochondrial ROS production on reperfusion and be of benefit in kidney transplantation, particularly as grafts from both DBD and DCD donors show near maximal succinate accumulation following organ retrieval and cold storage. However, it was not possible to inhibit mitochondrial ROS production using malonate ester pro-drugs administered prior to ischaemia, during organ preservation or at reperfusion in a mouse or pig model of kidney transplantation as measured by the mitochondrial ROS probe, MitoB. However, MitoB may be limited in its ability to accurately measure the burst of ROS from mitochondria on reperfusion, warranting further investigation of malonate ester prodrugs in kidney transplantation

using other markers of ROS production and oxidative damage. Conversely, it may be that more targeted approaches are required to deliver malonate to mitochondria at a sufficient rate and concentration to inhibit SDH effectively (and this will be discussed in further detail in Chapter 6). Nevertheless, three translational models of kidney transplantation in mice, pigs and humans have been further characterised in this chapter and may be used to inform future experiments and investigate other potential mitochondrial compounds.

Chapter 5

Consequences of Mitochondrial ROS Production in Kidney Transplantation

5.1 Introduction

As previously discussed, mitochondrial ROS production on reperfusion is thought to initiate much of the downstream damage resulting from IRI [15] [16] [276]. The large and sudden burst of superoxide produced by mitochondria on reperfusion may overwhelm cellular antioxidant defences resulting in damage to DNA, lipids and proteins and culminating in the activation of cell death pathways and necrosis [276] [277]. In turn, cell death resulting from ROS production may lead to the release of damage associated molecular patterns (DAMPs) and exacerbation of the sterile inflammatory response following IRI which may ultimately influence the extent of tissue repair versus fibrosis [16] [114]. Inhibition of the burst of superoxide from mitochondrial on reperfusion may therefore help to reduce the overall level of tissue injury, degree of cell death and severity of inflammation following IRI with important consequences for subsequent organ function and survival. This is particularly pertinent to kidney transplantation, where IRI is inherent to current transplant practices. Not only have concerns regarding IRI restricted the use of organs from the current donor pool but IRI is also thought to play a central role in initial graft function, graft survival and the risk of organ rejection as discussed in Chapter 1 [9] [10] [6] [107].

Malonate ester prodrugs were not shown to inhibit mitochondrial ROS production on initial reperfusion as measured by the ratiometric probe MitoB in Chapter 4. However, as previously discussed, MitoB may have limited ability to measure a burst of superoxide from mitochondria and administration of malonate ester prodrugs may still have had a protective effect. To investigate this possibility further, it was first important to better characterise the

level of injury that occurs on reperfusion in the different translational models of renal IRI and kidney transplantation in mice, pigs and humans and to identify suitable biomarkers of oxidative damage, cell death and kidney function that could be used to assess the protective effect of malonate ester-prodrugs in subsequent treatment experiments. This required a more detailed understanding of the fate of superoxide produced from mitochondria on reperfusion and different biological markers that could be used to assess levels of oxidative stress.

As described in Chapter 1, superoxide produced by mitochondria on reperfusion is rapidly dismutated to hydrogen peroxide by the enzyme manganese superoxide dismutase (MnSOD) [177]. Hydrogen peroxide is relatively unreactive with most biological molecules due to its high activation energy but readily undergoes one electron oxidations in the presence of a transition metal to form either a hydroxyl radical (Fenton reaction) or an activated metal complex. Hydroxyl radicals have a much lower activation energy than hydrogen peroxide for electron abstraction and are extremely reactive with DNA, proteins and lipids, resulting in covalent modifications to the structure of these molecules, impairing their function (see Figure 5.1) [184] [183] [278]. Whilst, mitochondria possess a number of antioxidant defence mechanisms which aim to neutralise hydrogen peroxide and avert hydroxyl radical formation including the thiol peroxidases, peroxiredoxins and glutathione peroxidase (see Figure 5.2); these have evolved to protect against low levels of mitochondrial ROS production that occur during forward electron transport and may be overwhelmed by the large and rapid production of superoxide that occurs during IRI. As a result, the burst of mitochondrial ROS on reperfusion, alongside mitochondrial Ca^{2+} overload and restoration of intracellular pH, may trigger opening of the mitochondrial permeability pore (mPTP), dissipation of the mitochondrial membrane potential, ATP depletion and necrotic cell death following IRI [40] [41]. In addition, rupture of the outer mitochondrial membrane and release of cytochrome C may trigger apoptosis in more marginally affected tissue whilst oxidative damage to lipids, protein and DNA may activate other forms of regulated cell death [47] [177]. Whilst other sources of ROS such as xanthine oxidases and NADPH oxidases are likely to also contribute to oxidative damage following IRI, the initial burst of mitochondrial superoxide on reperfusion is thought to be a key initiator of much of the secondary damage leading to tissue injury [15] [16] [276]. Oxidative damage to lipids, proteins and DNA, in addition to levels of cell death, may therefore be used as an indirect measure of mitochondrial ROS production following IRI and used to assess the protective effect of malonate ester prodrugs on kidney injury and function at later stages of reperfusion.

In this Chapter, oxidative damage to mtDNA, proteins, lipids as well as changes in tissue glutathione concentration were investigated in the mouse model of renal IRI at 1, 6 and 24 h reperfusion. As this thesis was primarily focused on the effect of malonate ester

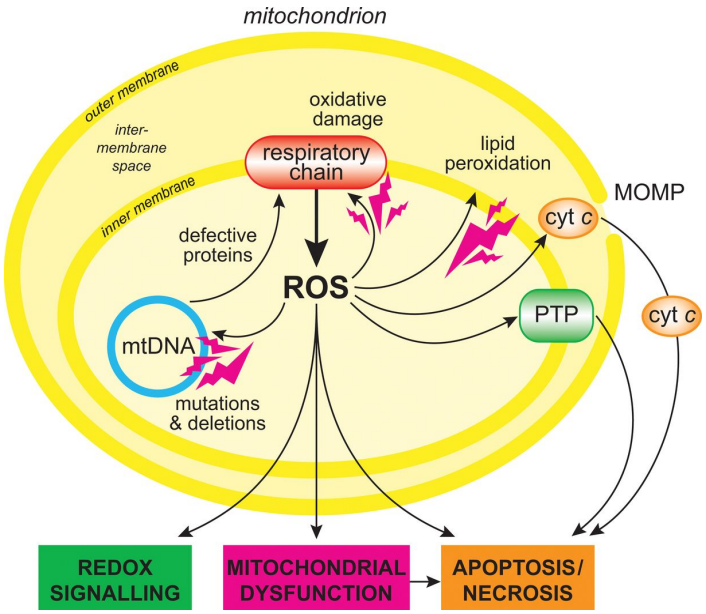

Figure 5.1 Mechanisms Leading to Oxidative Damage and Cell Death Following Mitochondrial ROS Production on Reperfusion. The burst of ROS from mitochondria on reperfusion may overwhelm mitochondrial antioxidant defence mechanisms leading to hydroxyl radical formation and oxidative damage to DNA, lipids and proteins. Mitochondrial DNA is particularly susceptible to oxidative damage due to its proximity to the site of mitochondrial ROS production as well as a lack of protective histones and a poor mtDNA repair mechanisms. The inner mitochondrial membrane is also susceptible to oxidative damage as it contains a large proportion of polyunsaturated fatty acids (PUFAs). Free radicals propagate within phospholipid bilayers containing PUFAs leading to changes in lipid structure, membrane permeability and generation of the lipid peroxidation products, 4-hydroxynonenal (4-HNE) and malondialdehyde (MDA). Lipid peroxidation products are also highly reactive molecules and may exacerbate oxidative tissue damage by causing further covalent modifications to DNA and proteins. Hydroxyl radicals (and other reactive species) may also react directly with proteins, leading to carbonyl formation (CO groups), protein-protein cross linkages and protein fragmentation. Not only may oxidative damage to proteins may impair their structure and function but also exacerbate oxidative damage to other structures if for example DNA polymerase proteins are no longer able to repair oxidative damage DNA or oxidative damage to mitochondrial respiratory chain components leads to further ROS production. Ultimately, mitochondrial ROS production may lead to opening of the mitochondrial permeability transition pore (mPTP) and necrotic cell death or induction of the mitochondrial outer membrane pore (MOMP) leading to cytochrome c (cyt C) release and apoptosis. In addition, accumulation of oxidative damage to lipids, proteins and DNA may trigger other pathways of regulated cell death. Adapted from Murphy (2009).

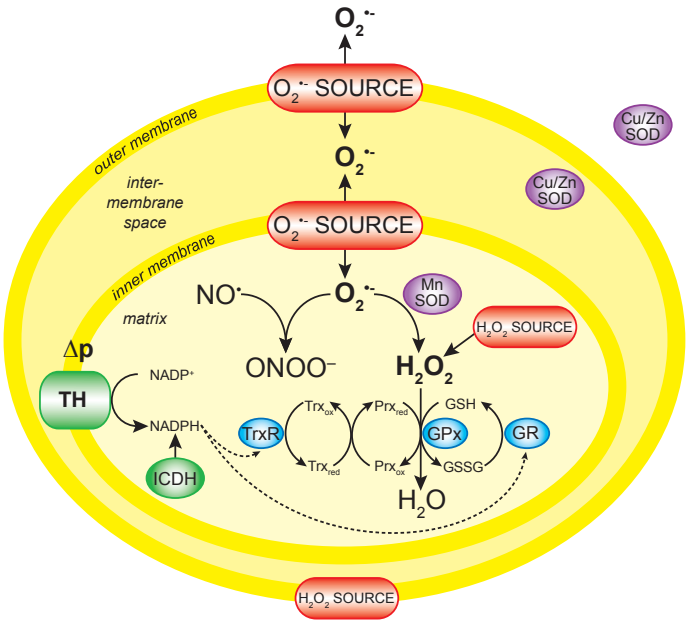

Figure 5.2 Antioxidant Defence Mechanisms Within Mitochondria. Mitochondria possess a number of thiol peroxidases, including peroxiredoxin and glutathione peroxidase which aim to neutralise hydrogen peroxide (H_2O_2) and avert hydroxyl radical formation ($OH^{\bullet}$). Glutathione peroxidase (GPx) catalyses the reaction of hydrogen peroxide with reduced glutathione (GSH) to form oxidised glutathione (GSSG), water and oxygen. Oxidised glutathione may subsequently be converted back to reduced glutathione (GSH) by reaction with NADPH, catalysed by glutathione reductase (GR). Meanwhile, peroxiredoxins (Prx and Trx) react with hydrogen peroxide to form interchain disulphide bonds, which may also be converted back to their reduced form by reaction with NADPH catalysed by thioredoxin reductases (TrxR). Adapted from Murphy (2009).

prodrugs on initial levels of kidney injury and function following IRI, later timepoints were not investigated. Following assessment of oxidative damage, different methods of quantifying the degree of cellular necrosis were investigated at 24 h reperfusion in the mouse model of renal IRI as well as the effect of varying periods of warm ischaemia on kidney function. As described above, this was to establish the most appropriate biomarkers and timepoints to assess the protective effect of malonate ester prodrugs in future treatment experiments. Similarly, the degree of cellular necrosis and organ function were also characterised in the pig and human translational models of kidney transplantation. However, the level injury could only be assessed for up to 6 h reperfusion in kidneys undergoing EVNP, after which increasing levels of red cell haemolysis were thought to adversely affect the physiological parameters of the perfusate and induce further tissue injury. After characterising the different models of renal IRI and kidney transplantation, the effect of malonate ester prodrugs on tissue injury, cell death and kidney function was investigated in the mouse and preliminary experiments in the pig when administered at different times during ischaemia reperfusion as discussed in previous Chapters. Investigation of the inflammatory response to IRI was outside the scope of this thesis but would form an important aspect of future work on malonate ester prodrugs, as discussed in Chapter 6.

5.1.1 Aims

1. To characterise the development of oxidative damage in the mouse model of renal IRI and translational model of kidney transplantation in the pig

2. To quantify the level cell death in the mouse model of renal IRI and translational model of kidney transplantation in the pig and human

3. To characterise the effect of IRI on kidney function in the mouse model of renal IRI and translational model of kidney transplantation in the pig and human

4. To determine the effect of malonate compounds administered prior to ischaemia (to simulate administration to the organ donor) and on reperfusion (to simulate administration to the organ recipient) in the mouse model of renal IRI

5. To determine the effect of malonate compounds administered prior to ischaemia (to simulate administration to the organ donor) and during back-table flush in preliminary experiments in the translational model of kidney transplantation in the pig

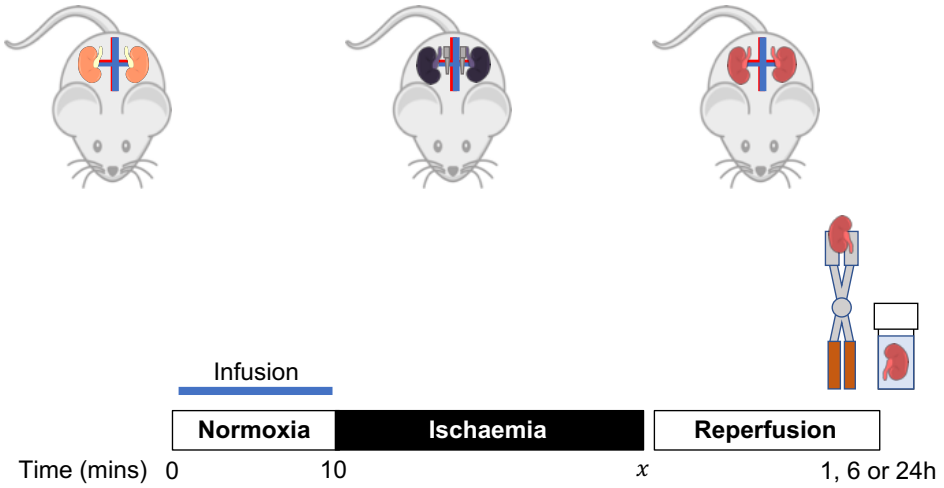

Figure 5.3 Investigating the Consequences of Ischaemia Reperfusion Injury in the Mouse Kidney. To investigate the consequences of ischaemia reperfusion injury in the mouse, kidneys were exposed to 20 or 25 mins warm ischaemia by placing a microserrefine clamp over the renal hila as previously described. Following ischaemia, the micro-serrefine clamps were removed and kidneys were reperfused for either 1, 6 or 24 h. At the end of the reperfusion period, one kidney was rapidly excised from the mouse under general anaesthesia and clamp frozen in LN2 using Wollenburg clamps whilst the second kidney was placed in formalin. A blood sample was also collected from the IVC immediately prior to kidney retrieval.

5.1.2 Hypothesis

Malonate ester pro-drugs may ameliorate IRI in kidney transplantation by reducing mitochondrial ROS production. This may subsequently lead to improved initial graft and reduced tissue injury following transplantation.

5.2 Assessment of Kidney Injury in the Mouse

To determine whether malonate compounds are able to ameliorate IRI in the mouse kidney, it was first necessary to better characterise the downstream consequences of IRI in order to select the most appropriate biological markers and end-points. Oxidative damage, cell death and kidney function were thus investigated following range of ischaemia and reperfusion times as shown in Figure 5.3.

5.2.1 Oxidative Damage

Reactive oxygen species produced by mitochondria during the initial reperfusion may react with cellular components such as proteins, lipids and DNA initiating much of the cellular

damage arising from IRI (see Figure 5.1). To better understand the development of oxidative damage within the kidney and to allow the selection of appropriate oxidative damage markers for use in treatment experiments, oxidative damage to mtDNA, proteins and lipids was measured at 1, 6 and 24 h reperfusion following either 20 or 25 mins warm ischaemia. Glutathione, a major component of cellular antioxidant defence pathways, was also measured at 1, 6 and 24 h reperfusion.

Oxidative Damage to Mitochondrial DNA

Oxidative damage to mitochondrial DNA (mtDNA) was measured using a quantitative PCR method. Oxidative damage to mtDNA blocks progression of the polymerase during PCR, reducing amplification of a long ($\sim$10 kb) target sequence relative to a short ($\sim$200 bp) target sequence which is used to control for mtDNA copy number [202]. Amplification of mitochondrial DNA following renal IRI in the mouse kidney is shown in Figure 5.4a. Mitochondrial DNA amplification was significantly increased at the end of 25 mins warm ischaemia and following 24 h reperfusion. This result was confusing and suggests the mtDNA at the end of ischaemia and at 24 h reperfusion contained less oxidative damage than control kidneys.

Protein Carbonyl Formation

Protein bound carbonyls resulting from oxidative damage to proteins were measured by derivatisation with DNP and detection with anti-DNP antibodies via an ELISA. Protein carbonyl concentration following renal IRI in the mouse is shown in Figure 5.4b. There was no significant difference in protein carbonyl concentration compared to control values at the end of 20 mins warm ischaemia (End-Isc) or following 1, 6 or 24 h reperfusion. Furthermore there was no significant difference between protein carbonyl concentration in control versus positive control samples which had under gone 8 h warm ischaemia at 36 °C in the carcass of euthanised mice, suggesting the assay may not have been sensitive enough to detect changes in protein carbonyl concentration in tissue homogenates

Lipid Peroxidation

Malondialdehyde, a major end product of lipid peroxidation, was detected by reaction with thiobarbituric acid and spectrophotometric measurement of thiobarbituric acid reactive species. Malondialdehyde concentration following renal IRI in the mouse is shown in Figure 5.4c and was calculated using the TBARS assay. Malondialdehyde concentration was

significantly increased at 24 h reperfusion compared to control values following 20 mins warm ischaemia.

Total Glutathione Concentration

Glutathione, a thiol-containing tripeptide, is a major cofactor for the thiol peroxidases, glutathione peroxidase and peroxiredoxins, involved in detoxification of hydrogen peroxide within mitochondria and may exist in both a reduced thiol form (GSH) and an oxidised disulfide form (GSSG) (see Figure 5.2). Total (reduced and oxidised) glutathione was measured using the glutathione recycling assay, during which the rate of TNB production from the reaction of GSH with DTNB is measured at 412 nm using a spectrophotometer and compared to the rate of TNB production in a set of GSH standards. During the assay, GSSG is 'recycled' back to GSH by GR meaning the total quantity of glutathione within the tissue (reduced and oxidised) is able to react with DTNB and contribute to TNB production. The total glutathione concentration in the kidney following renal IRI is shown in Figure 5.4d. Total glutathione was significantly decreased compared to control values at 1, 6 and 24 h reperfusion following 25 mins warm ischaemia.

5.2.2 Cell Death

A major consequence of IRI is cell death via both apoptotic and necrotic pathways [279]. Mitochondrial ROS produced during early reperfusion are thought to play a direct role in the induction of the mitochondrial permeability transition, apoptosis and necrosis in addition to their damaging effects on lipids, proteins and DNA which may also lead to the activation of cell death pathways [276]. To investigate how the level of cell death may be best quantified in the kidney following IRI for use in future treatment experiments, kidneys were exposed to various periods of warm ischaemia and cell death assessed by histological analysis and total adenosine nucleotide levels at 24 h reperfusion.

Histological Analysis

Histological analysis of haematoxylin and eosin (H&E) stained tissue sections was performed using ilastik software as described in Chapter 2. Representative images of H&E sections at 24 h reperfusion following varying periods of warm ischaemia are shown in Figure **??**a. The percentage of necrotic tissue calculated using ilastik software is shown in **??**b. Tissue necrosis at 24 h reperfusion increased with increasing warm ischaemia time and was significantly greater than control tissue following 15, 25, 30 and 45 mins warm ischaemia.

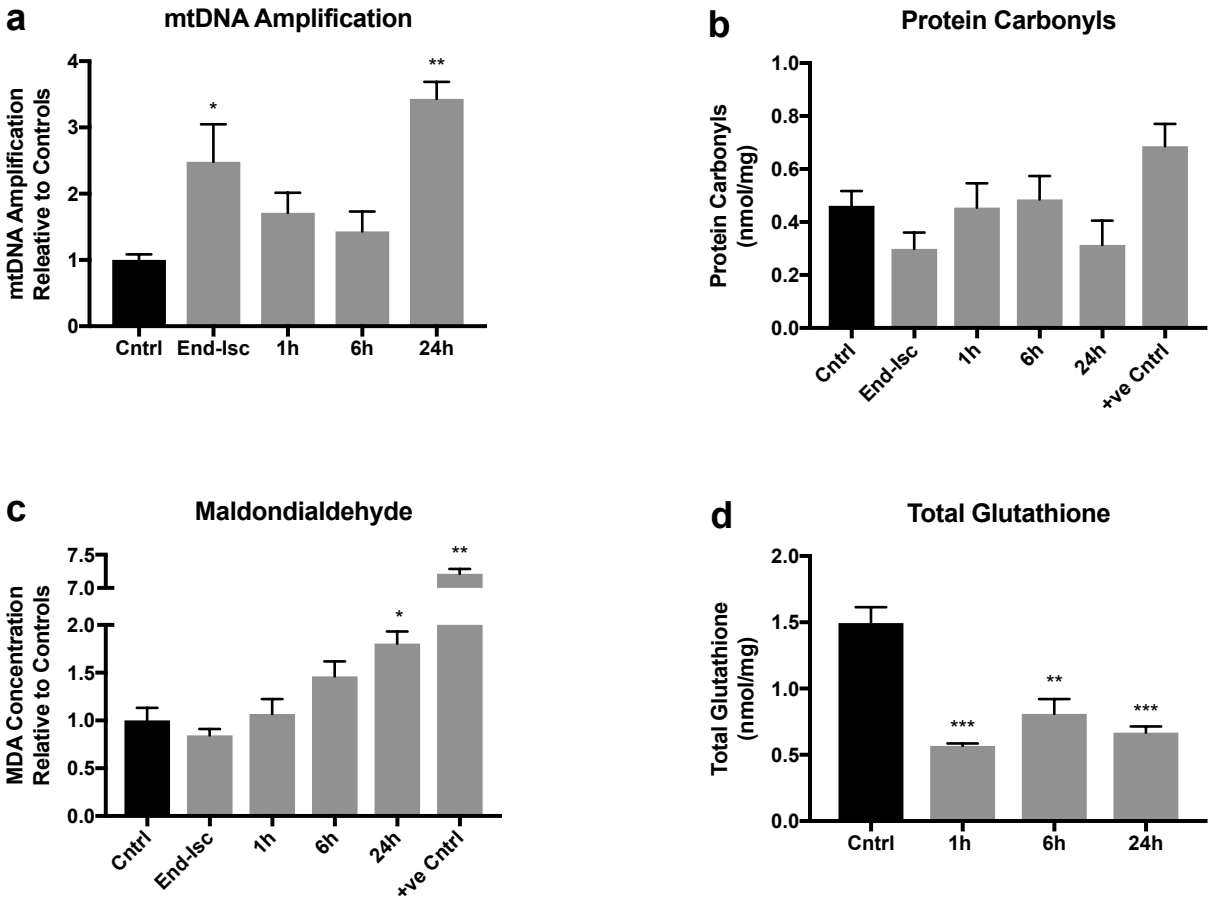

Figure 5.4 Characterisation of Oxidative Damage following Renal IRI in the Mouse (**a**) Amplification of mitochondrial DNA following 25 mins warm ischaemia (End-Isc) and at 1, 6 and 24 h reperfusion expressed relative to normoxic control values (n=4-6 except at 1 h where n=2). (**b**) Protein carbonyl concentration following 20 mins warm ischaemia (End-Isc) and at 1, 6 and 24h reperfusion compared to normoxic control values (n=4). (**c**) Tissue malondialdehyde (MDA) concentration following 20 mins warm ischaemia (End-Isc) and at 1, 6, and 24 h reperfusion expressed relative to normoxic control values (n=4). (**d**) Total glutathione concentration at 1, 6 and 24 h reperfusion following 25 mins warm ischaemia compared to normoxic control values (n=4 except 1 h where n=2). *P < 0.05, **P < 0.01, ***P < 0.001. P values were calculated by one-way analysis of variance (ANOVA) with Dunnett's multiple comparisons test. Data are mean ± SEM or where n=2 mean ± range. Measurement of tissue MDA concentration was performed by Ms Margaret M Huang (University of Cambridge Department of Surgery, UK).

ATP and ADP Concentration and Ratio

Tissue ATP and ADP nucleotide concentration may be used to estimate the level of necrosis following IRI as only viable cells are capable of regenerating their ATP and ADP levels following ischaemia. The sum of the ATP and ADP concentration at 24 h reperfusion following varying periods of warm ischaemia is shown is Figure **??**d and reflects levels necrosis measured in H&E sections. The sum of the ATP and ADP concentration at 24 h reperfusion was decreased with increasing warm ischaemic time and was significantly lower than control tissue following 30 and 45 mins warm ischaemia. One caveat, however, is that IRI may have resulted in other changes to cellular metabolism that may also contribute to reduced ATP and ADP levels. Nonetheless, the ATP/ADP ratio, shown in Figure **??**c, was not significantly different from controls values at 24 h reperfusion following increasing warm ischaemia times and the increased value following 25 mins warm ischaemia was possibly artifactual, suggesting large changes in cellular metabolism on reperfusion had not occured.

5.2.3 Kidney Function

Ultimately, the effect of IRI on organ function is the factor most critical for patient outcomes. To investigate the effect of IRI on organ function in the mouse kidney, serum creatinine and blood urea nitrogen concentration were measured at 24 h reperfusion following various periods of warm ischaemia.

Serum Creatinine Concentration

Creatinine is produced from the breakdown of phosphocreatinine in skeletal muscle and released into the blood at a relatively constant rate. It is then freely filtered from the blood by the kidney and excreted in the urine. As glomerular filtration rate (the rate of filtration of the blood by the kidneys) is also relatively constant under physiological conditions, a steady state serum creatinine concentration is established. If glomerular filtration rate decreases as a result of IRI, the ability of the kidneys to clear creatinine from the blood is reduced, leading to an increase in the level of serum creatinine. Serum creatinine concentration before and after IRI may therefore be used to assess kidney function. Figure 5.5a shows the SCr concentration in mice at 24 h reperfusion following various periods of warm ischaemia. Serum creatinine concentration was signficantly increased at 24 h reperfusion following 20, 25, 30 and 45 minutes warm ischaemia but not 15 or 18 minutes warm ischaemia. This is likely due to the large reserve capacity of the kidney with up to 50% of nephrons needing to be lost before a rise in serum creatinine concentration can be detected [234].

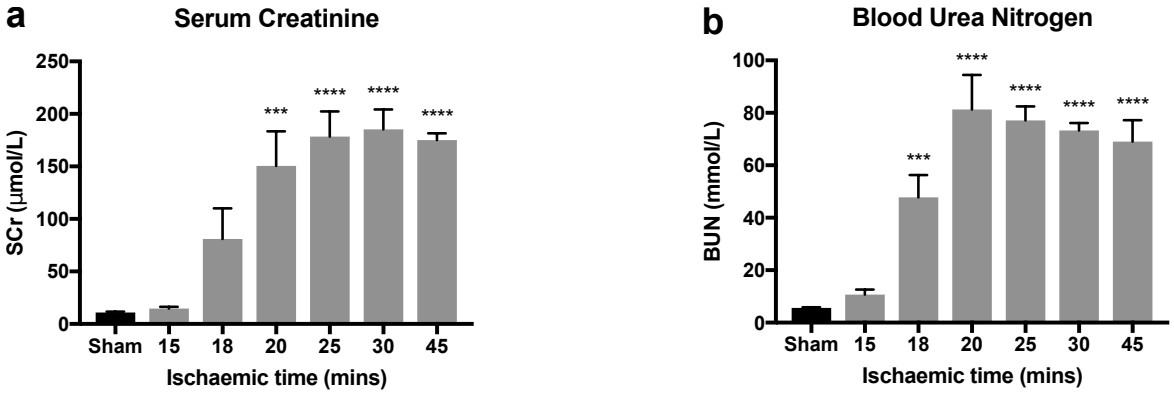

Figure 5.5 Kidney Function at 24 h Reperfusion in the Mouse Kidney Serum creatinine (**a**) (n=3-6) and blood urea nitrogen concentration (**b**) (n=3-6 except 45 mins where n=2) measured at 24 h reperfusion following various periods of warm ischaemia. ***P < 0.001, ****P < 0.0001. P values were calculated by one-way analysis of variance (ANOVA) with Dunnett's multiple comparisons test. Data are mean ± SEM or where n=2 mean ± range.

Blood Urea Nitrogen

Urea is produced from the breakdown of ammonia in the liver and cleared from the blood by the kidney in a similar manner to creatinine. If glomerular filtration rate decreases, the ability of the kidneys to clear urea is reduced leading to an increase in BUN concentration. Comparison of BUN concentration before and after IRI may therefore also be used to assess kidney function. Figure 5.5b shows the BUN concentration in the blood of mice at 24 h reperfusion following various periods of warm ischaemia. Blood urea nitrogen was significantly increased at 24 h reperfusion following 18, 20, 25, 30 and 45 mins warm ischaemia but not 15 mins warm ischaemia. Again, this was likely due to the large reserve capacity of the kidney.

5.3 Interim Summary I

A number of injury markers were investigated in the mouse model of renal IRI to determine the most appropriate measures and end-points for use in future treatment experiments. A significant increase in oxidative damage at 24 h reperfusion was detected using the TBARS assay of lipid peroxidation but not the protein carbonyl assay or mtDNA amplification assay suggesting the TBARS but not the protein carbonyl or mtDNA assay should be used in future experiments. Meanwhile, total glutathione levels were significantly decreased at 24 h reperfusion and may be used as an additional marker of oxidative stress following IRI. Cell death was quantified via analysis of H&E sections and adenosine nucleotide levels. The decrease in sum of ATP and ADP levels as a measure of cell death appeared to correlate with

analysis of H&E stained sections using a thresholding software as discussed in Chapter 2. Whilst a significant difference in the level of necrosis at 24 h reperfusion was only detected following 30 and 45 mins ischaemia via measurement of tissue ATP and ADP concentration, this may have been due to the low sample number investigated. Given the relative ease with which ATP and ADP concentration could be measured compared to the analysis of H&E sections, it was decided either method could be used to assess cell death in the kidney at 24 h reperfusion. Lastly, a significant increase in serum creatinine and BUN were measured at 24 h reperfusion following a warm ischaemia time of 20 minutes or greater and both measures could be used to assess kidney function in subsequent treatment experiments.

5.4 Assessment of Kidney Injury in the Pig

Whilst the mouse model of renal IRI is useful for the initial screening and identification of novel mitochondrial compounds, it is limited in its ability to replicate the clinical conditions of kidney transplantation. In order to aid in the translation of novel compounds, such as malonate ester prodrugs, from the mouse to human patients, a model of kidney transplantation was designed in the pig to more closely resemble the clinical conditions of organ donation. Furthermore, the pig kidney is similar in size, anatomy and physiology to the human, which may further aid in the translation process. As discussed in Chapter 4, pig kidneys were exposed to 30 mins warm ischaemia and 6 h cold ischaemia to simulate the conditions of donation after circulatory death and 0 mins warm ischaemia and 6 h cold storage to simulate the conditions of donation after brainstem death as shown in Figure 4.6. Whilst 30 mins warm ischaemia represents a more extreme warm ischaemia time rarely experienced by kidneys retrieved from DCD donors in the UK, this time was chosen to determine the full range of injury that may be experienced by pig kidneys in the model and to ensure there was sufficient therapeutic 'scope' for an improvement in kidney function to be measured in subsequent treatment experiments (see Section 4.4). As shown in Chapter 4, the metabolic changes that occur in pig kidneys exposed to 30 mins warm ischaemia and 6 h cold storage during ischaemia and reperfusion closely resemble those leading to mitochondrial ROS production during IRI in the mouse kidney whilst rapid recovery of ATP and ADP levels on reperfusion of pig kidneys exposed to 6 h cold storage only may have prevented mitochondrial ROS production from occurring (see Section 4.4). As such, a difference in organ function during EVNP may (partly) result from increased mitochondrial ROS production on reperfusion of pig kidneys exposed to 30 mins warm ischaemia and 6 h cold storage compared to pig kidneys exposed to 6 h cold storage only. In future treatment experiments aimed at reducing mitochondrial ROS production therefore, pig kidneys exposed to 30 min warm ischaemia

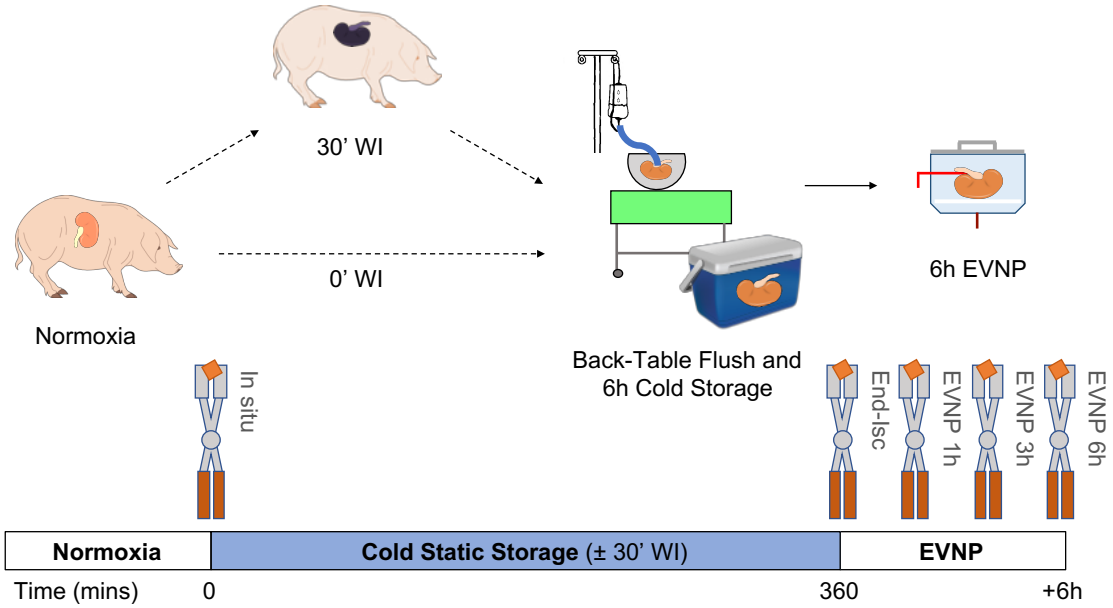

Figure 5.6 A Translational Model of Kidney DCD and DBD Donation and Transplantation in the Pig Pig kidneys were retrieved under general anaesthesia and exposed to either 30 mins warm ischaemia and 6 h cold static storage (30' WI) to simulate the conditions of DCD donation or 0 mins warm ischaemia and 6 h cold static storage (0' WI) to simulate the conditions of DBD donation. Kidneys were then reperfused using EVNP for 6 h. Tissue wedge biopsies were taken from pig kidneys *in situ* under conditions of normoxia prior to organ retreival (In situ), at the end of cold static storage (End-Isc) and at 1 (EVNP 1h), 3 (EVNP 3h) and 6 h (EVNP 6h) EVNP. Tissue wedge biopsies were rapidly clamp frozen in LN2 using Wollenburg clamps and stored at -70 °C until further proccesing and analysis. Mr Kourosh Saeb-Parsy (University of Cambridge Department of Surgery, UK) and Ms Krishnaa T Mahbubani (University of Cambridge Department of Surgery, UK) assisted with the surgical retrieval of kidneys from the pig.

and 6 h cold storage may act as a positive control whilst kidneys exposed to 6 h cold storage only may act as a negative control. The therapeutic 'scope' or range for improvement in subsequent treatment experiments would then be represented by the difference in organ function and injury between the two control groups.

To firstly determine whether an increase in mitochondrial ROS production on reperfusion led to a significant difference organ function and whether an appropriate therapeutic scope existed in the translational model of kidney transplantation in the pig, oxidative damage, kidney function and the degree of cellular necrosis were measured during 6 h EVNP as shown in Figure 4.6 and described in Chapter 2. Of note, pig kidneys were not perfused for longer than 6 h due to increasing haemolysis of red blood cells within the perfusion circuit. It was therefore not possible to investigate time points beyond 6 h reperfusion in the pig model of kidney transplantation as fresh pig blood to replace the perfusate at 6 h was not available.

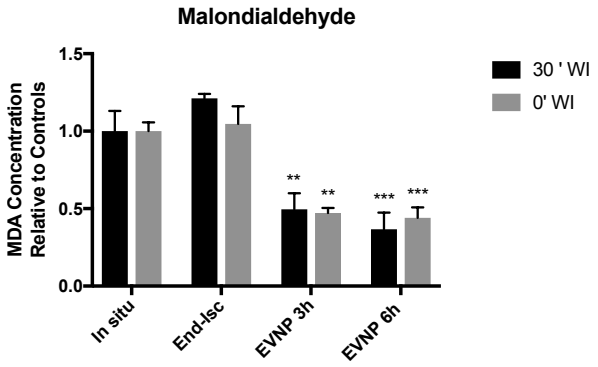

Figure 5.7 Comparison of Malondialdehyde Concentration in Kidneys Retrieved Under Conditions of DCD vs DBD donation in a Pig Model of Kidney Transplantation Tissue malondialdehyde (MDA) concentration in pig kidneys exposed to either 30 minutes warm ischaemia and 6 h cold storage to simulate conditions of DCD donation (30' WI) or 6 h cold storage only to simulate conditions of DBD donation (0' WI) under conditions of normoxia (In situ), at the end of ischaemia (End-Isc) and at 3 (EVNP 3h) and 6 h (EVNP 6h) EVNP as shown in Figure 5.6. n=3-4. Positive control value was 2.74 (n=1) (not shown). **P < 0.01, ***P < 0.001. P values were calculated by two-way analysis of variance (ANOVA) with Dunnett's multiple comparisons test. Data are mean ± SEM. Measurement of tissue MDA concentration was performed by Ms Margaret M Huang (University of Cambridge Department of Surgery, UK).

5.4.1 Oxidative Damage

Tissue malondialdehyde concentration was used to assess the level of oxidative damage following IRI in pig kidneys exposed to either 30 mins warm ischaemia and 6 h cold storage or 6 h cold storage only. Tissue MDA was measured using the TBARS assay as previously described. As shown in Figure 5.7, the tissue MDA concentration was significantly lower in kidneys exposed to both 30 mins warm ischaemia and 6 h cold storage (30' WI) and 6 h cold storage only (0' WI) at both 3 (EVNP 3h) and 6 h (EVNP 6h) reperfusion compared to *in situ* control levels (In situ). A reduction in tissue MDA concentration during EVNP was unexpected and whilst an equal wet weight of tissue was analysed for each time point, normalisation of values to the wet weight may have been affected by the development tissue oedema in kidneys during EVNP. Furthermore, tissue samples had been stored for over a year (at -70 °C) prior to analysis which may have also affected values measured. Nonetheless, comparison of values at 3 h and 6 h EVNP suggests further lipid peroxidation had not occurred during the second half of perfusion. As shown in the mouse, 6 h EVNP may have been too short a perfusion time for a significant increase in tissue MDA concentration to be measured by the TBARS assay. As discussed above, it was not possible to perfuse pig kidneys for longer durations in the current model due to increasing haemolysis of red blood cells within the perfusion circuit.

5.4.2 Cell Death

Acute tubular necrosis is reported as the primary cause of delayed graft function (DGF) in kidney transplantation [93] [280]. Grafts retrieved from DCD donors show increased rates of DGF on transplantation which is thought to relate to their increased exposure to warm ischaemia prior to cold *in situ* flush (although as shown in Chapter 3, cold *in situ* flush is often inefficient at rapidly cooling donor organs and similar metabolic changes are seen in DBD and DCD kidneys at the end of cold preservation). Higher rates of DGF in kidneys retrieved from DCD donors may therefore reflect a higher degree of acute tubular necrosis in DCD versus DBD grafts on transplantation. In the translational pig model of kidney transplantation described in Figure 5.6, pig kidneys were reperfused for 6 h using EVNP to simulate transplantation. However, 6 h reperfusion was too short for acute tubular necrosis to be identified on H&E stained sections and instead the sum of the ATP and ADP concentration was used to investigate the level of cell death [281] [282]. Figure 5.8 shows the tissue ATP/ADP ratio and total ATP and ADP nucleotide concentration in pig kidneys exposed to either 30 mins warm ischaemia and 6 h cold static storage (30' WI) or 0 mins warm ischaemia and 6 h cold static storage (0' WI). ATP and ADP concentrations were measured under conditions of normoxia prior to organ retrieval (In situ), at the end of ischaemia (End-Isc) and at 1 (EVNP 1h), 3 (EVNP 3h) and 6 h (EVNP 6h) EVNP.

The tissue ATP/ADP ratio (Figure 5.8a) and the sum of the ATP and ADP concentration (Figure 5.8b) was significantly decreased at the end of the ischaemic period (End-Isc) in kidneys exposed to 30 mins warm ischaemia and 6 h cold static storage (30' WI) and kidneys exposed to 0 mins warm ischaemia and 6 h cold static storage (0' WI) compared to normoxic controls (In situ). At 6 h EVNP, there was no significant difference in the ATP/ADP ratio (Figure 5.8a) in kidneys exposed to 30 mins warm ischaemia and 6 h cold static storage or 6 h cold static storage only compared to normoxic controls. However, the sum of the ATP and ADP concentration (Figure 5.8b) was significantly decreased in kidneys exposed to 30 mins warm ischaemia and 6 h cold static storage compared to normoxic controls versus kidneys that had been exposed to 6 h cold static storage only which were not significantly decreased. This suggests a greater level of cell death occurred in kidneys exposed to 30 mins warm ischaemia and 6 h cold static storage than in kidneys exposed to 6 h cold static storage only. However, other 'non-lethal' processes may also affect ATP and ADP levels following ischaemia reperfusion and interpretation of ATP and ADP levels should be conducted with caution.

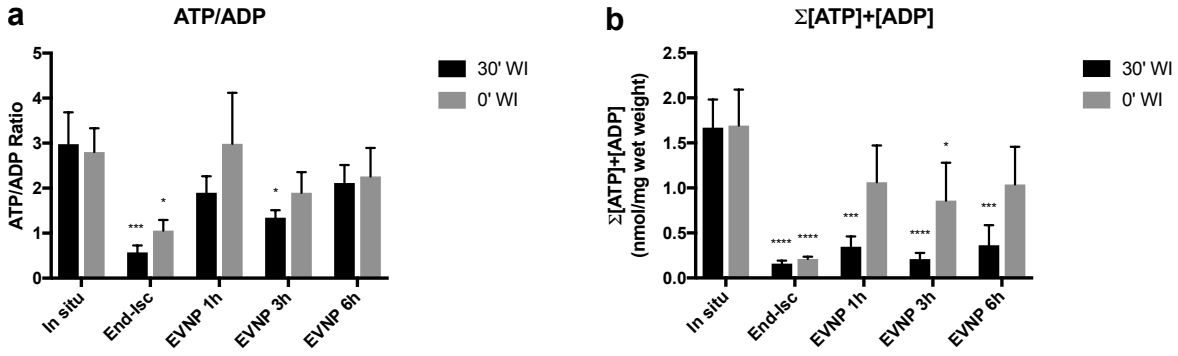

Figure 5.8 Comparison of the ATP/ADP Ratio and Sum of the ATP and ADP Concentration in Kidneys Retrieved Under Conditions of DCD vs DBD Donation in a Pig Model of Kidney Transplantation. Tissue ATP/ADP ratio (n=4) (**a**) and sum of the ATP and ADP concentration (n=4) (**b**) under conditions of normoxia (In situ) prior to ischaemia, at the end of cold static storage (End-Isc) and at 1 (EVNP 1h), 3 (EVNP 3h) and 6 h (EVNP 6h) EVNP. Pig kidneys were exposed to 30 mins warm ischaemia and 6 h cold static storage (30' WI) or 0 mins warm ischaemia and 6 h cold static storage (0' WI) to simulate the different conditions of DCD and DBD donation as shown in Figure 5.6. *P < 0.05, ***P < 0.001, ****P < 0.0001. P values were calculated by two-way analysis of variance (ANOVA) with Dunnett's multiple comparisons test. Data are mean ± SEM.

5.4.3 Kidney Function

Delayed graft function is most commonly defined as the requirement for dialysis within the first week post-transplantation (due to poor initial graft function) and is associated with increased patient morbidity, prolonged hospital admission, additional biopsy evaluation and increased healthcare costs [92]. As discussed above, grafts retrieved from DCD donors show increased rates of DGF on transplantation compared to grafts retrieved from DBD donors which is thought to relate to the increased exposure of DCD grafts to warm ischaemia [9]. To determine whether pig kidneys exposed to 30 mins warm ischaemia and 6 h cold storage showed reduced graft function on reperfusion compared to kidneys exposed to 0 mins warm ischaemia and 6 h cold storage, renal blood flow, urine output, reduction in SCr and FENa were monitored during EVNP as described in Chapter 2.

Renal Blood Flow

Renal blood flow during EVNP of kidneys exposed to 30 mins warm ischaemia and 6 h cold storage (30' WI) or 6 h cold storage only (0' WI) is shown in Figure 5.9a. The area under the curve (AUC) renal blood flow was used to compare the overall renal blood flow between kidneys during EVNP and is shown in Figure 5.10a. The AUC renal blood flow was significantly lower in kidneys exposed to 30 mins warm ischaemia and 6 h cold static storage (30' WI) than in kidneys exposed to 6 h cold static storage only (0' WI) suggesting kidneys

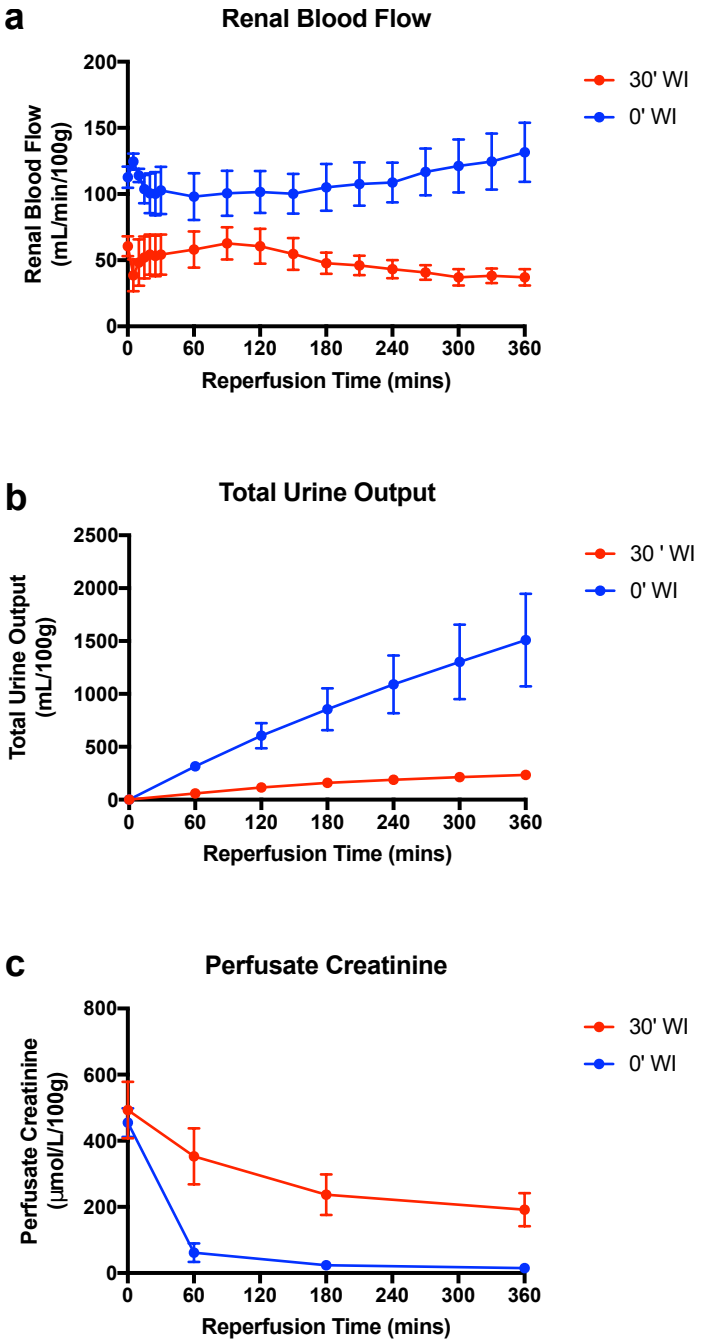

Figure 5.9 Renal Parameters during EVNP of Kidneys Retrieved Under Conditions of DCD vs DBD Donation in a Pig Model of Kidney Transplantation. Renal blood flow (n=4) (**a**), total urine output (n=4) (**b**) and perfusate creatinine concentration (n=4) (**c**) during 6 h EVNP in kidneys exposed to either 30 mins warm ischaemia and 6 h cold static storage to simulate DCD donation (30' WI) or 0 mins warm ischaemia and 6 h cold static storage to simulate DBD donation (0' WI) as shown in Figure 5.6. Data are mean ± SEM.

exposed to 30 mins warm ischaemia may have experienced increased vascular injury and kidney damage.

Total Urine Output

The urine output of kidneys exposed to 30 mins warm ischaemia and 6 h cold storage (30' WI) compared to kidneys exposed to 6 h cold storage only (0' WI) during EVNP is shown in Figure 5.9b. The total amount of urine produced by kidneys at the end of 6 h EVNP is shown in Figure 5.10b. Kidneys exposed to 30 mins warm ischaemia and 6 h cold static storage (30' WI) produced significantly less urine than in kidneys exposed to 6 h cold storage only (0' WI) during EVNP. This is likely due to increased vascular and tubular damage in kidneys exposed to 30 mins warm ischaemia resulting in increased tubular obstruction and a greater reduction in GFR.

Serum Creatinine

Creatinine was added to the perfusate at the start of EVNP and perfusate creatinine concentration measured at 1, 3 and 6 h reperfusion. During EVNP, the perfusate creatinine concentration gradually decreased as creatinine was cleared by the kidney and was not replaced as shown in Figure 5.9c. The AUC perfusate creatinine concentration was then calculated to reflect the rate of creatinine clearance from the perfusate in the circuit and act as a proxy of kidney function as shown in the Figure 5.10c. Kidneys that had been exposed to 30 mins warm ischaemia and 6 h cold static storage (30' WI) had a significantly greater AUC perfusate creatinine than kidneys exposed to 6 h cold static storage only (0' WI) suggesting they had a reduced clearance rate and poorer kidney function.

The AUC of perfusate creatinine concentration was measured as opposed to creatinine clearance as perfusate creatinine frequently decreased below detection limits in kidneys exposed to 6 h cold ischaemia only during the first hour of EVNP. This precluded accurate measurement of creatinine clearance in kidneys exposed to 6 h cold storage only, whereas the AUC serum creatinine could still be reliably calculated.

Fractional Excretion of Sodium

The FENa is the percentage of sodium filtered by the kidney which is excreted in the urine. Filtered sodium is reabsorbed by the proximal epithelial cells and fractional excretion of sodium in the healthy kidney is generally less than 1% [254]. However following IRI, FENa may increase as a result of proximal epithelial cell death, loss of cell polarity and tubule

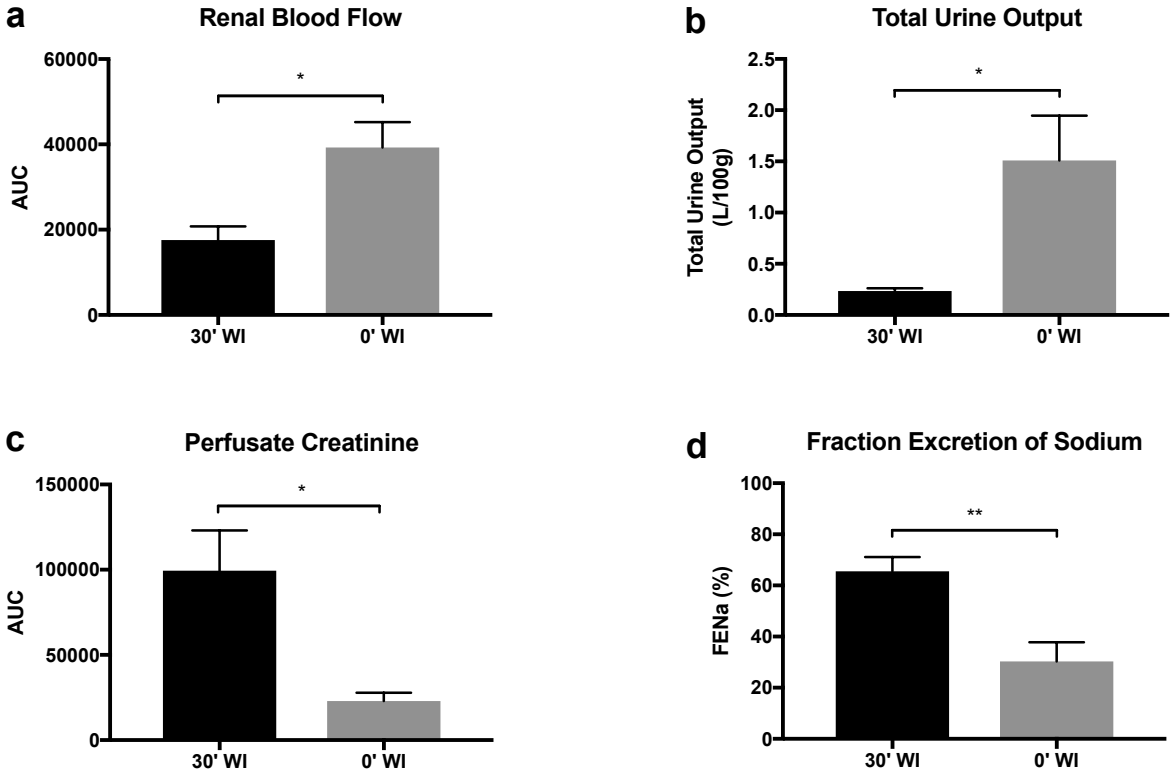

Figure 5.10 Comparison of Renal Function in Kidneys Retrieved Under Conditions of DCD vs DBD Donation in a Pig Model of Kidney Transplantation. Area under the curve (AUC) renal blood flow (n=4) (**a**), total urine output (n=4) (**b**), AUC serum creatinine concentration (n=4) (**c**) and fractional excretion of sodium (FENa) (n=4) (**d**) during 6 h EVNP of kidneys exposed to either 30 mins warm ischaemia and 6 h cold static storage to simulate DCD donation (30' WI) or 0 mins warm ischaemia and 6 h cold static storage to simulate DBD donation (0' WI) as shown in Figure 5.6. *P $<$ 0.05, **P $<$ 0.01. P values were calculated using an unpaired parametric t-test. Data are mean $\pm$ SEM.

damage [283]. The FENa during EVNP may therefore be used to assess the level of tissue damage in the kidney following IRI.

The FENa measured at 1 h EVNP is shown in Figure 5.10d. Fractional excretion of sodium was measured at 1 h EVNP as perfusate creatinine was mostly cleared by kidneys exposed to 6 h cold storage during this time and creatinine clearance required for the calculation of FENa could not be accurately determined at later time points. At 1 h EVNP, FENa was significantly greater in kidneys that had been exposed to 30 mins warm ischaemia and 6 h cold static storage (30' WI) than 6 h cold static storage only (0' WI). This suggests a greater level of tubular damage had occured in kidneys exposed to 30 mins warm ischaemia and 6 h cold static storage than in kidneys exposed to 6 h cold static storage only.

5.5 Assessment of Kidney Injury in the Human

To further aid in the translation of novel mitochondrial compounds from mouse models to human patients, EVNP of declined human kidneys could be used to investigate the efficacy, toxicity and therapeutic doses required to ameliorate mitochondrial ROS production in human tissue prior to use in clinical trials. However, as previously discussed, it was not possible (due to ethical and logistical constraints) to obtain a tissue biopsy from human kidneys prior to organ retrieval to act as a normoxic control sample. Instead, a translational model of human kidney transplantation in which declined human kidneys were reperfused for 1 h using EVNP followed by re-exposure to ischaemia and reperfusion was designed to enable the changes in tissue metabolites, injury and function to be investigated in human kidneys under more controlled conditions of IRI and compared to a normoxic baseline value obtained at the end of the 1 h EVNP period, as shown in Figure 5.11. Whilst declined human kidneys will have inevitably sustained some injury and damage during the initial 1 h of EVNP as well as an element of conditioning, this translational model is not dissimilar to conditions experienced by human kidneys that already undergo EVNP in a clinical setting. As succinate accumulation during ischaemia reperfusion is not affected by ischaemic preconditioning, this model enables the effect of novel mitochondrial compounds, such as malonate ester pro-drugs to be investigated [267] [140]. Furthermore, the effects of conditioning and differences in donor characteristics, mode of donation and prior ischaemia times between kidneys may be overcome in the model by using pairs of kidneys offered for research from the same donor. Both kidneys could undergo EVNP and re-exposure to ischaemia and reperfusion simultaneously with one kidney acting as an internal control for comparison with the second kidney undergoing treatment. Whilst pairs of kidneys were not used to generate initial pilot and feasibility data presented here, it is hoped that this strategy could be adopted in future treatment experiments to investigate the effect of malonate ester-prodrugs in human kidneys as discussed in Chapter 7.

5.5.1 Cell Death

The sum of the ATP and ADP concentration before and after IRI may be used as an approximation of cellular necrosis as previously described. Similar to pig, the duration of EVNP was too short for degree of necrosis in human kidneys to be reliably determined on H&E stained sections [281] [282]. Figure 5.12 shows the tissue ATP/ADP ratio and the sum of the ATP and ADP nucleotide concentration in the translational model of kidney transplantation using declined human kidneys described in Figure 5.11. The ATP/ADP ratio and sum of the ATP and ADP concentration was significantly decreased at the end of the initial period of

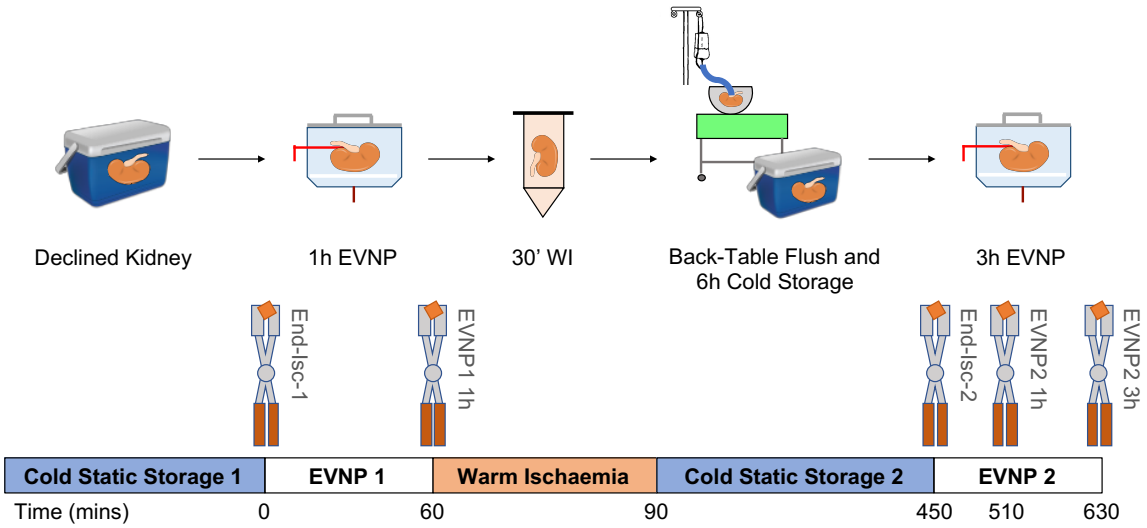

Figure 5.11 A Translational Model of Kidney Transplantation Using Declined Human Kidneys Declined human kidneys were accepted for research and underwent 1 h *ex vivo* normothermic perfusion (EVNP) on arrival to the laboratory. Kidneys were then exposed to 30 mins warm ischaemia at 36 °C followed by back-table flush and 6 h cold static storage. Kidneys then underwent a second 3 h period of EVNP. Tissue wedge biopsies were taken from kidneys at the end of cold static storage immediately prior to EVNP (End-Isc 1), at the end of 1 h EVNP (EVNP1 1h), at the end of the 30 mins warm ischaemia and 6 h cold static storage (End-Isc 2) and at 1 (EVNP2 1h) and 3 h (EVNP2 3h) during the second period of EVNP. Tissue wedge biopsies were rapidly frozen in LN2 using Wollenburg clamps and stored at -70 °C until further processing and analysis.

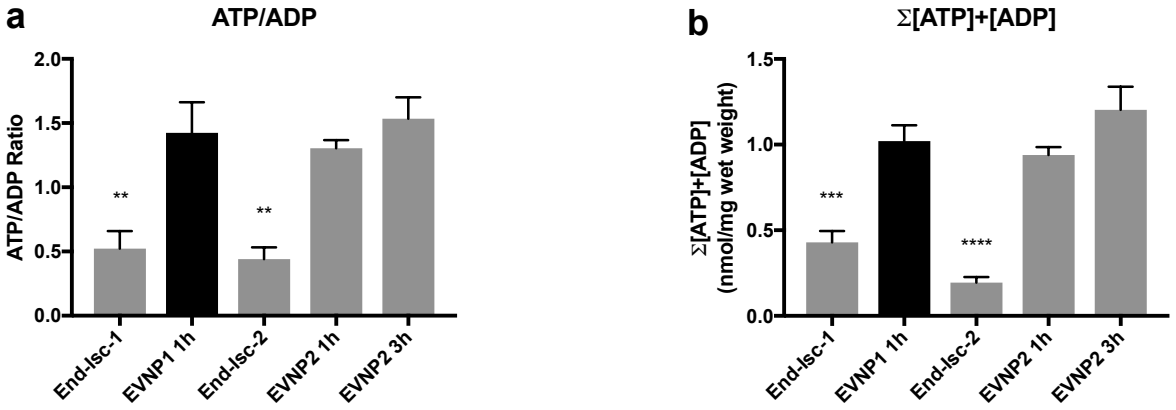

Figure 5.12 ATP/ADP Ratio and Sum of the ATP and ADP Concentration in a Translational Model of Kidney Transplantation Using Declined Human Kidneys Tissue ATP/ADP ratio (n=4) (**a**) and sum of the ATP and ADP concentration (n=4) (**b**) in declined human kidneys at the end of cold static storage (End-Isc-1), following 1 h EVNP (EVNP1 1h), at the end of 30 mins warm ischaemia and 6 h cold static storage (End-Isc-2) and at 1h (EVNP2 1h), 3 (EVNP2 3h) during a second period of EVNP as shown in Figure 5.11. **P < 0.01, ***P < 0.001 ****P < 0.0001. P values were calculated by one-way analysis of variance (ANOVA) with Dunnett's multiple comparisons test. Data are mean ± SEM.

cold static storage (End-Isc 1) and on re-exposure to 30 mins warm ischaemia and 6 h cold static storage (End-Isc-2) compared to the level following 1 h EVNP (EVNP1 1h). However, the ATP/ADP ratio and sum of the ATP and ADP concentration at 1 h (EVNP2 1h) and 3 h (EVNP2 3h) in the second period of EVNP was not significantly different from values measured at the end of the initial 1 h period EVNP (EVNP1 1h) suggesting further cellular necrosis had not occurred. However, it may be that kidneys reperfused for 1 h prior to re-exposure to warm and cold ischaemia had not fully recovered their ATP and ADP levels and that a higher initial ATP and ADP concentration may have been achieved if human kidneys were reperfused for longer prior to re-exposure to ischaemia. Nevertheless, in treatment experiments where paired kidneys from the same donor will be used (as discussed above and in Chapter 7), a comparison of the ATP and ADP concentration between the control and treatment kidney at different time points during EVNP may still provide important information about the protective effect of mitochondrial compounds on the kidney using this model.

5.5.2 Kidney Function

Figure 5.13 shows the renal parameters of declined human kidneys during the initial 1 h period of EVNP (EVNP1) and subsequent 3 h period of EVNP (EVNP2) following re-exposure of declined human kidneys to 30 mins warm ischaemia and 6 h cold storage as

described in Figure 5.11. Renal blood flow (Figure 5.13a) was greater in declined human kidneys during EVNP2 than EVNP1 however total urine output (Figure 5.13b), reduction in perfusate creatinine concentration (Figure 5.13c) and fractional excretion of sodium (Figure 5.13d) were similar before and after re-exposure to warm and cold ischaemia. As discussed above, Figure 5.13 represents preliminary pilot data to determine the feasibility of the model described in Figure 5.11. Data from both Figure 5.13 and Figure 5.12 suggest declined human kidneys are able to withstand 1 h EVNP followed by re-exposure to ischaemia and a subsequent 3 h period of EVNP as demonstrated by the recovery of both ATP and ADP levels and renal parameters. Together these findings suggest the model described in Figure 5.11 may be used to investigate the effect of novel malonate compounds in pairs of declined kidneys retrieved from the same donor, with one kidney acting as an internal control kidney and the second undergoing treatment. Mitochondrial ROS production, cell death and kidney function could then be compared between kidneys whilst controlling (as much as practically possible) for confounding factors related to the donor, retrieval process, prior ischaemia times and overall quality of the kidney graft.

5.6 Interim Summary II

A significant reduction in organ function and an increase in cellular necrosis was measured during 6 h EVNP in pig kidneys exposed to 30 mins warm ischaemia and 6 h cold storage compared to 6 h cold storage only. The reduction in organ function may have been due to increased mitochondrial ROS production in pig kidneys exposed to 30 minutes warm ischaemia and 6 h cold static storage versus 6 h cold storage only as discussed in Chapter 4. As such, the pig model of kidney transplantation described in Figure 5.6 may be used in subsequent treatment experiments aimed at reducing mitochondrial ROS production on reperfusion with pig kidneys exposed to 30 mins warm ischaemia and 6 h cold storage acting as a positive control and kidneys exposed to 6 h cold ischaemia only acting as a negative control. In addition, a model of kidney transplantation using declined human kidneys may further aid the translation of novel mitochondrial therapies from mouse models to human patients. Preliminary data has shown that declined human kidneys may withstand 1 h EVNP followed by re-exposure to 30 mins warm ischaemia and 6 h cold storage and a second 3 h period of EVNP. Pairs of declined human kidneys retrieved from the same donor could be used in future experiments to investigate the efficacy of novel mitochondrial compounds in human tissue using this model as described in Figure 5.11.

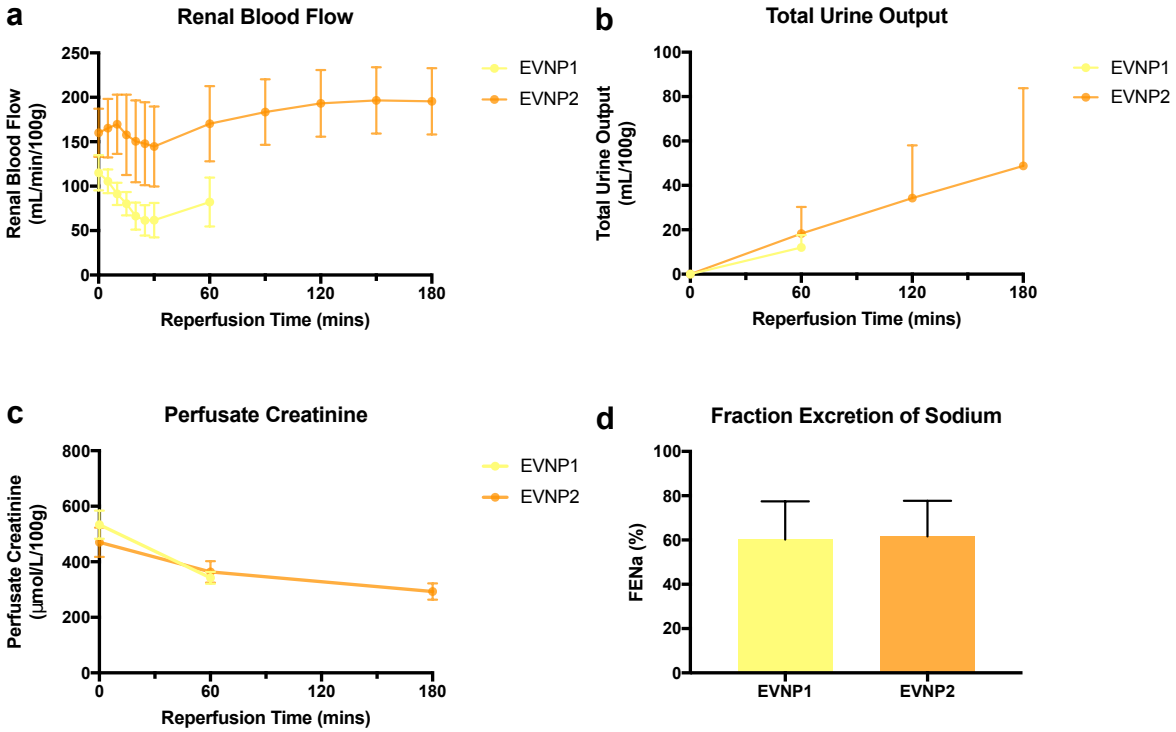

Figure 5.13 Renal Function during EVNP in a Translational Model of Kidney Transplantation Using Declined Human Kidneys Renal blood flow (n=4) (**a**), total urine output (n=4) (**b**) serum creatinine concentration (n=4) (**c**) and fractional excretion of sodium at 1 h reperfusion (n=4) (**d**) during EVNP of declined human kidneys. On arrival to the laboratory, declined human kidneys were perfused for 1 h (EVNP 1) before undergoing 30 mins warm ischaemia and 6 h cold static storage and a second period of 3 h EVNP (EVNP 2) as shown in Figure 5.11. Data are mean ± SEM.

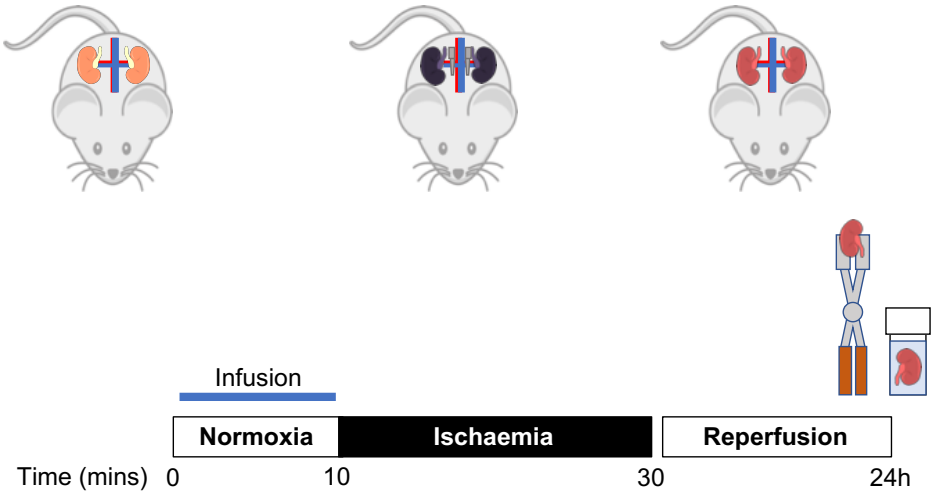

Figure 5.14 Administration of Malonate Compounds Prior to Warm Ischaemia in the Mouse Kidney. Mice were anaesthetised and the renal hila dissected. Malonate compounds were then administered as an infusion into the the IVC 10 mins prior to the onset of ischaemia. Immediately following infusion, the renal hila of both kidneys were occluded for 20 mins with a micro-serrefine clamp. The micro-serrefine clamps were then removed and both kidneys were reperfused for 24 h during which time mice were recovered in a heat cabinet maintained at 28 °C. At 24 h reperfusion, mice were re-anaesthetised and a blood sample was taken from the IVC. One kidney was then rapidly retrieved from the mouse and clamp frozen in LN2 using Wollenburg clamps whilst the second kidney was placed in 10% neutral buffered formalin. Clamp frozen kidneys were stored at -70 °C until further processing and analysis.

5.7 Effect of Malonate Ester Pro-Drugs on Kidney Injury in the Mouse

Whilst malonate ester prodrugs administered to the mouse kidney either before ischaemia or at the point of reperfusion were not shown to reduce mitochondrial ROS production as measured by the MitoP/MitoB ratio on reperfusion (see Chapter 4), as previously discussed, MitoB may be limited in its ability to specifically detect a burst of mitochondrial ROS production on reperfusion. Malonate ester prodrugs may have still had a protective effect on the mouse kidney during IRI either through inhibition of SDH or via another unknown mechanism. To investigate further, oxidative damage, cellular necrosis and kidney function were investigated at 24 h reperfusion in the mouse model of renal IRI where kidneys were treated with malonate ester prodrugs either before or after 20 mins warm ischaemia.

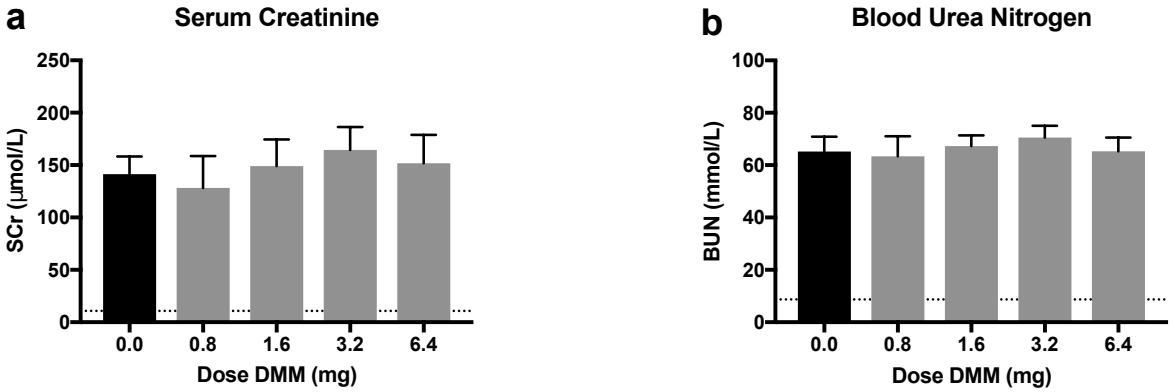

Figure 5.15 Kidney Function at 24 h Reperfusion Following Administration of DMM Prior To Warm Ischaemia in Mice. Serum creatinine (n=4) (**a**) and blood urea nitrogen concentration (n=4) (**b**) following 20 mins warm ischaemia and 24 h reperfuson. Dotted lines represent baseline control values. Dimethyl malonate (DMM) was administered as an infusion at various doses immediately prior to the onset of ischaemia as shown in Figure 5.14. Data are mean ± SEM.

5.7.1 Effect of DMM Administered Prior to Ischaemia

Dimethyl malonate was administered to mice as shown Figure 5.14. Tissue succinate and malonate concentrations in the mouse kidney following administration of DMM prior to ischaemia were previously presented in Chapter 3 (see Figure 3.20). Figure 5.15 shows the serum creatinine and blood urea nitrogen concentration at 24 h reperfusion following administration of DMM at range of doses. Administration of DMM prior to warm ischaemia showed no protection against kidney IRI as measured by serum creatinine concentration and blood urea nitrogen at 24 h reperfusion and is consistent with the finding DMM administered prior to ischaemia did not lead to a reduction in the accumulation of succinate during ischaemia or mitochondrial ROS production on reperfusion as shown in Figures 3.20 and 4.12.

5.7.2 Effect of DMM and MAM Administered at Reperfusion

Either 3.2 mg dimethyl malonate (DMM) or 0.32 mg diacetoxymethyl malonate (MAM) was administered to mice at reperfusion following 20 mins warm ischaemia as shown in Figure 5.16. The dose of DMM was based on the therapeutic dose previously reported in the mouse heart [14]. A 10x lower dose of MAM was chosen based preliminary *in vivo* data demonstrating more rapid hydrolysis of MAM compared to DMM within the kidney with a higher tissue malonate concentration being achieved (personal communication Mr Hiran A Prag). The tissue succinate and malonate concentrations following the administration of

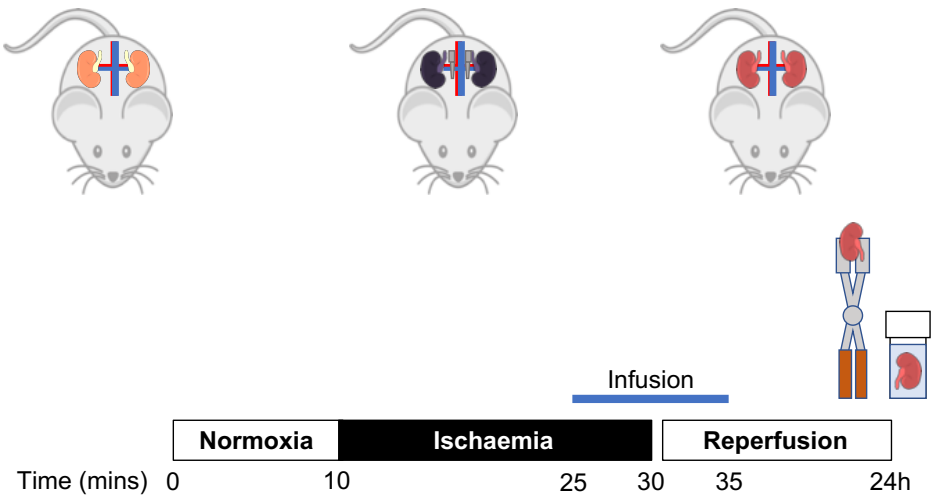

Figure 5.16 Administration of Malonate Compounds at Reperfusion of the Mouse Kidney. Mice were anaesthetised and the renal hila dissected. The renal hila of both kidneys was then occluded for 20 mins with a micro-serrefine clamp. A 10 min infusion of a malonate compound was started 5 mins prior to the onset of reperfusion as shown. At the end of 20 mins occlusion, both kidneys were reperfused for 24 h during which time mice were recovered in a heat cabinet maintained at 28 °C. At 24 h reperfusion, mice were re-anaesthetised and a blood sample was taken from the IVC. One kidney was then rapidly retrieved from the mouse and clamp frozen in LN2 using Wollenburg clamps whilst the second kidney was placed in 10% neutral buffered formalin. Clamp frozen kidneys were stored at -70 °C until further processing and analysis.

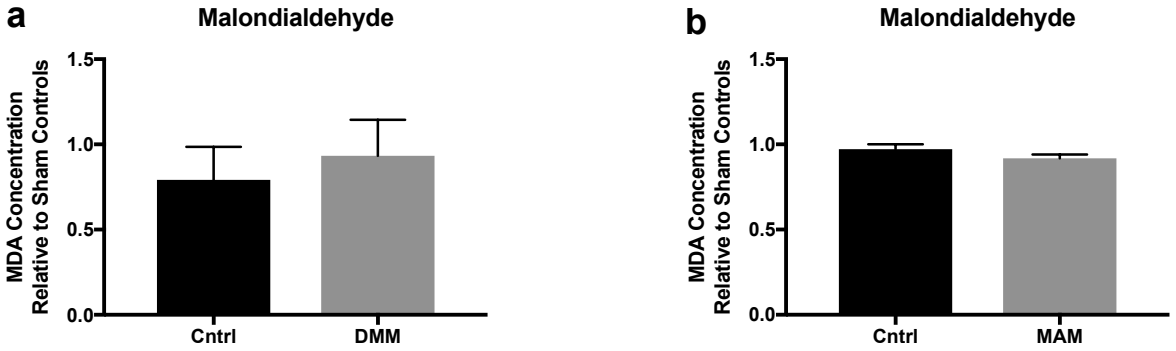

Figure 5.17 Tissue Malondialdehyde Concentration at 24 h Following Administration of DMM or MAM at Reperfusion Malondialdehyde (MDA) concentration measured using the TBARS assay at 24 h reperfusion in mouse kidneys exposed to 20 mins warm ischaemia. 3.2 mg DMM (n=6) (**a**) or 0.32 mg MAM (1% DMSO) (n=6) (**b**) were administered to mice on reperfusion as shown in Figure 5.16. Data are mean ± SEM. Measurement of tissue MDA concentration was performed by Ms Margaret M Huang (University of Cambridge Department of Surgery, UK).

either 3.2 mg DMM or 0.32 mg MAM at reperfusion in the mouse were previously presented in Chapter 4 (see Figures 4.14 and 4.15).

Effect on Oxidative Damage

Tissue malondialdehyde (MDA) concentration at 24 h reperfusion is shown in Figure 5.17. There was no significant difference in tissue MDA concentration at 24h reperfusion in either DMM or MAM treated kidneys compared to controls. Furthermore, tissue MDA concentration following IRI was not significantly different from values measured in sham operated control mice in contrast to values measured in Figure 5.4, re-emphasising the unreliability of this method for measuring MDA concentration in tissue homogenates.

Effect on Cell Death

Tissue ATP/ADP ratio and sum of the ATP and ADP concentration at 24 h reperfusion was used as a measured of cell death as described in Section 5.2.2 and is shown in Figure 5.18. There were no significant differences in ATP/ADP ratio (Figure 5.18a) or sum of the ATP and ADP concentration (Figure 5.18c) between saline controls and DMM treated kidneys at 24 h reperfusion. In MAM treated kidneys, the ATP/ADP ratio was significantly lower than in 1% DMSO controls at 24 h reperfusion (Figure 5.18b) but there was no significant difference in sum ATP and ADP concentration (Figure 5.18d). This suggests there was no significant difference in cell death between control and treatment groups in either DMM or MAM treated kidneys. Furthermore, the sum of the ATP and ADP concentration at 24 h reperfusion was similar to values in sham control kidneys suggesting little cell death occurred

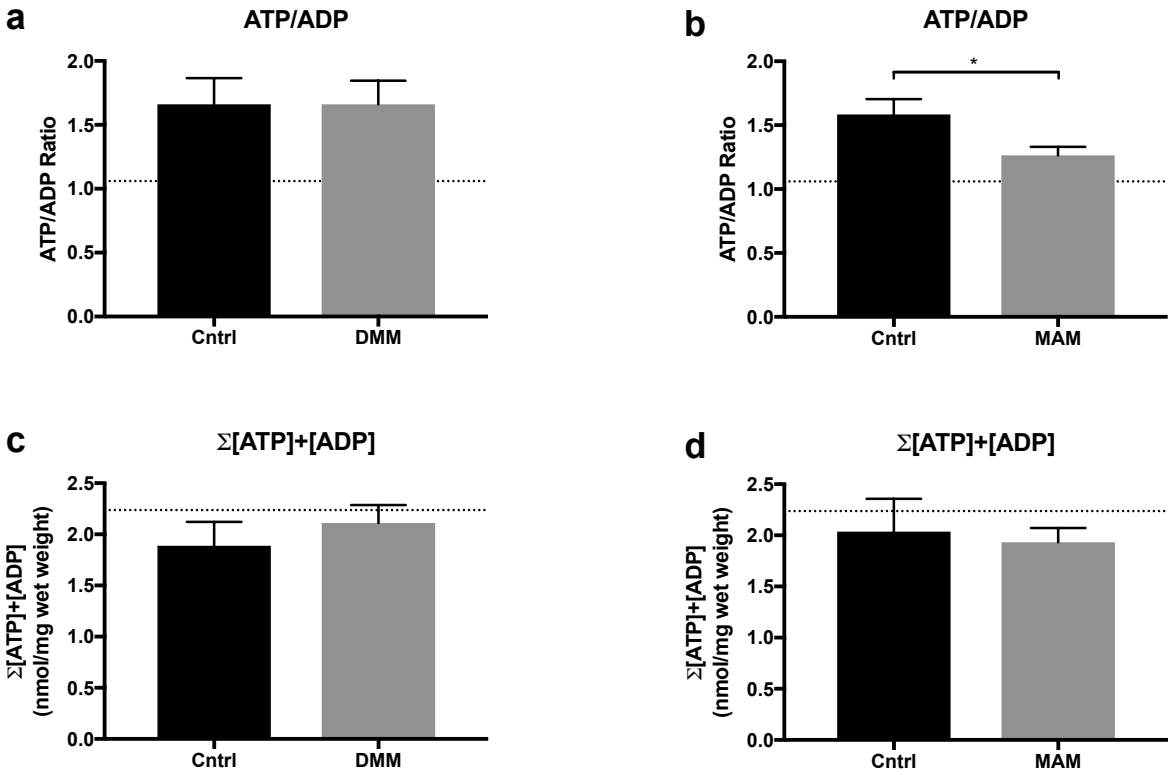

Figure 5.18 Tissue ATP and ADP Levels at 24 h Following Administration of DMM or MAM at Reperfusion. Tissue ATP/ADP (n=6) (**a**) and total ATP and ADP concentration (n=6) (**c**) following 20 mins warm ischaemia and 24 h reperfusion in DMM treated kidneys versus saline controls. Tissue ATP/ADP (n=6) (**b**) and total ATP and ADP concentration (n=6) (**d**) following 20 mins warm ischaemia and 24 h reperfusion in MAM (1%DMSO) treated kidneys versus 1% DMSO controls. DMM and MAM were administered as an infusion on reperfusion as shown in Figure 5.16. *P < 0.05. P values were calculated using an unpaired parametric t-test. Data are mean ± SEM.

overall. However, use of the tissue ATP and ADP concentration as a measure cell death is relatively non-specific and may be affected by other factors. More sensitive assays of cell death could instead be used to investigate the effect of DMM and MAM on reperfusion as discussed below.

Effect on Kidney Function

The serum creatinine and blood urea nitrogen concentration at 24 h reperfusion are shown in Figure 5.19. Serum creatinine concentration was significantly decreased at 24 h reperfusion in DMM (Figure 5.19a) and MAM (Figure 5.19b) treated kidneys compared to their corresponding controls. However, there was no significant difference in blood urea nitrogen concentration between DMM (Figure 5.19c) and MAM treated kidneys compared to controls (Figure 5.19c). This experiment may have been under powered given the variability of the

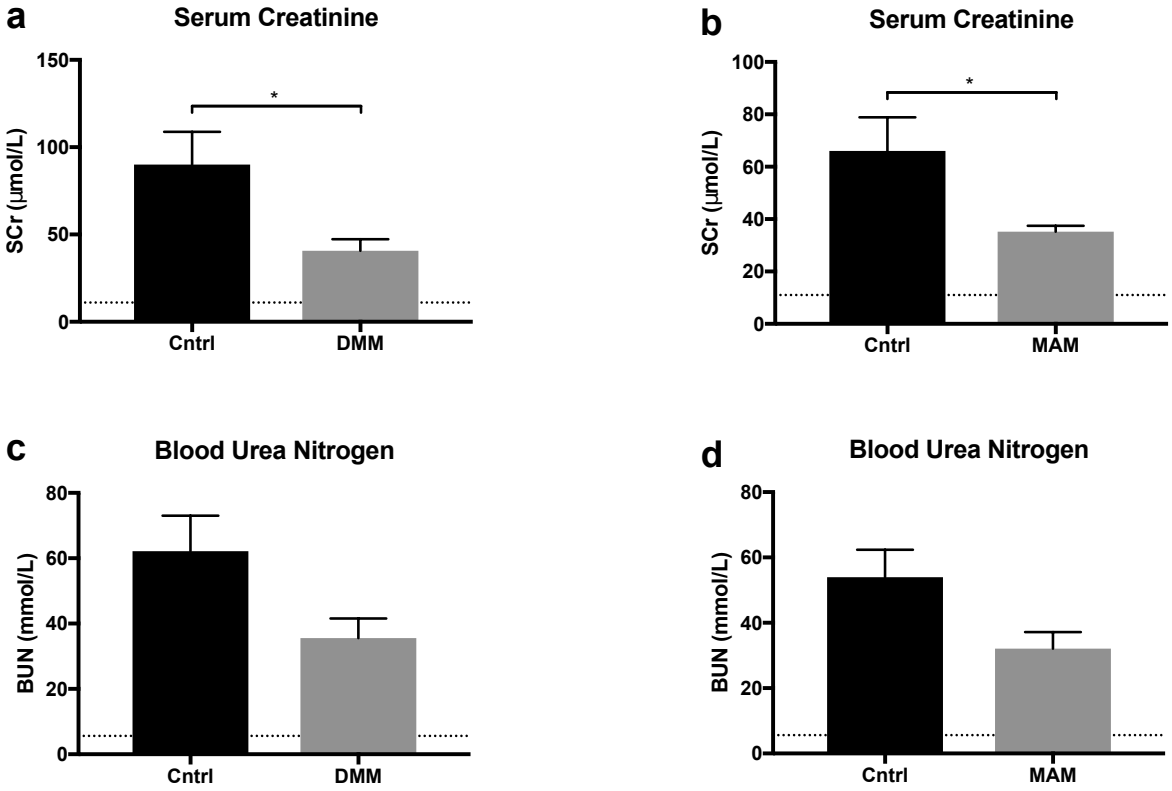

Figure 5.19 Kidney Function at 24 h Following Administration of DMM or MAM at Reperfusion. Serum creatinine (n=6) (**a**) and blood urea nitrogen concentration (n=6) (**c**) following 20 mins warm ischaemia and 24 h reperfuson in DMM treated kidneys versus saline controls. Serum creatinine (n=6) (**b**) and blood urea nitrogen concentration (n=6) (**d**) following 20 mins warm ischaemia and 24 h reperfuson in MAM (1% DMSO) treated kidneys versus 1% DMSO controls. DMM and MAM were administered as an infusion on reperfusion as shown in Figure 4.13. *P < 0.05. P values were calculated using an unpaired parametric t-test. Data are mean ± SEM.

model (see Discussion) and a trend towards an improvement in kidney function as measured by blood urea nitrogen was still observed.

5.8 Effect of Disodium Malonate on Kidney Injury in the Mouse

Disodium malonate (DSM) is the sodium salt of malonate and does not require hydrolysis by esterases within mitochondria, potentially leading to rapid inhibition of succinate dehydrogenase when administered during IRI. However, DSM is a charged molecule and is poorly taken up by cells under conditions of normoxia *in vitro* (personal communication, Hiran Prag). Nonetheless, DSM has previously been shown to reduce IRI when administered on

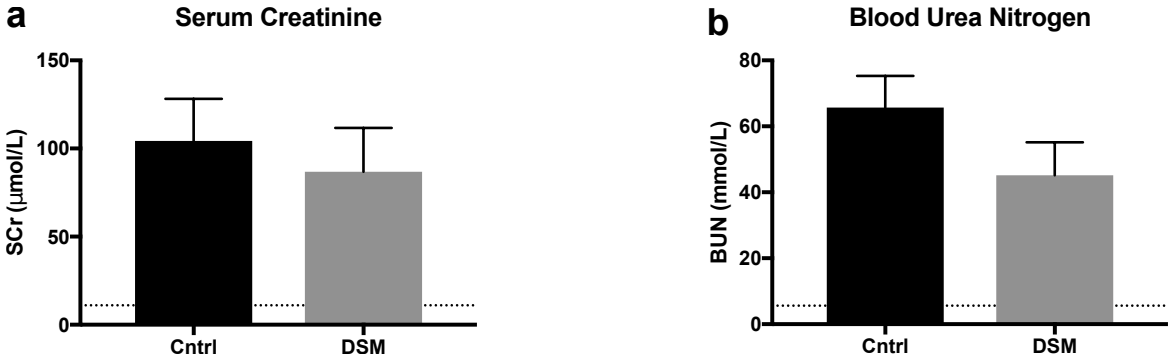

Figure 5.20 Kidney Function at 24 h Reperfusion Following Administration of DSM Prior To Warm Ischaemia in Mice. Serum creatinine (n=4) (**a**) and blood urea nitrogen concentration (n=4) (**b**) following 20 mins warm ischaemia and 24 h reperfusion. Dotted lines represent baseline control values. 3.2 mg disodium malonate (DSM) was administered as an infusion immediately prior to the onset of ischaemia as shown in Figure 5.14. Data are mean ± SEM.

reperfusion to the mouse and pig heart [194] [195]. To determine whether DSM is protective in kidney IRI, DSM was administered to mice immediately prior to 20 mins warm ischaemia as shown in Figure 5.14 or at reperfusion as shown in Figure 5.16.

5.8.1 Effect of DSM Administered Prior to Ischaemia

Disodium malonate was administered as an infusion immediately prior to 20 mins warm ischaemia as shown in Figure 5.14. A dose of 3.2 mg of DSM was administered based on the therapeutic dose of DMM reported in cardiac ischaemia reperfusion injury in mice [14]. Kidney function was then assessed by serum creatinine and BUN concentration at 24 h reperfusion as shown in Figure 5.20. There was no significant difference in serum creatinine concentration or BUN concentration in mice treated with DSM or saline controls at 24 h reperfusion suggesting DSM at a dose of 3.2 mg is not protective against IRI in the kidney when administered prior to ischaemia in mice.

5.8.2 Effect of DSM Administered on Reperfusion

Disodium malonate was also administered to mice at reperfusion following 20 mins warm ischaemia as shown in Figure 5.16. A dose of 0.38 mg was administered as an infusion based on the effective therapeutic dose administered at reperfusion in the heart [194]. Kidney function was then assessed by serum creatinine and BUN concentration at 24 h reperfusion as shown in Figure 5.21. There was no significant difference in serum creatinine concentration or blood urea nitrogen concentration in mice treated with DSM compared to saline controls

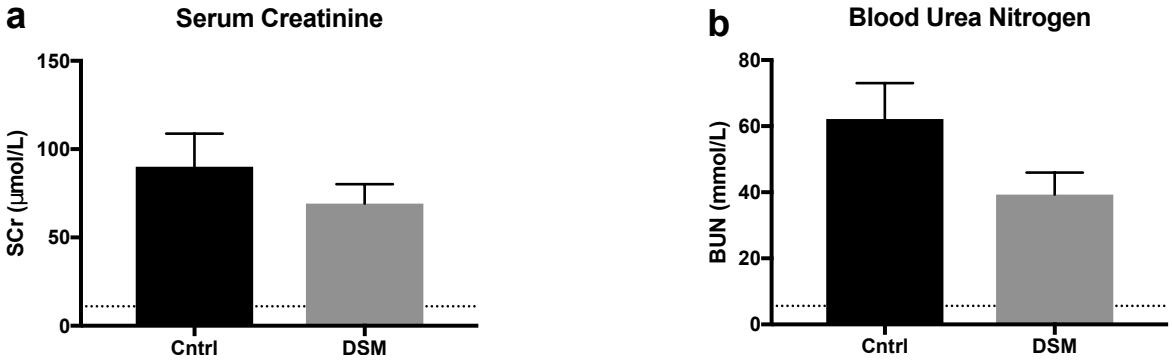

Figure 5.21 Kidney Function at 24 h Following Administration of DSM at Reperfusion in Mice Serum creatinine (n=6) (**a**) and blood urea nitrogen concentration (n=6) (**b**) following 20 mins warm ischaemia and 24 h reperfusion. Dotted lines represent baseline control values. 0.38 mg disodium malonate (DSM) was administered as an infusion at reperfusion as shown in Figure 5.16. Data are mean ± SEM.

at 24 h reperfusion suggesting DSM at a dose of 0.38 mg is not protective against IRI in the kidney when administered at reperfusion in mice.

5.9 Effect of Malonate Ester Pro-Drugs on Kidney Injury in the Pig

As previously discussed, the mouse model of renal IRI is limited in its ability to replicate the clinical conditions of kidney transplantation which may significantly affect a compounds efficacy. The effect of malonate ester prodrugs on kidney injury and function were thus also investigated in the pig model of kidney transplantation described in Section 5.4.

5.9.1 Effect of DMM Administered Prior to Ischaemia

The effect of DMM administered prior to ischaemia was investigated in a series of pilot experiments in the pig model of kidney transplantation as shown in Figure 5.22. As discussed in Section 3.9.2, a dose of 840 mg DMM was chosen based on allometric scaling of the therapeutic dose of DMM reported in the mouse heart [262] [14]. A 10x higher dose was also investigated in order to achieve similar tissue malonate concentrations in the pig kidney as in the mouse (see Figure 3.23). As these were preliminary experiments in which the appropriate dose and circulation time of DMM was still being determined, values for each dose and circulation time represent a single experiment and so statistical analysis of data was not possible.

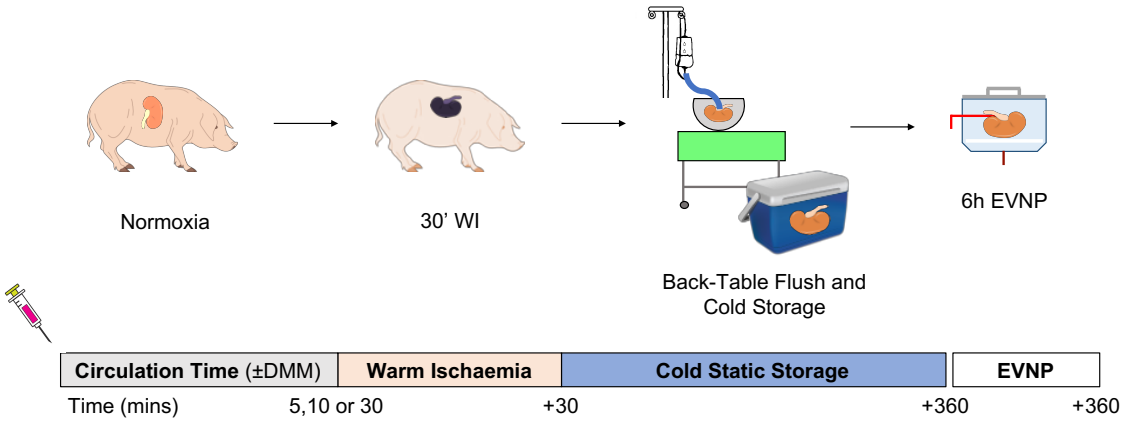

Figure 5.22 Administration of DMM Prior to Warm Ischaemia in the Pig Model of Kidney Transplantation. One kidney was retrieved from the pig prior to administration DMM and exposed to 30 mins warm ischaemia in order to act as a control (not shown). Dimethyl malonate (DMM) was then administered as a bolus injection into the ear vein of the pig and allowed to circulate systemically for 5, 10 or 30 minutes. The renal vessels of the second kidney were then tied and divided and the kidney was exposed to 30 mins warm ischaemia in abdomen of the pig maintained at 38 °C. During warm ischaemia pig kidneys became purple in colour due to the presence of deoxygenated blood within the microvasculature. Following 30 mins warm ischaemia, both kidneys underwent to 6 h cold static storage and then 6 h EVNP. Mr Kourosh Saeb-Parsy (University of Cambridge Department of Surgery, UK) and Ms Krishnaa T Mahbubani (University of Cambridge Department of Surgery, UK) assisted with the surgical retrieval of kidneys from the pig.

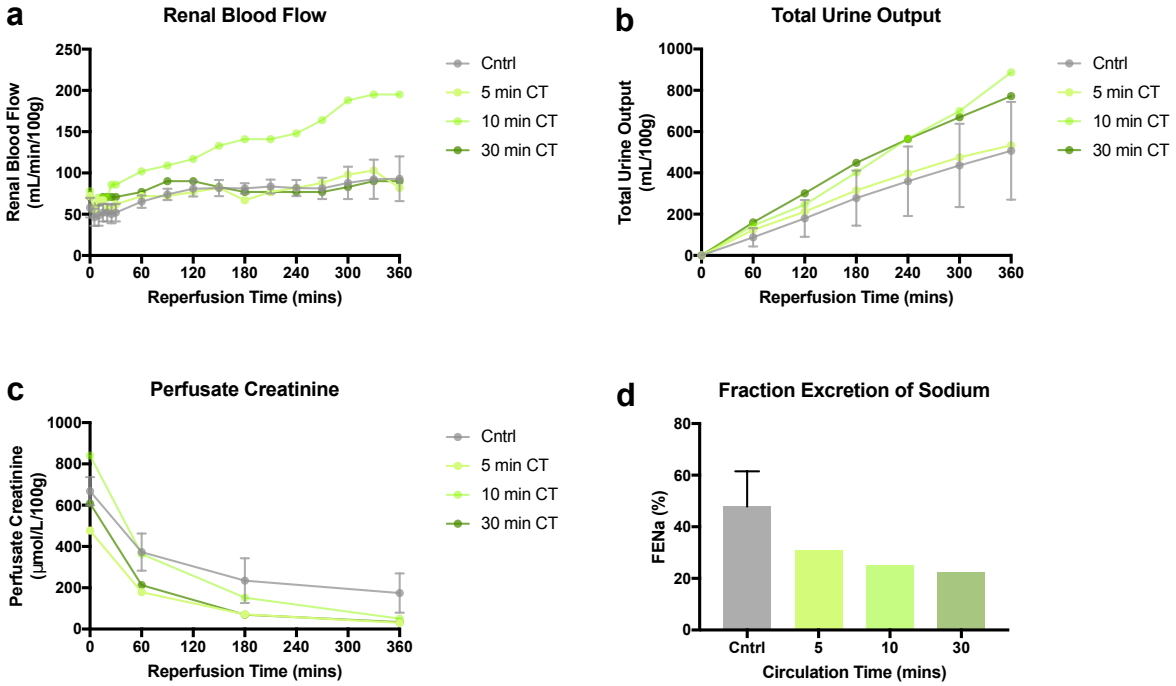

Figure 5.23 Effect of 840 mg DMM Administered Prior to Warm Ischaemia on Kidney Function during EVNP in a Pig Model of Kidney Transplantation. Renal blood flow (**a**), urine output (**b**), perfusate creatinine concentration (**c**) and fractional excretion of sodium (**d**) during 6 h EVNP of pig kidneys exposed 30 mins warm ischaemia and 6 h cold static storage. 840 mg DMM was administered as a bolus injection and allowed to circulate systemically in the pig for 5 (n=1), 10 (n=1) or 30 (n=1) mins prior to onset of warm ischaemia. Control kidneys (n=3) were retrieved from pigs prior to administration of DMM as described in Figure 5.22. Data are mean ± SEM.

The effect of 840 mg DMM administered prior to 30 mins warm ischaemia on kidney function during EVNP in the pig is shown in Figure 5.23. Following administration as a bolus dose into marginal ear vein, DMM was allowed to circulate systemically in the pig for either 5, 10 or 30 minutes prior to the onset of warm ischaemia and 6 h cold storage. A protective effect of 840 mg DMM during subsequent perfusion was not seen following either 5, 10 or 30 minutes circulation prior to warm ischaemia. This was largely due to variability in the control values for renal blood flow (Figure 5.23a), urine output (Figure 5.23b), perfusate creatinine concentration (Figure 5.23c) and fractional excretion of sodium (Figure 5.23d) and repeated experiments are likely needed before the effects of DMM on kidney function can be more reliably determined.

The effect of 8400 mg DMM administered prior to 30 mins warm ischaemia on kidney function during EVNP in the pig is shown in Figure 5.24. Following administration as a bolus dose into marginal ear vein, DMM was allowed to circulate systemically in the pig for either 5 or 10 minutes prior to the onset of warm ischaemia. 8400 mg DMM appeared to

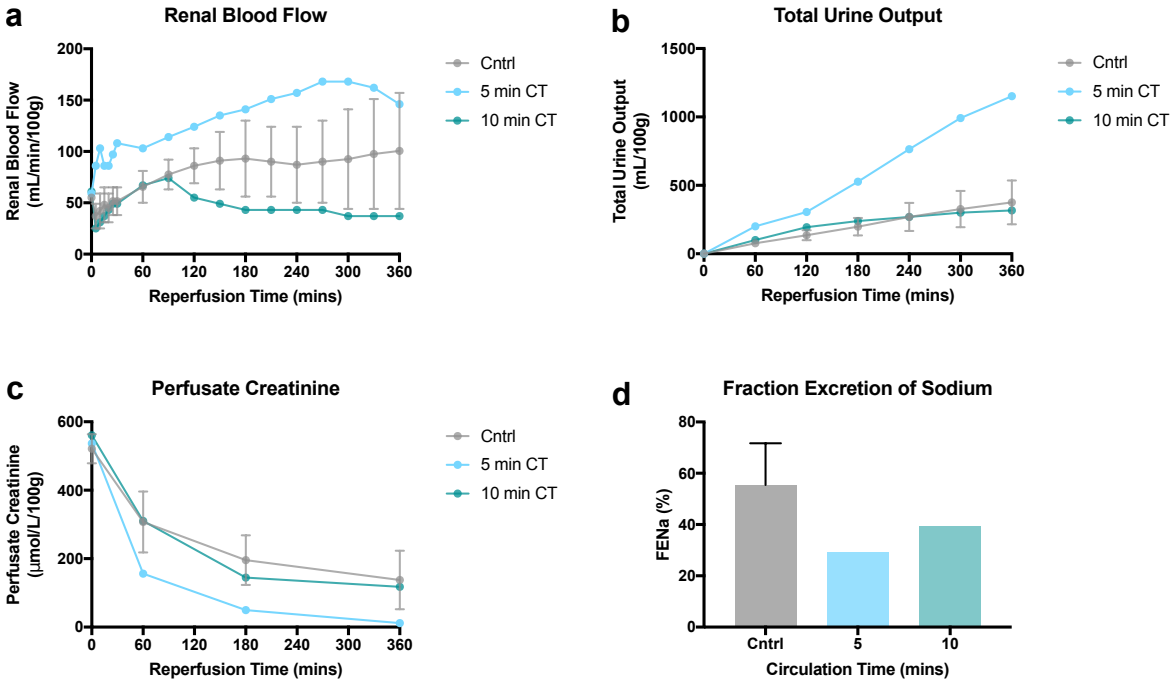

Figure 5.24 The Effect of 8400 mg DMM Adminstered Prior to Warm Ischaemia on Kidney Function during EVNP in a Pig Model of Kidney Transplantation. Renal blood flow (**a**), urine output (**b**), perfusate creatinine concentration (**c**) and fractional excretion of sodium (**d**) during 6 h EVNP of pig kidneys exposed to 30 mins warm ischaemia and 6 h cold static storage. 8400 mg DMM was administered as a bolus injection and allowed to circulate systemically in the pig for 5 (n=1) or 10 (n=1) minutes prior to the onset of warm ischaemia. Control kidneys (n=2) were retrieved from pigs prior to administration of DMM as described in Figure 5.22. Data are mean ± range.

lead to an improvement in renal function during EVNP when administered as a bolus dose 5 minutes prior to the onset of warm ischaemia across all parameters measured. However, the large variability in control values requires further experiments to be conducted before the protective effect at this dose and circulation time can be confirmed.

5.9.2 Effect of DMM Administered during Back-Table Flush

The effect of DMM administered during BTF was also investigated in a set of preliminary experiments in the pig model of kidney transplantation as shown in Figure 5.25. A dose of 80 mg DMM was administered to the kidney during BTF based on the weight of the pig kidney (∼100 g) and the previously reported therapeutic dose in the mouse (160 mg/kg). Kidneys were flushed with a total volume of 500 mL ice cold Soltran solution containing 16 mg/100 mL DMM. Allometric scaling was not used in this experiment as DMM was not administered systemically to the pig as discussed in Section 4.8.1.

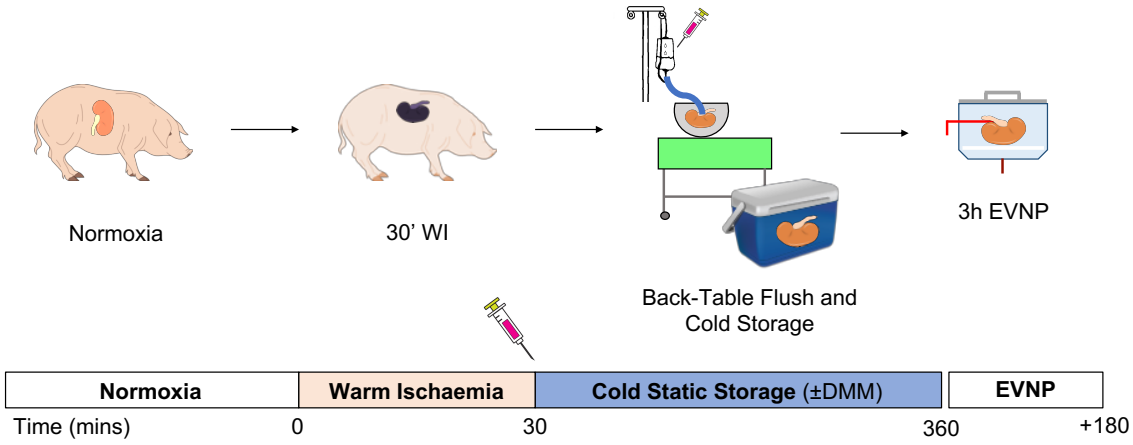

Figure 5.25 Adminstration of DMM During Back-Table Flush in a Pig Model of Kidney Transplantation. Kidneys were retrieved from pigs under general anaesthesia and exposed to 30 mins warm ischaemia (30' WI). During warm ischaemia, pig kidneys became purple in colour due to the presence of deoxygenated blood within the microvasculature. Following ischaemia, kidneys were then flushed with ice cold Soltran (Cntrl) or ice cold Soltran containing 80 mg DMM (DMM) and underwent 6 h cold static storage. Following cold static storage, kidneys were reperfused for 6 h using EVNP. Mr Jack L Martin (University of Cambridge Department of Surgery, UK) and Ms Krishnaa T Mahbubani (University of Cambridge Department of Surgery, UK) assisted with the surgical retrieval of kidneys from the pig.

Pig kidneys treated with DMM during BTF showed poorer function during EVNP compared to control kidneys as shown in Figure 5.26. However, one of the DMM treated kidney retrieved in this set of preliminary experiments had to be re-cannulated during EVNP as the presence of an early renal artery bifurcation led to the initial cannulation failing. As a result, one DMM treated kidney was exposed to a second period of warm ischaemia of roughly 10-20 mins during re-cannulation which may have had an adverse effect on subsequent kidney function. Given the variability in kidney function observed, the low *n* number and, second period of ischaemia experienced by one treatment kidney, further experiments are needed to determine the effect of DMM administered during BTF on kidney function.

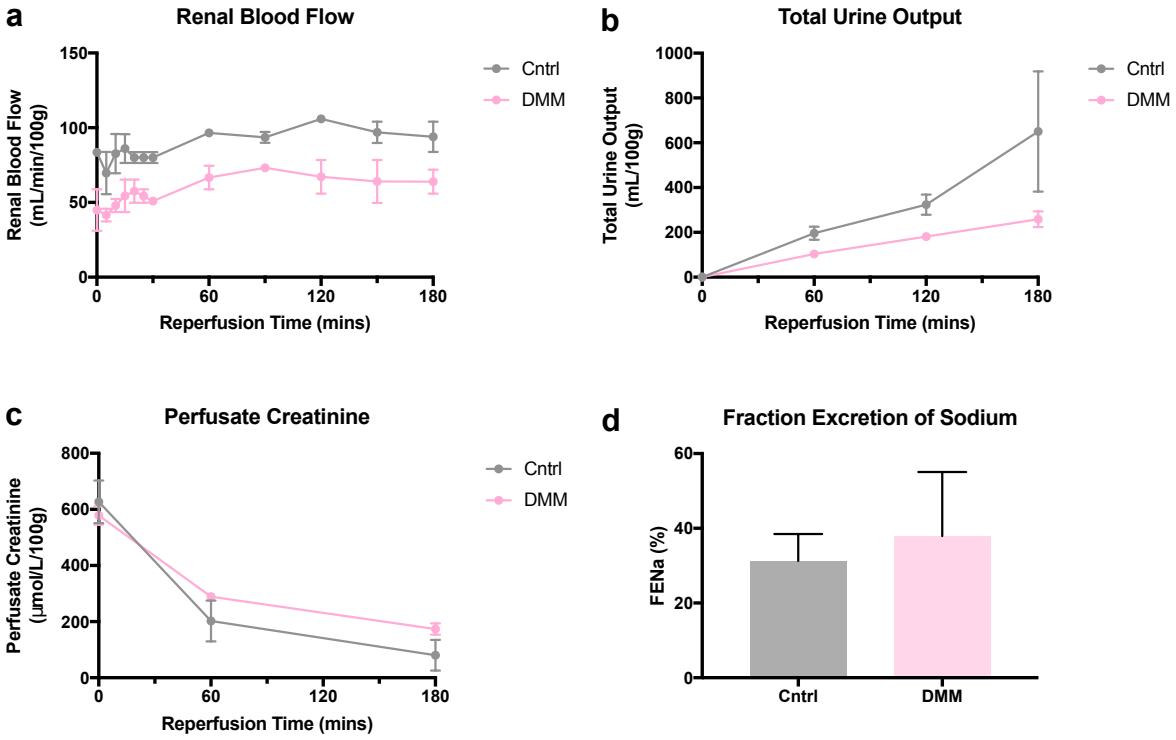

Figure 5.26 The Effect of 80 mg DMM Administered During Back-Table Flush on Kidney Function during EVNP in a Pig Model of Kidney Transplantation Renal blood flow (n=2) (**a**), urine output (n=2) (**b**), perfusate creatinine concentration (n=2) (**c**) and fractional excretion of sodium (n=2) (**d**) during 3 h EVNP of pig kidneys exposed to 30 mins warm ischaemia and 6 h cold static storage. 80 mg DMM was administered to pig kidneys during back-table flush as described in Figure 5.25. Data are mean ± range.

5.10 Discussion

5.10.1 Measurement of Oxidative Damage in the Mouse and Pig Kidney

Measurement of Oxidative Damage to Mitochondrial DNA

Oxidative damage to mtDNA may be inferred by the reduced amplification mtDNA during qPCR. This method was used to investigate mtDNA oxidative damage in the mouse model of renal IRI but not the translational model of kidney transplantation in the pig as the correct primers for pig mtDNA could not be obtained. Counterintuitively, mtDNA amplification was significantly increased compared to control values at 24 h reperfusion in the mouse kidney following 25 mins warm ischaemia. Whilst, this method has previously been used to demonstrate an increase oxidative damage to mtDNA following renal IRI in the mouse, kidneys were exposed to 45 mins warm ischaemia and may have experienced a more severe ischeamic injury [202]. The significant increase in mtDNA amplification relative to control values in Figure 5.4a however suggests mtDNA contained fewer lesions to disrupt the progress of the DNA polymerase during the PCR reaction. This may reflect an early reparative response in the kidney following IRI with the rapid loss of damaged mitochondrial DNA through mitophagy and shedding of mitochondria into extracellular vesicles or cell casts excreted in the urine [284] [285] [286]. Mitochondrial DNA could not be measured in the urine of mice from these experiments however as a sufficient volume of urine could not be collected. Alternatively, it may also be the case that the PCR method is limited in its ability to detect more subtle changes in mitochondrial DNA damage following shorter warm ischaemia times, particularly within a heterogeneous cell population with different sensitivities to ischaemia, such as in the kidney.

Measurement of Protein Carbonyl Formation

Protein carbonyl concentration was measured in the mouse model of renal IRI only. A significant increase in protein carbonyl concentration has previously been shown following 45 minutes warm ischaemia and 24 h reperfusion in this model [202]. In addition, protein carbonyl concentration has been used as a measure of oxidative damage in a mouse model of myocardial infarction [198]. However, there was no significant increase in protein carbonyl concentration at 1, 6 or 24 h reperfusion in kidneys that had been exposed to 20 mins warm ischaemia. This was probably due to the shorter warm ischaemia time investigated resulting in a less severe injury. However, prior to derivitisation, samples were homogenised in RIPA buffer and stored on ice whilst the protein concentration was calculated. During this time

further carbonyl formation may have occurred. Furthermore, the dynamic range of the ELISA used was relatively narrow and the protein carbonyl concentrations were close to the maximum value the assay could accurately measure. Protein carbonyl concentration therefore provides a very crude and unreliable measure of oxidative damage in this context and was not pursued any further.

Measurement of Lipid Peroxidation

Malondialdehyde concentration was investigated in the mouse model of renal IRI and a translational model of kidney transplantation in the pig. Tissue MDA concentration was significantly increased at 24 h reperfusion in the mouse kidney following 20 mins warm ischaemia. In the pig model of kidney transplantation, tissue MDA concentration was significantly decreased at 3 h and 6 h reperfusion. Malondialdehyde is a major end-product of lipid peroxidation along with 4-HNE and was measured in tissue homogenates by reaction with thiobarbituric acid to produce TBARS. However, not only is it very difficult to prevent further lipid peroxidation from occurring during the tissue extraction process but thiobarbituric acid may also react with other products within the homogenate leading to artificially elevated values of MDA in the assay. Whilst a positive control sample containing $FeCl_2$ and t-BHP as an oxidising agent was included to ensure samples had not reached saturation, this represented an unphysiological level of peroxidation and the assay did not have the sensitivity required to detect more subtle changes in physiological range. Instead, the increase in MDA concentration measured in the mouse kidney at 24 h reperfusion may reflect an increasing proportion of necrotic tissue within the kidney as supported by H&E staining (see below) Interestingly, ferroptosis results in lipid peroxidation and is reported as a major cell death pathway in the kidney following IRI [287] [288]. The gold-standard measurement of lipid peroxidation in tissues is via mass spectrometry of F_2-isoprostanes and could instead be used to measure lipid peroxidation in future treatment experiments [289]. However, difficulties again surround the stable extraction and analysis of F_2-isoprostanes from tissue homogenates and this technique is still being optimised.

Measurement of Total Glutathione Concentration

Measurement of total tissue glutathione concentration in tissue via the glutathione recycling assay may be used as a further marker of oxidative stress [177]. Glutathione plays an essential role in mitochondrial and cellular antioxidant defence mechanisms and is depleted during IRI [290]. The total tissue glutathione concentration was significantly decreased in the mouse kidney at 1, 6 and 24 h reperfusion. However, as glutathione may easily undergo further

oxidation during tissue extraction, it was not possible to accurately measure the oxidised to reduced glutathione ratio (GSSG:GSH) which may have provided further information on the tissue redox status. Furthermore, whilst glutathione depletion partly occurs due scavenging of reactive species (and thus can be used to measure oxidative death), depletion may also occur as a result of efflux of GSH across the plasma membrane [291]. This process may alter the redox status of the cell and is thought to play an important regulatory role in numerous cell death pathways [292].

5.10.2 Quantification of Cell Death in the Mouse, Pig and Human Kidney

Histological Analysis

The degree of cellular necrosis could be estimated in H&E sections of the mouse kidney at 24 h reperfusion using the image analysis software ilastik. As necrotic tissue is less eosinophilic than viable tissue, the software could be used to adjust the thresholds of the image and separate out the viable, necrotic and background areas (see Chapter 2) [293]. A set of training images were used to determine the image thresholds which were then applied to a separate set of images in order to calculate the average area of necrosis in each kidney. Using this method, a significant increase in tissue necrosis was measured at 24 h reperfusion following 15, 25, 30 and 45 mins warm ischaemia (with the level of necrosis increasing with warm ischaemic time). However, it was not possible to perform the same analysis in the pig and human model of kidney transplantation as the length of reperfusion was not long enough for the cellular changes associated with tissue necrosis to become evident on H&E sections [281] [282]. In addition, quantification of cellular necrosis via image thresholding was only possible in weakly stained tissue sections where there was a clear distinction between healthy and necrotic tissue. Where tissue sections were more heavily stained, use of threshold analysis was not possible. Furthermore, thresholds for viable and necrotic areas were subjectively determined in training images and it is unclear whether weaker eosin staining definitively represents tissue necrosis. Instead, terminal deoxynucleotidyl transferase dUTP nick end labelling (TUNEL) could be used in future experiments to provide a more objective measure of cell death. TUNEL staining uses a fluorescent probe to label 3'-hydroxy termini exposed during double strand DNA fragmentation that may then be imaged by immunofluorescence microscopy. Double-strand DNA fragmentation occurs in both apoptosis and necrosis and TUNEL staining is non-specific measure of cell death [294]. DNA fragmentation occurs at relatively early stage during cell death with the highest levels of TUNEL staining occurring 6 h after IRI in the mouse kidney [295]. As such, it may be that TUNEL staining could

also be used to detect the level of cellular necrosis at 6 h reperfusion in the pig and human translational model of kidney transplantation.

Measurement of ATP and ADP Concentration

The sum of the ATP and ADP concentration was used to estimate the level of cell necrosis in the mouse model of renal IRI at 24 h reperfusion as well as during 6 h EVNP in the pig and human model of kidney transplantation. The rational for using the sum of the ATP and ADP concentration to estimate the level of cell necrosis was only viable cells are theoretically capable of regenerating their ATP and ADP levels on reperfusion whilst the ATP and ADP concentration in dead or dying cells will be rapidly consumed or remain depleted following ischaemia. The level of tissue necrosis as measured by the sum of the ATP and ADP concentration at 24 h reperfusion in the mouse kidney generally reflected the level of necrosis measured in H&E tissue sections. However, changes in cellular metabolism following IRI could also lead to changes in the ATP and ADP concentration. For example, fatty acid droplets have been reported to accumulate in the cytoplasm of epithelial cells following renal IRI suggesting β-oxidation of fatty acids, the major energy source in the kidney, is impaired, such that whilst tissue is still viable, the ATP and ADP concentration may be reduced [296] [297]. Furthermore, damaged epithelial cells are thought to undergo a glycolytic shift away from the use of free fatty acids as a major fuel source following renal IRI which may also affect the tissue ATP and ADP concentration measured at later time points [298] [299].

In the pig and human translational models of kidney transplantation, kidneys were reperfused for a maximum period of 6 h EVNP. A significant reduction in the sum of the ATP and ADP concentration was measured in pig kidneys that had been exposed 30 mins warm ischaemia and 6 h cold storage during 6 h EVNP but not in kidneys exposed to 6 h cold storage only. This suggested an increased level of cellular necrosis occurred in pig kidneys exposed to 30 minutes warm ischaemia and 6 h cold storage compared to 6 h cold storage only and could be used to compare the level of necrosis in pig kidneys during EVNP in future treatment experiments. Meanwhile there was no significant difference in the sum of ATP and ADP concentration in human kidneys between the first and second periods of EVNP in the described model. However, the initial reperfusion period of 1 h may not have been long enough to allow full recovery of the ATP and ADP concentration in declined human kidneys prior to re-exposure to ischaemia and is a potential limitation of the model. Nevertheless, comparison of the ATP and ADP concentration in pairs of kidneys retrieved from the same donor with one kidney allocated to a treatment group and one acting as a control, could still be undertaken to make inferences about the level of cell necrosis under the

different experimental conditions and control for other confounding factors in the model such as ischaemic pre-conditioning and donor related factors. Ideally however, the sum of the ATP and ADP concentration should not be interpreted in isolation. Where histological methods of assessing cell death such as H&E or TUNEL staining are unavailable, quantification of caspase-3 activation by Western blotting may also be used to assess the level of apoptosis in clamp frozen tissue samples [198]. However, caspase-3 activation is a specific marker of apoptosis and may not wholly reflect the degree of cell death occurring via other pathways following renal IRI.

5.10.3 Measurement of Kidney Function in the Mouse, Pig and Human

Measurement of Kidney Function in the Mouse

Serum creatinine and BUN concentration were used to assess the level of kidney function in the mouse model of renal IRI at 24 h reperfusion. A significant reduction in kidney function was only detected after 20 mins warm ischaemia as measured by the SCr concentration and 18 mins warm ischaemia as measured by the BUN concentration. This was likely due to the large reserve capacity of the kidney with up to 50% of nephrons needing to be lost before a rise in serum creatinine concentration can be detected [234]. In addition, the degree of kidney injury as measured 24 h reperfusion is highly variable and may be affected by other factors including animal age, hydration status, core temperature during surgery, surgery time, anaesthesia, surgical trauma and post-recovery care [236]. However, strict measures, such as the use of a homeothermic monitoring system to maintain the temperature of the animal at 36.0 ± 0.5 °C throughout the procedure, were undertaken to control for these parameters as described in Chapter 2.

Measurement of Kidney Function in the Pig and Human

Renal blood flow, urine output, perfusate creatinine concentration and FENa were used to assess the function of pig and human kidneys during EVNP. In the translational model of kidney transplantation, kidneys exposed to 30 minutes warm ischaemia and 6 h cold storage had significantly reduced function during EVNP compared to kidneys exposed to 6 h cold static storage only. As previously discussed, the difference in function between the two group may have (partly) resulted from increased mitochondrial ROS production in kidneys exposed to 30 minutes warm ischaemia and 6 h cold storage compared to kidneys exposed to 6 h cold storage only. The model is therefore ideally suited to investigate the effect of novel mitochondrial compounds that target mitochondrial ROS production on kidney function

during EVNP, with kidneys exposed to 30 minutes warm ischaemia acting as a positive control and kidneys exposed to 6 cold storage only as a negative control.

Meanwhile, in preliminary human experiments, the values of renal blood flow, urine output, perfusate creatinine and FENa in the first and second period of EVNP were similar to values reported in human kidneys undergoing EVNP and then transplanted in the literature [250] [140]. This suggests declined human kidneys were able tolerate the re-exposure to ischaemia and reperfusion without adversely affecting renal function and that pairs of declined human kidneys retrieved from the same donor could be used to investigate the effect of novel mitochondrial compounds in human tissue prior to trials in humans as previously described.

5.10.4 Effect of Malonate Compounds Administered Prior to Ischaemia on Kidney Injury in the Mouse and Pig

There was no significant difference in kidney function at 24 h reperfusion in mice that had been treated with DMM or DSM prior warm ischaemia compared to untreated controls. This suggested DMM (at a dose of 0.8-6.4 mg) and DSM (at a dose of 3.2 mg) administered prior to ischaemia was not protective against IRI in the mouse kidney. In contrast DMM has previously been shown to protect against IRI when administered prior to ischaemia in a mouse model of myocardial infarction [14]. However, in this model, DMM was also administered to the mouse during ischaemia and the protective effect may have been due to a culmination of DMM present in the tissue during ischaemia and in the circulation on reperfusion. Whilst a high malonate concentration was achieved in the tissue during ischaemia (as shown in Figure 3.20), it is unclear what proportion of malonate is located within mitochondria as well as the quantity of malonate that may be flushed from the kidney on reperfusion and therefore unable to inhibit mitochondrial ROS production.

Meanwhile, administration of DMM prior to warm ischaemia in the pig model of kidney transplantation showed some protective effect in preliminary experiments, particularly at a dose of 8400 mg and a circulatory time of 5 mins. However, as discussed in Chapter 3, administration of 8400 mg DMM led to a short period cardiac depression when injected into the ear vein of the pig and may preclude its future use in human donation due to the risk premature circulatory arrest. Nonetheless, these experiments have aided in the development of the pig model of kidney transplantation and provided useful dosing information. Use of an infusion (which was not possible under the project licence in the current study) may enable higher doses of DMM to be administered to humans more safely without the risk of cardiac depression in future experiments as well as the use of alternative malonate ester

prodrugs such as MAM in which a higher tissue malonate concentration can be achieved with a lower concentration of the prodrug. Importantly however, as only one experiment was conducted for each condition, further experiments are needed to confirm the protective effect of malonate prodrugs administered prior to ischaemia in the pig before commencing human studies.

5.10.5 Effect of Malonate Ester Pro-Drugs Administered at Reperfusion on Kidney Injury in the Mouse and Pig

Administration of DMM and MAM on reperfusion of the mouse kidney lead to a significant reduction in serum creatinine but not BUN concentration at 24 h reperfusion compared to controls. However, given the high degree of variability within the mouse model, the experiment may have been underpowered. A post-hoc power analysis of data presented in Figure 5.19 suggests an n of 14 is required to achieve a β level of 0.1 and α level of 0.05, given the variability in BUN concentration between the two groups and a n of 10 given the variability serum creatinine concentration [300]. Nevertheless, the significant finding that administration of both DMM and MAM on reperfusion lead to an improvement in serum creatinine concentration at 24 h reperfusion in Figure 5.19 is encouraging. It is possible that the increased tissue malonate concentration within the tissue on reperfusion inhibited mitochondrial ROS production despite the fact a decrease in the MitoP/MitoB ratio on reperfusion was not measured was not measured in Chapter 4. As previously discussed, MitoB may be limited in its ability to specifically measure a burst of superoxide production from Complex I on initial reperfusion. Furthermore, as malonate compounds are rapidly degraded and excreted following administration, the concentration within tissues on reperfusion is only transiently raised and it is unlikely their protective effect occurs as a result of interaction with later downstream processes. Full dosing experiments, similar to those presented in Figure 3.20 should now be conducted for DMM and MAM administered at reperfusion to confirm their protective effect and optimal therapeutic concentration. In contrast to DMM and MAM, administration of DSM on reperfusion did not lead to a significant improvement in either serum creatinine or BUN concentration at 24 h reperfusion compared to controls suggesting DSM (at a dose of 0.38 mg) was not protective against IRI in the mouse kidney. However as only one DSM concentration was investigated, these experiments were extremely limited and full dosing studies with measurement of tissue succinate and malonate concentrations during ischaemia and on reperfusion should be conducted in future studies to fully determine whether or not DSM may have a protective effect in renal IRI and kidney transplantation.

Meanwhile, in a set of preliminary experiments, administration of DMM to the pig kidney during BTF did not lead to an improvement in kidney function as measured by renal blood flow, total urine output, perfusate creatinine or fractional excretion of sodium during subsequent reperfusion. However, as discussed above, one DMM treated kidney had to be re-cannulated during EVNP and underwent an additional period of warm ischaemia which may have led to a reduction in kidney function. Further experiments are needed before any conclusions can be drawn on the effect of DMM administered during BTF on initial kidney function in the pig model of kidney transplantation.

5.11 Summary

The data presented in this Chapter forms a preliminary experimental survey of the methods to assess kidney injury and function following IRI in the different transplant models. It was important to characterise the level of injury and organ function in the mouse model of renal IRI and pig and human translational model of kidney transplantation to determine the most appropriate endpoints and biological markers that could be used to assess the effect of novel mitochondrial therapies and reliably inform future clinical trials. A reliable marker of oxidative damage was not identified in the mouse or pig kidney and further work is needed to determine how the level of oxidative damage may be assessed in the kidney following IRI. Cell death was primarily assessed by the ATP and ADP concentration in the mouse, pig and human as well as analysis of H&E stained sections in the mouse. However, the analysis of the ATP and ADP concentration is an indirect measure of cellular necrosis and alternative measures of cell death such as TUNEL staining and caspase 3 activation should also be investigated in future experiments. Kidney function could be reliably assessed in the mouse, pig and human kidney however there was a large degree of variability within the mouse model requiring strict control of measures such as animal temperature during surgery. The pig and human translational models of kidney transplantation meanwhile were at greater risk of technical failures if the anatomy of the kidney was unsuitable for reperfusion or a problem was encountered with the reperfusion circuit, preventing definitive conclusions from being drawn from such experiments. It was also not possible to perfuse kidneys for more than 6 h following ischaemia reperfusion due to deterioration of the perfusate and red cell haemolysis and so the effect of novel compounds on kidney function could only be assessed early on in the injury process. In this Chapter, administration of DMM and MAM on reperfusion of the mouse kidney led to a significant improvement in kidney function at 24 h compared to controls. However, full dosing studies of DMM and MAM administered at reperfusion should now be conducted. In addition, these findings must be replicated in the pig and human

translational models of kidney transplantation to show that DMM and MAM may have the same protective effect under conditions that more closely resemble clinical transplantation. As very high concentrations of DMM are required to achieve therapeutic concentrations of malonate in the pig, more targeted approaches of malonate delivery with either 'tuned' malonate ester prodrugs (such as MAM) or mitochondrial targeted malonate prodrugs may be required to minimise the likelihood of adverse off target effects such as cardiac depression which would likely be unacceptable in human donors.

Chapter 6

General Discussion and Future Directions

6.1 General Discussion

The primary aim of this thesis was to determine whether malonate ester prodrugs may inhibit mitochondrial ROS production and thereby ameliorate IRI in kidney transplantation. This was investigated using a model of renal IRI in the mouse and translational models kidney transplantation in the pig and human. Much of the data presented in this thesis represents preliminary studies for the use of malonate ester prodrugs in a transplant setting. Whilst important inroads towards this goal have been made, a number of significant hurdles must still be overcome and are discussed in each of the sections below.

6.1.1 Measurement of Mitochondrial ROS Production *In Vivo*

In Chapter 4, the ratiometric, mass spectrometry probe MitoB was used to assess the level of mitochondrial ROS production on reperfusion in the mouse. However, MitoB was unable to detect a difference in mitochondrial ROS production on reperfusion between control kidneys and those treated with malonate ester prodrugs. Interestingly, however, administration of malonate ester prodrugs at reperfusion led to a reduction in tissue injury as measured by serum creatinine concentration suggesting the compounds had a protective effect (as shown in Chapter 5). This was likely due to the inhibition of mitochondrial ROS production as malonate concentrations were only transiently raised in the tissue excluding other later effects. This led to the suggestion that MitoB may be limited in its sensitivity to accurately measure the burst of superoxide produced by mitochondria on reperfusion or that the wrong time point to measure the MitoP/MitoB ratio on reperfusion had been selected (see Section 4.9.1).

The necessity of measuring mitochondrial ROS production *in vivo* is an important discussion point, given the technical challenges and the fact malonate has been shown to inhibit mitochondrial ROS production *in vitro* using other more accurate assays [14]. However, as previously discussed, the *in vitro* environment can differ greatly from the physiological conditions present within an organ or tissue *in vivo*. Therefore, during the early stages of drug development and translation, it is important to examine potential reasons why a particular compound that proved promising *in vitro* experiments did not lead to the desired effect *in vivo*.

Assuming the mechanism of mitochondrial ROS production during IRI described by Chouchani et al [15] may be applied to the kidney (as was done in this thesis), a lack of efficacy of malonate ester prodrugs may occur under a number of circumstances. First, the malonate compound may not have entered mitochondria rapidly enough or to the correct concentration to inhibit SDH at the appropriate time point leading to either succinate accumulation during ischaemia or rapid oxidation of succinate on reperfusion. Alternatively, the malonate compound may have successfully inhibited either succinate accumulation or oxidation, leading to a reduction in mitochondrial ROS production but not tissue injury. This would imply that succinate-driven mitochondrial ROS production may not significantly contribute to IRI *in vivo* as *in vitro*. Lastly, our assumption that the rapid oxidation of succinate on reperfusion is the primary driver of mitochondrial ROS production in the kidney may be incorrect. In this scenario, malonate may successfully inhibit either succinate accumulation during ischaemia or oxidation on reperfusion without affecting mitochondrial ROS production and would imply mitochondrial ROS production and tissue injury occur primarily through other mechanisms.

Distinguishing between the different scenarios described above and formally testing our assumption that succinate is a key driver of mitochondrial ROS production in the kidney (particularly as most previous has been conducted in the heart) is therefore fundamental in furthering the translation of malonate ester prodrugs to clinical transplant practice. However, this will require more sensitive methods of measuring mitochondrial ROS production *in vivo* to be identified. This will allow the mechanism of mitochondrial ROS production in the kidney to be tested under more physiological conditions *in vivo*, either by altering the mitochondrial membrane potential e.g. with oligomycin or uncouplers, or succinate concentration e.g. with AMS, during IRI [193]. Subsequently, if the mechanism described by Chouchani et al holds true in the kidney, the effect of malonate ester prodrugs on mitochondrial ROS production could be investigated with greater clarity and confidence in a similar manner to MitoB experiments presented in Chapter 4. If mass spectrometry suggests malonate does not reach sufficient concentrations in the tissue to inhibit SDH during ischaemia or reperfusion

(by comparing to either mass spectrometry measures of succinate concentration or more sensitive measures of mitochondrial ROS production), then alternative strategies, such as the use of the mitochondrial-targeting TPP moiety, can instead be investigated. Alternatively, if mass spectrometry suggests malonate does sufficiently inhibit SDH in a particular experiment, then more accurate and sensitive measures of mitochondrial ROS production will allow decisions on the relevance of a particular mechanism or target of mitochondrial ROS production in the kidney to be made with more certainty.

As briefly discussed, there are a number of other techniques that may be used to measure mitochondrial ROS production *in vivo*, either directly or indirectly. Direct measures include the use of spin trapping and electron spin resonance (ESR) . Electron spin resonance measures a quantum property of electrons called spin. In essence, unpaired electrons may act as a small magnet and align in parallel or opposition (antiparallel) to an external magnetic field, creating two possible energy levels for the electron. If electromagnetic radiation of the correct energy (usually in the microwave range) is then applied to the molecule containing the unpaired electron, it will be used to move the electron from the lower energy level to the upper one, producing an absorbance spectrum which can be used to identify the molecule. Electron spin resonance is too insensitive to measure superoxide and hydroxyl radicals, however larger compounds or spin traps may specifically react with oxygen radicals to form a stable radical that can subsequently be detected by ESR. Spin traps may be administered *in vivo* and subsequently extracted from clamp frozen tissue for analysis via ESR. For example, hydroxylamine spin traps have previously been used to measure superoxide production on reperfusion in a rat model of pancreas transplantation [301]. Mitochondrial ROS production during IRI may specifically be measured using TPP-hydroxylamine spin traps, such as Mito-TEMPO. Mito-TEMPO, which reacts with superoxide, has a rate constant of $\sim 10^3$-10^4 M^{-1} s^{-1} and will compete for the superoxide signal on reperfusion with MnSOD that has a rate constant of 6.8 x 10^8 M^{-1} s^{-1} [302] [303]. Whilst MitoTEMPO is approximately 4-5 magnitudes less reactive with superoxide than MnSOD, this difference is much less than the difference between MitoB (rate constant ~ 9 M^{-1} s^{-1}) and the peroxidases (rate constant 2 x 10^7 M^{-1} s^{-1}) for hydrogen peroxide [268]. Mito-TEMPO may therefore be better suited to detecting the transient and rapid increase in mitochondrial ROS production that occurs during IRI. However, ESR requires specialist equipment and expertise that were not available during this thesis. Instead, detection of mitochondrial ROS production *in vivo* could be further investigated using the newly designed mass spectrometry probe MitoNeoD. MitoNeoD reacts with superoxide at a rate of $\sim 10^4$ M^{-1} s^{-1} and similar to Mito-TEMPO, may be better able to compete for the mitochondrial ROS signal upon reperfusion [304].

Meanwhile, indirect measures of mitochondrial ROS production include the aconitase assay as described in Chapter 4 or additional markers of oxidative damage not investigated in this thesis. These include F_2-isoprostanes or hydroxylation products of aromatic compounds, such as phenylalanine, administered prior to ischaemia [305] [306]. However, problems again exist in the stable extraction of these markers without causing additional oxidation that may affect the subsequent level of oxidative damage measured. Furthermore, whilst the aconitase assay is relatively specific for mitochondrial superoxide production, other measures of oxidative damage may not discriminate between ROS species or sites of ROS of production and therefore require careful interpretation [272]. Nevertheless, these approaches could be used in future experiments either individually or in combination to establish a reliable marker for mitochondrial ROS production on reperfusion.

6.1.2 Characterisation of the Translational Models of Kidney Transplantation in Mice, Pigs and Humans

In this thesis a number of translational animal models were used to investigate the role of mitochondrial ROS production in kidney transplantation. As discussed in Chapter 1, translational models play an essential role in bridging the gap between the laboratory bench and patient bedside. This is important as many models used early on in the drug development process may oversimplify the mechanisms leading to tissue injury [307]. By closely simulating the clinical conditions of disease, translational models may help to identify compounds likely to be efficacious in humans at an earlier stage of drug development. This would allow the limited resources available to a drug development to be allocated more efficiently and economically. In this thesis, the importance of using translational models in transplant research was emphasised in Chapter 3 where the metabolic changes that occurred during kidney retrieval and cold storage were much greater in the pig and human than in the mouse.

Whilst the mouse model of renal IRI may not have accurately reflected many aspects of organ transplantation, it was nevertheless useful in identifying promising compounds in the early stages of drug development. In comparison to the pig and human models of kidney transplantation, the mouse model of renal IRI enabled rapid screening of novel malonate ester prodrugs administered at different timepoints during IRI. The surgical procedure was also relatively simple, requiring less training compared to more complex models described in Chapter 1. However, depending on the outcome measured, the mouse model of renal IRI could be variable requiring large sample sizes to achieve an appropriate level of power as discussed in Chapter 5. This was partly due to the large number of confounding factors that may affect IRI, including animal temperature, hydration status and method of anaesthesia.

However, strict measures were taken to control for these factors as described in Chapter 2. The mouse model of renal IRI will thus continue to be useful for the screening of future malonate and other mitochondrial compounds and aid in their early translation from *in vitro* models to clinical transplantation.

Meanwhile, the pig model enabled the effect of mitochondrial ROS production to be investigated in the kidney under the conditions that more closely resemble transplant practices. In addition, the size, anatomy and physiology of the pig kidney is closely related to that in the human [242] [243]. However, pig kidneys exposed to 6 h cold ischaemia in the model more closely resemble LD grafts than DBD grafts which are associated with additional damaged related to the catecholamine and cytokine storms. Similarly, pig kidneys exposed to warm ischaemia likely experienced a more extreme level of injury than typically encountered DCD grafts in the UK. This time was chosen to investigate the full injury that may be experienced in the model as discussed in Chapters 4 and 5 however, it is also worth re-emphasising young and healthy pigs were used compared to human organ donors who commonly suffer from multiple comorbidities and are typically older in age. Nevertheless, a key advantage of the model is that malonate compounds may be administered to the pig at different stages during the transplant process that closely reflects clinical practice and it is possible to train a non-surgical professional (myself) to retrieve kidneys from the pig independently.

As discussed in Chapter 1, pig kidneys were not transplanted into recipients but reperfused using EVNP. This was logistically and economically more practical than performing full transplant studies in the pig at this early stage of drug development. Moreover, *ex vivo* perfusion enables close monitoring of kidney function during the initial reperfusion period and for multiple tissue, blood and urine samples to be taken from the kidney that would not be possible in full transplant experiments [247]. Of note, EVNP is already used in clinical practice and the data gained from experiments in the pig may help to further understand the effects of EVNP in clinical transplantation [139]. Nonetheless, as discussed in Chapter 5, EVNP of pig (and human) kidneys is currently limited to approximately 6 h due to haemolysis of red blood cells within the perfusion circuit. The perfusion time may be extended further if fresh porcine blood was available to replace the initial perfusate. However this was not possible in this thesis and would likely require another pig of the same blood type to act as a blood donor. It is thus likely that full transplant studies would be required to investigate the effect of mitochondrial ROS production and malonate ester prodrugs at longer timepoints following transplantation. Importantly, full transplant experiments should only be conducted with the most promising compounds already tested in the pig and human EVNP model of kidney transplantation in future experiments.

Lastly, a novel method for investigating the efficacy of mitochondrial compounds in human tissue was developed as part of this thesis. Declined human kidneys offered for research were reperfused for 1 h using EVNP in order to 'reset' their metabolic profile before being re-exposed to ischaemia and reperfusion as described in Chapter 5. It is hoped that this model could be used to further identify the most efficacious compounds for use in humans as well as informing future clinical trials. As discussed in Chapter 5, an element of conditioning is unavoidable in the model but may be controlled for by using pairs of kidneys from the same donor. Furthermore, the model is not dissimilar to the use EVNP in clinical transplantation and may again help to further understand the protective mechanisms of this technique [139]. The model is also very similar to the pig model and comparisons may be made between the two species to further aid in the identification of the most efficacious compounds for use in future trials. However, the reperfusion of human kidneys is also limited by the haemolysis of red blood cells within the perfusate and whilst this may be more easily replaced than in the pig model, it is still difficult to maintain the kidney on the circuit for long periods due to the deterioration of other perfusion parameters. Nevertheless, the effect of mitochondrial compounds on initial ROS production and injury may be easily assessed in the human kidney using EVNP and provide important dosing and toxicity information for use in future human trials.

6.1.3 Use of Malonate Ester Prodrugs to Inhibit Mitochondrial ROS Production in Kidney Transplantation

As described in Chapter 1, mitochondrial ROS production during IRI may be targeted via a number of different strategies [15] [17]. The main focus of this thesis however was to determine whether malonate ester prodrugs may be used to inhibit mitochondrial ROS production that occurs during IRI in kidney transplantation.

Malonate is a competitive inhibitor of SDH and may inhibit mitochondrial ROS production by inhibiting either the accumulation of succinate that occurs via reverse action of SDH during ischaemia or rapid oxidation of succinate by SDH that drives RET and ROS production on reperfusion. However, to effectively achieve either one of these goals, malonate must be present within mitochondrial at the correct dose and time [308]. As discussed previously, malonate is a charged molecule and must therefore be administered in a cell permeable form to pass through lipid membranes *in vivo*. The negatively charged groups on malonate are covered by an alkyl moieties in malonate ester prodrugs via formation of an ester bonds; however, these must be subsequently hydrolysed by intracellular esterases in order to release active malonate and for SDH inhibition to occur. Sufficient time prior to either ischaemia or

reperfusion must therefore be available to allow malonate ester prodrugs to accumulate and undergo hydrolysis within mitochondria.

In most clinical scenarios involving IRI, the onset of ischaemia is unpredictable and the only opportunity to administer therapies aimed at reducing mitochondrial ROS production is at the point of reperfusion. In such instances, malonate ester prodrugs (or other mitochondrial compounds) must rapidly accumulate within mitochondria in their active form to inhibit mitochondrial ROS production. As the burst of mitochondrial ROS production occurs rapidly on reperfusion, many compounds do not reach sufficient concentrations in the tissue to effectively inhibit this process and prevent subsequent injury [309]. However, organ transplantation is unique in that the onset of ischaemia is more easily anticipated and there are multiple opportunities to administer mitochondrial therapies during the retrieval, preservation and transplant process, as described in Chapter 1. This may facilitate the use of compounds that would not otherwise be effective in other forms of IRI.

In this thesis, the efficacy of malonate ester prodrugs administered either prior to ischaemia or at reperfusion was first investigated in the mouse model of renal IRI to screen for the most promising compounds for future use in the pig and human models of kidney transplantation. In Chapter 3, I investigated whether malonate ester prodrugs administered prior to the onset of ischaemia may inhibit SDH reversal and succinate accumulation. Administration of malonate ester prodrugs prior to ischaemia did not lead to a reduction in succinate accumulation in the mouse model of renal IRI despite clear inhibition of SDH activity. As discussed, succinate may also accumulate through alternative pathways during ischaemia, including glutaminolysis and canonical CAC activity, and the effective inhibition of succinate accumulation in the kidney requires further investigation [14] [175]. Malonate ester prodrugs were also administered prior to ischaemia in the pig model of kidney transplantation in Chapter 3. However, a definitive conclusion on the effect of malonate ester prodrugs on succinate accumulation could not be drawn from these pilot experiments. Nevertheless, important dosing and timing information was obtained for future use.

In Chapters 4 and 5, I investigated whether malonate ester prodrugs administered prior to ischaemia or at the point reprfusion may instead inhibit mitochondrial ROS production. Administration of malonate ester prodrugs prior to ischaemia or at the point of reperfusion did not lead to a reduction in mitochondrial ROS production as measured by the ratiometric probe MitoB in the mouse model of renal IRI. However, as discussed above, MitoB may be limited in its sensitivity to accurately measure the rapid burst of mitochondrial ROS on reperfusion and other measures of mitochondrial ROS and oxidative damage should ideally be investigated in future experiments. Nevertheless, administration of either DMM or MAM at the point of reperfusion led to an improvement in kidney function as measured by the

serum creatinine concentration at 24 h reperfusion. Whilst this suggested both DMM and MAM were hydrolysed rapidly enough to inhibit succinate oxidation and ROS production within the ischaemic tissue on reperfusion, a 10-fold lower dose of MAM compared to DMM was able to achieve the same protective effect. As previously discussed, MAM is hydrolysed more rapidly by PLE than DMM *in vitro* and malonate accumulates more rapidly and to higher concentration in the kidney when MAM and DMM are administered as an intravenous injection to mice (personal communication, Hiran Prag). This may explain the greater efficacy of MAM compared to DMM *in vivo*. Furthermore, the lower concentration of MAM required will likely reduce the degree of adverse, off-target effects of these compounds. This is particularly important for the clinical translation of malonate ester prodrugs, as the high dose DMM currently used in the pig led to cardiac depression and is unlikely to be approved for use in human kidney transplantation as discussed in Chapter 5. Further dosing studies of DMM and MAM administered at reperfusion should now be conducted in the mouse, similar to those presented in Figure 3.20, to find the optimal therapeutic range of each compound.

In addition, the concentration of malonate prodrugs required to inhibit mitochondrial ROS production on reperfusion may be reduced even further with the future use of mitochondrial targeted malonate compounds, as described in Chapter 1. These compounds typically comprise a TPP cation linked by a carbon chain with the intended mitochondrial cargo. The positively charged TPP cation is strongly attracted to the negatively charged inner mitochondrial membrane potential, accumulating several hundred-fold within the mitochondrial matrix. A promising compound currently under development in our Lab is TPP_{11}-malonate, which when given at a 10x lower dose to MAM at reperfusion (e.g. 1.6 mg/kg versus 16 mg/kg) led to a similar reduction in infarct size in a mouse model of myocardial infarction (personal communication, Hiran A Prag). The effect of TPP-linked malonate esters on mitochondrial ROS production in kidney transplantation may subsequently be investigated in future experiments using the models described in this thesis.

Lastly, the use of malonate ester prodrugs to inhibit mitochondrial ROS production on reperfusion was also investigated in the pig model of kidney transplantation. These experiments demonstrated that malonate ester prodrugs given during back-table flush may undergo hydrolysis during subsequent cold preservation, such that sufficient levels of malonate were present in the tissue to inhibit mitochondrial ROS production on reperfusion. This is important, as administration of novel therapies during back-table flush currently represents the easiest approach to incorporating the use of malonate ester prodrugs into clinical practice. Administration of novel compounds to the isolated organ during back-table flush may also have a number of other advantages over their administration to the organ donor or recipient.

For example, off-target and toxic effects to other organs can be avoided, possibly allowing larger concentrations of the compound to be used; conversely, organ specific delivery may enable a lower concentration of the compound to be used. The optimal dose and time to administration malonate ester prodrugs in kidney transplantation still requires further investigation. The pig and human translational models of kidney transplantation described and characterised in the this thesis will play an important role in these future experiments.

6.2 Future Directions

The future directions of this projection can be divided into short and long term objectives. In the short-term, future experiments should focus on the two main areas discussed above. Firstly, more accurate and sensitive methods of measuring mitochondrial ROS production during IRI *in vivo* should be identified, and secondly, preliminary findings in the mouse should now be investigated under conditions that more closely resemble clinical transplantation in the pig and human models. To aid in this process, further dosing experiments in the mouse and additional markers of tissue damage, cell death and inflammation should be identified in the pig and human models as discussed above and in Chapter 5. In the longer-term, two other areas are of particular interest in renal IRI and kidney transplantation. These include the effect of mitochondrial damage following IRI on long-term kidney function and the additional roles of succinate accumulation during IRI and subsequent tissue repair. These processes are discussed in detail below and may form important targets for future mitochondrial therapies.

6.2.1 Effect of Mitochondrial ROS Production on Long-Term Graft Function and Survival in Kidney Transplantation

As discussed in Chapter 1, the IRI that occurs during kidney transplantation may influence long-term graft function and survival. Whilst this thesis primarily focused on the effect of mitochondrial ROS production on initial graft function following IRI, improving long term graft function and survival is also incredibly important in helping to reduce organ demand and improve patient morbidity and mortality. As described in Chapter 1, maladaptive repair following IRI in the kidney may promote a persistent pro-inflammatory milieu, G2/M cell cycle arrest of tubular cells and the development of tissue fibrosis, during which mitochondrial dysfunction is thought to play a central role [114] [299]. Interestingly, SS-31, a mitochondria-targeted peptide, administered for 6 weeks, following kidney IRI in rats, led to improved mitochondrial integrity, reduced expression of pro-inflammatory markers and

arrested interstitial fibrosis [310]. Mitochondrial damage following IRI may therefore also play an important role in chronic graft dysfunction following kidney transplantation.

Malonate ester prodrugs are not suited to the inhibition of persistent mitochondrial ROS production that occurs following IRI in CKD as this is likely produced by through an alternative mechanism to rapid succinate oxidation and RET [177]. However, inhibition of mitochondrial ROS production during initial reperfusion may improve mitochondrial function on reperfusion and dampen the immune response to IRI which may subsequently alter the development of chronic graft dysfunction. This hypothesis could be investigated in future experiments using the mouse model of renal IRI described in this thesis. The ischaemia time of 20 mins used to investigate the effect of malonate ester prodrugs on initial kidney injury in the mouse is known to be non-lethal and has previously been used to investigate the mRNA changes for up to 12 months after IRI [240].

6.2.2 Additional Roles of Increased Succinate Levels in IRI and Kidney Transplantation

In addition to its role in mitochondrial ROS production, succinate is increasingly recognised as an important signalling molecule that may communicate the metabolic status of the mitochondria to the nucleus of the cell and the surrounding extracellular tissue. This is achieved through numerous mechanisms as shown in Figure 6.1 and has been implicated in several regulatory and inflammatory processes [164] [311]. In particular, increased succinate levels stabilise the transcription factor HIF-1α via direct inhibition of prolyl hydroxylases (PHD) in macrophages, driving them towards their M1 pro-inflammatory phenotype and has been shown to exacerbate tissue injury in a mouse model of rheumatoid arthritis [312] [313]. Succinate has also been shown to increase the activation of dendritic cells via the G-protein coupled receptor, SUCNR1, leading to an increased rate of skin graft rejection in WT compared to Sucnr1$^{-/-}$ mice [314]. Furthermore, succinate is thought to mediate the release of renin in the kidney whilst chronic activation of SUCNR1 in renal epithelial cells may contribute to tubular interstitial fibrosis in diabetic kidney disease [315] [316]. Increased succinate may also affect proteins involved in cellular metabolism via post-translational modifications such as lysine succinylation and inhibit JMJD histone demethylases and TET hydroxylases at very high (millimolar) concentrations leading to epigenetic changes to nuclear DNA.

As demonstrated in this thesis, succinate accumulates 5-10 fold in human kidneys during organ retrieval and cold preservation whilst approximately two-thirds of accumulated succinate is ‘washed’ out of ischaemic tissue on reperfusion [175] [317]. Increased levels

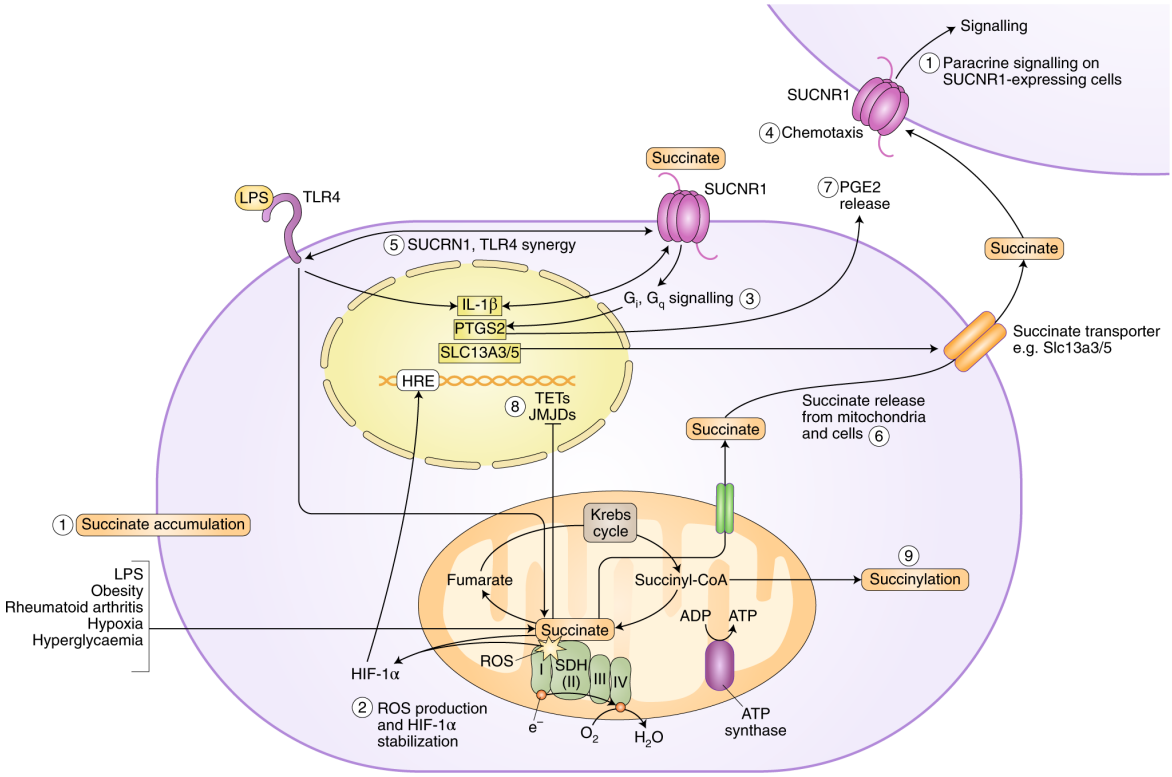

Figure 6.1 Succinate Signalling in Kidney Transplantation. Accumulation of succinate that occurs during ischaemia may lead to the stabilisation of HIF-1α, lysine residue succinylation and SUCNR1 activation. On reperfusion, a large proportion of accumulated succinate is 'washed out' of tissues where it may mediate further signalling roles. In particular, increased succinate has been shown to promote a pro-inflammatory phenotype via HIF-1α stabilisation in macrophages, which may exacerbate the acute inflammatory response to IRI in kidney transplantation. In addition, succinate may increase the activation of dendritic cells via the SUCNR1 receptor, promoting graft rejection. Meanwhile, chronic activation of SUCNR1 in renal epithelial cells may contribute to the development of tubulointerstitial fibrosis whilst lysine succinylation may impair the function of numerous metabolic enzymes including ICDH, GAPDH, PDH and SDH. Finally, succinate is not thought to accumulate to levels required to inhibit JMJD and TET enzymes (typically milli-molar concentrations) and induce epigenetic changes under conditions of IRI. Figure adapted from Ryan et al (2019).

of succinate that occur during IRI may therefore play additional roles in tissue injury in kidney transplantation, particularly in inflammatory cell pathways. This could have important consequences for the overall level of injury that occurs following IRI in the kidney as well as long-term graft function and survival. The additional roles of succinate in kidney injury should therefore be investigated in future experiments using the models of renal IRI and kidney transplantation described in this thesis. In particular, the effect of succinate inhibition on macrophage activation following IRI could be investigated using flow cytometry in a similar manner to Peruzzotti-Jametti et al (2018) who showed macrophage activation was reduced in the brain of mice when transplanted with neural stem cells that reduced the CSF concentration of succinate [318].

6.3 Final Summary

In this thesis, I showed the metabolic changes required for mitochondrial ROS production on reperfusion occur in grafts retrieved from all donor types and may partly relate to the difficulty in effectively cooling organs to prevent rapid succinate accumulation that occurs during warm ischaemia. I also showed the ratiometric probe, MitoB, may be limited in its sensitivity to accurately quantify the burst of superoxide from kidney mitochondria on reperfusion; however, the metabolic changes that drive mitochondrial ROS production on reperfusion *in vitro* occur in the mouse, pig and human models of renal IRI and kidney transplantation *in vivo*. I then showed malonate ester prodrugs administered at reperfusion (but not prior to ischaemia) led to an improvement in kidney function following renal IRI in the mouse. Of note, a 10x lower dose of MAM could achieve the same protective effect as DMM which may have important implications for the future translation of these compounds. Lastly, I presented preliminary experiments in the pig and human models of kidney transplantation which have provided important dosing and timing information for the use malonate ester prodrugs in these models. Future experiments should now aim to determine whether malonate ester prodrugs (or mitochondria-targeted malonate compounds) may have the same protective effect in the pig and human models of kidney transplantation via the strategies discussed above. As these models closely resemble the conditions of clinical transplantation, it is hoped the results from experiments in the pig and human model may go on to inform the use of malonate ester prodrugs in future clinical trials.

References

[1] M Tonelli, N Wiebe, G Knoll, A Bello, S Browne, D Jadhav, S Klarenbach, and J Gill. Systematic review: kidney transplantation compared with dialysis in clinically relevant outcomes. *American journal of transplantation*, 11(10):2093–2109, 2011.

[2] NHS Blood and Transplant. Annual report on kidney transplantation - report for 2018/2019. Aug 2019.

[3] UK Renal Registry (2019). Uk renal registry 21st annual report - data to 31/12/2017, bristol uk. *Available from https://www.renalreg.org/publications-reports/.*

[4] Rachel J Johnson, Lisa L Bradbury, Kate Martin, James Neuberger, et al. Organ donation and transplantation in the uk—the last decade: a report from the uk national transplant registry. *Transplantation*, 97:S1–S27, 2014.

[5] J Nath, M Field, SR Ebbs, T Smith, D McGrogan, J Al-Shakarchi, J Hodson, S Mellor, and A Ready. Evolution of renal transplant practice over the past decade: a uk center experience. In *Transplantation proceedings*, volume 47, pages 1700–1704. Elsevier, 2015.

[6] M Cavaillé-Coll, S Bala, E Velidedeoglu, A Hernandez, P Archdeacon, G Gonzalez, C Neuland, J Meyer, and R Albrecht. Summary of fda workshop on ischemia reperfusion injury in kidney transplantation. *American journal of transplantation*, 13(5):1134–1148, 2013.

[7] Julia Menke, Daniel Sollinger, Beate Schamberger, Uwe Heemann, and Jens Lutz. The effect of ischemia/reperfusion on the kidney graft. *Current opinion in organ transplantation*, 19(4):395–400, 2014.

[8] Dominic M Summers, Rachel J Johnson, Alex Hudson, David Collett, Christopher J Watson, and J Andrew Bradley. Effect of donor age and cold storage time on outcome in recipients of kidneys donated after circulatory death in the uk: a cohort study. *The Lancet*, 381(9868):727–734, 2013.

[9] Dominic M Summers, Christopher JE Watson, Gavin J Pettigrew, Rachel J Johnson, David Collett, James M Neuberger, and J Andrew Bradley. Kidney donation after circulatory death (dcd): state of the art. *Kidney international*, 88(2):241–249, 2015.

[10] Chris J Callaghan, Simon JF Harper, Kourosh Saeb-Parsy, Alex Hudson, Paul Gibbs, Christopher JE Watson, Raaj K Praseedom, Andrew J Butler, Gavin J Pettigrew, and J Andrew Bradley. The discard of deceased donor kidneys in the uk. *Clinical transplantation*, 28(3):345–353, 2014.

[11] Sumit Mohan, Mariana C Chiles, Rachel E Patzer, Stephen O Pastan, S Ali Husain, Dustin J Carpenter, Geoffrey K Dube, R John Crew, Lloyd E Ratner, and David J Cohen. Factors leading to the discard of deceased donor kidneys in the united states. *Kidney international*, 94(1):187–198, 2018.

[12] Claudio Ponticelli. Ischaemia-reperfusion injury: a major protagonist in kidney transplantation. *Nephrology Dialysis Transplantation*, 29(6):1134–1140, 2013.

[13] Borja Ibanez, Gerd Heusch, Michel Ovize, and Frans Van de Werf. Evolving therapies for myocardial ischemia/reperfusion injury. *Journal of the American College of Cardiology*, 65(14):1454–1471, 2015.

[14] Edward T Chouchani, Victoria R Pell, Edoardo Gaude, Dunja Aksentijević, Stephanie Y Sundier, Ellen L Robb, Angela Logan, Sergiy M Nadtochiy, Emily NJ Ord, Anthony C Smith, et al. Ischaemic accumulation of succinate controls reperfusion injury through mitochondrial ros. *Nature*, 515(7527):431, 2014.

[15] Edward T Chouchani, Victoria R Pell, Andrew M James, Lorraine M Work, Kourosh Saeb-Parsy, Christian Frezza, Thomas Krieg, and Michael P Murphy. A unifying mechanism for mitochondrial superoxide production during ischemia-reperfusion injury. *Cell metabolism*, 23(2):254–263, 2016.

[16] Holger K Eltzschig and Tobias Eckle. Ischemia and reperfusion—from mechanism to translation. *Nature medicine*, 17(11):1391, 2011.

[17] Michael P Murphy and Richard C Hartley. Mitochondria as a therapeutic target for common pathologies. *Nature Reviews Drug Discovery*, 17(12):865, 2018.

[18] Derek J Hausenloy and Derek M Yellon. Myocardial ischemia-reperfusion injury: a neglected therapeutic target. *The Journal of clinical investigation*, 123(1):92–100, 2013.

[19] Derek M Yellon and Derek J Hausenloy. Myocardial reperfusion injury. *New England Journal of Medicine*, 357(11):1121–1135, 2007.

[20] Thomas H Sanderson, Christian A Reynolds, Rita Kumar, Karin Przyklenk, and Maik Hüttemann. Molecular mechanisms of ischemia–reperfusion injury in brain: pivotal role of the mitochondrial membrane potential in reactive oxygen species generation. *Molecular neurobiology*, 47(1):9–23, 2013.

[21] Edward J Lesnefsky, Qun Chen, Bernard Tandler, and Charles L Hoppel. Mitochondrial dysfunction and myocardial ischemia-reperfusion: implications for novel therapies. *Annual review of pharmacology and toxicology*, 57:535–565, 2017.

[22] May Nour, Fabien Scalzo, and David S Liebeskind. Ischemia-reperfusion injury in stroke. *Interventional neurology*, 1(3-4):185–199, 2012.

[23] Victoria R Pell, Edward T Chouchani, Christian Frezza, Michael P Murphy, and Thomas Krieg. Succinate metabolism: a new therapeutic target for myocardial reperfusion injury. *Cardiovascular Research*, 111(2):134–141, 2016.

[24] Nicole M Valenzuela and Elaine F Reed. Antibody-mediated rejection across solid organ transplants: manifestations, mechanisms, and therapies. *The Journal of clinical investigation*, 127(7):2492–2504, 2017.

[25] Jamie L Todd and Scott M Palmer. Danger signals in regulating the immune response to solid organ transplantation. *The Journal of clinical investigation*, 127(7):2464–2472, 2017.

[26] Faouzi Braza, Sophie Brouard, Steve Chadban, and Daniel R Goldstein. Role of tlrs and damps in allograft inflammation and transplant outcomes. *Nature Reviews Nephrology*, 12(5):281, 2016.

[27] Maurizio Salvadori, Giuseppina Rosso, and Elisabetta Bertoni. Update on ischemia-reperfusion injury in kidney transplantation: Pathogenesis and treatment. *World journal of transplantation*, 5(2):52, 2015.

[28] LH Opie. Acute metabolic response in myocardial infarction. *Heart*, 33(Suppl):129–137, 1971.

[29] Gary J Grover, Karnail S Atwal, Paul G Sleph, Feng-Li Wang, Hossain Monshizadegan, Thomas Monticello, and David W Green. Excessive atp hydrolysis in ischemic myocardium by mitochondrial f1f0-atpase: effect of selective pharmacological inhibition of mitochondrial atpase hydrolase activity. *American Journal of Physiology-Heart and Circulatory Physiology*, 287(4):H1747–H1755, 2004.

[30] Catia Barsotti and Piero L Ipata. Metabolic regulation of atp breakdown and of adenosine production in rat brain extracts. *The international journal of biochemistry & cell biology*, 36(11):2214–2225, 2004.

[31] Morris Karmazyn. The role of the myocardial sodium-hydrogen exchanger in mediating ischemic and reperfusion injury: From amiloride to cariporide a. *Annals of the New York Academy of Sciences*, 874(1):326–334, 1999.

[32] C Steenbergen, TA Fralix, and E Murphy. Role of increased cytosolic free calcium concentration in myocardial ischemic injury. *Basic research in cardiology*, 88(5):456–470, 1993.

[33] Elizabeth Murphy and Charles Steenbergen. Mechanisms underlying acute protection from cardiac ischemia-reperfusion injury. *Physiological reviews*, 88(2):581–609, 2008.

[34] Rex L Jamison. The role of cellular swelling in the pathogenesis of organ ischemia. *Western Journal of Medicine*, 120(3):205, 1974.

[35] Edgardo E Guibert, Alexander Y Petrenko, Cecilia L Balaban, Alexander Y Somov, Joaquín V Rodriguez, and Barry J Fuller. Organ preservation: current concepts and new strategies for the next decade. *Transfusion Medicine and Hemotherapy*, 38(2):125–142, 2011.

[36] CJE Watson and JH Dark. Organ transplantation: historical perspective and current practice. *British journal of anaesthesia*, 108(suppl_1):i29–i42, 2012.

[37] Patricia M Schulte. The effects of temperature on aerobic metabolism: towards a mechanistic understanding of the responses of ectotherms to a changing environment. *Journal of Experimental Biology*, 218(12):1856–1866, 2015.

[38] Xin Pan, Jie Liu, Tiffany Nguyen, Chengyu Liu, Junhui Sun, Yanjie Teng, Maria M Fergusson, Ilsa I Rovira, Michele Allen, Danielle A Springer, et al. The physiological role of mitochondrial calcium revealed by mice lacking the mitochondrial calcium uniporter. *Nature cell biology*, 15(12):1464, 2013.

[39] D Neil Granger and Peter R Kvietys. Reperfusion injury and reactive oxygen species: the evolution of a concept. *Redox biology*, 6:524–551, 2015.

[40] Elinor J Griffiths and Andrew P Halestrap. Mitochondrial non-specific pores remain closed during cardiac ischaemia, but open upon reperfusion. *Biochemical Journal*, 307(1):93–98, 1995.

[41] JJ Lemasters, JM Bond, E Chacon, IS Harper, SH Kaplan, H Ohata, DR Trollinger, B Herman, and WE Cascio. The ph paradox in ischemia-reperfusion injury to cardiac myocytes. In *Myocardial Ischemia: Mechanisms, Reperfusion, Protection*, pages 99–114. Springer, 1996.

[42] Christopher P Baines, Robert A Kaiser, Nicole H Purcell, N Scott Blair, Hanna Osinska, Michael A Hambleton, Eric W Brunskill, M Richard Sayen, Roberta A Gottlieb, Gerald W Dorn, et al. Loss of cyclophilin d reveals a critical role for mitochondrial permeability transition in cell death. *Nature*, 434(7033):658, 2005.

[43] Sang-Bing Ong, Parisa Samangouei, Siavash Beikoghli Kalkhoran, and Derek J Hausenloy. The mitochondrial permeability transition pore and its role in myocardial ischemia reperfusion injury. *Journal of molecular and cellular cardiology*, 78:23–34, 2015.

[44] Paolo Bernardi and Fabio Di Lisa. The mitochondrial permeability transition pore: molecular nature and role as a target in cardioprotection. *Journal of molecular and cellular cardiology*, 78:100–106, 2015.

[45] Martin Crompton. The mitochondrial permeability transition pore and its role in cell death. *Biochemical journal*, 341(2):233–249, 1999.

[46] Frank Eefting, Benno Rensing, Jochem Wigman, Willem Jan Pannekoek, Wai Ming Liu, Maarten Jan Cramer, Daniel J Lips, and Pieter A Doevendans. Role of apoptosis in reperfusion injury. *Cardiovascular Research*, 61(3):414–426, 2004.

[47] Stefan W Ryter, Hong Pyo Kim, Alexander Hoetzel, Jeong W Park, Kiichi Nakahira, Xue Wang, and Augustine MK Choi. Mechanisms of cell death in oxidative stress. *Antioxidants & redox signaling*, 9(1):49–89, 2007.

[48] A Phillip West and Gerald S Shadel. Mitochondrial dna in innate immune responses and inflammatory pathology. *Nature Reviews Immunology*, 17(6):363, 2017.

[49] Jack L Martin, Anja V Gruszczyk, Timothy E Beach, Michael P Murphy, and Kourosh Saeb-Parsy. Mitochondrial mechanisms and therapeutics in ischaemia reperfusion injury. *Pediatric Nephrology*, 34(7):1167–1174, 2019.

[50] Jeremy S Leventhal and Bernd Schröppel. Toll-like receptors in transplantation: sensing and reacting to injury. *Kidney international*, 81(9):826–832, 2012.

[51] Keir Pittman and Paul Kubes. Damage-associated molecular patterns control neutrophil recruitment. *Journal of innate immunity*, 5(4):315–323, 2013.

[52] Daniel N Mori, Daniel Kreisel, James N Fullerton, Derek W Gilroy, and Daniel R Goldstein. Inflammatory triggers of acute rejection of organ allografts. *Immunological reviews*, 258(1):132–144, 2014.

[53] Fadi G Lakkis. Where is the alloimmune response initiated? *American Journal of Transplantation*, 3(3):241–242, 2003.

[54] Pippa Bailey, Anusha Edwards, and Aisling E Courtney. Living kidney donation. *BMJ*, 354, 2016.

[55] Rachel J Johnson, Joanne E Allen, Susan V Fuggle, J Andrew Bradley, Chris Rudge, et al. Early experience of paired living kidney donation in the united kingdom. *Transplantation*, 86(12):1672–1677, 2008.

[56] John Oram and Paul Murphy. Diagnosis of death. *Continuing Education in Anaesthesia, Critical Care & Pain*, 11(3):77–81, 2011.

[57] EM Bos, HGD Leuvenink, H Van Goor, and RJ Ploeg. Kidney grafts from brain dead donors: Inferior quality or opportunity for improvement? *Kidney international*, 72(7):797–805, 2007.

[58] Paul I Terasaki, J Michael Cecka, David W Gjertson, and Steven Takemoto. High survival rates of kidney transplants from spousal and living unrelated donors. *New England Journal of Medicine*, 333(6):333–336, 1995.

[59] JI Roodnat, IC Van Riemsdijk, PGH Mulder, I Doxiadis, FHJ Claas, JNM Ijzermans, T van Gelder, and W Weimar. The superior results of living-donor renal transplantation are not completely caused by selection or short cold ischemia time: a single-center, multivariate analysis. *Transplantation*, 75(12):2014–2018, 2003.

[60] Welmoet H Westendorp, Henri G Leuvenink, and Rutger J Ploeg. Brain death induced renal injury. *Current opinion in organ transplantation*, 16(2):151–156, 2011.

[61] Ryan P Watts, Ogilvie Thom, and John F Fraser. Inflammatory signalling associated with brain dead organ donation: from brain injury to brain stem death and posttransplant ischaemia reperfusion injury. *Journal of transplantation*, 2013, 2013.

[62] D Novitzky. Detrimental effects of brain death on the potential organ donor. In *Transplantation proceedings*, volume 29, pages 3770–3772. Elsevier, 1997.

[63] JAB Van der Hoeven, S Lindell, R Van Schilfgaarde, G Molema, GJ Ter Horst, JH Southard, and RJ Ploeg. Donor brain death reduces survival after transplantation in rat livers preserved for 20 hr1. *Transplantation*, 72(10):1632–1636, 2001.

[64] J Pratschke, MJ Wilhelm, M Kusaka, M Basker, DKC Cooper, WW Hancock, and NL Tilney. Brain death and its influence on donor organ quality and outcome after transplantation1. *Transplantation*, 67(3):343–348, 1999.

[65] Dominic M Summers, Rachel J Johnson, Joanne Allen, Susan V Fuggle, David Collett, Christopher J Watson, and J Andrew Bradley. Analysis of factors that affect outcome after transplantation of kidneys donated after cardiac death in the uk: a cohort study. *The Lancet*, 376(9749):1303–1311, 2010.

[66] JE Locke, DL Segev, DS Warren, F Dominici, CE Simpkins, and RA Montgomery. Outcomes of kidneys from donors after cardiac death: implications for allocation and preservation. *American journal of transplantation*, 7(7):1797–1807, 2007.

[67] NHS Blood and Transplant. National standards for organ retrival from deceased donors. *Available from: https://bts.org.uk/operational-guidelines/*, 2012.

[68] AWN Reid, Simon Harper, Chris H Jackson, AC Wells, DM Summers, O Gjorgjimajkoska, LD Sharples, JA Bradley, and GJ Pettigrew. Expansion of the kidney donor pool by using cardiac death donors with prolonged time to cardiorespiratory arrest. *American journal of transplantation*, 11(5):995–1005, 2011.

[69] Friedrich K Port, Jennifer L Bragg-Gresham, Robert A Metzger, Dawn M Dykstra, Brenda W Gillespie, Eric W Young, Francis L Delmonico, James J Wynn, Robert M Merion, Robert A Wolfe, et al. Donor characteristics associated with reduced graft survival: an approach to expanding the pool of kidney donors1. *Transplantation*, 74(9):1281–1286, 2002.

[70] Christopher JE Watson, Rachel J Johnson, Rhiannon Birch, Dave Collett, and J Andrew Bradley. A simplified donor risk index for predicting outcome after deceased donor kidney transplantation. *Transplantation*, 93(3):314–318, 2012.

[71] Andrew Siedlecki, William Irish, and Daniel C Brennan. Delayed graft function in the kidney transplant. *American journal of transplantation*, 11(11):2279–2296, 2011.

[72] SK Singh and SJ Kim. Does expanded criteria donor status modify the outcomes of kidney transplantation from donors after cardiac death? *American Journal of Transplantation*, 13(2):329–336, 2013.

[73] James F Gillooly, James H Brown, Geoffrey B West, Van M Savage, and Eric L Charnov. Effects of size and temperature on metabolic rate. *science*, 293(5538):2248–2251, 2001.

[74] LK Kayler, TR Srinivas, and JD Schold. Influence of cit-induced dgf on kidney transplant outcomes. *American Journal of Transplantation*, 11(12):2657–2664, 2011.

[75] Gerhard Opelz and Bernd Döhler. Multicenter analysis of kidney preservation. *Transplantation*, 83(3):247–253, 2007.

[76] J Adam van der Vliet, Michiel C Warlé, CL Sarah Cheung, Steven Teerenstra, and Andries J Hoitsma. Influence of prolonged cold ischemia in renal transplantation. *Clinical transplantation*, 25(6):E612–E616, 2011.

[77] LK Kayler, J Magliocca, I Zendejas, TR Srinivas, and JD Schold. Impact of cold ischemia time on graft survival among ecd transplant recipients: a paired kidney analysis. *American journal of transplantation*, 11(12):2647–2656, 2011.

[78] Olivier Aubert, Nassim Kamar, Dewi Vernerey, Denis Viglietti, Frank Martinez, Jean-Paul Duong-Van-Huyen, Dominique Eladari, Jean-Philippe Empana, Marion Rabant, Jerome Verine, et al. Long term outcomes of transplantation using kidneys from expanded criteria donors: prospective, population based cohort study. *bmj*, 351:h3557, 2015.

[79] Agnes Debout, Yohann Foucher, Katy Trébern-Launay, Christophe Legendre, Henri Kreis, Georges Mourad, Valérie Garrigue, Emmanuel Morelon, Fanny Buron, Lionel Rostaing, et al. Each additional hour of cold ischemia time significantly increases the risk of graft failure and mortality following renal transplantation. *Kidney international*, 87(2):343–349, 2015.

[80] J Nath, J Hodson, SW Canbilen, J Al Shakarchi, NG Inston, A Sharif, and AR Ready. Effect of cold ischaemia time on outcome after living donor renal transplantation. *British Journal of Surgery*, 103(9):1230–1236, 2016.

[81] Benoît Feuillu, Luc Cormier, Luc Frimat, Michele Kessler, Mohamed Amrani, Philippe Mangin, and Jacques Hubert. Kidney warming during transplantation. *Transplant international*, 16(5):307–312, 2003.

[82] L Heylen, M Naesens, I Jochmans, D Monbaliu, E Lerut, K Claes, S Heye, P Verhamme, W Coosemans, B Bammens, et al. The effect of anastomosis time on outcome in recipients of kidneys donated after brain death: a cohort study. *American Journal of Transplantation*, 15(11):2900–2907, 2015.

[83] Karim Marzouk, Joseph Lawen, Ian Alwayn, and Bryce A Kiberd. The impact of vascular anastomosis time on early kidney transplant outcomes. *Transplantation research*, 2(1):8, 2013.

[84] Line Heylen, Jacques Pirenne, Undine Samuel, Ineke Tieken, Maarten Naesens, Ben Sprangers, and Ina Jochmans. The impact of anastomosis time during kidney transplantation on graft loss: a eurotransplant cohort study. *American journal of transplantation*, 17(3):724–732, 2017.

[85] Annemarie Weissenbacher, Rupert Oberhuber, Benno Cardini, Sascha Weiss, Hanno Ulmer, Claudia Bösmüller, Stefan Schneeberger, Johann Pratschke, and Robert Öllinger. The faster the better: anastomosis time influences patient survival after deceased donor kidney transplantation. *Transplant International*, 28(5):535–543, 2015.

[86] Karthik K Tennankore, S Joseph Kim, Ian PJ Alwayn, and Bryce A Kiberd. Prolonged warm ischemia time is associated with graft failure and mortality after kidney transplantation. *Kidney international*, 89(3):648–658, 2016.

[87] D Kamińska, K Kościelska-Kasprzak, P Chudoba, and M Klinger. Kidney injury due to warm ischemia during transplantation can be reduced. *American Journal of Transplantation*, 16(5):1639–1639, 2016.

[88] M Szostek, M Pacholczyk, B Łαgiewska, R Danielewicz, J Wałaszwski, and W Rowiński. Effective surface cooling of the kidney during vascular anastomosis decreases the risk of delayed kidney function after transplantation. *Transplant International*, 9:S84–S85, 1996.

[89] Bernd Schröppel and Christophe Legendre. Delayed kidney graft function: from mechanism to translation. *Kidney international*, 86(2):251–258, 2014.

[90] Mona D Doshi, Neha Garg, Peter P Reese, and Chirag R Parikh. Recipient risk factors associated with delayed graft function: a paired kidney analysis. *Transplantation*, 91(6):666–671, 2011.

[91] MO Hamed, Y Chen, L Pasea, CJ Watson, N Torpey, JA Bradley, G Pettigrew, and K Saeb-Parsy. Early graft loss after kidney transplantation: risk factors and consequences. *American Journal of Transplantation*, 15(6):1632–1643, 2015.

[92] Dermot H Mallon, Dominic M Summers, J Andrew Bradley, and Gavin J Pettigrew. Defining delayed graft function after renal transplantation: simplest is best. *Transplantation*, 96(10):885–889, 2013.

[93] Eric Lechevallier, Bertrand Dussol, Aline Luccioni, Xavier Thirion, Henri Vacher-Copomat, Khalil Jaber, Philippe Brunet, Françoise Leonetti, Olivier Lavelle, Christian Coulange, et al. Posttransplantation acute tubular necrosis: risk factors and implications for graft survival. *American journal of kidney diseases*, 32(6):984–991, 1998.

[94] Mondher Ounissi, Mejda Cherif, Taieb Ben Abdallah, Mongi Bacha, Hafedh Hedri, Ezzedine Abderrahim, Rym Goucha, Adel Kheder, Riadh Ben Slama, Amine Derouiche, et al. Risk factors and consequences of delayed graft function. *Saudi Journal of Kidney Diseases and Transplantation*, 24(2):243, 2013.

[95] Sri G Yarlagadda, Steven G Coca, Richard N Formica Jr, Emilio D Poggio, and Chirag R Parikh. Association between delayed graft function and allograft and patient survival: a systematic review and meta-analysis. *Nephrology dialysis transplantation*, 24(3):1039–1047, 2008.

[96] Tiffany J Zens, Juan S Danobeitia, Glen Leverson, Peter J Chlebeck, Laura J Zitur, Robert R Redfield, Anthony M D'Alessandro, Scott Odorico, Dixon B Kaufman, and Luis A Fernandez. The impact of kidney donor profile index on delayed graft function and transplant outcomes: A single-center analysis. *Clinical transplantation*, 32(3):e13190, 2018.

[97] Martin Chaumont, Judith Racapé, Nilufer Broeders, Fadoua El Mountahi, Annick Massart, Thomas Baudoux, Jean-Michel Hougardy, Dimitri Mikhalsky, Anwar Hamade, Alain Le Moine, et al. Delayed graft function in kidney transplants: time evolution, role of acute rejection, risk factors, and impact on patient and graft outcome. *Journal of transplantation*, 2015, 2015.

[98] Wai H Lim, David W Johnson, Armando Teixeira-Pinto, and Germaine Wong. Association between duration of delayed graft function, acute rejection, and allograft outcome after deceased donor kidney transplantation. *Transplantation*, 103(2):412–419, 2019.

[99] Deepa Jayaram, Mallika Kommareddi, Randall S Sung, and Fu L Luan. Delayed graft function requiring more than one-time dialysis treatment is associated with inferior clinical outcomes. *Clinical transplantation*, 26(5):E536–E543, 2012.

[100] Caitlyn Marek, Benjamin Thomson, Ahmed Shoker, Patrick P Luke, and Michael AJ Moser. The prognostic value of time needed on dialysis in patients with delayed graft function. *Nephrology dialysis transplantation*, 29(1):203–208, 2013.

[101] Tainá Veras de Sandes-Freitas, Cláudia Rosso Felipe, Wilson Ferreira Aguiar, Marina Pontello Cristelli, Helio Tedesco-Silva, and José Osmar Medina-Pestana. Prolonged delayed graft function is associated with inferior patient and kidney allograft survivals. *PLoS One*, 10(12):e0144188, 2015.

[102] Walter G Land. The role of postischemic reperfusion injury and other nonantigen-dependent inflammatory pathways in transplantation. *Transplantation*, 79(5):505–514, 2005.

[103] PF Halloran, J Homik, N Goes, SL Lui, J Urmson, V Ramassar, and SM Cockfield. The "injury response": a concept linking nonspecific injury, acute rejection, and long-term transplant outcomes. In *Transplantation proceedings*, volume 29, pages 79–81. Elsevier, 1997.

[104] Mollie Jurewicz, Ayumi Takakura, Andrea Augello, Said Movahedi Naini, Takaharu Ichimura, Kambiz Zandi-Nejad, and Reza Abdi. Ischemic injury enhances dendritic cell immunogenicity via tlr4 and nf-κb activation. *The Journal of Immunology*, 184(6):2939–2948, 2010.

[105] Miguel Ascon, Dolores B Ascon, Manchang Liu, Chris Cheadle, Chaitali Sarkar, Lorraine Racusen, Heitham T Hassoun, and Hamid Rabb. Renal ischemia-reperfusion leads to long term infiltration of activated and effector-memory t lymphocytes. *Kidney international*, 75(5):526–535, 2009.

[106] Richard Fuquay, Brandon Renner, Liudmila Kulik, James W McCullough, Claudia Amura, Derek Strassheim, Roberta Pelanda, Raul Torres, and Joshua M Thurman. Renal ischemia-reperfusion injury amplifies the humoral immune response. *Journal of the American Society of Nephrology*, 24(7):1063–1072, 2013.

[107] Hailin Zhao, Azeem Alam, Aurelie Pac Soo, Andrew JT George, and Daqing Ma. Ischemia-reperfusion injury reduces long term renal graft survival: mechanism and beyond. *EBioMedicine*, 28:31–42, 2018.

[108] Panduranga S Rao and Akinlolu Ojo. The alphabet soup of kidney transplantation: Scd, dcd, ecd—fundamentals for the practicing nephrologist. *Clinical Journal of the American Society of Nephrology*, 4(11):1827–1831, 2009.

[109] J Hassanzadeh, AA Hashiani, A Rajaeefard, H Salahi, E Khedmati, F Kakaei, S Nikeghbalian, and A Malek-Hossein. Long-term survival of living donor renal transplants: A single center study. *Indian journal of nephrology*, 20(4):179, 2010.

[110] Hannah Burton, Lydia Iyamu Perisanidou, Retha Steenkamp, Rebecca Evans, Lisa Mumford, Katharine M Evans, Fergus J Caskey, and Rachel Hilton. Causes of renal allograft failure in the uk: trends in uk renal registry and national health service blood and transplant data from 2000 to 2013. *Nephrology Dialysis Transplantation*, 34(2):355–364, 2018.

[111] Piergiorgio Messa, Claudio Ponticelli, and Luisa Berardinelli. Coming back to dialysis after kidney transplant failure. *Nephrology Dialysis Transplantation*, 23(9):2738–2742, 2008.

[112] D Ansell, UP Udayaraj, R Steenkamp, and CRK Dudley. Chronic renal failure in kidney transplant recipients. do they receive optimum care?: data from the uk renal registry. *American journal of transplantation*, 7(5):1167–1176, 2007.

[113] Lakhmir S Chawla, Paul W Eggers, Robert A Star, and Paul L Kimmel. Acute kidney injury and chronic kidney disease as interconnected syndromes. *New England Journal of Medicine*, 371(1):58–66, 2014.

[114] David A Ferenbach and Joseph V Bonventre. Mechanisms of maladaptive repair after aki leading to accelerated kidney ageing and ckd. *Nature Reviews Nephrology*, 11(5):264, 2015.

[115] Chunyuan Guo, Guie Dong, Xinling Liang, and Zheng Dong. Epigenetic regulation in aki and kidney repair: mechanisms and therapeutic implications. *Nature Reviews Nephrology*, page 1, 2019.

[116] Line Heylen, Bernard Thienpont, Maarten Naesens, Diether Lambrechts, and Ben Sprangers. The emerging role of dna methylation in kidney transplantation: a perspective. *American Journal of Transplantation*, 16(4):1070–1078, 2016.

[117] Gerhard R Situmorang and Neil S Sheerin. Ischaemia reperfusion injury: mechanisms of progression to chronic graft dysfunction. *Pediatric Nephrology*, 34(6):951–963, 2019.

[118] Rachel J Johnson, Susan V Fuggle, Lisa Mumford, J Andrew Bradley, John LR Forsythe, Chris J Rudge, Kidney Advisory Group of NHS Blood, Transplant, et al. A new uk 2006 national kidney allocation scheme for deceased heart-beating donor kidneys. *Transplantation*, 89(4):387–394, 2010.

[119] Craig J Taylor, Vasilis Kosmoliaptsis, Linda D Sharples, Davide Prezzi, C Helen Morgan, Timothy Key, Afzal N Chaudhry, Irum Amin, Menna R Clatworthy, Andrew J Butler, et al. Ten-year experience of selective omission of the pretransplant crossmatch test in deceased donor kidney transplantation. *Transplantation*, 89(2):185–193, 2010.

[120] Chris J Callaghan, Lisa Mumford, Laura Pankhurst, Richard J Baker, J Andrew Bradley, and Christopher JE Watson. Early outcomes of the new uk deceased donor kidney fast-track offering scheme. *Transplantation*, 101(12):2888–2897, 2017.

[121] Tanja C Saat, Eline K van den Akker, Jan NM IJzermans, Frank JMF Dor, and Ron WF de Bruin. Improving the outcome of kidney transplantation by ameliorating renal ischemia reperfusion injury: lost in translation? *Journal of translational medicine*, 14(1):20, 2016.

[122] Sarah Anne Hosgood, E Thompson, T Moore, CH Wilson, and Michael Lennard Nicholson. Normothermic machine perfusion for the assessment and transplantation of declined human kidneys from donation after circulatory death donors. *British Journal of Surgery*, 105(4):388–394, 2018.

[123] John OO Ayorinde, Dominic M Summers, Laura Pankhurst, Emma Laing, Alison J Deary, Karla Hemming, Edward CF Wilson, Victoria Bardsley, Desley A Neil, and Gavin J Pettigrew. Preimplantation trial of histopathology in renal allografts (pithia): a stepped-wedge cluster randomised controlled trial protocol. *BMJ open*, 9(1):e026166, 2019.

[124] Xinmiao Shi, Jicheng Lv, Wenke Han, Xuhui Zhong, Xinfang Xie, Baige Su, and Jie Ding. What is the impact of human leukocyte antigen mismatching on graft survival and mortality in renal transplantation? a meta-analysis of 23 cohort studies involving 486,608 recipients. *BMC nephrology*, 19(1):116, 2018.

[125] Chris Dudley and Paul Harden. Renal association clinical practice guideline on the assessment of the potential kidney transplant recipient. *Nephron*, 118:c209, 2011.

[126] Diana A Wu, Christopher J Watson, J Andrew Bradley, Rachel J Johnson, John L Forsythe, and Gabriel C Oniscu. Global trends and challenges in deceased donor kidney allocation. *Kidney international*, 91(6):1287–1299, 2017.

[127] Sarah A Hosgood, Bin Yang, Atul Bagul, Ismail H Mohamed, and Michael L Nicholson. A comparison of hypothermic machine perfusion versus static cold storage in an experimental model of renal ischemia reperfusion injury. *Transplantation*, 89(7):830–837, 2010.

[128] Cyril Moers, Jacqueline M Smits, Mark-Hugo J Maathuis, Jürgen Treckmann, Frank van Gelder, Bogdan P Napieralski, Margitta van Kasterop-Kutz, Jaap J Homan van der Heide, Jean-Paul Squifflet, Ernest van Heurn, et al. Machine perfusion or cold storage in deceased-donor kidney transplantation. *New England Journal of Medicine*, 360(1):7–19, 2009.

[129] Cyril Moers, Jacques Pirenne, Andreas Paul, and Rutger J. Ploeg. Machine perfusion or cold storage in deceased-donor kidney transplantation. *New England Journal of Medicine*, 366(8):770–771, 2012. PMID: 22356343.

[130] CJE Watson, AC Wells, RJ Roberts, JA Akoh, PJ Friend, M Akyol, FR Calder, JE Allen, MN Jones, D Collett, et al. Cold machine perfusion versus static cold storage of kidneys donated after cardiac death: a uk multicenter randomized controlled trial. *American Journal of Transplantation*, 10(9):1991–1999, 2010.

[131] Jürgen Treckmann, Cyril Moers, Jacqueline M Smits, Anja Gallinat, Mark-Hugo J Maathuis, Margitta van Kasterop-Kutz, Ina Jochmans, Jaap J Homan van der Heide, Jean-Paul Squifflet, Ernest Van Heurn, et al. Machine perfusion versus cold storage for preservation of kidneys from expanded criteria donors after brain death. *Transplant International*, 24(6):548–554, 2011.

[132] Samuel J Tingle, Rodrigo S Figueiredo, John AG Moir, Michael Goodfellow, David Talbot, and Colin H Wilson. Machine perfusion preservation versus static cold storage for deceased donor kidney transplantation. *Cochrane Database of Systematic Reviews*, (3), 2019.

[133] Ina Jochmans, John M O'Callaghan, Jacques Pirenne, and Rutger J Ploeg. Hypothermic machine perfusion of kidneys retrieved from standard and high-risk donors. *Transplant international*, 28(6):665–676, 2015.

[134] Franziska Alexandra Meister, Zoltan Czigany, Jan Bednarsch, Jörg Böcker, Iakovos Amygdalos, Daniel Antonio Morales Santana, Katharina Rietzler, Marcus Moeller, René Tolba, Peter Boor, et al. Hypothermic oxygenated machine perfusion of extended criteria kidney allografts from brain dead donors: Protocol for a prospective pilot study. *JMIR research protocols*, 8(10):e14622, 2019.

[135] Phillipp Dutkowski, James V Guarrera, Jeroen De Jonge, Paulo N Martins, Robert J Porte, and Pierre-Alain Clavien. Evolving trends in machine perfusion for liver transplantation. *Gastroenterology*, 156(6):1542–1547, 2019.

[136] Sarah A Hosgood, Ernest van Heurn, and Michael L Nicholson. Normothermic machine perfusion of the kidney: better conditioning and repair? *Transplant International*, 28(6):657–664, 2015.

[137] ML Nicholson and SA Hosgood. Renal transplantation after ex vivo normothermic perfusion: the first clinical study. *American Journal of Transplantation*, 13(5):1246–1252, 2013.

[138] David Nasralla, Constantin C Coussios, Hynek Mergental, M Zeeshan Akhtar, Andrew J Butler, Carlo DL Ceresa, Virginia Chiocchia, Susan J Dutton, Juan Carlos García-Valdecasas, Nigel Heaton, et al. A randomized trial of normothermic preservation in liver transplantation. *Nature*, 557(7703):50, 2018.

[139] Sarah A Hosgood, Kourosh Saeb-Parsy, Colin Wilson, Christopher Callaghan, Dave Collett, and Michael L Nicholson. Protocol of a randomised controlled, open-label trial of ex vivo normothermic perfusion versus static cold storage in donation after circulatory death renal transplantation. *BMJ open*, 7(1):e012237, 2017.

[140] Sarah Anne Hosgood, Kourosh Saeb-Parsy, MO Hamed, and Michael Lennard Nicholson. Successful transplantation of human kidneys deemed untransplantable but resuscitated by ex vivo normothermic machine perfusion. *American Journal of Transplantation*, 16(11):3282–3285, 2016.

[141] Benoit Barrou, Claire Billault, and Armelle Nicolas-Robin. The use of extracorporeal membranous oxygenation in donors after cardiac death. *Current opinion in organ transplantation*, 18(2):148–153, 2013.

[142] Ricard Valero, Catiana Cabrer, Frederic Oppenheimer, Esteve Trias, Jacinto Sánchez-Ibáñez, Francisco M De Cabo, Aurora Navarro, David Paredes, Antonio Alcaraz, Rafael Gutiérrez, et al. Normothermic recirculation reduces primary graft dysfunction of kidneys obtained from non-heart-beating donors. *Transplant international*, 13(4):303–310, 2000.

[143] Andrew J Butler, Lucy V Randle, and Christopher JE Watson. Normothermic regional perfusion for donation after circulatory death without prior heparinization. *Transplantation*, 97(12):1272–1278, 2014.

[144] GC Oniscu, LV Randle, P Muiesan, AJ Butler, IS Currie, MTPR Perera, JL Forsythe, and CJE Watson. In situ normothermic regional perfusion for controlled donation after circulatory death—the united kingdom experience. *American Journal of Transplantation*, 14(12):2846–2854, 2014.

[145] Stephen O'Neill and Gabriel C Oniscu. Donor pretreatment and machine perfusion: current views. *Current Opinion in Organ Transplantation*, 25(1):59–65, 2020.

[146] Andrew J Roger, Sergio A Muñoz-Gómez, and Ryoma Kamikawa. The origin and diversification of mitochondria. *Current Biology*, 27(21):R1177–R1192, 2017.

[147] Nick Lane and William Martin. The energetics of genome complexity. *Nature*, 467(7318):929, 2010.

[148] Payam A Gammage and Christian Frezza. Mitochondrial dna: the overlooked oncogenome? *BMC biology*, 17(1):53, 2019.

[149] Terrence G Frey and Carmen A Mannella. The internal structure of mitochondria. *Trends in biochemical sciences*, 25(7):319–324, 2000.

[150] Nikolaus Pfanner, Bettina Warscheid, and Nils Wiedemann. Mitochondrial proteins: from biogenesis to functional networks. *Nature Reviews Molecular Cell Biology*, 20(5):267–284, 2019.

[151] Michael W Gray, Gertraud Burger, and B Franz Lang. Mitochondrial evolution. *Science*, 283(5407):1476–1481, 1999.

[152] Varda Shoshan-Barmatz, Vito De Pinto, Markus Zweckstetter, Ziv Raviv, Nurit Keinan, and Nir Arbel. Vdac, a multi-functional mitochondrial protein regulating cell life and death. *Molecular aspects of medicine*, 31(3):227–285, 2010.

[153] Nils Wiedemann, Ann E Frazier, and Nikolaus Pfanner. The protein import machinery of mitochondria. *Journal of Biological Chemistry*, 279(15):14473–14476, 2004.

[154] Edmund RS Kunji. The role and structure of mitochondrial carriers. *FEBS letters*, 564(3):239–244, 2004.

[155] Nils Wiedemann and Nikolaus Pfanner. Mitochondrial machineries for protein import and assembly. *Annual review of biochemistry*, 86:685–714, 2017.

[156] Christof Osman, Mathias Haag, Christoph Potting, Jonathan Rodenfels, Phat Vinh Dip, Felix T Wieland, Britta Brügger, Benedikt Westermann, and Thomas Langer. The genetic interactome of prohibitins: coordinated control of cardiolipin and phosphatidylethanolamine by conserved regulators in mitochondria. *The Journal of cell biology*, 184(4):583–596, 2009.

[157] Nadia Terziyska, Thomas Lutz, Christian Kozany, Dejana Mokranjac, Nikola Mesecke, Walter Neupert, Johannes M Herrmann, and Kai Hell. Mia40, a novel factor for protein import into the intermembrane space of mitochondria is able to bind metal ions. *FEBS letters*, 579(1):179–184, 2005.

[158] Werner Kühlbrandt. Structure and function of mitochondrial membrane protein complexes. *BMC biology*, 13(1):89, 2015.

[159] Jonathan R Friedman and Jodi Nunnari. Mitochondrial form and function. *Nature*, 505(7483):335, 2014.

[160] Timothy Wai and Thomas Langer. Mitochondrial dynamics and metabolic regulation. *Trends in Endocrinology & Metabolism*, 27(2):105–117, 2016.

[161] Akinori Eiyama and Koji Okamoto. Pink1/parkin-mediated mitophagy in mammalian cells. *Current opinion in cell biology*, 33:95–101, 2015.

[162] Marc Liesa and Orian S Shirihai. Mitochondrial dynamics in the regulation of nutrient utilization and energy expenditure. *Cell metabolism*, 17(4):491–506, 2013.

[163] Leonid A Sazanov. A giant molecular proton pump: structure and mechanism of respiratory complex i. *Nature Reviews Molecular Cell Biology*, 16(6):375, 2015.

[164] Dylan G Ryan, Michael P Murphy, Christian Frezza, Hiran A Prag, Edward T Chouchani, Luke A O'Neill, and Evanna L Mills. Coupling krebs cycle metabolites to signalling in immunity and cancer. *Nature metabolism*, 1(1):16, 2019.

[165] Fei Sun, Xia Huo, Yujia Zhai, Aojin Wang, Jianxing Xu, Dan Su, Mark Bartlam, and Zihe Rao. Crystal structure of mitochondrial respiratory membrane protein complex ii. *Cell*, 121(7):1043–1057, 2005.

[166] Joseph J Braymer and Roland Lill. Iron–sulfur cluster biogenesis and trafficking in mitochondria. *Journal of Biological Chemistry*, 292(31):12754–12763, 2017.

[167] Alexander Galkin, Stefan Dröse, and Ulrich Brandt. The proton pumping stoichiometry of purified mitochondrial complex i reconstituted into proteoliposomes. *Biochimica et Biophysica Acta (BBA)-Bioenergetics*, 1757(12):1575–1581, 2006.

[168] Ian N Watt, Martin G Montgomery, Michael J Runswick, Andrew GW Leslie, and John E Walker. Bioenergetic cost of making an adenosine triphosphate molecule in animal mitochondria. *Proceedings of the National Academy of Sciences*, 107(39):16823–16827, 2010.

[169] Pallavi Bhargava and Rick G Schnellmann. Mitochondrial energetics in the kidney. *Nature Reviews Nephrology*, 13(10):629, 2017.

[170] Joseph V Bonventre and Li Yang. Cellular pathophysiology of ischemic acute kidney injury. *The Journal of clinical investigation*, 121(11):4210–4221, 2011.

[171] Josephine M Forbes and David R Thorburn. Mitochondrial dysfunction in diabetic kidney disease. *Nature Reviews Nephrology*, 14(5):291, 2018.

[172] Thomas P Keeley and Giovanni E Mann. Defining physiological normoxia for improved translation of cell physiology to animal models and humans. *Physiological Reviews*, 99(1):161–234, 2018.

[173] Paul M O'Connor, Warwick P Anderson, Michelle M Kett, and Roger G Evans. Renal preglomerular arterial–venous o2 shunting is a structural anti-oxidant defence mechanism of the renal cortex. *Clinical and experimental pharmacology and physiology*, 33(7):637–641, 2006.

[174] Andrey Y Abramov, Antonella Scorziello, and Michael R Duchen. Three distinct mechanisms generate oxygen free radicals in neurons and contribute to cell death during anoxia and reoxygenation. *Journal of Neuroscience*, 27(5):1129–1138, 2007.

[175] Jimmy Zhang, Yves T Wang, James H Miller, Mary M Day, Joshua C Munger, and Paul S Brookes. Accumulation of succinate in cardiac ischemia primarily occurs via canonical krebs cycle activity. *Cell reports*, 23(9):2617–2628, 2018.

[176] Qun Chen, Shadi Moghaddas, Charles L Hoppel, and Edward J Lesnefsky. Reversible blockade of electron transport during ischemia protects mitochondria and decreases myocardial injury following reperfusion. *Journal of Pharmacology and Experimental Therapeutics*, 319(3):1405–1412, 2006.

[177] Michael P Murphy. How mitochondria produce reactive oxygen species. *Biochemical journal*, 417(1):1–13, 2009.

[178] Joe M McCord. Oxygen-derived free radicals in postischemic tissue injury. *New England Journal of Medicine*, 312(3):159–163, 1985.

[179] Karen Bedard and Karl-Heinz Krause. The nox family of ros-generating nadph oxidases: physiology and pathophysiology. *Physiological reviews*, 87(1):245–313, 2007.

[180] Paul D Ray, Bo-Wen Huang, and Yoshiaki Tsuji. Reactive oxygen species (ros) homeostasis and redox regulation in cellular signaling. *Cellular signalling*, 24(5):981–990, 2012.

[181] Laura A Sena and Navdeep S Chandel. Physiological roles of mitochondrial reactive oxygen species. *Molecular cell*, 48(2):158–167, 2012.

[182] Giang T Nguyen, Erin R Green, and Joan Mecsas. Neutrophils to the roscue: mechanisms of nadph oxidase activation and bacterial resistance. *Frontiers in cellular and infection microbiology*, 7:373, 2017.

[183] Christine C Winterbourn. Reconciling the chemistry and biology of reactive oxygen species. *Nature chemical biology*, 4(5):278, 2008.

[184] Christine C Winterbourn. The biological chemistry of hydrogen peroxide. In *Methods in enzymology*, volume 528, pages 3–25. Elsevier, 2013.

[185] Esra Birben, Umit Murat Sahiner, Cansin Sackesen, Serpil Erzurum, and Omer Kalayci. Oxidative stress and antioxidant defense. *World Allergy Organization Journal*, 5(1):9, 2012.

[186] Michael P Murphy. Mitochondrial thiols in antioxidant protection and redox signaling: distinct roles for glutathionylation and other thiol modifications. *Antioxidants & redox signaling*, 16(6):476–495, 2012.

[187] Kira M Holmström and Toren Finkel. Cellular mechanisms and physiological consequences of redox-dependent signalling. *Nature reviews Molecular cell biology*, 15(6):411, 2014.

[188] Yuliya Mikhed, Andreas Daiber, and Sebastian Steven. Mitochondrial oxidative stress, mitochondrial dna damage and their role in age-related vascular dysfunction. *International journal of molecular sciences*, 16(7):15918–15953, 2015.

[189] Günther Daum. Lipids of mitochondria. *Biochimica et Biophysica Acta (BBA)-Reviews on Biomembranes*, 822(1):1–42, 1985.

[190] Ethan J Anderson, Lalage A Katunga, and Monte S Willis. Mitochondria as a source and target of lipid peroxidation products in healthy and diseased heart. *Clinical and Experimental Pharmacology and Physiology*, 39(2):179–193, 2012.

[191] Daniela Weber, Michael J Davies, and Tilman Grune. Determination of protein carbonyls in plasma, cell extracts, tissue homogenates, isolated proteins: focus on sample preparation and derivatization conditions. *Redox biology*, 5:367–380, 2015.

[192] Barbara S Berlett and Earl R Stadtman. Protein oxidation in aging, disease, and oxidative stress. *Journal of Biological Chemistry*, 272(33):20313–20316, 1997.

[193] Jack L Martin, Ana SH Costa, Anja V Gruszczyk, Timothy E Beach, Fay M Allen, Hiran A Prag, Elizabeth C Hinchy, Krishnaa Mahbubani, Mazin Hamed, Laura Tronci, et al. Succinate accumulation drives ischaemia-reperfusion injury during organ transplantation. *Nature Metabolism*, pages 1–9, 2019.

[194] Laura Valls-Lacalle, Ignasi Barba, Elisabet Miro-Casas, Juan José Alburquerque-Béjar, Marisol Ruiz-Meana, Marina Fuertes-Agudo, Antonio Rodríguez-Sinovas, and David García-Dorado. Succinate dehydrogenase inhibition with malonate during reperfusion reduces infarct size by preventing mitochondrial permeability transition. *Cardiovascular research*, 109(3):374–384, 2015.

[195] Laura Valls-Lacalle, Ignasi Barba, Elisabet Miró-Casas, Marisol Ruiz-Meana, Antonio Rodríguez-Sinovas, and David García-Dorado. Selective inhibition of succinate dehydrogenase in reperfused myocardium with intracoronary malonate reduces infarct size. *Scientific reports*, 8(1):2442, 2018.

[196] Edward J Lesnefsky, Qun Chen, Shadi Moghaddas, Medhat O Hassan, Bernard Tandler, and Charles L Hoppel. Blockade of electron transport during ischemia protects cardiac mitochondria. *Journal of Biological Chemistry*, 279(46):47961–47967, 2004.

[197] Marion Babot, Amanda Birch, Paola Labarbuta, and Alexander Galkin. Characterisation of the active/de-active transition of mitochondrial complex i. *Biochimica et Biophysica Acta (BBA)-Bioenergetics*, 1837(7):1083–1092, 2014.

[198] Edward T Chouchani, Carmen Methner, Sergiy M Nadtochiy, Angela Logan, Victoria R Pell, Shujing Ding, Andrew M James, Helena M Cochemé, Johannes Reinhold, Kathryn S Lilley, et al. Cardioprotection by s-nitrosation of a cysteine switch on mitochondrial complex i. *Nature medicine*, 19(6):753, 2013.

[199] Robin AJ Smith, Richard C Hartley, Helena M Cocheme, and Michael P Murphy. Mitochondrial pharmacology. *Trends in pharmacological sciences*, 33(6):341–352, 2012.

[200] Michael P Murphy. Understanding and preventing mitochondrial oxidative damage. *Biochemical Society Transactions*, 44(5):1219–1226, 2016.

[201] Victoria J Adlam, Joanne C Harrison, Carolyn M Porteous, Andrew M James, Robin AJ Smith, Michael P Murphy, and Ivan A Sammut. Targeting an antioxidant to mitochondria decreases cardiac ischemia-reperfusion injury. *The FASEB Journal*, 19(9):1088–1095, 2005.

[202] Anna J Dare, Eleanor A Bolton, Gavin J Pettigrew, J Andrew Bradley, Kourosh Saeb-Parsy, and Michael P Murphy. Protection against renal ischemia–reperfusion injury in vivo by the mitochondria targeted antioxidant mitoq. *Redox biology*, 5:163–168, 2015.

[203] Anna J Dare, Angela Logan, Tracy A Prime, Sebastian Rogatti, Martin Goddard, Eleanor M Bolton, J Andrew Bradley, Gavin J Pettigrew, Michael P Murphy, and Kourosh Saeb-Parsy. The mitochondria-targeted anti-oxidant mitoq decreases ischemia-reperfusion injury in a murine syngeneic heart transplant model. *The Journal of Heart and Lung Transplantation*, 34(11):1471–1480, 2015.

[204] Alexander B Kotlyar and Andrei D Vinogradov. Interaction of the membrane-bound succinate dehydrogenase with substrate and competitive inhibitors. *Biochimica et Biophysica Acta (BBA)-Protein Structure and Molecular Enzymology*, 784(1):24–34, 1984.

[205] Anna Stepanova, Yevgeniya Shurubor, Federica Valsecchi, Giovanni Manfredi, and Alexander Galkin. Differential susceptibility of mitochondrial complex ii to inhibition by oxaloacetate in brain and heart. *Biochimica et Biophysica Acta (BBA)-Bioenergetics*, 1857(9):1561–1568, 2016.

[206] Leslie Hellerman, Oscar K Reiss, SS Parmar, John Wein, NL Lasser, et al. Studies on succinate dehydrogenase. effect of monoethyl oxaloacetate, acetylene dicarboxylate, and thyroxine. *Journal of Biological Chemistry*, 235(8):2468–2474, 1960.

[207] Jiri Neuzil, Jeffrey C Dyason, Ruth Freeman, Lan-Feng Dong, Lubomir Prochazka, Xiu-Fang Wang, Immo Scheffler, and Stephen J Ralph. Mitocans as anti-cancer agents targeting mitochondria: lessons from studies with vitamin e analogues, inhibitors of complex ii. *Journal of bioenergetics and biomembranes*, 39(1):65–72, 2007.

[208] Hezhen Wang, Bader Huwaimel, Kshitij Verma, James Miller, Todd M Germain, Nihar Kinarivala, Dimitri Pappas, Paul S Brookes, and Paul C Trippier. Synthesis and antineoplastic evaluation of mitochondrial complex ii (succinate dehydrogenase) inhibitors derived from atpenin a5. *ChemMedChem*, 12(13):1033–1044, 2017.

[209] Caitlyn E Bowman, Susana Rodriguez, Ebru S Selen Alpergin, Michelle G Acoba, Liang Zhao, Thomas Hartung, Steven M Claypool, Paul A Watkins, and Michael J Wolfgang. The mammalian malonyl-coa synthetase acsf3 is required for mitochondrial protein malonylation and metabolic efficiency. *Cell chemical biology*, 24(6):673–684, 2017.

[210] Jia Yin and Joanne Wang. Renal drug transporters and their significance in drug–drug interactions. *Acta Pharmaceutica Sinica B*, 6(5):363–373, 2016.

[211] Jarkko Rautio, Nicholas A Meanwell, Li Di, and Michael J Hageman. The expanding role of prodrugs in contemporary drug design and development. *Nature Reviews Drug Discovery*, 17(8):559, 2018.

[212] M Jason Hatfield, Robyn A Umans, Janice L Hyatt, Carol C Edwards, Monika Wierdl, Lyudmila Tsurkan, Michael R Taylor, and Philip M Potter. Carboxylesterases: General detoxifying enzymes. *Chemico-biological interactions*, 259:327–331, 2016.

[213] Earl W Morgan, BF Yan, Denise Greenway, Dennis R Petersen, and Andrew Parkinson. Purification and characterization of two rat-liver microsomal carboxylesterases (hydrolase a and b). *Archives of biochemistry and biophysics*, 315(2):495–512, 1994.

[214] Tetsuo Satoh and Masakiyo Hosokawa. Structure, function and regulation of carboxylesterases. *Chemico-biological interactions*, 162(3):195–211, 2006.

[215] Rolf Mentlein, Hella Rix-Matzen, and Eberhard Heymann. Subcellular localization of non-specific carboxylesterases, acylcarnitine hydrolase, monoacylglycerol lipase and palmitoyl-coa hydrolase in rat liver. *Biochimica et Biophysica Acta (BBA)-General Subjects*, 964(3):319–328, 1988.

[216] MF Ross, GF Kelso, FH Blaikie, AM James, HM Cocheme, A Filipovska, Tatiana Da Ros, TR Hurd, RAJ Smith, and MP Murphy. Lipophilic triphenylphosphonium cations as tools in mitochondrial bioenergetics and free radical biology. *Biochemistry (Moscow)*, 70(2):222–230, 2005.

[217] Jens Ripcke, Kim Zarse, Michael Ristow, and Marc Birringer. Small-molecule targeting of the mitochondrial compartment with an endogenously cleaved reversible tag. *Chembiochem*, 10(10):1689–1696, 2009.

[218] Carolyn M Porteous, Angela Logan, Cameron Evans, Elizabeth C Ledgerwood, David K Menon, Franklin Aigbirhio, Robin AJ Smith, and Michael P Murphy. Rapid uptake of lipophilic triphenylphosphonium cations by mitochondria in vivo following intravenous injection: implications for mitochondria-specific therapies and probes. *Biochimica et Biophysica Acta (BBA)-General Subjects*, 1800(9):1009–1017, 2010.

[219] Barry J Snow, Fiona L Rolfe, Michelle M Lockhart, Christopher M Frampton, John D O'Sullivan, Victor Fung, Robin AJ Smith, Michael P Murphy, Kenneth M Taylor, and Protect Study Group. A double-blind, placebo-controlled study to assess the mitochondria-targeted antioxidant mitoq as a disease-modifying therapy in parkinson's disease. *Movement Disorders*, 25(11):1670–1674, 2010.

[220] Robin AJ Smith, Richard C Hartley, and Michael P Murphy. Mitochondria-targeted small molecule therapeutics and probes. *Antioxidants & redox signaling*, 15(12):3021–3038, 2011.

[221] DW McKeown, RS Bonser, and JA Kellum. Management of the heartbeating brain-dead organ donor. *British journal of anaesthesia*, 108(suppl_1):i96–i107, 2012.

[222] UK Donation Ethics Committee et al. An ethical framework for controlled donation after circulatory death. *London: Academy of Medical Royal Colleges*, 2011.

[223] James M DuBois, Francis L Delmonico, and Anthony M D'Alessandro. When organ donors are still patients: is premortem use of heparin ethically acceptable? *American Journal of Critical Care*, 16(4):396–400, 2007.

[224] UK Donation Ethics Committee et al. Interventions before death to optimise donor organ quality and improve transplant outcomes: guidance from the uk donation ethics committee. *London: Academy of Medical Royal Colleges*, 2014.

[225] Jenna R DiRito, Sarah A Hosgood, Gregory T Tietjen, and Michael L Nicholson. The future of marginal kidney repair in the context of normothermic machine perfusion. *American Journal of Transplantation*, 18(10):2400–2408, 2018.

[226] Ahmer Hameed, Natasha Rogers, Henry Pleass, Bo Lu, Ray Miraziz, and Wayne Hawthorne. Intra-renal delivery of drugs targeting ischemia-reperfusion injury of the kidney using normothermic machine perfusion. *Transplantation*, 102:S700, 2018.

[227] Tristan M Snowsill, Jason Moore, Ruben E Mujica Mota, Jaime L Peters, Tracey L Jones-Hughes, Nicola J Huxley, Helen F Coelho, Marcela Haasova, Chris Cooper, Jenny A Lowe, et al. Immunosuppressive agents in adult kidney transplantation in the national health service: a model-based economic evaluation. *Nephrology Dialysis Transplantation*, 32(7):1251–1259, 2017.

[228] H Tse George, Emily E Hesketh, Michael Clay, Gary Borthwick, Jeremy Hughes, and Lorna P Marson. Mouse kidney transplantation: Models of allograft rejection. *JoVE (Journal of Visualized Experiments)*, 92(e52163), 2014.

[229] Anita S Chong, Maria-Luisa Alegre, Michelle L Miller, and Robert L Fairchild. Lessons and limits of mouse models. *Cold Spring Harbor perspectives in medicine*, 3(12):a015495, 2013.

[230] M Skoskiewicz, C Chase, HJ Winn, and PS Russell. Kidney transplants between mice of graded immunogenetic diversity. *Transplant Proc*, 5(721), 1973.

[231] Fangmin Ge and Weihua Gong. Strategies for successfully establishing a kidney transplant in a mouse model. *Exp Clin Transplant*, 9(5):287–94, 2011.

[232] Longhui Qiu and Zheng Jenny Zhang. Therapeutic strategies of kidney transplant ischemia reperfusion injury: Insight from mouse models. *Biomedical journal of scientific & technical research*, 14(5), 2019.

[233] George Hondag Tse, Jeremy Hughes, and Lorna Palmer Marson. Systematic review of mouse kidney transplantation. *Transplant International*, 26(12):1149–1160, 2013.

[234] Aashish Sharma, Marìa Jimena Mucino, and Claudio Ronco. Renal functional reserve and renal recovery after acute kidney injury. *Nephron Clinical Practice*, 127(1-4):94–100, 2014.

[235] Yin-Wu Bao, Yuan Yuan, Jiang-Hua Chen, and Wei-Qiang Lin. Kidney disease models: tools to identify mechanisms and potential therapeutic targets. *Zoological research*, 39(2):72, 2018.

[236] Qingqing Wei and Zheng Dong. Mouse model of ischemic acute kidney injury: technical notes and tricks. *American Journal of Physiology-Renal Physiology*, 303(11):F1487–F1494, 2012.

[237] Nathalie Le Clef, Anja Verhulst, Patrick C D'Haese, and Benjamin A Vervaet. Unilateral renal ischemia-reperfusion as a robust model for acute to chronic kidney injury in mice. *PloS one*, 11(3):e0152153, 2016.

[238] Sean E Kennedy and Jonathan H Erlich. Murine renal ischaemia-reperfusion injury (methods in renal research paper). *Nephrology*, 13(5):390–396, 2008.

[239] Pietro E Cippà, Bo Sun, Jing Liu, Liang Chen, Maarten Naesens, and Andrew P McMahon. Transcriptional trajectories of human kidney injury progression. *JCI insight*, 3(22), 2018.

[240] Jing Liu, Sanjeev Kumar, Egor Dolzhenko, Gregory F Alvarado, Jinjin Guo, Can Lu, Yibu Chen, Meng Li, Mark C Dessing, Riana K Parvez, et al. Molecular characterization of the transition from acute to chronic kidney injury following ischemia/reperfusion. *JCI insight*, 2(18), 2017.

[241] Alexandra Wendler and Martin Wehling. The translatability of animal models for clinical development: biomarkers and disease models. *Current opinion in pharmacology*, 10(5):601–606, 2010.

[242] Allan D Kirk. Crossing the bridge: large animal models in translational transplantation research. *Immunological reviews*, 196(1):176–196, 2003.

[243] S Giraud, F Favreau, N Chatauret, R Thuillier, S Maiga, and T Hauet. Contribution of large pig for renal ischemia-reperfusion and transplantation studies: the preclinical model. *BioMed Research International*, 2011, 2011.

[244] Matthew N Simmons, Martin J Schreiber, and Inderbir S Gill. Surgical renal ischemia: a contemporary overview. *The Journal of urology*, 180(1):19–30, 2008.

[245] Eiji Kobayashi, Shuji Hishikawa, Takumi Teratani, and Alan T Lefor. The pig as a model for translational research: overview of porcine animal models at jichi medical university. *Transplantation research*, 1(1):8, 2012.

[246] Marco A Pereira-Sampaio, Luciano A Favorito, and Francisco JB Sampaio. Pig kidney: anatomical relationships between the intrarenal arteries and the kidney collecting system. applied study for urological research and surgical training. *The Journal of urology*, 172(5):2077–2081, 2004.

[247] Rohan Kumar, Wen Yuan Chung, Ashley Robert Dennison, and Giuseppe Garcea. Ex vivo porcine organ perfusion models as a suitable platform for translational transplant research. *Artificial organs*, 41(9):E69–E79, 2017.

[248] Simon JF Harper, Sarah A Hosgood, Helen L Waller, Bin Yang, Mark D Kay, Ines Goncalves, and Michael L Nicholson. The effect of warm ischemic time on renal function and injury in the isolated hemoperfused kidney. *Transplantation*, 86(3):445–451, 2008.

[249] Sarah A Hosgood, Tom Moore, Theresa Kleverlaan, Tom Adams, and Michael L Nicholson. Haemoadsorption reduces the inflammatory response and improves blood flow during ex vivo renal perfusion in an experimental model. *Journal of translational medicine*, 15(1):216, 2017.

[250] Sarah A Hosgood, AD Barlow, J Dormer, and ML Nicholson. The use of ex-vivo normothermic perfusion for the resuscitation and assessment of human kidneys discarded because of inadequate in situ perfusion. *Journal of translational medicine*, 13(1):329, 2015.

[251] Sarah A Hosgood and Michael L Nicholson. First in man renal transplantation after ex vivo normothermic perfusion. *Transplantation*, 92(7):735–738, 2011.

[252] Gregory T Tietjen, Sarah A Hosgood, Jenna DiRito, Jiajia Cui, Deeksha Deep, Eric Song, Jan R Kraehling, Alexandra S Piotrowski-Daspit, Nancy C Kirkiles-Smith, Rafia Al-Lamki, et al. Nanoparticle targeting to the endothelium during normothermic machine perfusion of human kidneys. *Science translational medicine*, 9(418):eaam6764, 2017.

[253] John R. Ferdinand, Sarah A. Hosgood, Tom Moore, Christopher J. Ward, Tomas Castro-Dopico, Michael L. Nicholson, and Menna R. Clatworthy. Investigation of the transcriptional profile of human kidneys during machine perfusion reveals potential benefits of haemoadsorption. *bioRxiv*, 2019.

[254] Robert W Steiner. Interpreting the fractional excretion of sodium. *The American journal of medicine*, 77(4):699–702, 1984.

[255] Bernard L Strehler. Bioluminescence assay: principles and practice. *Methods Biochem Anal*, 16:99–181, 1968.

[256] JV Passonneau and VR Lauderdale. A comparison of three methods of glycogen measurement in tissues. *Analytical biochemistry*, 60(2):405–412, 1974.

[257] Janine H Santos, Joel N Meyer, Bhaskar S Mandavilli, and Bennett Van Houten. Quantitative pcr-based measurement of nuclear and mitochondrial dna damage and repair in mammalian cells. In *DNA Repair Protocols*, pages 183–199. Springer, 2006.

[258] Geoffrey F Kelso, Carolyn M Porteous, Carolyn V Coulter, Gillian Hughes, William K Porteous, Elizabeth C Ledgerwood, Robin AJ Smith, and Michael P Murphy. Selective targeting of a redox-active ubiquinone to mitochondria within cells antioxidant and antiapoptotic properties. *Journal of Biological Chemistry*, 276(7):4588–4596, 2001.

[259] Owen W Griffith. Determination of glutathione and glutathione disulfide using glutathione reductase and 2-vinylpyridine. *Analytical biochemistry*, 106(1):207–212, 1980.

[260] Christoph Sommer, C. Strähle, Ullrich Köthe, and Fred A. Hamprecht. ilastik: Interactive learning and segmentation toolkit. In *Eighth IEEE International Symposium on Biomedical Imaging (ISBI 2011).Proceedings*, pages 230–233, 2011. 1.

[261] Johannes Schindelin, Ignacio Arganda-Carreras, Erwin Frise, Verena Kaynig, Mark Longair, Tobias Pietzsch, Stephan Preibisch, Curtis Rueden, Stephan Saalfeld, Benjamin Schmid, et al. Fiji: an open-source platform for biological-image analysis. *Nature methods*, 9(7):676, 2012.

[262] Vijay Sharma and John H McNeill. To scale or not to scale: the principles of dose extrapolation. *British journal of pharmacology*, 157(6):907–921, 2009.

[263] T Ahmed. Pharmacokinetics of drugs following iv bolus, iv infusion, and oral administration. *Basic Pharmacokinetic Concepts and Some Clinical Applications2015*, 2015.

[264] Thomas GJ Kuipers, Joyce Hellegering, Mostafa El Moumni, Christina Krikke, Jan Willem Haveman, Stefan P Berger, Henri G Leuvenink, and Robert A Pol. Kidney temperature course during living organ procurement and transplantation. *Transplant international*, 30(2):162–169, 2017.

[265] Marcel CG Van De Poll, Peter B Soeters, Nicolaas EP Deutz, Kenneth CH Fearon, and Cornelis HC Dejong. Renal metabolism of amino acids: its role in interorgan amino acid exchange. *The American journal of clinical nutrition*, 79(2):185–197, 2004.

[266] Cholsoon Jang, Li Chen, and Joshua D Rabinowitz. Metabolomics and isotope tracing. *Cell*, 173(4):822–837, 2018.

[267] Victoria R Pell, Ana-Mishel Spiroski, John Mulvey, Nils Burger, Ana SH Costa, Angela Logan, Anja V Gruszczyk, Tiziana Rosa, Andrew M James, Christian Frezza, et al. Ischemic preconditioning protects against cardiac ischemia reperfusion injury without affecting succinate accumulation or oxidation. *Journal of molecular and cellular cardiology*, 123:88–91, 2018.

[268] Angela Logan, Helena M Cochemé, Pamela Boon Li Pun, Nadezda Apostolova, Robin AJ Smith, Lesley Larsen, David S Larsen, Andrew M James, Ian M Fearnley, Sebastian Rogatti, et al. Using exomarkers to assess mitochondrial reactive species in vivo. *Biochimica et Biophysica Acta (BBA)-General Subjects*, 1840(2):923–930, 2014.

[269] Helena M Cochemé, Caroline Quin, Stephen J McQuaker, Filipe Cabreiro, Angela Logan, Tracy A Prime, Irina Abakumova, Jigna V Patel, Ian M Fearnley, Andrew M James, et al. Measurement of h2o2 within living drosophila during aging using a ratiometric mass spectrometry probe targeted to the mitochondrial matrix. *Cell metabolism*, 13(3):340–350, 2011.

[270] R Houston Thompson, Brian R Lane, Christine M Lohse, Bradley C Leibovich, Amr Fergany, Igor Frank, Inderbir S Gill, Michael L Blute, and Steven C Campbell. Every minute counts when the renal hilum is clamped during partial nephrectomy. *European urology*, 58(3):340–345, 2010.

[271] Brian R Lane, Paul Russo, Robert G Uzzo, Adrian V Hernandez, Stephen A Boorjian, R Houston Thompson, Amr F Fergany, Thomas E Love, and Steven C Campbell. Comparison of cold and warm ischemia during partial nephrectomy in 660 solitary kidneys reveals predominant role of nonmodifiable factors in determining ultimate renal function. *The Journal of urology*, 185(2):421–427, 2011.

[272] Michael P Murphy, Arne Holmgren, Nils-Göran Larsson, Barry Halliwell, Christopher J Chang, Balaraman Kalyanaraman, Sue Goo Rhee, Paul J Thornalley, Linda Partridge, David Gems, et al. Unraveling the biological roles of reactive oxygen species. *Cell metabolism*, 13(4):361–366, 2011.

[273] Johannes K Ehinger, Sarah Piel, Rhonan Ford, Michael Karlsson, Fredrik Sjövall, Eleonor Åsander Frostner, Saori Morota, Robert W Taylor, Doug M Turnbull, Clive Cornell, et al. Cell-permeable succinate prodrugs bypass mitochondrial complex i deficiency. *Nature communications*, 7:12317, 2016.

[274] Paul R Gardner. Aconitase: sensitive target and measure of superoxide. In *Methods in enzymology*, volume 349, pages 9–23. Elsevier, 2002.

[275] Donna R Trollinger, Wayne E Cascio, and John J Lemasters. Selective loading of rhod 2 into mitochondria shows mitochondrial ca2+ transients during the contractile cycle in adult rabbit cardiac myocytes. *Biochemical and biophysical research communications*, 236(3):738–742, 1997.

[276] Theodore Kalogeris, Yimin Bao, and Ronald J Korthuis. Mitochondrial reactive oxygen species: a double edged sword in ischemia/reperfusion vs preconditioning. *Redox biology*, 2:702–714, 2014.

[277] Gianluca Farrugia and Rena Balzan. Oxidative stress and programmed cell death in yeast. *Frontiers in oncology*, 2:64, 2012.

[278] Susana Cadenas. Ros and redox signaling in myocardial ischemia-reperfusion injury and cardioprotection. *Free Radical Biology and Medicine*, 117:76–89, 2018.

[279] Zhi-Qing Zhao, Masanori Nakamura, Ning-Ping Wang, Josiah N Wilcox, Steven Shearer, Russell S Ronson, Robert A Guyton, and Jakob Vinten-Johansen. Reperfusion induces myocardial apoptotic cell death. *Cardiovascular research*, 45(3):651–660, 2000.

[280] W Gwinner, K Hinzmann, U Erdbruegger, I Scheffner, V Broecker, B Vaske, H Kreipe, H Haller, A Schwarz, and M Mengel. Acute tubular injury in protocol biopsies of renal grafts: prevalence, associated factors and effect on long-term function. *American Journal of Transplantation*, 8(8):1684–1693, 2008.

[281] S Op den Dries, N Karimian, ME Sutton, AC Westerkamp, MWN Nijsten, ASH Gouw, J Wiersema-Buist, T Lisman, HGD Leuvenink, and RJ Porte. Ex vivo normothermic machine perfusion and viability testing of discarded human donor livers. *American Journal of Transplantation*, 13(5):1327–1335, 2013.

[282] Annemarie Weissenbacher, Letizia Lo Faro, Olga Boubriak, Maria F Soares, Ian S Roberts, James P Hunter, Daniel Voyce, Nikolay Mikov, Andrew Cook, Rutger J Ploeg, et al. Twenty-four–hour normothermic perfusion of discarded human kidneys with urine recirculation. *American Journal of Transplantation*, 19(1):178–192, 2019.

[283] Asif A Sharfuddin and Bruce A Molitoris. Pathophysiology of ischemic acute kidney injury. *Nature Reviews Nephrology*, 7(4):189, 2011.

[284] Qiongyuan Hu, Jianan Ren, Huajian Ren, Jie Wu, Xiuwen Wu, Song Liu, Gefei Wang, Guosheng Gu, Kun Guo, and Jieshou Li. Urinary mitochondrial dna identifies renal dysfunction and mitochondrial damage in sepsis-induced acute kidney injury. *Oxidative medicine and cellular longevity*, 2018, 2018.

[285] Chengyuan Tang, Hailong Han, Mingjuan Yan, Shiyao Zhu, Jing Liu, Zhiwen Liu, Liyu He, Jieqiong Tan, Yu Liu, Hong Liu, et al. Pink1-prkn/park2 pathway of mitophagy is activated to protect against renal ischemia-reperfusion injury. *Autophagy*, 14(5):880–897, 2018.

[286] Lin-Li Lv, Ye Feng, Tao-Tao Tang, and Bi-Cheng Liu. New insight into the role of extracellular vesicles in kidney disease. *Journal of cellular and molecular medicine*, 23(2):731–739, 2019.

[287] Andreas Linkermann, Rachid Skouta, Nina Himmerkus, Shrikant R Mulay, Christin Dewitz, Federica De Zen, Agnes Prokai, Gabriele Zuchtriegel, Fritz Krombach, Patrick-Simon Welz, et al. Synchronized renal tubular cell death involves ferroptosis. *Proceedings of the National Academy of Sciences*, 111(47):16836–16841, 2014.

[288] Brent R Stockwell, Jose Pedro Friedmann Angeli, Hülya Bayir, Ashley I Bush, Marcus Conrad, Scott J Dixon, Simone Fulda, Sergio Gascón, Stavroula K Hatzios, Valerian E Kagan, et al. Ferroptosis: a regulated cell death nexus linking metabolism, redox biology, and disease. *Cell*, 171(2):273–285, 2017.

[289] Domenico Praticò, Joshua Rokach, John Lawson, and Garret A FitzGerald. F2-isoprostanes as indices of lipid peroxidation in inflammatory diseases. *Chemistry and physics of lipids*, 128(1-2):165–171, 2004.

[290] Mehmet Kaya Ozer, Hakan Parlakpinar, Yilmaz Cigremis, Muharrem Ucar, Nigar Vardi, and Ahmet Acet. Ischemia-reperfusion leads to depletion of glutathione content and augmentation of malondialdehyde production in the rat heart from overproduction of oxidants: can caffeic acid phenethyl ester (cape) protect the heart? *Molecular and cellular biochemistry*, 273(1-2):169–175, 2005.

[291] Hartmut Jaeschke. Vascular oxidant stress and hepatic ischemia/reperfusion injury. *Free radical research communications*, 13(1):737–743, 1991.

[292] Rodrigo Franco and John A Cidlowski. Glutathione efflux and cell death. *Antioxidants & redox signaling*, 17(12):1694–1713, 2012.

[293] Susan A Elmore, Darlene Dixon, James R Hailey, Takanori Harada, Ronald A Herbert, Robert R Maronpot, Thomas Nolte, Jerold E Rehg, Susanne Rittinghausen, Thomas J Rosol, et al. Recommendations from the inhand apoptosis/necrosis working group. *Toxicologic pathology*, 44(2):173–188, 2016.

[294] Bettina Grasl-Kraupp, Branislav Ruttkay-Nedecky, Helga Koudelka, Krystyna Bukowska, Wilfried Bursch, and Rolf Schulte-Hermann. In situ detection of fragmented dna (tunel assay) fails to discriminate among apoptosis, necrosis, and autolytic cell death: a cautionary note. *Hepatology*, 21(5):1465–1468, 1995.

[295] Daigo Nakazawa, Santhosh V Kumar, Julian Marschner, Jyaysi Desai, Alexander Holderied, Lukas Rath, Franziska Kraft, Yutian Lei, Yuichiro Fukasawa, Gilbert W Moeckel, et al. Histones and neutrophil extracellular traps enhance tubular necrosis and remote organ injury in ischemic aki. *Journal of the American Society of Nephrology*, 28(6):1753–1768, 2017.

[296] Mei T Tran, Zsuzsanna K Zsengeller, Anders H Berg, Eliyahu V Khankin, Manoj K Bhasin, Wondong Kim, Clary B Clish, Isaac E Stillman, S Ananth Karumanchi, Eugene P Rhee, et al. Pgc1α drives nad biosynthesis linking oxidative metabolism to renal protection. *Nature*, 531(7595):528, 2016.

[297] Thorsten Feldkamp, Andreas Kribben, Nancy F Roeser, Ruth A Senter, and Joel M Weinberg. Accumulation of nonesterified fatty acids causes the sustained energetic deficit in kidney proximal tubules after hypoxia-reoxygenation. *American Journal of Physiology-Renal Physiology*, 290(2):F465–F477, 2006.

[298] Noémie Simon and Alexandre Hertig. Alteration of fatty acid oxidation in tubular epithelial cells: from acute kidney injury to renal fibrogenesis. *Frontiers in medicine*, 2:52, 2015.

[299] Hyun Mi Kang, Seon Ho Ahn, Peter Choi, Yi-An Ko, Seung Hyeok Han, Frank Chinga, Ae Seo Deok Park, Jianling Tao, Kumar Sharma, James Pullman, et al. Defective fatty acid oxidation in renal tubular epithelial cells has a key role in kidney fibrosis development. *Nature medicine*, 21(1):37, 2015.

[300] Michael FW Festing and Douglas G Altman. Guidelines for the design and statistical analysis of experiments using laboratory animals. *ILAR journal*, 43(4):244–258, 2002.

[301] Hannes P Neeff, Ernst Von Dobschuetz, Olaf Sommer, Ulrich T Hopt, and Oliver Drognitz. In vivo quantification of oxygen-free radical release in experimental pancreas transplantation. *Transplant International*, 21(11):1081–1089, 2008.

[302] Sergey I Dikalov and David G Harrison. Methods for detection of mitochondrial and cellular reactive oxygen species. *Antioxidants & redox signaling*, 20(2):372–382, 2014.

[303] B Gray and AJ Carmichael. Kinetics of superoxide scavenging by dismutase enzymes and manganese mimics determined by electron spin resonance. *Biochemical Journal*, 281(3):795–802, 1992.

[304] Maria M Shchepinova, Andrew G Cairns, Tracy A Prime, Angela Logan, Andrew M James, Andrew R Hall, Sara Vidoni, Sabine Arndt, Stuart T Caldwell, Hiran A Prag, et al. Mitoneod: a mitochondria-targeted superoxide probe. *Cell chemical biology*, 24(10):1285–1298, 2017.

[305] H Sakamoto, TB Corcoran, JG Laffey, and GD Shorten. Isoprostanes–markers of ischaemia reperfusion injury. *European journal of anaesthesiology*, 19(8):550–559, 2002.

[306] Jian-Zhong Sun, Harparkash Kaur, Barry Halliwell, Xiao-Ying Li, and Roberto Bolli. Use of aromatic hydroxylation of phenylalanine to measure production of hydroxyl radicals after myocardial ischemia in vivo. direct evidence for a pathogenetic role of the hydroxyl radical in myocardial stunning. *Circulation Research*, 73(3):534–549, 1993.

[307] Pedro R Lowenstein and Maria G Castro. Uncertainty in the translation of preclinical experiments to clinical trials. why do most phase iii clinical trials fail? *Current gene therapy*, 9(5):368–374, 2009.

[308] Duvaraka Kula-Alwar, Hiran A Prag, and Thomas Krieg. Targeting succinate metabolism in ischemia/reperfusion injury. *Circulation*, 140(24):1968–1970, 2019.

[309] Lance B Becker. New concepts in reactive oxygen species and cardiovascular reperfusion physiology. *Cardiovascular research*, 61(3):461–470, 2004.

[310] Hazel H Szeto, Shaoyi Liu, Yi Soong, Surya V Seshan, Leona Cohen-Gould, Viacheslav Manichev, Leonard C Feldman, and Torgny Gustafsson. Mitochondria protection after acute ischemia prevents prolonged upregulation of il-1β and il-18 and arrests ckd. *Journal of the American Society of Nephrology*, 28(5):1437–1449, 2017.

[311] Christian Frezza. Mitochondrial metabolites: undercover signalling molecules. *Interface focus*, 7(2):20160100, 2017.

[312] GM Tannahill, AM Curtis, J Adamik, EM Palsson-McDermott, AF McGettrick, G Goel, C Frezza, NJ Bernard, B Kelly, NH Foley, et al. Succinate is an inflammatory signal that induces il-1β through hif-1α. *Nature*, 496(7444):238, 2013.

[313] Amanda Littlewood-Evans, Sophie Sarret, Verena Apfel, Perrine Loesle, Janet Dawson, Juan Zhang, Alban Muller, Bruno Tigani, Rainer Kneuer, Saijel Patel, et al. Gpr91 senses extracellular succinate released from inflammatory macrophages and exacerbates rheumatoid arthritis. *Journal of Experimental Medicine*, 213(9):1655–1662, 2016.

[314] Tina Rubic, Günther Lametschwandtner, Sandra Jost, Sonja Hinteregger, Julia Kund, Nicole Carballido-Perrig, Christoph Schwärzler, Tobias Junt, Hans Voshol, Josef G Meingassner, et al. Triggering the succinate receptor gpr91 on dendritic cells enhances immunity. *Nature immunology*, 9(11):1261, 2008.

[315] Weihai He, Frederick J-P Miao, Daniel C-H Lin, Ralf T Schwandner, Zhulun Wang, Jinhai Gao, Jin-Long Chen, Hui Tian, and Lei Ling. Citric acid cycle intermediates as ligands for orphan g-protein-coupled receptors. *Nature*, 429(6988):188, 2004.

[316] Ana Carolina Ariza, Peter MT Deen, and Joris Hubertus Robben. The succinate receptor as a novel therapeutic target for oxidative and metabolic stress-related conditions. *Frontiers in endocrinology*, 3:22, 2012.

[317] Matthias Kohlhauer, Sam Dawkins, Ana SH Costa, Regent Lee, Timothy Young, Victoria R Pell, Robin P Choudhury, Adrian P Banning, Rajesh K Kharbanda, Oxford Acute Myocardial Infarction (OxAMI) Study, et al. Metabolomic profiling in acute st-segment–elevation myocardial infarction identifies succinate as an early marker of human ischemia–reperfusion injury. *Journal of the American Heart Association*, 7(8):e007546, 2018.

[318] Luca Peruzzotti-Jametti, Joshua D Bernstock, Nunzio Vicario, Ana SH Costa, Chee Keong Kwok, Tommaso Leonardi, Lee M Booty, Iacopo Bicci, Beatrice Balzarotti, Giulio Volpe, et al. Macrophage-derived extracellular succinate licenses neural stem cells to suppress chronic neuroinflammation. *Cell Stem Cell*, 22(3):355–368, 2018.